May 1976 WRRI Report No. 073

STUDIES ON RAINFALL-RUNOFF MODELING

3. Converging Overland Flow

Partial Technical Completion Report
Project No. 3109-206

STUDIES ON RAINFALL-RUNOFF MODELING

3. Converging Over Land Flow

Vijay P. Singh, Assistant Professor of Hydrology

Partial Technical Completion Report

Project No. 3109-206

New Mexico Water Resources Research Institute
in cooperation with
New Mexico Institute of Mining and Technology
Socorro, New Mexico 87801

May 1976

The work upon which this report is based was supported in part by funds provided through the New Mexico Water Resources Research Institute by the Department of the Interior, Office of Water Research and Technology as authorized under the Water Resources Research Act of 1964, Public Law 88-379 as amended, under project number 3109-206.

LIST OF CONTENTS

LIST OF FIGURES

LIST OF TABLES

ABSTRACT

In the traditional formulation of kinematic wave theory the kinematic wave friction relationship parameter is treated as constant. The present study relaxes this assumption of parameter constancy, allows continuous spatial variability in the parameter and attempts to develop a more general formulation of the kinematic wave theory. This concept of parameter variability leads to a completely distributed model, and might hopefully eliminate the necessity of utilizing a complex network model to represent the watershed system. Furthermore, this more general formulation appears to reduce the complexity of modeling watershed surface runoff and save greatly the computational time and effort.

A converging geometry is chosen to represent the natural watershed geometry, and is utilized to develop the converging overland flow model. A laboratory investigation is performed to study the behavior of kinematic wave parameters. It is demonstrated that for many hydrologic problems the kinematic wave parameter n can be fixed at 1.5 and thus the two-parameter model can be reduced to a one-parameter model.

The converging overland flow model is studied on a number of natural, agricultural watersheds. It is found that the topographic map of a watershed is sufficient to transform its natural geometry into an equivalent converging geometry. The concept of both parameter constancy and variability is studied in detail on several agricultural watersheds. The model, in both lumped and distributed forms, is applied to predict surface runoff from several of these watersheds.

The converging overland flow on infiltrating watersheds is formulated as a free boundary problem. Mathematical solutions are developed to study the effect of infiltration on nonlinear overland flow dynamics. To develop

explicit solutions rainfall and infiltration are represented by simple space-and-time invariant functions.

ACKNOWLEDGEMENTS

The chapters on analytical mathematics are essentially an outgrowth of the author's collaborative work with Dr. Bernard Sherman, Professor of Mathematics, New Mexico Institute of Mining and Technology, Socorro, New Mexico. Prof. Sherman's contribution in this regard is gratefully appreciated. Part of laboratory investigation, reported herein, was conducted at Colorado State University Engineering Research Center while the author was working there toward a Ph.D. degree in Civil Engineering under the guidance of Dr. D. A. Woolhiser, Supervisory Research Hydraulic Engineer, USDA-ARS. Assistance of Dr. Woolhiser and Colorado State University is gratefully acknowledged.

CHAPTER 1

INTRODUCTION

1.1 GENERAL REMARKS

Since its formulation by Lighthill and Whitham (1955), its application to watershed modeling by Henderson and Wooding (1964) and Wooding (1965a, 1965b, 1966), and the subsequent demonstration of its applicability, in general, to problems of hydrologic significance by Woolhiser and Ligget (1967), the kinematic wave theory has been increasingly utilized in numerous investigations on watershed runoff modeling (Brakensiek, 1967; Woolhiser, 1969; Kibler and Woolhiser, 1970; Woolhiser et al, 1970; Eagleson, 1972; Singh, 1974, 1975a, 1975b; Rovey, 1974; Li, 1974; Lane, 1975). In these investigations the formulation of kinemetic wave theory has been as follows:

The continuity equation for the plane section,

$$\frac{\partial h}{\partial t} + \frac{\partial Q}{\partial x} = q(x,t) \tag{1-1}$$

and the kinematic approximation to momentum equation,

$$Q = uh = \alpha h^n \tag{1-2}$$

where h = local depth of flow, u = local average velocity, $q(x,t)$ = rate of effective lateral inflow varying in time and space, Q = rate of outflow per unit width, x = space coordinate, t = time coordinate, n = exponent between 1 and 3 inclusive, and α = the kinematic wave friction relationship parameter.

Equations (1-1) and (1-2) constitute what is called as the traditional formulation of kinemative wave theory. A close examination of Eqs. (1-1) and (1-2) can easily show that the structure of a kinematic wave model of watershed surface runoff will depend on (1) the characterization of the parameter α , and (2) the geometric configuration chosen to

represent the natural watershed geometry. It is apparent from Eq. (1-2) that in the traditional formulation the kinematic wave friction relationship parameter α does not vary in time or space. One approach that partly relaxes this assumption of parameter constancy is to employ a network model which considers the parameter to be different for different elements in the network geometry.

Most natural drainage systems have a very complex surface configuration. For purposes of hydrograph simulation it is necessary to transform the complex configuration into a simpler one having a similar hydrologic response. In the recent past four alternate simplified geometric configurations have been proposed to represent the geometry of a natural watershed. Accordingly, mathematical models of watershed surface runoff based on kinematic wave theory can be classified into four groups:

1. Converging overland flow model
2. Wooding's model
3. Composite section model
4. Cascade model

These models entail varying degrees of geometric abstractions, and are either lumped or at most quasi-distributed depending upon the characterization of the parameter α .

The converging overland flow model (Woolhiser, 1969; Singh, 1974, 1975a, 1975b) is a lumped parameter model. Of all it has the highest degree of geometric abstraction. It is shown in Fig. 1-1 where L_o denotes the length of flow region, r the degree of convergence, θ the interior angle, and S_o the ground slope. Wooding's model (Wooding, 1965a, 1965b, 1966) has relatively lesser degree of geometric abstraction. This is also a lumped parameter model, or at most quasi-distributed

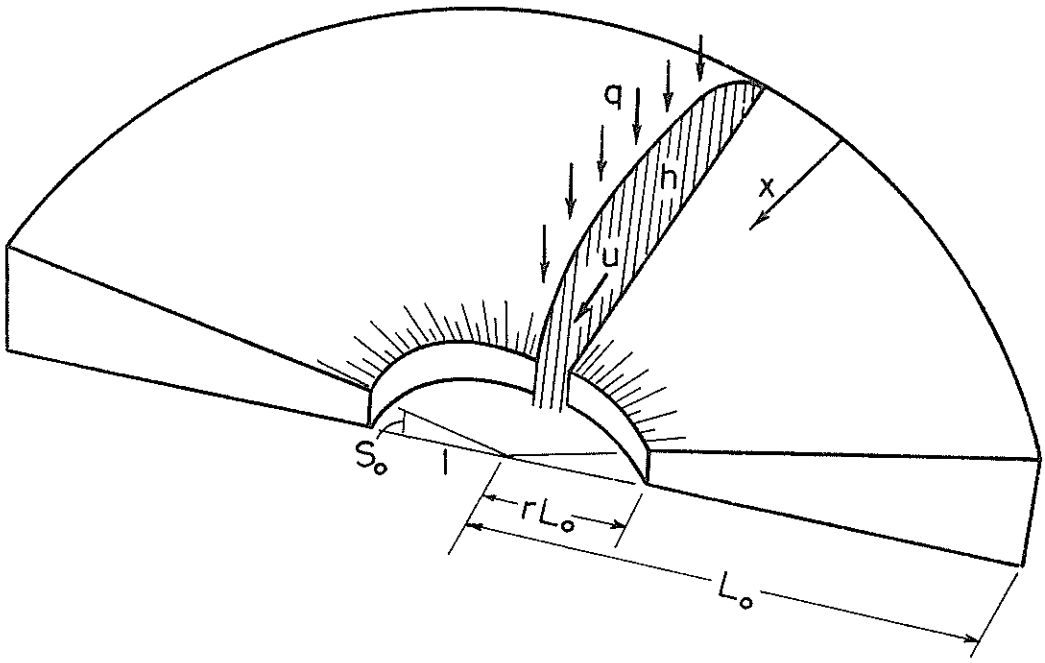

Fig. 1-1. Geometry of converging section.

if the parameter α is allowed to vary from one element to another in the network geometry. The model geometry is V-shaped having two planes discharging into a channel as shown in Fig. 1-2 where W denotes the plane width and L_o the plane length. The composite section model (Singh, 1974, 1975b) has even lesser degree of abstraction. This model will be quasi-distributed if the parameter α is allowed to be different for different elements in the network geometry. The model geometry is shown in Fig. 1-3 where $L_o(1 - r)$ denotes the length of converging flow, which is equal to the length of the plane and W the width of the plane which is equal to the length of the channel. It should be pointed out that the length of flow over the plane must be normal to the channel; it can therefore be computed directly from $L_o(1 - r)$ and the interior angle θ of the converging section. Obviously this geometry is a combination of the geometries of the two previous models. The cascade model (Brakensiek, 1967; Kibler and Woolhiser, 1970; Singh, 1974) has the least order of abstraction and hence more close to reality. The model geometry consists of planes and channels as shown in Fig. 1-4 where there are N planes, having length L_k and width L_{ck}, discharging into a channel of width W_c and length L_c; k denotes a dummy index. The arrangement of planes and channels will naturally differ from one watershed to another. Permitting the parameter α to vary from one element to another will make the cascade model a quasi-distributed model. Although a cascade model can be made so complex as to provide an almost perfect representation of the watershed system, it will be too complex and too time consuming to be of any real operational value.

A consideration of watershed runoff dynamics might suggest that the watershed surface roughness characteristics have more predominent influence on the runoff generation process than the watershed geometry as such.

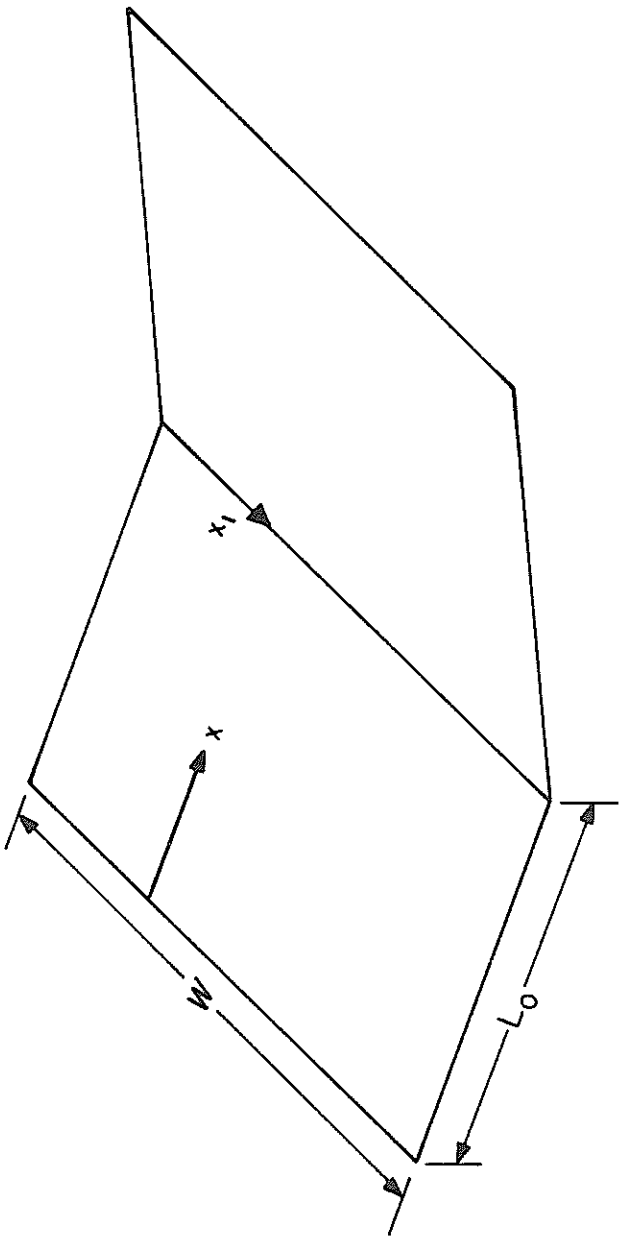

Fig. 1-2. Geometry of Wooding's runoff model.

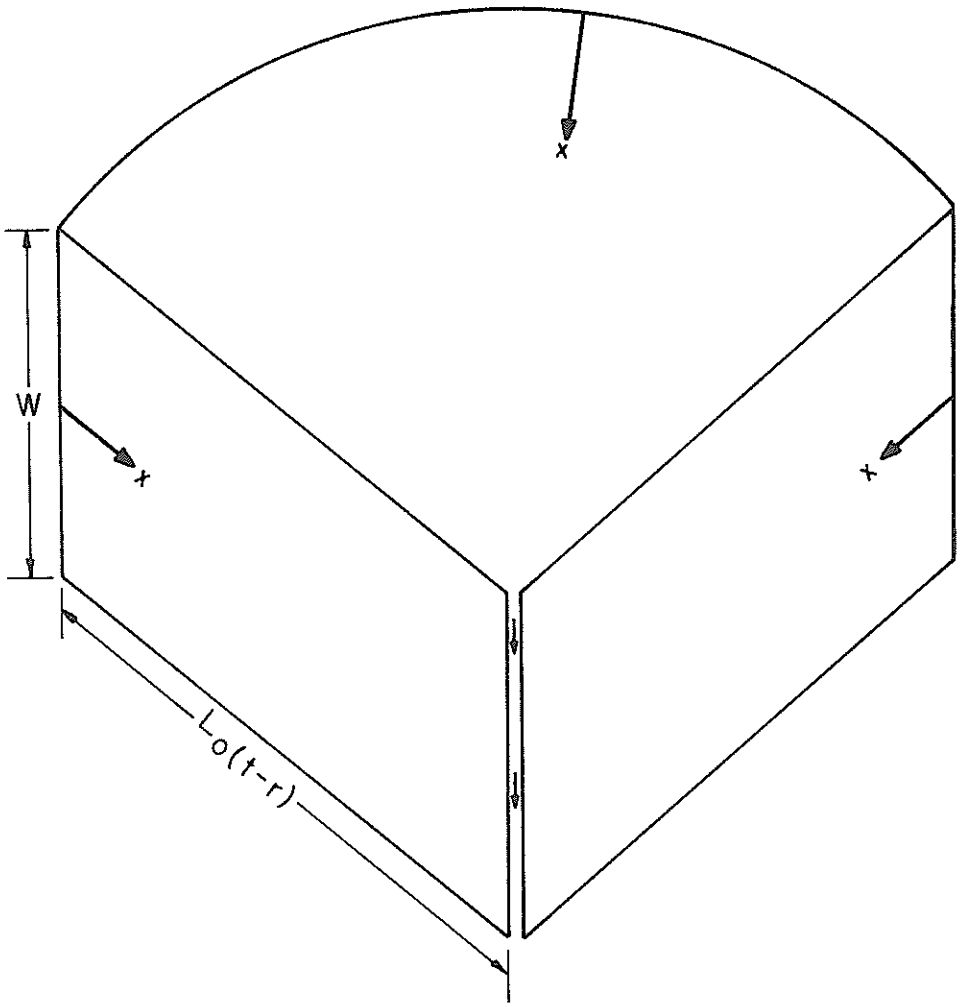

Fig. 1-3. Geometry of a composite section.

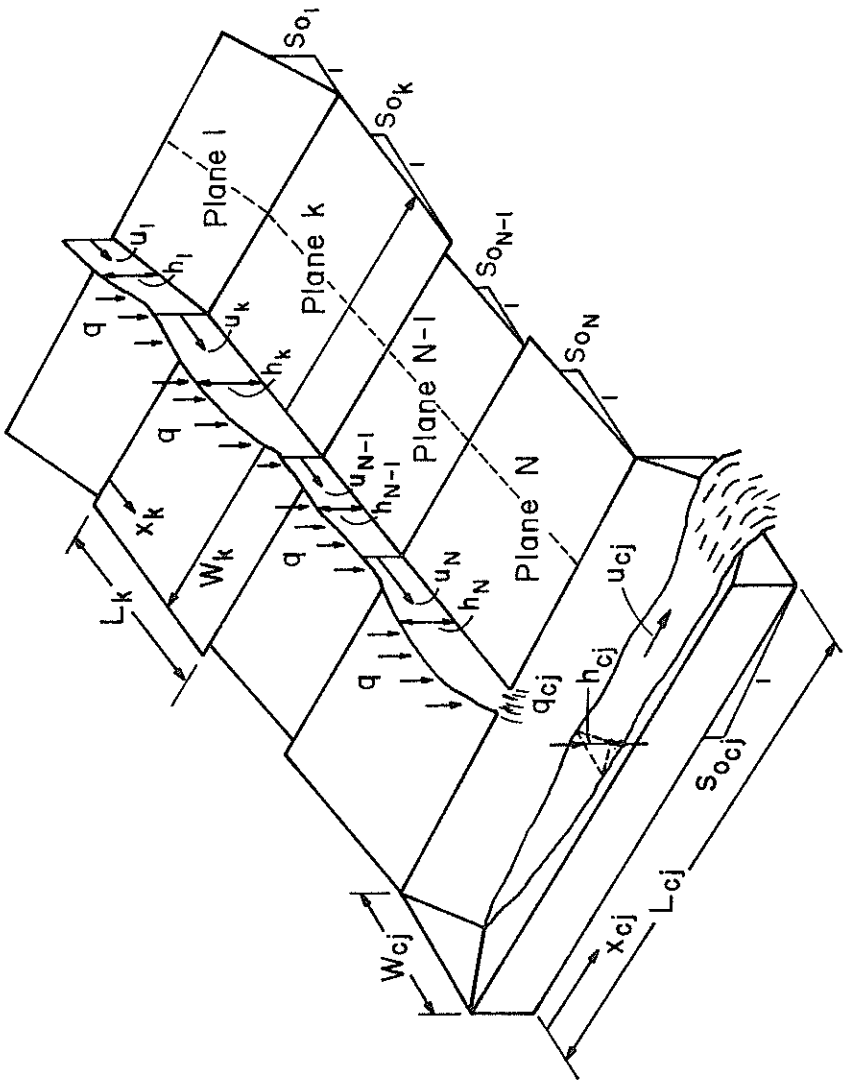

Fig. 1-4. Cascade of N planes discharging into the j^{th} channel.

This contention was expressed in a recent study by Singh (1974) which concluded that regardless of its complexity the geometry of a natural watershed could be transformed into a simple converging geometry which would preserve the hydrologic response to a large extent. This same view was expressed much earlier by Woolhiser (1969). Besides their obvious simplicity this premise might be another explanation for the popularity of such simple geometries as converging geometry and V-shaped geometry in representation of a natural watershed.

In the present study the roughness characteristics are being represented by the parameter α . It may then be argued that the above geometrical configurations have been advanced primarily to better represent the spatial distribution of the parameter α. It is then suggested that the necessity of a complex geometric configuration can be eliminated by employing a simple geometry and allowing the parameter α to vary continuously in space. By so doing the resulting model will be simpler in geometry (for example, a converging geometry or a plane geometry) and completely distributed. It will be interesting to note that this concept of parameter variability is not an artificial one, but is consistent with runoff dynamics. Before proceeding further, it must be made clear that by no means we are suggesting here that geometrical details will have no influence on runoff process at all.

In the present study we will examine the physical plausibility of the concept of parameter variability utilizing a converging section, and test by considering its application to natural agricultural watersheds. This examination will be conducted in light of the development of a systematic treatment to the problem of surface runoff.

1.2 OBJECTIVES

The objectives of this study are:

1. To conduct a laboratory investigation of the lumped parameter converging overland flow model.

2. To test the lumped parameter converging overland flow model on natural agricultural watersheds.

3. To develop mathematics of distributed converging overland flow.

4. To test the distributed converging overland flow model on natural agricultural watersheds.

5. To develop mathematical solutions for infiltrating watersheds.

CHAPTER 2

MATHEMATICAL SOLUTIONS FOR CONVERGING OVERLAND FLOW FROM IMPERVIOUS WATERSHEDS

2.1 GENERAL REMARKS

The kinematic wave equations of continuity and momentum for a converging section (Singh, 1974) can be written respectively in most general one-dimensional form (see appendix A) as:

$$\frac{\partial h}{\partial t} + u\frac{\partial h}{\partial t} + h\frac{\partial u}{\partial x} = q(x,t) + \frac{uh}{(L_o - x)} \tag{2-1}$$

$$Q = uh = \alpha(x,t)h^n \tag{2-2}$$

where h = local depth of flow, u = local average velocity, $q(x,t)$ = rate of effective lateral inflow varying in both time and space, Q = rate of outflow per unit width, x = space coordinate, t = time coordinate, L_o = length of the converging section, n = exponent, an index of non-linearity and greater than 1, and α = kinematic wave friction relationship parameter. These equations are derived in appendix A. Here the parameter α is a function of both time and space. For a specified rainfall duration T, $q(x,t) = 0$ when $t>T$, and $q(x,t) > 0$ when $t \leq T$. Substituting Eq. (2-2) into Eq. (2-1) we obtain:

$$\frac{\partial h}{\partial t} + n\alpha(x,t)h^{n-1}\frac{\partial h}{\partial x} = q(x,t) + \frac{\alpha(x,t)h^n}{(L_o - x)} - h^n\frac{\partial \alpha(x,t)}{\partial x} \tag{2-3}$$

Equation (2-3) holds in $S = \{0<x<L_o(1-r),\ t>0\}$. Depending upon the functional forms or distributional characteristics of $\alpha(x,t)$ and $q(x,t)$ we can have sixteen special cases of Eq. (2-3):

When $\alpha(x,t) = \alpha$, a constant, then

(1) $q(x,t) = q$, constant

(2) $q(x,t) = q(x)$

(3) $q(x,t) = q(t)$

(4) $q(x,t)$

When $\alpha(x,t) = \alpha(x)$ then

(5) $q(x,t) = q$

(6) $q(x,t) = q(x)$

(7) $q(x,t) = q(t)$

(8) $q(x,t)$

When $\alpha(x,t) = \alpha(t)$ then

(9) $q(x,t) = q$

(10) $q(x,t) = q(x)$

(11) $q(x,t) = q(t)$

(12) $q(x,t)$

When $\alpha(x,t) = \alpha(x,t)$ then

(13) $q(x,t) = q$

(14) $q(x,t) = q(x)$

(15) $q(x,t) = q(t)$

(16) $q(x,t)$

However, it may be interesting to note the two special cases:

1. When the parameter α is constant then Eq. (2-3) becomes:

$$\frac{\partial h}{\partial t} + n\alpha h^{n-1} \frac{\partial h}{\partial x} = q(x,t) + \frac{\alpha h^n}{(L_o - x)} \tag{2-4}$$

This case has been investigated by Woolhiser (1969), Woolhiser et al (1970) and Singh (1974, 1975a, 1975b, 1975c, 1975d, 1975e).

2. When the parameter α is a function of space only, then Eq. (2-3) becomes:

$$\frac{\partial h}{\partial t} + n\alpha(x) h^{n-1} \frac{\partial h}{\partial t} = q(x,t) + \frac{\alpha(x) h^n}{(L_o - x)} - h^n \frac{\partial \alpha(x)}{\partial x} \tag{2-5}$$

This case has not been investigated before and the present study attempts to do it. It is apparent that the former case given by Eq. (2-4) is also a special case of the latter given by Eq. (2-5).

2.2 MATHEMATICAL SOLUTIONS

We desire solution of Eq. (2-5). In the context of watershed surface runoff problem it is reasonable to assume the boundary conditions representing an initially dry surface:

$$h(x,0) = 0 \qquad 0 \leq x \leq L_0(1-r) \tag{2-6}$$

$$h(0,t) = 0 \qquad 0 \leq t \leq T$$

It is physically plausible that $h(0,t)$ should not be specified for $t>T$; that is, the solution of Eq. (2-5) in S below t=T subject to Eq. (2-6) should extend into S above t=T. This will be seen to be true in the ensuing mathematical discussion.

It must be pointed out that here $q(x,t)$ forms input to the model. Its hydrological significance is twofold:

(1) Rainfall or any other source of lateral inflow will directly contribute to input. This implies that the watershed surface is impervious, and infiltration is disregarded. This is true for parking lots, highways, runways, etc.

(2) Rainfall excess may form the input to the model. Here infiltration is considered and subtracted off from rainfall to yield rainfall excess. An important implication of this notion of rainfall-excess is that infiltration is allowed to take place only during the period of rainfall. As soon as rainfall ceases to exist, infiltration is assumed to cease simultaneously. This assumption, although far from reality, has been and continues to be used in most studies on hydrologic modeling.

In developing solutions of Eqs. (2-5) and (2-6) the method of characteristics appears to be most practical. The essence of the method lies in reducing a partial differential equation to a system of ordinary differential equations called the characteristic equations. Thus the

characteristic equations of Eq. (2-5) are:

$$\frac{dt}{ds} = 1$$

$$\frac{dx}{ds} = n\alpha(x)h^{n-1}$$

$$\frac{dh}{ds} = q(x,t) + \frac{\alpha(x)h^n}{(L_o-x)} - h^n \frac{d\alpha(x)}{dx}$$

where s is a parameter. Then the characteristic curves of Eq. (2-5) are given by the solution of the above system of ordinary differential equations. Through each point of space (x,t,h) there passes a unique characteristic curve. The solution of Eqs. (2-5) and (2-6) is the surface formed by all the characteristic curves passing through the segment $t = o$, $o \leq x \leq L_o(1-r)$ and the segment $x = o$, $o \leq t \leq T$ (in appendix B we will show that this solution extends into all of S above $t = T$). Figure 2-1 shows the projections of these characteristic curves onto the x - t plane. To obtain the surface formed by the characteristic curves we may take x as parameter instead of s. Then we have:

$$\frac{dt}{dx} = \frac{1}{n\alpha(x)h^{n-1}} \tag{2-7}$$

$$\frac{dh}{dx} = \frac{q(x,t)}{n\alpha(x)h^{n-1}} + \frac{h}{n(L_o-x)} - \frac{h}{n\alpha(x)} \frac{d\alpha(x)}{dx} \tag{2-8}$$

The initial conditions are:

$$t(o) = t_o \; ; \; h(o) = o$$

or

$$t(x_o) = o \; ; \; h(x_o) = o$$

The solution of Eqs. (2-7) and (2-8) will be the solution of Eq. (2-5). To obtain the solution of Eqs. (2-7) and (2-8) we distinguish two cases:

1. Case A: The characteristic curve $t = t(x,o)$ through the origin (0,0) intersects $x = L_o(1-r)$ (the downstream boundary) before it intersects $t = T$ (the duration of rainfall $q(x,t)$). This case will result in equilibrium hydrograph, and is shown in Fig. 2-2. Thus $t^* \leq T$. The

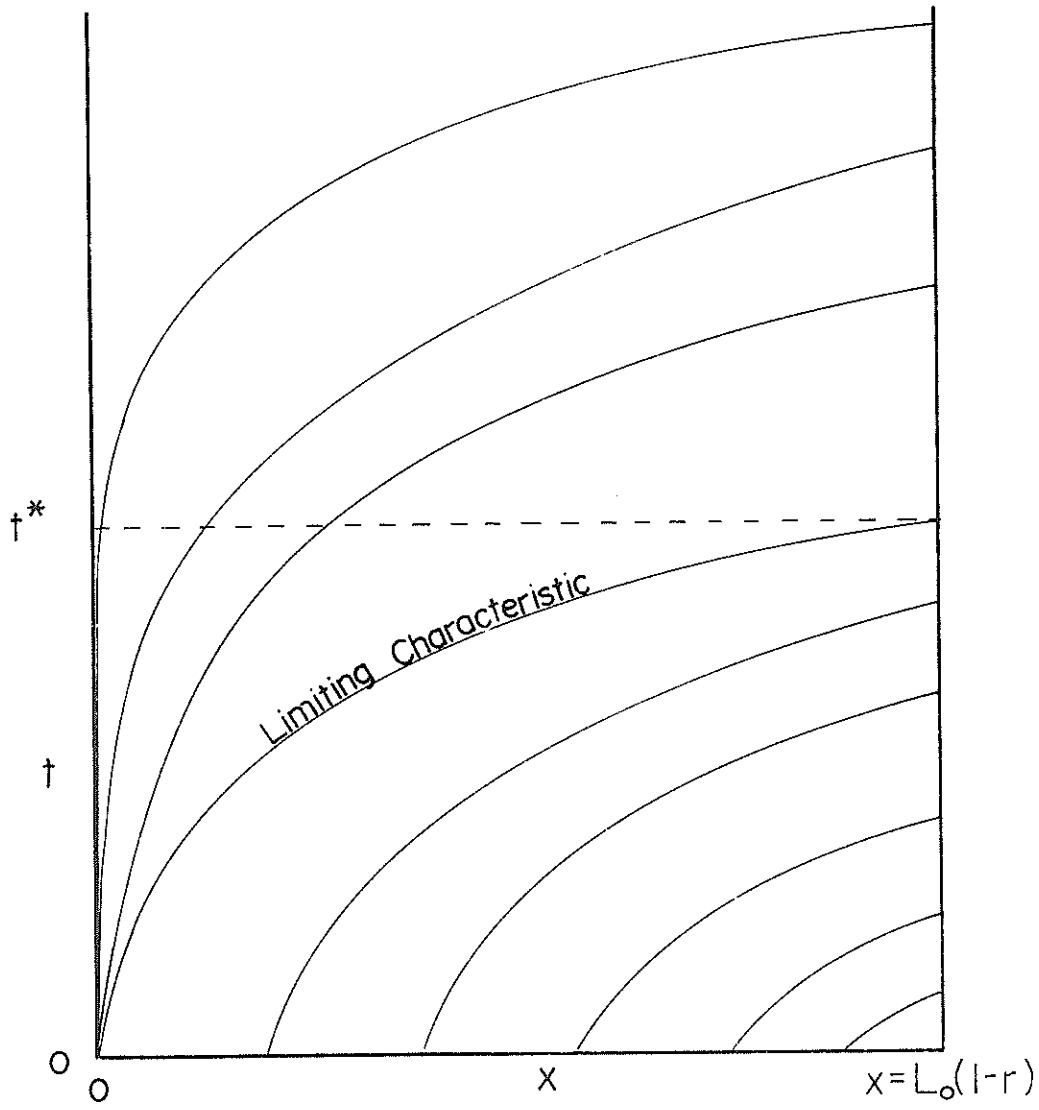

Fig. 2-1. The kinematic wave diagram.

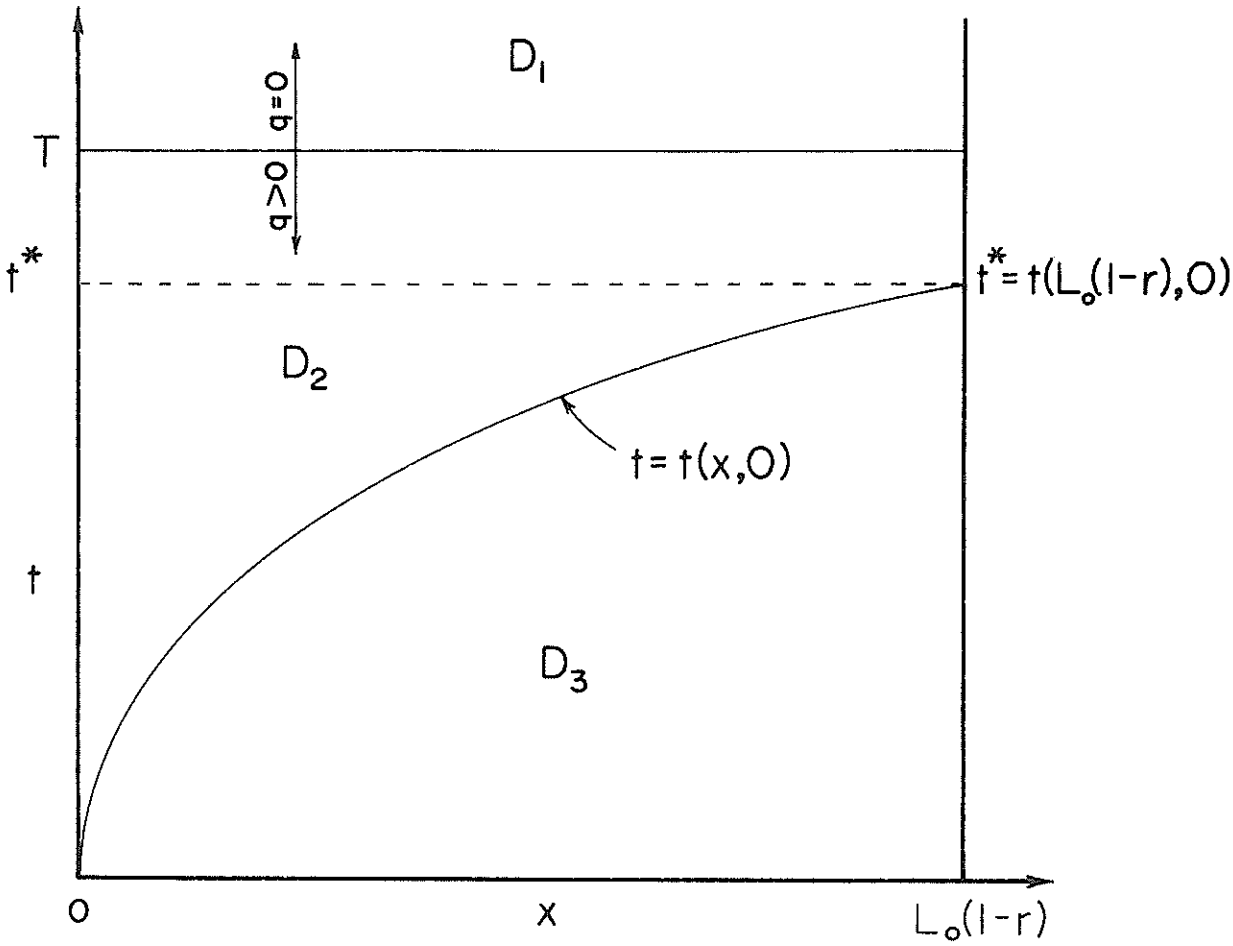

Fig. 2-2. Solution domain for equilibrium hydrograph.

characteristic issuing from the origin is called as the limiting characteristic. Here t* is identical to watershed equilibrium time.

2. Case B. The characteristic curve $t = t(x,o)$ through the origin (o,o) intersects $t = T$ before it intersects the downstream boundary $x = L_o(1-r)$. This case will result in partial equilibrium hydrograph and is shown in Fig. 2-3. Thus $t^* > T$ for this case. Here t* will depend on T, and is not equal to t* of case A.

The solutions to these two cases will completely characterize the surface runoff hydrograph. We will develop mathematical solutions to these two cases.

2.2.1 Case A: Equilibrium Situation

We can write the input $q(x,t)$ as:

$$q(x,t) = \begin{cases} q(x,t) & o \leq t \leq T \quad ; T \geq t^* \\ o & t > T \end{cases}$$

where T = rainfall duration, and t* = time taken by the limiting characteristic to intersect the downstream boundary. It must be noted that here t* is independent of T, and may be characterized as the watershed equilibrium time. For this case we divide the solution domain into four subdomains as shown in Fig. 2-2. First, we wish to obtain the surface formed by the characteristics passing through the t-axis. We have:

Domain D_2. For this domain we can write our initial conditions as:

$$t(o) = t_o \quad ; o \leq t_o \leq T \qquad (2\text{-}9)$$

$$h(o) = o$$

The solution surface is then expressed in terms of x and t_o where:

$$t = t(x,t_o)$$

$$h = h(x,t_o)$$

$$x = x$$

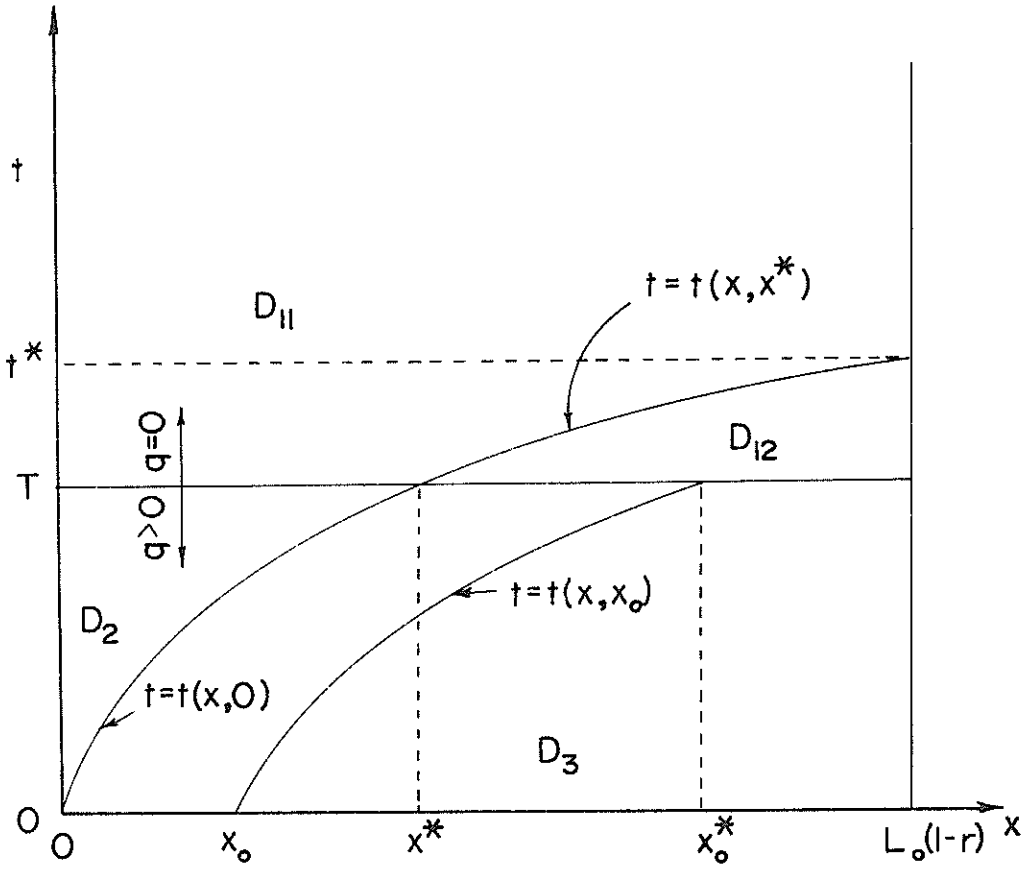

Fig. 2-3. Solution domain for partial equilibrium hydrograph.

We will assume that, under appropriate conditions on $\alpha(x)$ and $q(x,t)$, the curves $t = t(x,t_o)$ do not, for distinct values of t_o, intersect in S. It will be seen in appendix C that this is true for $q(x,t) = q$, a constant. $t(x,t_o)$ is an increasing function of x for fixed t_o since $h(x) > o$ in S (from Eq. (2-10) below) and, by our nonintersection assumption, it is an increasing function of t_o. Thus we can solve for t_o in $t = t(x,t_o)$ and we can, therefore, express h as a function of x and t. We can write Eq. (2-8) as:

$$\frac{d}{dx}\left\{\alpha(x)h^n(L_o - x)\right\} = (L_o - x)q(x,t)$$

Integrating and using the condition $h(o) = o$ we obtain:

$$(L_o - x)\alpha(x)h^n = \int_o^x (L_o - \xi)q(\xi,t(\xi,t_o))d\xi$$

Thus we have:

$$h(x,t_o) = \left\{\frac{1}{\alpha(x)(L_o - x)}\int_o^x (L_o - \xi)q(\xi,t(\xi,t_o))d\xi\right\}^{\frac{1}{n}} \qquad (2\text{-}10)$$

Inserting Eq. (2-10) into Eq. (2-7) we get:

$$\frac{dt}{dx} = \frac{1}{n\alpha(x)}\left\{\frac{1}{(L_o - x)\alpha(x)}\int_o^x (L_o - \xi)q(\xi,t(\xi,t_o))d\xi\right\}^{\frac{1-n}{n}}$$

Upon integration,

$$t(x,t_o) = t_o + \int_o^x \frac{1}{n\alpha(\eta)}\left\{\frac{1}{\alpha(\eta)(L_o - \eta)}\int_o^\eta (L_o - \xi)q(\xi,t(\xi,t_o))d\xi\right\}^{\frac{1-n}{n}} d\eta \qquad (2\text{-}11)$$

Equation (2-11) is a nonlinear integral equation for $t(x,t_o)$ whose solution will obviously depend on the functional form of $\alpha(x)$ in space and that of $q(x,t)$ in time and space. Inserting the solution of Eq. (2-11) into Eq. (2-10) we get $h(x,t_o)$. There can be seven special cases of Eqs. (2-10) and (2-11) that we now examine:

1. If $q(x,t)$ is constant then we get explicit solutions:

$$h(x,t_o) = \left\{\frac{(L_o^2 - (L_o - x)^2)q}{2\alpha(x)(L_o - x)}\right\}^{\frac{1}{n}} \tag{2-12}$$

$$t(x,t_o) = t_o + \frac{q^{\frac{1-n}{n}}}{n}\int_o^x (\alpha(\eta))^{-\frac{1}{n}}\left\{\frac{L_o^2 - (L_o - \eta)^2}{2(L_o - \eta)}\right\}^{\frac{1-n}{n}} d\eta \tag{2-13}$$

2. If $q(x,t)$ varies in space only, then we obtain:

$$h(x,t_o) = \left\{\frac{1}{\alpha(x)(L_o - x)}\int_o^x (L_o - \xi)q(\xi)d\xi\right\}^{\frac{1}{n}} \tag{2-14}$$

$$t(x,t_o) = t_o + \frac{1}{n}\int_o^x \left\{\frac{1}{\alpha(\eta)}\right\}^{\frac{1}{n}}(L_o - \eta)^{\frac{n-1}{n}}\left\{\int_o^\eta (L_o - \xi)q(\xi)d\xi\right\}^{\frac{1-n}{n}} d\eta \tag{2-15}$$

3. If $q(x,t)$ varies in time only, then we have:

$$h(x,t_o) = \left\{\frac{1}{\alpha(x)(L_o - x)}\int_o^x (L_o - \xi)q(t(\xi,t_o))d\xi\right\}^{\frac{1}{n}} \tag{2-16}$$

$$t(x,t_o) = t_o + \frac{1}{n}\int_o^x \left\{\frac{1}{\alpha(\eta)}\right\}^{\frac{1}{n}}\left(L_o - \eta\right)^{\frac{n-1}{n}}\left\{\int_o^\eta (L_o - \xi)q(t(\xi,t_o))d\xi\right\}^{\frac{1-n}{n}} d\eta \tag{2-17}$$

4. If $\alpha(x)$ and $q(x,t)$ both are constant then we get:

$$h(x,t_o) = \left\{\frac{(2L_o x - x^2)q}{2\alpha(L_o - x)}\right\}^{\frac{1}{n}} \tag{2-18}$$

$$t(x,t_o) = t_o + \left(\frac{2}{q}\right)^{\frac{n-1}{n}}\left(\frac{1}{\alpha}\right)^{\frac{1}{n}}\frac{1}{n}\int_o^x \left\{\frac{(L_o - \xi)}{2L_o\xi - \xi^2}\right\}^{\frac{n-1}{n}} d\xi \tag{2-19}$$

Equation (2-19) is, however, expressible in terms of Beta functions as follows:

$$t(x,t_o) = t_o + \frac{1}{n}\left(\frac{2}{q}\right)^{\frac{n-1}{n}}\left(\frac{1}{\alpha}\right)^{\frac{1}{n}}\int_o^x \left\{\frac{(L_o - \xi)}{L_o^2 - (L_o - \xi)^2}\right\}^{\frac{n-1}{n}} d\xi$$

Substituting $\eta = \left(\frac{L_o - \xi}{L_o}\right)^2$,

$$t(x,t_o) = t_o + \frac{q}{n}^{\frac{1-n}{n}}\left(\frac{L_o}{2\alpha}\right)^{\frac{1}{n}}\int_{\left(\frac{L_o - x}{L_o}\right)^2}^{1} \eta^{-\frac{1}{2n}}(1-\eta)^{\frac{1}{n}-1}\, d\eta$$

$$= t_o + \frac{q}{n}^{\frac{1-n}{n}}\left(\frac{L_o}{2\alpha}\right)^{\frac{1}{n}}\int_{\left(\frac{L_o - x}{L_o}\right)^2}^{1} \eta^{\left(1-\frac{1}{2n}\right)-1}(1-\eta)^{\frac{1}{n}-1}\, d\eta$$

$$= t_o + \frac{q}{n}^{\frac{1-n}{n}}\left(\frac{L_o}{2\alpha}\right)^{\frac{1}{n}}\left\{\int_o^1 \eta^{\left(1-\frac{1}{2n}\right)-1}(1-\eta)^{\frac{1}{n}-1}\, d\eta - \int_o^{\left(\frac{L_o - x}{L_o}\right)^2} \eta^{\left(1-\frac{1}{2n}\right)-1}(1-\eta)^{\frac{1}{n}-1}\, d\eta\right\}$$

$$= t_o + \frac{q}{n}^{\frac{1-n}{n}}\left(\frac{L_o}{2\alpha}\right)^{\frac{1}{n}}\left\{\beta(a;b) - \beta_\phi(a;b)\right\} \qquad (2\text{-}20)$$

where $a = (1 - \frac{1}{2n})$, $b = \frac{1}{n}$, and $\phi = \left(\frac{L_o - x}{L_o}\right)^2$. The quantity β, without a subscript, denotes a complete Beta function and can be expressed in terms of Gamma function as:

$$\beta(a;b) = \frac{\Gamma(a)\Gamma(b)}{\Gamma(a + b)} \tag{2-21}$$

However, β, with a subscript, denotes incomplete Beta function and has the following mathematical connotation:

$$\beta_\phi(a;b) = \int_o^\phi \xi^{a-1}(1 - \xi)^{b-1}\, d\xi \quad ; \; a > o \; ; \; b > o \; ; \; \phi \in (o,1) \tag{2-22}$$

$$\simeq \frac{\phi^a(1 - \phi)^b}{a}\left\{1 + \sum_{j=o}^{\infty} \frac{\beta(a + 1;\, j + 1)}{\beta(a + b;\, j + 1)}\, \phi^{j+1}\right\} \tag{2-23}$$

Using Eqs.(2-21) - (2-23) we can write Eq. (2-20) as:

$$t(x,t_o) = t_o + \frac{q^{\frac{1-n}{n}}}{n}\left(\frac{L_o}{2\alpha}\right)^{\frac{1}{n}}\left\{\frac{\Gamma\left(1 - \frac{1}{2n}\right)\Gamma\left(\frac{1}{n}\right)}{\Gamma\left(1 + \frac{1}{2n}\right)} - \frac{\left(\frac{L_o - x}{L_o}\right)^{2 - \frac{1}{n}}\left[1 - \left(\frac{L_o - x}{L_o}\right)^2\right]^{\frac{1}{n}}}{\left(1 - \frac{1}{2n}\right)}\right.$$

$$\left.\left[1 + \sum_{j=o}^{\infty} \frac{\beta\left(2 - \frac{1}{2n}\,;\, j + 1\right)}{\beta\left(1 + \frac{1}{2n}\,;\, j + 1\right)}\left(\frac{L_o - x}{L_o}\right)^{2(j+1)}\right]\right\} \tag{2-24}$$

5. If $\alpha(x)$ is constant but $q(x,t)$ varies in both time and space then we get:

$$h(x,t_o) = \left\{\frac{1}{\alpha(L_o - x)}\int_o^x (L_o - \xi)\, q(\xi, t(\xi,t_o))\, d\xi\right\}^{\frac{1}{n}} \tag{2-25}$$

$$t(x,t_o) = t_o + \frac{1}{n}\left(\frac{1}{\alpha}\right)^{\frac{1}{n}}\int_o^x (L_o - \eta)^{\frac{n-1}{n}}\left\{\int_o^\eta q(\xi, t(\xi,t_o))\, d\xi\right\}^{\frac{1-n}{n}} d\eta \tag{2-26}$$

6. If $\alpha(x)$ is constant but $q(x,t)$ varies in space only, then we obtain:

$$h(x,t_o) = \left\{ \frac{1}{\alpha(L_o - x)} \int_o^x q(\xi)(L_o - \xi)d\xi \right\}^{\frac{1}{n}} \tag{2-27}$$

$$t(x,t_o) = t_o + \frac{1}{n}\left(\frac{1}{\alpha}\right)^{\frac{1}{n}} \int_o^x (L_o - \eta)^{\frac{n-1}{n}} \left\{ \int_o^\eta q(\xi)(L_o - \xi)d\xi \right\}^{\frac{1-n}{n}} d\eta \tag{2-28}$$

7. If $\alpha(x)$ is constant but $q(x,t)$ varies in time only, then we get:

$$h(x,t_o) = \left\{ \frac{1}{\alpha(L_o - x)} \int_o^x q(t(\xi,t_o))\ (L_o - \xi)d\xi \right\}^{\frac{1}{n}} \tag{2-29}$$

$$t(x,t_o) = t_o + \frac{1}{n}\left(\frac{1}{\alpha}\right)^{\frac{1}{n}} \int_o^x (L_o - \eta)^{\frac{n-1}{n}} \left\{ \int_o^\eta q(t(\xi,t_o))\ (L_o - \xi)d\xi \right\}^{\frac{1-n}{n}} d\eta \tag{2-30}$$

From these solutions we observe that in the strip $\{o \le x \le L_o(1 - r)\ ;\ t(x,o) \le t \le T\} \equiv D_2$ the surface h, as a function of x and t, depends only on x if $q(x,t)$ is constant or varies only in space, regardless of the functional form of $\alpha(x)$. We also note that the characteristics issuing from the non-negative t-axis will have t-axis as their tangent. In particular, Eq. (2-7) implies that $\frac{dt}{dx} \Rightarrow \infty$ at $x = o$, $t_o = o$.

Domain D_3. To obtain the surface containing the x-axis, that is, h in D_3, we solve Eqs. (2-7) and (2-8) subject to the boundary conditions:

$$t(x_o) = o \quad ; \quad o \le x_o \le L_o(1-r)$$

$$h(x_o) = o$$

Then the solution surface is expressed in terms of x and x_o:

$t = t(x,x_o)$

$h = h(x,x_o)$

$x = x$

We again assume that the curves $t = t(x,t_o)$ do not intersect for distinct values of x_o. Thus $t(x,x_o)$ is, for fixed x_o, an increasing function of x and, for fixed x, a decreasing function of x_o. This nonintersection property will be proved in appendix C under the condition $q(x,t)$ a constant and $\alpha(x)$ an increasing function of x.

The solution of Eqs. (2-7) and (2-8) subject to the above specified boundary conditions is:

$$h(x,x_o) = \left\{ \frac{1}{\alpha(x)(L_o - x)} \int_{x_o}^{x} q(\xi,t(\xi,x_o))\ (L_o - \xi)d\xi \right\}^{\frac{1}{n}} \tag{2-31}$$

$$t(x,x_o) = \frac{1}{n} \int_{x_o}^{x} \left(\frac{1}{\alpha(\eta)}\right)^{\frac{1}{n}} (L_o - \eta)^{\frac{n-1}{n}} \left\{ \int_{x_o}^{\eta} q(\xi,t(\xi,x_o))\ (L_o - \xi)d\xi \right\}^{\frac{1-n}{n}} d\eta \tag{2-32}$$

Equation (2-32) is a nonlinear integral equation for $t(x,x_o)$, the solution of which will obviously depend on the functional forms of $\alpha(x)$ and $q(x,t)$. We get $h(x,x_o)$ by inserting the solution of Eq. (2-32) into Eq. (2-31). The seven special cases for this domain are:

1. If $q(x,t)$ is constant, we get explicit solutions:

$$h(x,x_o) = \left\{ \frac{q\left[(L_o - x_o)^2 - (L_o - x)^2\right]}{2\alpha(x)\ (L_o - x)} \right\}^{\frac{1-n}{n}} \tag{2-33}$$

$$t(x,x_o) = \frac{q^{\frac{1-n}{n}}}{n} \int_{x_o}^{x} \left\{\frac{1}{\alpha(\eta)}\right\}^{\frac{1}{n}} \left\{ \frac{(L_o - x_o)^2 - (L_o - \eta)^2}{2(L_o - \eta)} \right\}^{\frac{1-n}{n}} d\eta \tag{2-34}$$

2. If $q(x,t)$ varies in space only, then we have:

$$h(x,x_o) = \left\{ \frac{1}{\alpha(x)(L_o - x)} \int_{x_o}^{x} q(\xi)(L_o - \xi)\, d\xi \right\}^{\frac{1}{n}} \tag{2-35}$$

$$t(x,x_o) = \frac{1}{n} \int_{x_o}^{x} \left\{ \frac{1}{\alpha(\eta)} \right\}^{\frac{1}{n}} (L_o - \eta)^{\frac{n-1}{n}} \left\{ \int_{x_o}^{\eta} q(\xi)(L_o - \xi)\, d\xi \right\}^{\frac{1-n}{n}} d\eta \tag{2-36}$$

3. If $q(x,t)$ varies in time only, then we get:

$$h(x,x_o) = \left\{ \frac{1}{\alpha(x)(L_o - x)} \int_{x_o}^{x} q(t(\xi,x_o))\ (L_o - \xi)\, d\xi \right\}^{\frac{1}{n}} \tag{2-37}$$

$$t(x,x_o) = \frac{1}{n} \int_{x_o}^{x} \left\{ \frac{1}{\alpha(\eta)} \right\}^{\frac{1}{n}} (L_o - \eta)^{\frac{n-1}{n}} \left\{ \int_{x_o}^{\eta} q(t(\xi,x_o))\ (L_o - \xi)\, d\xi \right\}^{\frac{1-n}{n}} d\eta \tag{2-38}$$

4. If $q(x,t)$ and $\alpha(x)$ both are constant then we get:

$$h(x,x_o) = \left\{ \frac{q\left[2L_o(x - x_o) - (x^2 - x_o^2)\right]}{2\alpha(L_o - x)} \right\}^{\frac{1}{n}} \tag{2-39}$$

$$t(x,x_o) = \left(\frac{2}{q}\right)^{\frac{n-1}{n}} \left(\frac{1}{\alpha}\right)^{\frac{1}{n}} \frac{1}{n} \int_{x_o}^{x} \left\{ \frac{2L_o(\xi - x_o) - (\xi^2 - x_o^2)}{(L_o - \xi)} \right\}^{\frac{1-n}{n}} d\xi \tag{2-40}$$

$$= \left(\frac{2}{q}\right)^{\frac{n-1}{n}} \left(\frac{1}{\alpha}\right)^{\frac{1}{n}} \frac{1}{n} \int_{x_o}^{x} \left\{ \frac{(L_o - \xi)}{(L_o - x_o)^2 - (L_o - \xi)^2} \right\}^{\frac{n-1}{n}} d\xi$$

Substituting the transformation $\eta = \left(\frac{L_o - \xi}{L_o - x_o}\right)^2$ and making proper algebraic manipulations we get:

$$t(x,x_o) = \left(\frac{1}{q}\right)^{\frac{n-1}{n}} \left(\frac{L_o - x_o}{2\alpha}\right)^{\frac{1}{n}} \frac{1}{n} \int_{\left(\frac{L_o - x}{L_o - x_o}\right)^2}^{1} \eta^{\left(1 - \frac{1}{2n}\right) - 1} (1 - \eta)^{\frac{1}{n} - 1} d\eta \quad (2\text{-}41)$$

Equation (2-41) is expressible in terms of Beta function. We can write:

$$t(x,x_o) = \left(\frac{1}{q}\right)^{\frac{n-1}{n}} \left(\frac{L_o - x_o}{2\alpha}\right)^{\frac{1}{n}} \frac{1}{n} \left\{ \int_o^1 \eta^{\left(1 - \frac{1}{2n}\right) - 1} (1 - \eta)^{\frac{1}{n} - 1} d\eta - \int_o^{\left(\frac{L_o - x}{L_o - x_o}\right)^2} \eta^{\left(1 - \frac{1}{2n}\right) - 1} (1 - \eta)^{\frac{1}{n} - 1} d\eta \right\}$$

$$= \left(\frac{1}{q}\right)^{\frac{n-1}{n}} \left(\frac{L_o - x_o}{2\alpha}\right)^{\frac{1}{n}} \frac{1}{n} \left\{ \frac{\Gamma\left(1 - \frac{1}{2n}\right)\Gamma\left(\frac{1}{n}\right)}{\Gamma\left(1 + \frac{1}{2n}\right)} - \left(\frac{L_o - x}{L_o - x_o}\right)^{2 - \frac{1}{n}} \left\{ 1 - \left(\frac{L_o - x}{L_o - x_o}\right)^2 \right\}^{\frac{1}{n}} \right.$$

$$\left. \frac{1}{\left(1 - \frac{1}{2n}\right)} \left[1 + \sum_{j=o}^{\infty} \frac{\beta\left(2 - \frac{1}{2n} ; j + 1\right)}{\beta\left(1 + \frac{1}{2n} ; j + 1\right)} \left(\frac{L_o - x}{L_o - x_o}\right)^{2(j+1)} \right] \right\} \quad (2\text{-}42)$$

5. If $\alpha(x)$ is constant but $q(x,t)$ varies in both space and time, then we obtain:

$$h(x,x_o) = \left\{ \frac{1}{\alpha} \frac{1}{(L_o - x)} \int_{x_o}^{x} q(t,t(\xi,x_o)) \ (L_o - \xi) \ d\xi \right\}^{\frac{1}{n}} \tag{2-43}$$

$$t(x,x_o) = \frac{1}{n}\left(\frac{1}{\alpha}\right)^{\frac{1}{n}} \int_{x_o}^{x} (L_o - \eta)^{\frac{n-1}{n}} \left\{ \int_{x_o}^{\eta} q(\xi,t(\xi,x_o)) \ (L_o - \xi) \ d\xi \right\}^{\frac{1-n}{n}} d\eta \tag{2-44}$$

6. If $\alpha(x)$ is constant but $q(x,t)$ varies in space only, then we obtain:

$$h(x,x_o) = \left(\frac{1}{\alpha}\right)^{\frac{1}{n}} \left\{ \frac{1}{(L_o - x)} \int_{x_o}^{x} q(\xi) \ (L_o - \xi) \ d\xi \right\}^{\frac{1}{n}} \tag{2-45}$$

$$t(x,x_o) = \left(\frac{1}{\alpha}\right)^{\frac{1}{n}} \frac{1}{n} \int_{x_o}^{x} (L_o - \eta)^{\frac{n-1}{n}} \left\{ \int_{x_o}^{\eta} q(\xi) \ (L_o - \xi) \ d\xi \right\}^{\frac{1-n}{n}} d\eta \tag{2-46}$$

7. If $\alpha(x)$ is constant but $q(x,t)$ varies in time only, then we get:

$$h(x,x_o) = \left(\frac{1}{\alpha}\right)^{\frac{1}{n}} \left\{ \frac{1}{(L_o - x)} \int_{x_o}^{x} q(t(\xi,x_o)) \ (L_o - \xi) \ d\xi \right\}^{\frac{1}{n}} \tag{2-47}$$

$$t(x,x_o) = \frac{1}{n}\left(\frac{1}{\alpha}\right)^{\frac{1}{n}} \int_{x_o}^{x} (L_o - \eta)^{\frac{n-1}{n}} \left\{ \int_{x_o}^{\eta} q(t(\xi,t_o)) \ (L_o - \xi) \ d\xi \right\}^{\frac{1}{n}} \tag{2-48}$$

From the above solutions it is clear that in domain D_3 h, as a function of x and t, now depends on both x and t.

Domain D_1. We must modify Eqs. (2-7) and (2-8) subject to the condition $q(x,t) = o$ for $t > T$. Thus we have:

$$\frac{dt}{dx} = \frac{1}{n\alpha(x)h^{n-1}} \tag{2-49}$$

$$\frac{dh}{dx} = \frac{h}{n(L_o - x)} - \frac{h}{n\alpha(x)} \frac{d\alpha(x)}{dx} \tag{2-50}$$

Then our initial condition will become:

$$t(x_o^*) = T \tag{2-51}$$

$$h(x_o^*) = h(x_o^*,T) = h_o$$

where $h(x_o^*)$ is obtained from Eqs. (2-9) and (2-10). The solution in domain D_1 will be expressed in terms of x and x_o^*:

$$t = t(x,x_o^*)$$

$$h = h(x,x_o^*)$$

$$x = x$$

The solution of Eqs. (2-49) and (2-50) in conjunction with Eq. (2-51) is:

$$h(x,x_o^*) = h_o \left\{\frac{(L_o - x_o^*)\alpha(x_o^*)}{(L_o - x)\alpha(x)}\right\}^{\frac{1}{n}} \tag{2-52}$$

$$t(x,x_o^*) = T + \frac{h_o^{1-n}}{n} \left\{\alpha(x_o^*)(L_o - x_o^*)\right\}^{\frac{1-n}{n}} \int_{x_o^*}^{x} \left\{\frac{1}{\alpha(\xi)}\right\}^{\frac{1}{n}} \left\{L_o - \xi\right\}^{\frac{n-1}{n}} d\xi \tag{2-53}$$

Equation (2-53) is a nonlinear integral equation for $t(x,x_o^*)$, the solution of which will depend on functional forms of $\alpha(x)$ and $q(x,t)$. By

inserting the solution of Eq. (2-53) into Eq. (2-52) we get $h(x,x_o^*)$.

Again we examine the seven special cases:

1. If $q(x,t)$ is constant then the solution is:

$$h_o = \left\{ \frac{q(L_o^2 - (L_o - x_o^*)^2)}{2\alpha(x_o^*)(L_o - x_o^*)} \right\}^{\frac{1}{n}} \tag{2-54}$$

$$h(x,x_o^*) = \left\{ \frac{q(L_o^2 - (L_o - x_o^*)^2)}{2\alpha(x)(L_o - x)} \right\}^{\frac{1}{n}} \tag{2-55}$$

$$t(x,x_o^*) = T + \frac{1}{n} \left\{ \frac{q}{2}\left[L_o^2 - (L_o - x_o^*)^2 \right] \right\}^{\frac{1-n}{n}} \int_{x_o^*}^{x} \left\{ \frac{1}{\alpha(\xi)} \right\}^{\frac{1}{n}} \left\{ L_o - \xi \right\}^{\frac{n-1}{n}} d\xi \tag{2-56}$$

2. If $q(x,t)$ varies in space only, then we obtain:

$$h_o = \left\{ \frac{1}{\alpha(x_o^*)(L_o - x_o^*)} \int_o^{x_o^*} q(\xi)(L_o - \xi) d\xi \right\}^{\frac{1}{n}} \tag{2-57}$$

$$h(x,x_o^*) = \left\{ \frac{1}{\alpha(x)(L_o - x)} \int_o^{x_o} q(\xi)(L_o - \xi)\, d\xi \right\}^{\frac{1}{n}} \tag{2-58}$$

$$t(x,x_o^*) = T + \frac{1}{n} \left\{ \int_o^{x_o^*} q(\xi)(L_o - \xi)\, d\xi \right\}^{\frac{1-n}{n}} \int_{x_o^*}^{x} \left\{ \frac{1}{\alpha(\xi)} \right\}^{\frac{1}{n}} \left\{ L_o - \xi \right\}^{\frac{n-1}{n}} d\xi \tag{2-59}$$

3. If $q(x,t)$ varies in time only, then we obtain:

$$h_o = \left\{ \frac{1}{\alpha(x_o^*)(L_o - x_o^*)} \int_o^{x_o^*} (L_o - \xi)\, q\,(t(\xi,t_o))\, d\xi \right\}^{\frac{1}{n}} \tag{2-60}$$

$$h(x,x_o^*) = \left\{ \frac{1}{(L_o - x)\alpha(x)} \int_o^{x_o^*} (L_o - \xi)\, q\,(t(\xi,t_o))\, d\xi \right\}^{\frac{1}{n}} \tag{2-61}$$

$$t(x,x_o^*) = T + \frac{1}{n} \left\{ \int_o^{x_o^*} (L_o - \xi)\, q\,(t(\xi,t_o))\, d\xi \right\}^{\frac{1-n}{n}}$$

$$\int_{x_o}^{x} \left\{\frac{1}{\alpha(\xi)}\right\}^{\frac{1}{n}} \left\{L_o - \xi\right\}^{\frac{n-1}{n}} d\xi \tag{2-62}$$

4. If both $\alpha(x)$ and $q(x,t)$ are constant then we get:

$$h_o = \left\{ \frac{(2L_o x_o^* - x_o^{*2})q}{2\alpha(L_o - x_o^*)} \right\}^{\frac{1}{n}} \tag{2-63}$$

$$h(x,x_o^*) = \left\{ \frac{q(2L_o x_o^* - x_o^{*2})}{2\alpha(L_o - x)} \right\}^{\frac{1}{n}} \tag{2-64}$$

$$t(x,x_o^*) = T + \left\{\frac{q}{2}(2L_o x_o^* - x_o^{*2})\right\}^{\frac{1-n}{n}} \left(\frac{1}{\alpha}\right)^{\frac{1}{n}} \frac{1}{(2n-1)} \left\{(L_o - x)^{\frac{2n-1}{n}} - (L_o - x_o^*)^{\frac{2n-1}{n}}\right\} \quad (2\text{-}65)$$

5. If $\alpha(x)$ is constant but $q(x,t)$ varies in both time and space, then we get:

$$h_o = \left\{\frac{1}{\alpha(L_o - x_o^*)} \int_o^{x_o^*} q(\xi, t(\xi, t_o))\ (L_o - \xi)\ d\xi\right\}^{\frac{1}{n}} \quad (2\text{-}66)$$

$$h(x,x_o^*) = \left\{\frac{1}{\alpha(L_o - x)} \int_o^{x_o^*} q(\xi, t(\xi, t_o))\ (L_o - \xi)\ d\xi\right\}^{\frac{1}{n}} \quad (2\text{-}67)$$

$$t(x,x_o^*) = T + \left\{\int_o^{x_o^*} q(\xi, t(\xi, t_o))\ (L_o - \xi)\ d\xi\right\}^{\frac{1-n}{n}} \left(\frac{1}{\alpha}\right)^{\frac{1}{n}}$$

$$\left\{\frac{(L_o - x)^{\frac{2n-1}{n}} - (L_o - x_o^*)^{\frac{2n-1}{n}}}{(2n-1)}\right\} \quad (2\text{-}68)$$

6. If $\alpha(x)$ is constant but $q(x,t)$ varies in space only, then we obtain:

$$h_o = \left\{\frac{1}{\alpha(L_o - x_o^*)} \int_o^{x_o^*} q(\xi)\ (L_o - \xi)\ d\xi\right\}^{\frac{1}{n}} \quad (2\text{-}69)$$

$$h(x,x_o^*) = \left\{ \frac{1}{\alpha(L_o - x)} \int_o^{x_o^*} q(\xi)\ (L_o - \xi)\ d\xi \right\}^{\frac{1}{n}} \tag{2-70}$$

$$t(x,x_o^*) = T + \left\{ \int_o^{x_o^*} q(\xi)\ (L_o - \xi)\ d\xi \right\}^{\frac{1-n}{n}} \left(\frac{1}{\alpha}\right)^{\frac{1}{n}} \left\{ \frac{(L_o - x)^{\frac{2n-1}{n}} - (L_o - x_o^*)^{\frac{2n-1}{n}}}{(2n - 1)} \right\} \tag{2-71}$$

7. If $\alpha(x)$ is constant but $q(x,t)$ varies in time only, then we obtain:

$$h_o = \left\{ \frac{1}{\alpha(L_o - x_o^*)} \int_o^{x_o^*} q(t(\xi,t_o))\ (L_o - \xi)\ d\xi \right\}^{\frac{1}{n}} \tag{2-72}$$

$$h(x,x_o^*) = \left\{ \frac{1}{\alpha(L_o - x)} \int_o^{x_o^*} q(t(\xi,t_o))\ (L_o - \xi)\ d\xi \right\}^{\frac{1}{n}} \tag{2-73}$$

$$t(x,x_o^*) = T + \left\{ \int_o^{x_o^*} q(t(\xi,t_o))\ (L_o - \xi)\ d\xi \right\}^{\frac{1-n}{n}} \left(\frac{1}{\alpha}\right)^{\frac{1}{n}}$$

$$\left\{ \frac{(L_o - x)^{\frac{2n-1}{n}} - (L_o - x_o^*)^{\frac{2n-1}{n}}}{(2n - 1)} \right\} \tag{2-74}$$

It is clear from the above discussion that in domain D_1, h depends on both x and t. The curves $t = t(x,x_o)$ fill out the entire domain D_1 as x_o^* ranges from o to $L_o(1 - r)$. We now summarize the case A, $t^* \leq T$.

(1) In domain D_3 the solution is given by Eqs. (2-31) and (2-32). Here the parameter x_o assumes values on the segment $o \leq x \leq L_o(1 - r)$, $t = o$.

(2) In domain D_2 the solution is given by Eqs. (2-10) and (2-11). Here the parameter t_o assumes values on the segment $x = o$, $o \leq t \leq T$.

(3) In domain D_1 the solution is given by Eqs. (2-52) and (2-53). Here the parameter x_o^* assumes values on the segment $o \leq x \leq L_o$, $t = T$.

We now consider, in case A with $q(x,t) = q$, h as a function of t for fixed x, that is, we want to know the appearance of the curve cut out of the surface $h(x,t)$ by a plane perpendicular to the x axis. In domain D_3 we have:

$$\frac{\partial h(x,t)}{\partial t} = \frac{\partial h(x,x_o)}{\partial x_o} \qquad \frac{\partial x_o}{\partial t} = \frac{h_{x_o}(x,x_o)}{t_{x_o}(x,x_o)} \tag{2-75}$$

From Eqs. (2-33) and (2-34) we see that $h_{x_o}(x,x_o) < o$. From these equations it also follows, although the discussion is more complicated, that $t_{x_o}(x,x_o) < o$. Thus $h_t(x,t) > o$ if $(x,t) \varepsilon D_3$. In domain D_2, $h(x,t)$ is independent of t for time-invariant input and for space-invariant input. In domain D_1, we have from Eqs. (2-55) and (2-56), $h_{x_o}^*(x,x_o^*) > o$ and $t_{x_o}^*(x,x_o^*) < o$. Thus $h_t(x,t) < o$. From Eq. (2-56) $t \to \infty$ for fixed x is equivalent to $x_o^* \to o$ for fixed x, and from Eq. (2-55) $h(x,t) \to o$ as $t \to \infty$. It then follows that, for a fixed value of x, the function $h(x,t)$, due to a pulse input, has the appearance as shown in Fig. 2-4. We may obtain the approximate behavior of $h(x,t)$ for large t (and therefore small x_o^*) by setting $x_o^* = o$ in the integral in Eq. (2-56) and eliminating x_o^* between Eq. (2-55) and (2-56):

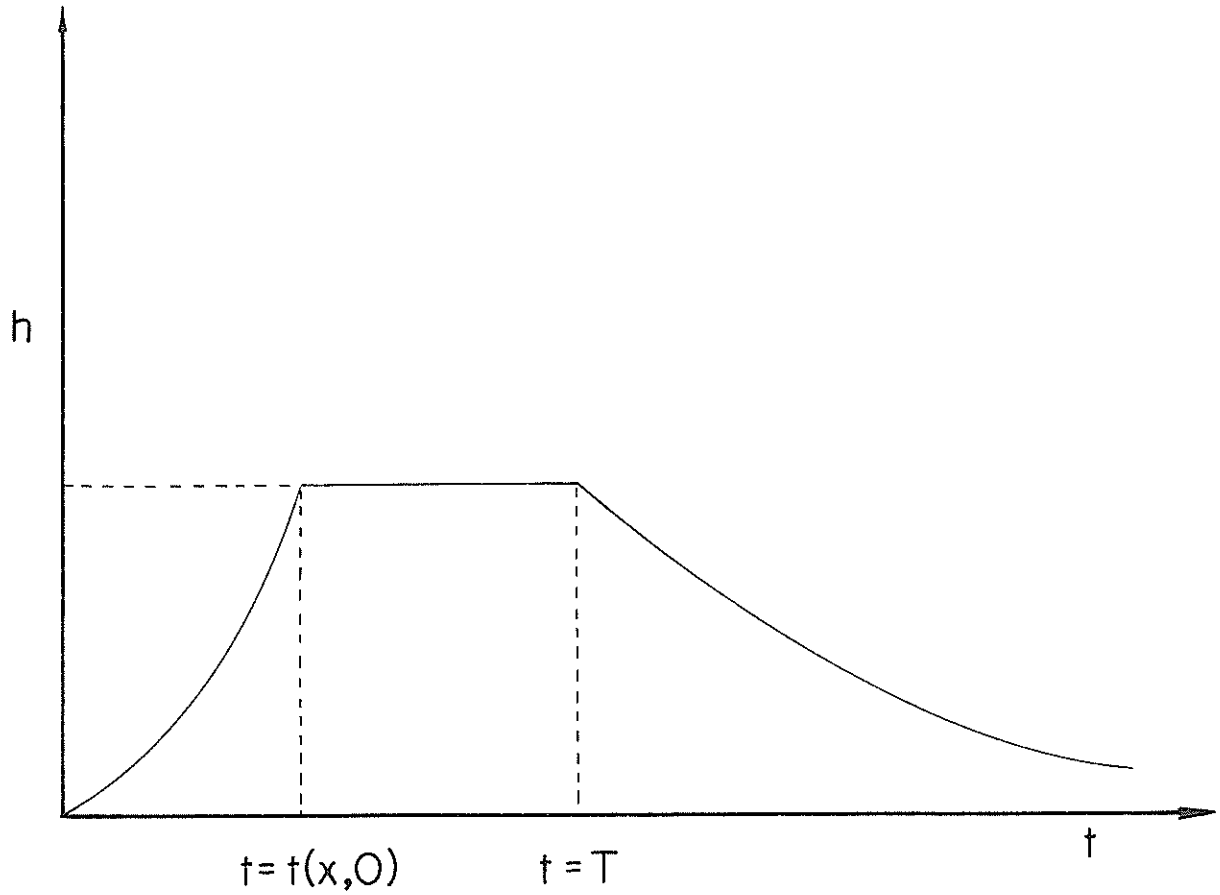

Fig. 2-4. The depth of flow at x for equilibrium case, $t^* \leq T$, $q(x,t) = q$.

$$h(x,t) = \frac{\psi(x)}{(t - T)^{\frac{1}{n-1}}}$$

$$\text{where } \psi(x) = \frac{\left[\int_o^x (\alpha(\eta))^{-\frac{1}{n}} (L_o - \eta)^{\frac{n-1}{n}} d\eta\right]^{\frac{1}{n-1}}}{n^{\frac{1}{n-1}} \left\{\alpha(x)(L_o - x)\right\}^{\frac{1}{n}}}$$

We note that the decline of h to o as $t \to \infty$ is not exponential. Thus, if $n = 1.5$, $h(x,t)$ goes to zero as t^{-2}. In Table 2-1 we summarize the conditions leading to explicit analytic solutions.

It may be instructive at this point to determine the equilibrium time and the equilibrium depth; both these quantities will be given when the characteristic curve passing through the origin (o,o) intersects the downstream boundary $L_o(1 - r)$. For case A equilibrium time will be the same as t^* in Fig. 2-2, and will be independent of rainfall pattern and duration. Thus we have:

$$h_e = \left\{\frac{1}{L_o r \gamma} \int_o^{L_o(1-r)} (L_o - \xi)\, q\,(\xi, t(\xi))\, d\xi\right\}^{\frac{1}{n}} \tag{2-76}$$

$$t_e = \int_o^{L_o(1-r)} \frac{1}{n\alpha(\eta)} \left\{\frac{1}{\alpha(\eta)(L_o - \eta)} \int_o^{\eta} (L_o - \xi)\, q\,(\xi, t(\xi))\, d\xi\right\}^{\frac{1-n}{n}} d\eta \tag{2-77}$$

where γ is the value of $\alpha(x)$ at $x = L_o(1 - r)$, h_e the equilibrium depth at $x = L_o(1 - r)$, and t_e equilibrium time at $x = L_o(1 - r)$. Let

Table 2-1. Conditions leading to analytical solutions for equilibrium and partial equilibrium hydrographs

Case number	Parameter $\alpha(x)$		Input $q(x,t)$				Analytical Solutions		Remarks
	Constant	Varying in space	Constant	Varying in space only	Varying in time only	Varying in both space and time	Complete	Part	
1		X				X		X	The functional forms of $\alpha(x)$ and $q(x,t)$ will determine the form of solutions
2		X	X				X		The functional form of $\alpha(x)$ will determine the form of solutions
3		X		X				X	The functional forms of $\alpha(x)$ and $q(x)$ will determine the form of solutions
4		X			X			X	The functional forms of $\alpha(x)$ and $q(t)$ will determine the form of solutions
5	X					X		X	The functional form of $q(x,t)$ will determine the form of solutions
6	X		X				X		
7	X			X				X	The functional form of $q(x)$ will determine the form of solutions
8	X				X			X	The functional form of $q(t)$ will determine the form of solutions

us now determine the equilibrium depth and time for the seven special cases:

1. If q(x,t) is constant then we get:

$$h_e = \left\{\frac{qL_o(1 - r^2)}{2r\gamma}\right\}^{\frac{1}{n}} \tag{2-78}$$

$$t_e = \frac{q^{\frac{1-n}{n}}}{n} \int_o^{L_o(1-r)} \left\{\frac{1}{\alpha(\eta)}\right\}^{\frac{1}{n}} \left\{\frac{L_o^2 - (L_o - \eta)^2}{2(L_o - \eta)}\right\}^{\frac{1-n}{n}} d\eta \tag{2-79}$$

2. If q(x,t) varies in space only, then we obtain:

$$h_e = \left\{\frac{1}{\gamma L_o r} \int_o^{L_o(1-r)} q(\xi)\ (L_o - \xi)\ d\xi\right\}^{\frac{1}{n}} \tag{2-80}$$

$$t_e = \frac{1}{n} \int_o^{L_o(1-r)} \left\{\frac{1}{\alpha(\eta)}\right\}^{\frac{1}{n}} \left\{L_o - \eta\right\}^{\frac{n-1}{n}} \left\{\int_o^{\eta} (L_o - \xi)\ q\ (\xi)\ d\xi\right\}^{\frac{1-n}{n}} d\eta \tag{2-81}$$

3. If q(x,t) varies in time only, then we obtain:

$$h_e = \left\{\frac{1}{\gamma L_o r} \int_o^{L_o(1-r)} (L_o - \xi)\ q\ (t(\xi))\ d\xi\right\}^{\frac{1}{n}} \tag{2-82}$$

$$t_e = \frac{1}{n} \int_o^{L_o(1-r)} \left\{\frac{1}{\alpha(\eta)}\right\}^{\frac{1}{n}} \left\{L_o - \eta\right\}^{\frac{n-1}{n}} \left\{ \int_o^{\eta} (L_o - \xi)\ q\ (t(\xi))\ d\xi \right\}^{\frac{1-n}{n}} d\eta \qquad (2\text{-}83)$$

4. If $\alpha(x)$ and $q(x,t)$ both are constant then we get:

$$h_e = \left\{\frac{qL_o(1 - r^2)}{2\alpha r}\right\}^{\frac{1}{n}} \qquad (2\text{-}84)$$

$$t_e = \frac{1}{n}\left(\frac{2}{q}\right)^{\frac{n-1}{n}}\left(\frac{L_o}{\alpha}\right)^{\frac{1}{n}} \left\{\frac{\Gamma(1 - \frac{1}{2n})\Gamma(\frac{1}{n})}{\Gamma(1 + \frac{1}{2n})} - \frac{(r)^{2-\frac{1}{n}}(1 - r)^{\frac{1}{n}}}{(1 - \frac{1}{2n})}\right.$$

$$\left.\left[1 + \sum_{j=o}^{\infty} \frac{\beta(2 - \frac{1}{2n}\ ;\ j + 1)}{\beta(1 + \frac{1}{2n}\ ;\ j + 1)} (r)^{2(j+1)}\right]\right\} \qquad (2\text{-}85)$$

If however r is small, as is the case most often, we can simply write:

$$t_e = \frac{1}{n}\left(\frac{2}{q}\right)^{\frac{n-1}{n}}\left(\frac{L_o}{\alpha}\right)^{\frac{1}{n}} \frac{\Gamma(1 - \frac{1}{2n})\Gamma(\frac{1}{n})}{\Gamma(1 + \frac{1}{2n})} \qquad (2\text{-}86)$$

5. If $\alpha(x)$ is constant but $q(x,t)$ varies in both space and time then we have:

$$h_e = \left\{\frac{1}{\alpha L_o r} \int_o^{L_o(1-r)} q(\xi, t(\xi))\ (L_o - \xi)\ d\xi\right\}^{\frac{1}{n}} \qquad (2\text{-}87)$$

$$t_e = \frac{1}{n}\left(\frac{1}{\alpha}\right)^{\frac{1}{n}} \int_o^{L_o(1-r)} (L_o - \eta)^{\frac{n-1}{n}} \left\{ \int_o^{\eta} q(\xi, t(\xi))\, d\xi \right\}^{\frac{1-n}{n}} d\eta \qquad (2\text{-}88)$$

6. If $\alpha(x)$ is constant but $q(x,t)$ varies in space only, then we obtain:

$$h_e = \left\{ \frac{1}{\alpha L_o r} \int_o^{L_o(1-r)} q(\xi)(L_o - \xi)\, d\xi \right\}^{\frac{1}{n}} \qquad (2\text{-}89)$$

$$t_e = \frac{1}{n}\left(\frac{1}{\alpha}\right)^{\frac{1}{n}} \int_o^{L_o(1-r)} (L_o - \eta)^{\frac{n-1}{n}} \left\{ \int_o^{\eta} q(\xi)(L_o - \xi)\, d\xi \right\}^{\frac{1-n}{n}} d\eta \qquad (2\text{-}90)$$

7. If $\alpha(x)$ is constant but $q(x,t)$ varies in time only, then we get:

$$h_e = \left\{ \frac{1}{\alpha L_o r} \int_o^{L_o(1-r)} (L_o - \xi)\, q\,(t(\xi))\, d\xi \right\}^{\frac{1}{n}} \qquad (2\text{-}91)$$

$$t_e = \frac{1}{n}\left(\frac{1}{\alpha}\right)^{\frac{1}{n}} \int_o^{L_o(1-r)} (L_o - \eta)^{\frac{n-1}{n}} \left\{ \int_o^{\eta} q(t(\xi))\, (L_o - \xi)\, d\xi \right\}^{\frac{1-n}{n}} d\eta \qquad (2\text{-}92)$$

2.2.2 Case B: Partial Equilibrium Case

We can write the input as:

$$q(x,t) = \begin{cases} q(x,t) & o \leq t \leq T \quad , \quad T < t^* \\ o & \text{otherwise} \end{cases}$$

This case is somewhat more complicated. The quantity t^* will depend on

T. The solution domain is shown in Fig. 2-3, and is divided into four parts. Let x^* be the solution of $T = t(x,o)$. Let D_{11} be the domain above the line $t = T$ and above the curve $t = t(x,x^*)$. The curve $t = t(x,x^*)$ is just the propagation of $t = t(x,o)$ beyond $t = T$. Let D_{12} be the domain bounded by $t = T$, $t = t(x,x^*)$, and $x = L_o$. The domain D_2 is bounded by $t = T$, $x = o$ and the curve $t = t(x,o)$. The domain D_3 is bounded by $t = t(x,o)$, $t = T$, $t = o$ and $x = L_o(1 - r)$.

Domain D_2. The solution is given by Eqs. (2-10) and (2-11)

Domain D_3. The solution is given by Eqs. (2-31) and (2-32)

Domain D_{11}. Let $o < x_o^* \leq x^*$, $t = T$, then the solution is given by Eqs. (2-52) and (2-53)

Domain D_{12}. Let x_o^* be the solution of $T = t(x,x_o)$, that is the value of x where the curve $t = t(x,x_o)$ given by Eq. (2-32) intersects the line $t = T$. Then along the segment $x^* < x_o^* < L_o(1 - r)$, $t = T$, we have from Eq. (2-31):

$$h(x_o^*,x_o) = \left\{ \frac{1}{\alpha(x_o^*)(L_o - x_o^*)} \int_{x_o}^{x_o^*} (L_o - \xi)\, q\, (\xi, t(\xi,x_o))\, d\xi \right\}^{\frac{1}{n}} \tag{2-93}$$

Now we solve the two differential equations given by Eqs. (2-49) and (2-50) subject to the initial conditions:

$t(x_o^*) = T$

$h(x_o^*) = h(x_o^*, x_o)$

Then the solution follows:

$$h(x;x_o^*,x_o) = h(x_o^*,x_o) \left\{ \frac{(L_o - x_o^*)\alpha(x_o^*)}{(L_o - x)\alpha(x)} \right\}^{\frac{1}{n}} \tag{2-94}$$

or

$$h(x;x_o^*,\ x_o) = \left\{ \frac{1}{(L_o - x)\alpha(x)} \int_{x_o}^{x_o^*} (L_o - \xi)\ q\ (\xi, t(\xi, x_o))\ d\xi \right\}^{\frac{1}{n}} \tag{2-95}$$

$$t(x;x_o^*,x_o) = T + \frac{1}{n}(h(x_o^*,x_o))^{1-n} \left\{(L_o - x_o^*)\alpha(x_o^*)\right\}^{\frac{1-n}{n}} \int_{x_o^*}^{x} (L_o - \xi)^{\frac{n-1}{n}} \left[\frac{1}{\alpha(\xi)}\right]^{\frac{1}{n}} d\xi \tag{2-96}$$

Here x_o^* and x_o are bound by the relation:

$$T = \int_{x_o}^{x_o^*} \frac{(L_o - \eta)^{\frac{n-1}{n}}}{n(\alpha(\eta))^{\frac{1}{n}}} \left[\int_{x_o}^{\eta} (L_o - \xi)\ q\ (\xi, t(\xi, x_o))\ d\xi \right]^{\frac{1-n}{n}} d\eta \tag{2-97}$$

Thus in Eqs. (2-95) and (2-96) we may think of x_o^* as the parameter in which case we have to replace x_o which appears in these equations by its solution to Eq. (2-97) in terms of x_o^*. On the other hand we may think of x_o as the parameter in Eqs. (2-95) and (2-96); in that case we have to replace x_o^* in these equations by its solution to Eq. (2-97). Since, in Eq. (2-97) x_o^* is an increasing function of x_o, the correspondence between x_o^* and x_o is one to one. We now examine the seven special cases:

1. If q(x,t) is constant then we obtain:

$$h(x_o^*,\ x_o) = \left\{ \frac{q}{2} \frac{(L_o - x_o)^2 - (L_o - x_o^*)^2}{\alpha(x_o^*)(L_o - x_o^*)} \right\}^{\frac{1}{n}} \tag{2-98}$$

$$h(x;x_o^*,x_o) = \left\{ \frac{q}{2} \frac{(L_o - x_o)^2 - (L_o - x_o^*)^2}{(L_o - x)\alpha(x)} \right\}^{\frac{1}{n}} \tag{2-99}$$

$$t(x;x_o^*,x_o) = T + \frac{1}{n}\left[\frac{q}{2}\left\{(L_o - x_o)^2 - (L_o - x_o^*)^2\right\}\right]^{\frac{1-n}{n}} \int_{x_o^*}^{x} \left(\frac{1}{\alpha(\xi)}\right)^{\frac{1}{n}} (L_o - \xi)^{\frac{n-1}{n}}\, d\xi \qquad (2\text{-}100)$$

2. If $q(x,t)$ varies in space only, then we obtain:

$$h(x_o^*,x_o) = \left\{\frac{1}{\alpha(x_o^*)(L_o - x_o^*)} \int_{x_o}^{x_o^*} (L_o - \xi)\, q(\xi)\, d\xi\right\}^{\frac{1}{n}} \qquad (2\text{-}101)$$

$$h(x;x_o^*,x_o) = \left\{\frac{1}{(L_o - x)\alpha(x)} \int_{x_o}^{x_o^*} (L_o - \xi)\, q(\xi)\, d\xi\right\}^{\frac{1}{n}} \qquad (2\text{-}102)$$

$$t(x;x_o^*,x_o) = T + \frac{1}{n}\left\{\int_{x_o}^{x_o^*} (L_o - \xi)\, q(\xi)\, d\xi\right\}^{\frac{1-n}{n}} \int_{x_o}^{x_o^*} (L_o - \eta)^{\frac{n-1}{n}} \left(\frac{1}{\alpha(\eta)}\right)^{\frac{1}{n}} d\xi \qquad (2\text{-}103)$$

3. If $q(x,t)$ varies in time only, then we obtain:

$$h(x_o^*,\ x_o) = \left\{\frac{1}{\alpha(x_o^*)(L_o - x_o^*)} \int_{x_o}^{x_o^*} (L_o - \xi)\, q(t(\xi,x_o))\, d\xi\right\}^{\frac{1}{n}} \qquad (2\text{-}104)$$

$$h(x;x_o^*,x_o) = \left\{\frac{1}{(L_o - x)\alpha(x)} \int_{x_o}^{x_o^*} (L_o - \xi)\, q(t(\xi,x_o))\, d\xi\right\}^{\frac{1}{n}} \qquad (2\text{-}105)$$

$$t(x;x_o^*,\ x_o) = T + \frac{1}{n}\left\{\int_{x_o}^{x_o^*} (L_o - \xi)\ q(t(\xi,x_o))\ d\xi\right\}^{\frac{1}{n}}$$

$$\int_{x_o}^{x_o^*} (L_o - \eta)^{\frac{n-1}{n}} \left[\frac{1}{\alpha(\eta)}\right]^{\frac{1}{n}} d\eta \qquad (2\text{-}106)$$

4. If $\alpha(x)$ and $q(x,t)$ both are constant then we obtain:

$$h(x_o^*,\ x_o) = \left\{\frac{q}{2}\ \frac{(L_o - x_o)^2 - (L_o - x_o^*)^2}{\alpha(L_o - x_o^*)}\right\}^{\frac{1}{n}} \qquad (2\text{-}107)$$

$$h(x;x_o^*,x_o) = \left\{\frac{q}{2}\ \frac{(L_o - x_o)^2 - (L_o - x_o^*)^2}{\alpha(L_o - x)}\right\}^{\frac{1}{n}} \qquad (2\text{-}108)$$

$$t(x;x_o^*,x_o) = T + \left[\frac{q}{2}\left\{(L_o - x_o)^2 - (L_o - x_o^*)^2\right\}\right]^{\frac{1-n}{n}} \left(\frac{1}{\alpha}\right)^{\frac{1}{n}}$$

$$\left[\frac{(L_o - x_o^*)^{\frac{2n-1}{n}} - (L_o - x)^{\frac{2n-1}{n}}}{(2n - 1)}\right] \qquad (2\text{-}109)$$

5. If $\alpha(x)$ is constant but $q(x,t)$ varies in time and space then we obtain:

$$h(x_o^*,x_o) = \left\{\frac{1}{(L_o - x_o^*)\alpha}\int_{x_o}^{x_o^*} (L_o - \xi)\ q(\xi,t(\xi,x_o))\ d\xi\right\}^{\frac{1}{n}} \qquad (2\text{-}110)$$

$$h(x;x_o^*,x_o) = \left\{ \frac{1}{(L_o - x)\alpha} \int_{x_o}^{x_o^*} (L_o - \xi)\, q(\xi, t(\xi,x_o))\, d\xi \right\}^{\frac{1}{n}} \tag{2-111}$$

$$t(x;x_o^*,x_o) = T + \left\{ \int_{x_o}^{x_o^*} (L_o - \xi)\, q(\xi, t(\xi,x_o))\, d\xi \right\}^{\frac{1}{n}} \left(\frac{1}{\alpha}\right)^{\frac{1}{n}}$$

$$\left[\frac{(L_o - x_o^*)^{\frac{2n-1}{n}} - (L_o - x)^{\frac{2n-1}{n}}}{(2n-1)} \right] \tag{2-112}$$

6. If $\alpha(x)$ is constant but $q(x,t)$ varies in space only, then we get:

$$h(x_o^*,x_o) = \left\{ \frac{1}{(L_o - x_o^*)\alpha} \int_{x_o}^{x_o^*} (L_o - \xi)\, q(\xi)\, d\xi \right\}^{\frac{1}{n}} \tag{2-113}$$

$$h(x;x_o^*,x_o) = \left\{ \frac{1}{(L_o - x)\alpha} \int_{x_o}^{x_o^*} (L_o - \xi)\, q(\xi)\, d\xi \right\}^{\frac{1}{n}} \tag{2-114}$$

$$t(x;x_o^*,x_o) = T + \left\{ \int_{x_o}^{x_o^*} (L_o - \xi)\, q(\xi)\, d\xi \right\}^{\frac{1}{n}} \left(\frac{1}{\alpha}\right)^{\frac{1}{n}}$$

$$\left[\frac{(L_o - x_o^*)^{\frac{2n-1}{n}} - (L_o - x)^{\frac{2n-1}{n}}}{(2n-1)} \right] \tag{2-115}$$

7. If $\alpha(x)$ is constant but $q(x,t)$ varies in time only, then we obtain:

$$h(x_o^*,x_o) = \left\{ \frac{1}{(L_o - x_o^*)\alpha} \int_{x_o}^{x_o^*} (L_o - \xi)\, q\,(t(\xi,x_o))\, d\xi \right\}^{\frac{1}{n}} \tag{2-116}$$

$$h(x;x_o^*,x_o) = \left\{ \frac{1}{\alpha(L_o - x_o)} \int_{x_o}^{x_o^*} (L_o - \xi)\, q\,(t(\xi,x_o))\, d\xi \right\}^{\frac{1}{n}} \tag{2-117}$$

$$t(x;x_o^*,x_o) = T + \left\{ \int_{x_o}^{x_o^*} (L_o - \xi)\, q\,(t(\xi,x_o))\, d\xi \right\}^{\frac{1}{n}} \left(\frac{1}{\alpha}\right)^{\frac{1}{n}}$$

$$\left[\frac{(L_o - x_o^*)^{\frac{2n-1}{n}} - (L_o - x)^{\frac{2n-1}{n}}}{(2n-1)} \right] \tag{2-118}$$

We summarize the case B, $t^* > T$:

(1) In domain D_3 the solution is given by Eqs. (2-31) and (2-32). Here the parameter assumes values on the segment $o \leq x \leq L_o(1 - r)$, $t = o$.

(2) In domain D_2 the solution is given by Eqs. (2-10) and (2-11). Here the parameter t_o assumes values on the segment $x = o$, $o \leq t \leq T$.

(3) In domain D_{11} the solution is given by Eqs. (2-52) and (2-53), where x_o is replaced in these equations by x_o^*. The parameter x_o^* assumes values on the segment $o \leq x_o^* \leq x^*$, $t = T$.

(4) In domain D_{12} the solution is given by Eqs. (2-95) and (2-96) where x_o is replaced by x_o^* in these equations. The parameter x_o^* assumes values on the segment $o \leq x_o^* \leq (L_o(1 - r) - x^*)$. Here we may regard either x_o or x_o^* as the parameter.

As in case A we consider h as a function of t for fixed x when $q(x,t) = q$. In case B this behavior of $h(x,t)$ is the same as in case A for $o < x < x^*$ as shown in Fig 2-4. If $x^* \leq x \leq L_o(1 - r)$ then $h(x,t)$ is an increasing function of t if $(x,t) \in D_3$, and it is a decreasing function of t if $(x,t) \in D_{11}$; the arguments are the same as in case A. It remains to consider the behavior of $h(x,t)$ when x is fixed and $(x,t) \in D_{12}$; the maximum of $h(x,t)$, for x fixed, will occur in D_{12}, possibly on $t = T$ or on $t = t(x,x^*)$. We have:

$$h_t(x,t) = h_{x_o}(x;x_o^*(x_o),x_o)\ \frac{\partial x_o(x,t)}{\partial t}$$

$$= \frac{h_{x_o}(x;x_o^*(x_o),x_o)}{t_{x_o}(x;x_o^*(x_o),x_o)} \tag{2-119}$$

$$h_{x_o}(x;x_o^*(x_o),x_o) = h_{x_o}{}^*(x;x_o^*,x_o)\ \frac{dx_o^*}{dx_o} + h_{x_o}(x;x_o^*,x_o) \tag{2-120}$$

Using Eq. (2-98) we get from Eq. (2-120):

$$h_{x_o}(x;x_o^*(x_o),x_o) = \frac{2}{n}\left(\frac{q}{2}\right)^{\frac{1}{n}} \frac{\left[(x_o^* - x)(2L_o - x_o - x_o^*)\right]^{\frac{1}{n}-1}}{\left[\alpha(x)(L_o - x)\right]^{\frac{1}{n}}}$$

$$\left[(L_o - x_o^*)\ \frac{dx_o^*}{dx_o} - (L_o - x_o)\right]$$

Thus the sign of $h_{x_o}(x;x_o^*(x_o),x_o)$ is determined by the sign of

$$\left[(L_o - x_o^*)\frac{dx_o^*}{dx_o} - (L_o - x_o)\right] \tag{2-121}$$

We consider now the special case when $\alpha(x) = \alpha$, constant. Then Eq. (2-97) becomes:

$$T = \frac{1}{n}\left(\frac{2}{q}\right)^{\frac{n-1}{n}}\left(\frac{1}{\alpha}\right)^{\frac{1}{n}}\int_{x_o}^{x_o^*}\left[\frac{L_o - \eta}{(\eta - x_o)(2L_o - x_o - \eta)}\right]^{\frac{n-1}{n}} d\eta \tag{2-122}$$

We introduce the change of variable $(L_o - \eta) = (L_o - x_o)\xi$. Then Eq. (2-122) becomes:

$$\frac{T\alpha^{\frac{1}{n}}}{\left(\frac{2}{q}\right)^{\frac{n-1}{n}}}(L_o - x_o)^{-\frac{1}{n}} = \int_{\left(\frac{L_o - x_o^*}{L_o - x_o}\right)}^{1}\left(\frac{\xi}{1 - \xi^2}\right)^{\frac{n-1}{n}} d\xi \tag{2-123}$$

Differentiating on both sides of Eq. (2-123) with respect to x_o we get:

$$\frac{T\alpha^{\frac{1}{n}}}{n\left(\frac{2}{q}\right)^{\frac{n-1}{n}}}(L_o - x_o)^{-\frac{1}{n}-1} = -\left[\frac{(L_o - x_o)(L_o - x_o^*)}{(L_o - x_o)^2(L_o - x_o^*)^2}\right]^{\frac{n-1}{n}}$$

$$\left\{\frac{-1}{(L_o - x_o)}\frac{dx_o^*}{dx_o} + \frac{L_o - x_o^*}{(L_o - x_o)^2}\right\} \tag{2-124}$$

Solving Eq. (2-124) for $\frac{dx_o^*}{dx_o}$ we obtain:

$$\frac{dx_o^*}{dx_o} = \frac{T(\alpha)^{\frac{1}{n}}}{n\left(\frac{2}{q}\right)^{\frac{n-1}{n}}} \frac{\left[(L_o - x_o)^2 - (L_o - x_o^*)^2\right]^{\frac{n-1}{n}} + (L_o - x_o^*)^{2-\frac{1}{n}}}{(L_o - x_o)(L_o - x_o^*)^{\frac{n-1}{n}}} \tag{2-125}$$

Then Eq. (2-121) becomes:

$$\frac{\left\{(L_o - x_o)^2 - (L_o - x_o^*)^2\right\}^{\frac{n-1}{n}}}{(L_o - x_o)} \left[\frac{T\alpha^{\frac{1}{n}}}{n\left(\frac{2}{q}\right)^{\frac{n-1}{n}}} (L_o - x_o^*)^{\frac{1}{n}} - \left\{(L_o - x_o)^2 - (L_o - x_o^*)^2\right\}^{\frac{1}{n}}\right] \tag{2-126}$$

Invoking the identity

$$a^N - b^N = (a - b) \sum_{k=1}^{N} a^{N-k} b^{k-1}$$

the bracked term in Eq. (2-126) is nonpositive if and only if

$$\sigma(L_o - x_o^*) - \left\{(L_o - x_o)^2 - (L_o - x_o^*)^2\right\} \tag{2-127}$$

is nonpositive, where $\sigma = \alpha\left\{\frac{T}{n}\left(\frac{q}{2}\right)^{\frac{n-1}{n}}\right\}^n$. We can write Eq. (2-127) as:

$$(L_o - x_o)^2 \left[\left(\frac{L_o - x_o^*}{L_o - x_o} \right)^2 + \frac{\sigma}{(L_o - x_o)} \frac{L - x_o^*}{L - x_o} - 1 \right]$$

$$= (L_o - x_o)^2 \left[\mu^2 + \mu \left(\frac{1}{n} \int_{\mu}^{1} \left(\frac{\xi}{1 - \xi^2} \right)^{\frac{n-1}{n}} d\xi \right)^n - 1 \right] \qquad (2\text{-}128)$$

where $\mu = (L_o - x_o^*)/(L_o - x_o)$. We have $o < \mu < 1$. Let $F(\mu)$ be the bracket on the right side of Eq. (2-128). Since

$$\frac{\xi}{1 + \xi} \leq \frac{1}{2} \quad , \quad o \leq \xi \leq 1$$

we have:

$$\left(\frac{\xi}{1 - \xi^2} \right)^{\frac{n-1}{n}} \leq \left(\frac{1}{2} \right)^{\frac{n-1}{n}} \frac{1}{(1 - \xi)^{\frac{n-1}{n}}} \quad , \quad o \leq \xi \leq 1$$

and

$$\left(\frac{1}{n} \int_{\mu}^{1} \left(\frac{\xi}{1 - \xi^2} \right)^{\frac{n-1}{n}} d\xi \right)^n < \left(\frac{1}{n} \left(\frac{1}{2} \right)^{\frac{n-1}{n}} \int_{\mu}^{1} (1 - \xi)^{-1 - \frac{1}{n}} d\xi \right)^n$$

$$= \frac{1}{2^{n-1}} (1 - \mu)$$

Thus

$$F(\mu) < \mu^2 + \frac{1}{2^{n-1}} \mu(1 - \mu) - 1 = \left(1 - \frac{1}{2^{n-1}} \right) \mu^2 + \frac{1}{2^{n-1}} \mu - 1 < o$$

if $n > o$ and $o < \mu < 1$. We conclude then, that when $\alpha(x) = \alpha$, $h_{x_o}(x;x_o^*(x_o),x_o) < o$. Since $t_{x_o}(x;x_o^*(x_o),x_o) < o$ we see that, when $\alpha(x) = \alpha$, $h(x,t)$ is an increasing function of t for fixed x when $(x,t) \in D_{12}$. Thus the maximum of $h(x,t)$, as a function of t for fixed x, $x^* < x \leq L_o(1 - r)$ is reached on the curve $t = t(x,x^*)$ (See appendix D for additional details). We summarize the behavior, in case B, of $h(x,t)$ for fixed x (see Fig. 2-5):

(1) If $o < x < x^*$, $h(x,t)$ increases if $(x,t) \in D_3$, is independent of t if $(x,t) \in D_2$, and decreases if $(x,t) \in D_{11}$. $h(x,t) \to o$ as $t \to \infty$.

(2) If $x^* \leq x \leq L_o(1 - r)$, $h(x,t)$ increases if $(x,t) \in D_3$, achieves its maximum in the interval $T \leq t \leq t(x,x^*)$ and decreases if $(x,t) \in D_{11}$. $h(x,t) \to o$ as $t \to \infty$. If $\alpha(x) =$ constant, $h(x,t)$ increases in the interval $T \leq t \leq t(x,x^*)$ so that the maximum is reached on $t = t(x,x^*)$.

In case A we have from Eqs. (2-12) and (2-13):

$$h_{max}(x) = \left(\frac{q}{2}\right)^{\frac{1}{n}} \left[\frac{2L_o x - x^2}{\alpha(x)(L_o - x)}\right]^{\frac{1}{n}} \tag{2-129}$$

$$t_{max}(x) = \left\{t;t(x,o) \leq x \leq T\right\} \tag{2-130}$$

In case B Eqs. (2-128) and (2-130) also hold if $o < x \leq x^*$; where x^* is the root of $T = t(x,o)$. If $x^* < x \leq L_o(1 - r)$ and $\alpha(x) = \alpha$ then from Eq. (2-55) we have:

$$h_{max}(x) = \left(\frac{q}{2}\right)^{\frac{1}{n}} \left[\frac{2L_o x - x}{\alpha(L_o - x)}\right]^{\frac{1}{n}} \tag{2-131}$$

and from Eq. (2-56):

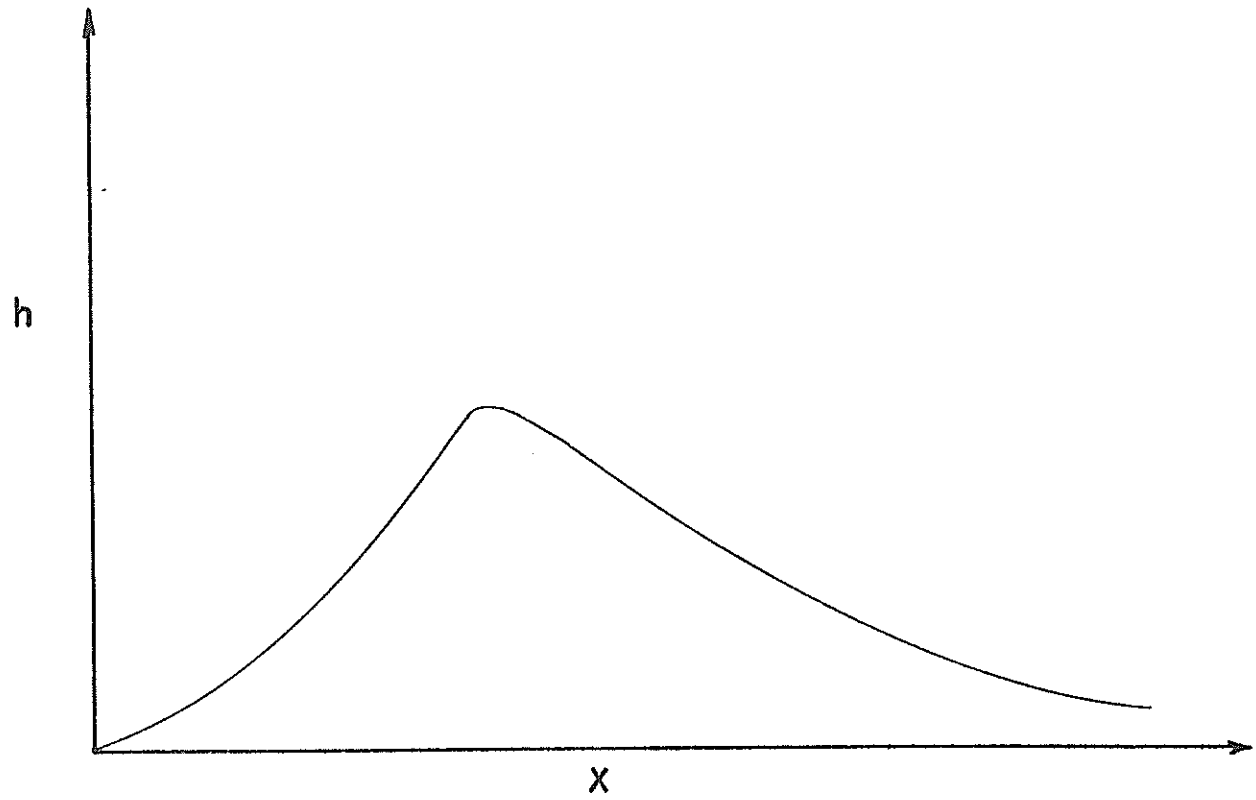

Fig. 2-5. Depth of flow at x for partial equilibrium hydrograph, $T < t^*$, $q(x,t) = q$.

$$t_{max}(x) = T + \left(\frac{q}{2}\right)^{\frac{n-1}{n}} \frac{1}{2n-1}\left(\frac{1}{\alpha}\right)^{\frac{1}{n}}\left(\frac{1}{2L_o x^* - x^{*2}}\right)^{\frac{n-1}{n}}\left[(L - x^*)^{\frac{2n-1}{n}} - (L - x)^{\frac{2n-1}{n}}\right] \quad (2\text{-}132)$$

2.2.3 Definition of t*

We define t* as the time of intersection of $t = t(x,o)$ with $x = L_o(1 - r)$ in case A, and as the time of intersection of $t = t(x,x^*)$ with $x = L_o(1 - r)$ in case B. Thus t* is a function of T. Define $T_o = F(L_o(1 - r))$. Then $t^*(T) = T_o$ when $T \geq T_o$ and, when $T < T_o$, $t^*(T)$ is defined, through x^*, by

$$T = F(x^*) \quad (2\text{-}133)$$

$$t^* = F(x^*) + \frac{1}{n}\left(\frac{2}{q}\right)^{\frac{n-1}{n}}\left(\frac{1}{2L_o x^* - x^{*2}}\right)^{\frac{n-1}{n}} \int_{x^*}^{L_o(1-r)} \frac{(L_o - \eta)^{\frac{n-1}{n}}}{(\alpha(\eta))^{\frac{1}{n}}}\, d\eta \quad (2\text{-}134)$$

Since

$$\frac{dt^*}{dT} = \frac{dt^*}{dx^*}\frac{dx^*}{dT} = \frac{dt^*}{dx^*} \Big/ F'(x^*)$$

and since $F'(x^*) > o$, the sign of dt^*/dT is the same as the sign of dt^*/dx^*. Using Eq. (2-134) it is easily seen that $dt^*/dx^* < o$. Thus $t^*(T)$ is a decreasing function of T in $o < T < T_o$ as shown in Fig. 2-6. As $T \to o$, $x^* \to o$, and we see from Eq. (2-134) that $t^* \to \infty$.

We will now try to establish the explicit functional relationship between t* and T. From Fig. 2-3 we see that $t^* = T + \Delta t$ where Δt is the difference between t* and T, or the time of propagation of $t(x,o)$ beyond $t = T$ until the downstream boundary. Hence our interest is in the determination of Δt. Thus we have from Eq. (2-53):

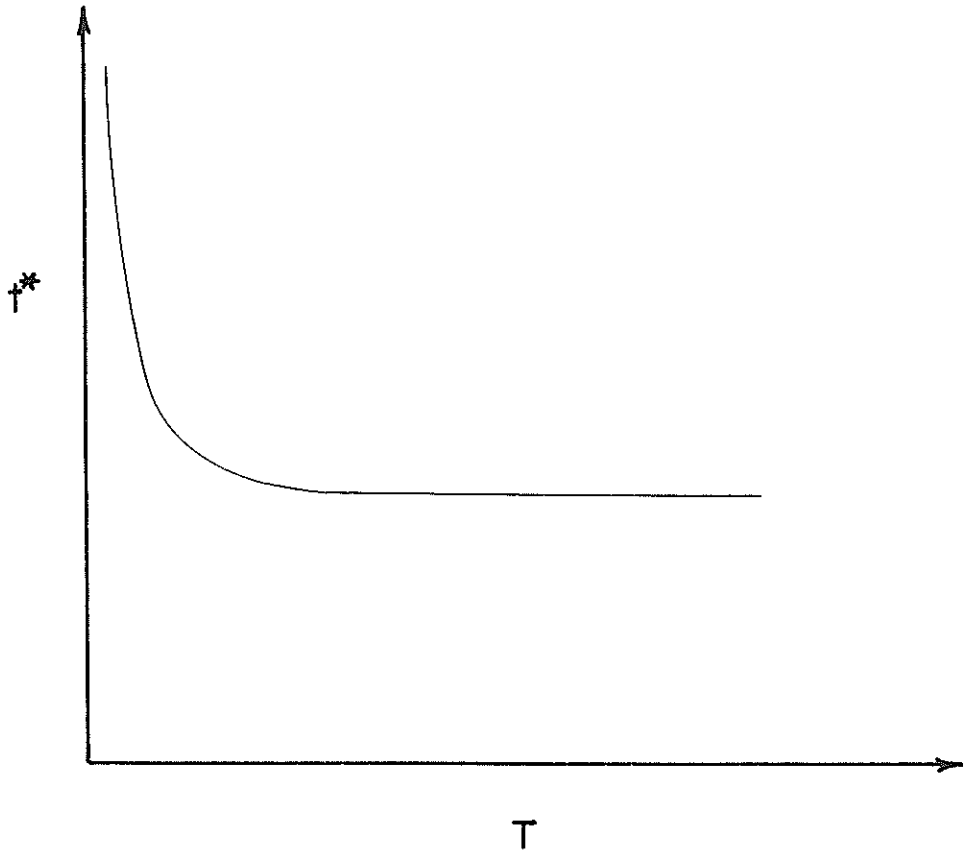

Fig. 2-6. t* as a function of T, rainfall duration.

$$t^* = T + \frac{1}{n}\left\{\int_o^{x^*} (L_o - \xi)\, q(\xi, t(\xi))\, d\xi\right\}^{\frac{1-n}{n}} \int_{x^*}^{L_o(1-r)} \left(\frac{1}{\alpha(\eta)}\right)^{\frac{1}{n}} (L_o - \eta)^{\frac{n-1}{n}}\, d\eta \qquad (2\text{-}135)$$

We shall give the quantity t^* for all seven cases:

1. If $q(x,t)$ is constant then we get:

$$t^* = T + q^{\frac{1-n}{n}} (L_o - x^*)^{\frac{1}{n}} \int_{x^*}^{L_o(1-r)} \left(\frac{1}{\alpha(\eta)}\right)^{\frac{1}{n}} (L_o - \eta)^{\frac{n-1}{n}}\, d\eta \qquad (2\text{-}136)$$

2. If $q(x,t)$ varies in space only, then we obtain:

$$t^* = T + \frac{1}{n}\left\{\int_o^{x^*} (L_o - \xi)\, q(\xi)\, d\xi\right\}^{\frac{1-n}{n}} \int_{x^*}^{L_o(1-r)} \left(\frac{1}{\alpha(\eta)}\right)^{\frac{1}{n}} (L_o - \eta)^{\frac{n-1}{n}}\, d\eta \qquad (2\text{-}137)$$

3. If $q(x,t)$ varies in time only, then we obtain:

$$t^* = T + \frac{1}{n}\left\{\int_o^{x^*} (L_o - \xi)\, q\,(t(\xi))\, d\xi\right\}^{\frac{1-n}{n}} \int_{x^*}^{L_o(1-r)} \left(\frac{1}{\alpha(\eta)}\right)^{\frac{1}{n}} (L_o - \eta)^{\frac{n-1}{n}}\, d\eta \qquad (2\text{-}138)$$

4. If both $\alpha(x)$ and $q(x,t)$ are constant then we obtain:

$$t^* = T + nq^{\frac{1-n}{n}} (L_o - x^*)^{\frac{1}{n}} \left(\frac{1}{\alpha}\right)^{\frac{1}{n}} \frac{\left\{(L_o - x^*)^{\frac{2n-1}{n}} - (L_o r)^{\frac{2n-1}{n}}\right\}}{(2n-1)} \qquad (2\text{-}139)$$

5. If $\alpha(x)$ is constant but $q(x,t)$ varies in both time and space:

$$t^* = T + \left(\frac{1}{\alpha}\right)^{\frac{1}{n}} \frac{\left\{(L_o - x^*)^{\frac{2n-1}{n}} - (L_o r)^{\frac{2n-1}{n}}\right\}}{(2n-1)} \left\{\int_o^{x^*} (L_o - \xi)\, q\,(\xi, t(\xi))\, d\xi\right\}^{\frac{1-n}{n}} \qquad (2\text{-}140)$$

6. If $\alpha(x)$ is constant but $q(x,t)$ varies in space only, then we obtain:

$$t^* = T + \left(\frac{1}{\alpha}\right)^{\frac{1}{n}} \frac{\left\{(L_o - x^*)^{\frac{2n-1}{n}} - (L_o r)^{\frac{2n-1}{n}}\right\}}{(2n-1)} \left\{\int_o^{x^*} (L_o - \xi)\, q(\xi)\, d\xi\right\}^{\frac{1-n}{n}} \qquad (2\text{-}141)$$

7. If $\alpha(x)$ is constant but $q(x,t)$ varies in time only, then we obtain:

$$t^* = T + \left(\frac{1}{\alpha}\right)^{\frac{1}{n}} \frac{\left\{(L_o - x^*)^{\frac{2n-1}{n}} - (L_o r)^{\frac{2n-1}{n}}\right\}}{(2n-1)} \left\{\int_o^{x^*} (L_o \xi)\, q(\xi)\, d\xi\right\}^{\frac{1-n}{n}} \qquad (2\text{-}142)$$

We must, however, determine x^* before we can hope to determine the partial equilibrium hydrograph. This quantity can be determined by solving for the limiting characteristic curve $t(x,o)$, passing through the origin, at the point in (x,t) plane where it intersects the segment $t = T$. That is,

$$T = \int_o^{x^*} \frac{1}{n\alpha(\eta)} \left\{\frac{1}{\alpha(\eta)(L_o - \eta)} \int_o^{\eta} (L_o - \xi)\, q\,(\xi, t(\xi))\, d\xi\right\}^{\frac{1-n}{n}} d\eta \qquad (2\text{-}143)$$

Now we will consider all seven special cases.

1. If $q(x,t)$ is constant then we get:

$$T = \frac{q^{\frac{1-n}{n}}}{n} \int_o^{x^*} \left\{\frac{1}{\alpha(\eta)}\right\}^{\frac{1}{n}} \left\{\frac{L_o^2 - (L_o - \eta)^2}{2(L_o - \eta)}\right\}^{\frac{1-n}{n}} d\eta \qquad (2\text{-}144)$$

2. If q(x,t) varies in space only then we get:

$$T = \frac{1}{n}\int_{o}^{x^*} \left\{\frac{1}{\alpha(\eta)}\right\}^{\frac{1}{n}} \left\{L_o - \eta\right\}^{\frac{n-1}{n}} \left\{\int_{o}^{\eta} (L_o - \xi)\, q(\xi)\, d\xi\right\}^{\frac{1-n}{n}} d\eta \qquad (2\text{-}145)$$

3. If q(x,t) varies in time only, then we obtain:

$$T = \frac{1}{n}\int_{o}^{L_o(1-r)} \left\{\frac{1}{\alpha(\eta)}\right\}^{\frac{1}{n}} \left\{L_o - \eta\right\}^{\frac{n-1}{n}} \left\{\int_{o}^{\eta} (L_o - \xi)\, q\,(t(\xi))\, d\xi\right\}^{\frac{1-n}{n}} d\eta \qquad (2\text{-}146)$$

4. If $\alpha(x)$ and $q(x,t)$ both are constant then we get:

$$T = \frac{1}{n}\left(\frac{1}{q}\right)^{\frac{n-1}{n}} \left(\frac{L_o}{2\alpha}\right)^{\frac{1}{n}} \left\{ \frac{\Gamma\left(1 - \frac{1}{2n}\right)\Gamma\left(\frac{1}{n}\right)}{\Gamma\left(1 + \frac{1}{2n}\right)} - \frac{\left(\frac{L_o - x^*}{L_o}\right)^{2 - \frac{1}{n}} \left\{1 - \left(\frac{L_o - x^*}{L_o}\right)^2\right\}^{\frac{1}{n}}}{\left(1 - \frac{1}{2n}\right)} \right.$$

$$\left. \left[1 + \sum_{j=o}^{\infty} \frac{\beta\left(2 - \frac{1}{2n}\,;\, j+1\right)}{\beta\left(1 + \frac{1}{2n}\,;\, j+1\right)} \left(\frac{L_o - x^*}{L_o}\right)^{2(j+1)}\right] \right\} \qquad (2\text{-}147)$$

5. If $\alpha(x)$ is constant but $q(x,t)$ varies in both space and time, then we have:

$$T = \frac{1}{n}\left(\frac{1}{\alpha}\right)^{\frac{1}{n}} \int_{o}^{x^*} (L_o - \eta)^{\frac{n-1}{n}} \left\{\int_{o}^{\eta} q(\xi, t(\xi))\, d\xi\right\}^{\frac{1-n}{n}} d\eta \qquad (2\text{-}148)$$

6. If $\alpha(x)$ is constant but $q(x,t)$ varies in space only, then we get:

$$T = \frac{1}{n}\left(\frac{1}{\alpha}\right)^{\frac{1}{n}} \int_0^{x^*} (L_o - \eta)^{\frac{n-1}{n}} \left\{ \int_0^{\eta} q(\xi)(L_o - \xi)\, d\xi \right\}^{\frac{1-n}{n}} d\eta \qquad (2\text{-}149)$$

7. If $\alpha(x)$ is constant but $q(x,t)$ varies in time only, then we get:

$$T = \frac{1}{n}\left(\frac{1}{\alpha}\right)^{\frac{1}{n}} \int_0^{x^*} (L_o - \eta)^{\frac{n-1}{n}} \left\{ \int_0^{\eta} q(t(\xi))\ (L_o - \xi)\, d\xi \right\}^{\frac{1-n}{n}} d\eta \qquad (2\text{-}150)$$

2.2.4 Criterion to Distinguish Equilibrium and Partial Equilibrium Situations

One question arises: how can we distinguish cases A and B beforehand? It turns out that there is a simple criterion, when $q(x,t) = q$, which distinguishes cases A and B. From Eq. (2-13) we obtain, by setting $t_o = o$ and the left side equal to T,

$$T = \frac{1}{n}\left(\frac{2}{q}\right)^{\frac{n-1}{n}} \int_0^{x} \left(\frac{1}{\alpha(\eta)}\right)^{\frac{1}{n}} \left(\frac{L_o - \eta}{2L_o\eta - \eta^2}\right)^{\frac{n-1}{n}} d\eta \qquad (2\text{-}151)$$

Equation (2-151) has a root x^* between o and $L_o(1 - r)$ in case B and does not have a root in case A. Since the right side, F(x), of Eq. (2-151) is an increasing function of x, it is sufficient to determine the value of F at $x = L_o(1 - r)$:

$F(L_o(1 - r)) \leq T$, case A

$F(L_o(1 - r)) > T$, case B

CHAPTER 3

CONVERGING FLOW ON INFILTRATING WATERSHEDS

3.1 GENERAL REMARKS

The overland flow and infiltration have been extensively studied as separate components of hydrologic cycle (Woolhiser and Ligget, 1967; Woolhiser, 1969; Kibler and Woolhiser, 1970; Singh, 1974; Lane, 1975; Philip, 1957; Hanks and Bowers, 1962; Whisler and Klute, 1965; Rubin, 1966). A combined study of these two phases is required for modeling overland flow. Barring a few exceptions, notably the work by Smith (1970) and Smith and Woolhiser (1971), the conventional approach (Wooding, 1965; Eagleson, 1972; Singh, 1975f) to combine these phases has been through the familiar notion of so-called rainfall-excess. In this approach infiltration is independently determined and subtracted off from rainfall; the residual is termed as rainfall-excess, which forms input to the overland flow model. It seems that this concept of rainfall-excess is more of an artifice than a reality. The processes of infiltration and runoff occur almost simultaneously in nature during and after the occurrence of rainfall and, therefore, must be studied together. In this chapter we develop a combined treatment of infiltration and overland flow on a converging surface. The combined treatment will be useful in studying the effect of infiltration on nonlinear watershed runoff dynamics. It goes without saying that unlike the conventional approach, the present approach does not require an independent, apriori determination of infiltration; rather by specifying an infiltration function, infiltration and overland flow are simultaneously determined. Interestingly enough, this evolves into a free boundary problem.

3.2 MATHEMATICAL SOLUTIONS FOR CONVERGING FLOW ON INFILTRATING SURFACES

In the previous chapter, infiltration of water through the ground surface was either disregarded or considered through rainfall-excess. In this chapter we treat infiltration and overland flow simultaneously. Let $f(x,t)$ be the rate of infiltration; f is dependent on the depth of flow, h, in the following sense:

$f(x,t) > o$ if $h(x,t) > o$

$f(x,t) = o$ if $h(x,t) = o$

We will assume further that

$q(x,t) > f(x,t)$; $o \leq t \leq T$, $o \leq x \leq L_o(1-r)$

All the symbols retain their same meaning. Then the continuity and momentum equations are:

$$\frac{\partial h}{\partial t} + \frac{\partial (uh)}{\partial x} = q(x,t) - f(x,t) + \frac{uh}{(L_o - x)} \tag{3-1}$$

$$Q = uh = \alpha(x)\, h^n \tag{3-2}$$

As before $n > 1$, and $q(x,t) = o$ when $t > T$. The initial and boundary conditions are:

$$\begin{aligned} &h(x,o) = o \ , \quad o \leq x \leq L_o(1-r) \\ &h(o,t) = o \ , \quad o \leq t \leq T \end{aligned} \tag{3-3}$$

It is plausible on physical grounds that there will be a curve $t = t^o(x)$ in $\{t \geq T \ ; \ o \leq x \leq L_o(1-r)\}$, starting at $x = o$, $t = T$, and such that $h(x,t^o(x)) = o$. This curve gives the time history of the water edge as it progresses from $x = o$ to $x = L_o(1-r)$. Equations (3-1) and (3-2) are satisfied in $S = \{o < t < t^o(x) \ , \ o < x < L_o(1-r)\}$. Thus $t = t^o(x)$ is a free boundary, and Eqs. (3-1) to (3-3) and $h(x,t^o(x)) = o$ form a free boundary problem. In the domain above the curve $t = t^o(x)$, $h(x,t) = o$. The determination of the free boundary $t = t^o(x)$ is, as we will see, relatively simple when q and f are

constant (see Fig. 3-1); in this study we will discuss only that case in detail.

Eliminating u between Eqs. (3-1) and (3-2) we get:

$$\frac{\partial h}{\partial t} + n\,\alpha(x)\,h^{n-1}\,\frac{\partial h}{\partial x} = q(x,t) - f(x,t) + \frac{\alpha(x)\,h^{n}}{(L_o - x)} - \alpha'(x)\,h^{n} \qquad (3\text{-}4)$$

Then the characteristic equations are:

$$\frac{dt}{ds} = 1$$

$$\frac{dx}{ds} = n\,\alpha(x)\,h^{n-1}$$

$$\frac{dh}{ds} = q(x,t) - f(x,t) + \frac{\alpha(x)\,h^{n}}{(L_o - x)} - \alpha'(x)\,h^{n}$$

The solution of Eqs. (3-4) and (3-3) is the surface $h(x,t)$ formed by all the characteristic curves through the segment $t = o$, $o \leq x \leq L_o(1-r)$ and the segment $x = o$, $o \leq t \leq T$. The free boundary $t = t^{o}(x)$ is the locus $h(x,t) = o$ in the (x,t) plane. If we take x as a parameter then the characteristic curves are given by:

$$\frac{dt}{dx} = \frac{1}{n\,\alpha(x)\,h^{n-1}} \qquad (3\text{-}5)$$

$$\frac{dh}{dx} = \frac{q(x,t) - f(x,t)}{n\,\alpha(x)\,h^{n-1}} + \frac{h}{n(L_o - x)} - \frac{\alpha'(x)\,h}{n\,\alpha(x)} \qquad (3\text{-}6)$$

and the initial conditions are:

$$t(o) = t_o \quad , \quad h(o) = o \quad , \quad o \leq t_o \leq T \qquad (3\text{-}7)$$

or

$$t(x_o) = o \quad , \quad h(x_o) = o \quad , \quad o \leq x_o \leq L_o(1-r) \qquad (3\text{-}8)$$

We assume that the curves $t = t(x,t_o)$, which are the solutions of Eqs. (3-5) - (3-7), do not intersect for distinct values of t_o .

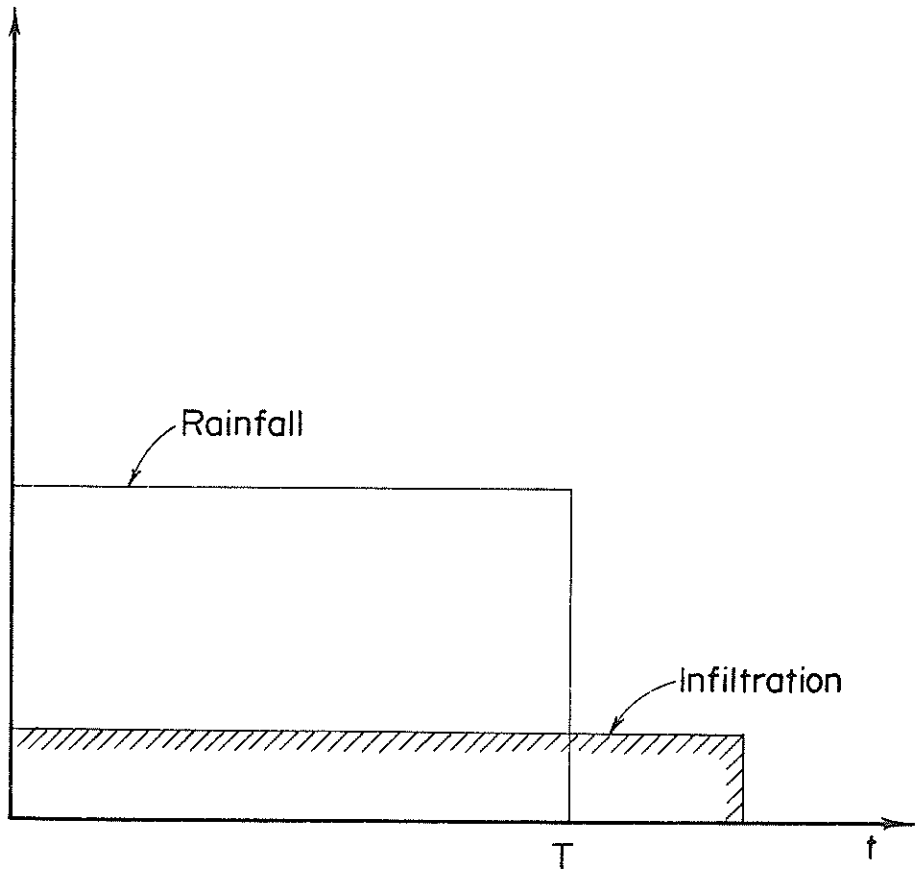

Fig. 3-1. Rainfall and infiltration, constant in time and space.

Similarly we assume that the curves $t = t(x,x_o)$ which are the solutions of Eqs. (3-5), (3-6) and (3-8), do not intersect for distinct values of x_o. This is true when q and f are constant and $(L_o - x)/\alpha(x)$ is a decreasing function of x; it is known from the previous chapter when $t \leq T$, i.e., in domains D_2 and D_3 (Fig. 3-2) and when $t > T$, it is proved in appendix E.

We distinguish three cases A, B_1 and B_2 which depend on the relative disposition of the three curves $t = t^o(x)$, $t = T$, and $t = t(x,o)$ ($t = t(x,x^*)$ is the prolongation of $t = t(x,o)$ to the right of $x = x^*$) as shown in Figs. 3-2 - 3-4.

Case A. $t^o(x) > T > t(x,o)$, $o < x \leq L_o(1-r)$

Case B_1. $t^o(x) > T$ and $t^o(x) > t(x,o)$, but $t = T$ and $t = t(x,o)$ intersect at $x = x^*$, i.e., $T = t(x^*,o)$ and $o < x^* < L_o(1-r)$.

Case B_2. $t^o(x) > T$ but $t = T$ and $t = t(x,o)$ intersect at $x = x^*$ and $t = t^o(x)$ and $t = t(x,x^*)$ intersect at $x = \bar{x}$, i.e., $t^o(\bar{x}) = t(\bar{x},x^*)$ and $o < \bar{x} < L_o(1-r)$.

Since $t^o(x)$ and $t(x,o)$ are not known until we have solved the problem, it appears that we cannot distinguish these cases beforehand. But in the special case which we consider in this paper, $q(x,t)$ and $f(x,t)$ both constant, we can distinguish the three cases beforehand. The domains D_1, D_2 and D_3 in case A, and the domains D_{11}, D_{12}, D_2 and D_3 in cases B_1 and B_2 are indicated in Figs. 3-2 - 3-4 respectively.

3.2.1 Case A: Equilibrium Situation

In case A the solutions in domains D_2 and D_3, when q and f are constant, are obtained from the discussion in chapter 2. Let us define:

$$q^* = q - f$$

$$\beta^* = \left(\frac{q^*}{2}\right)^{\frac{1}{n}}$$

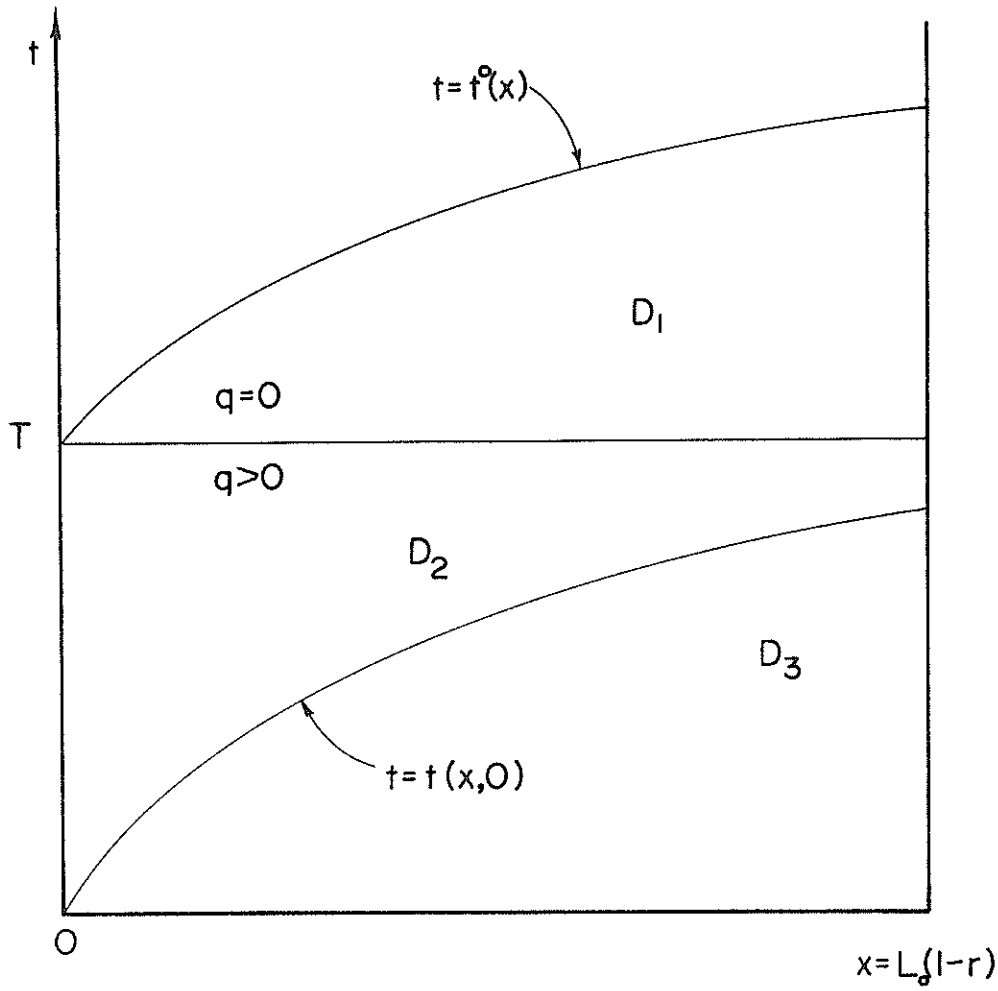

Fig. 3-2. Solution domain for equilibrium case A.

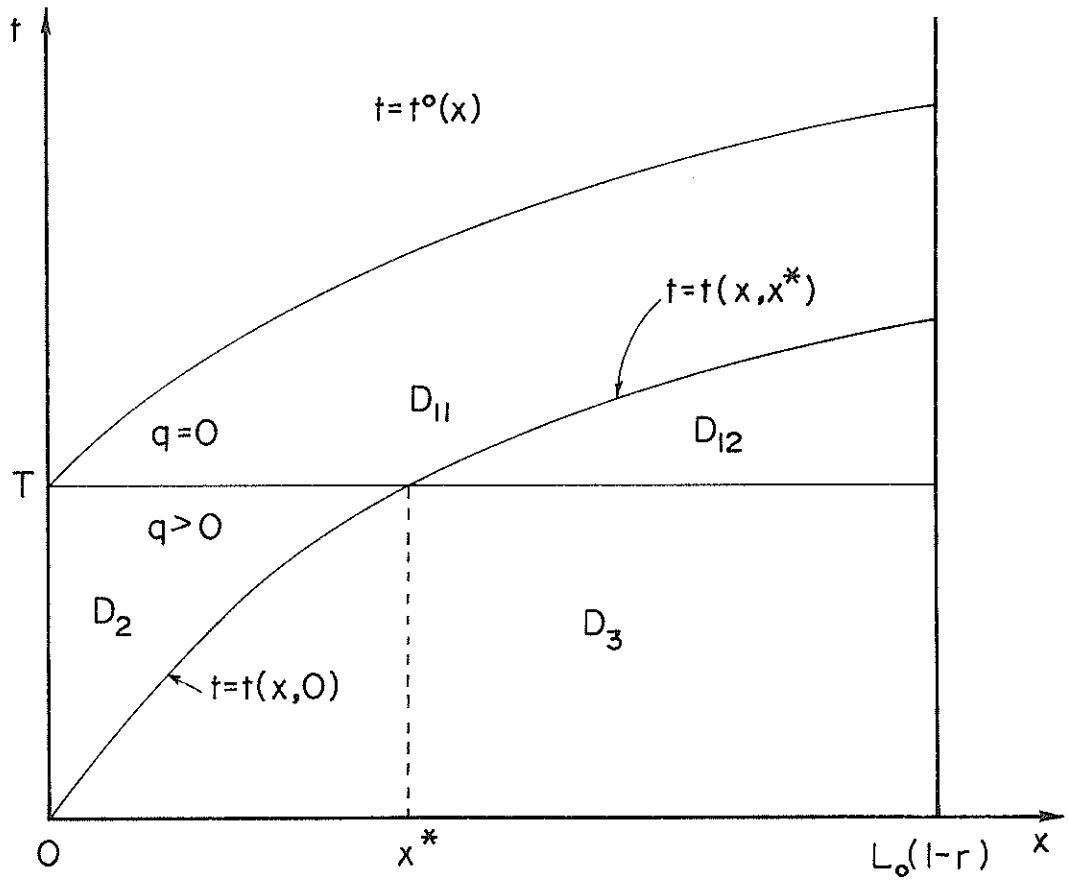

Fig. 3-3. Solution domain for partial equilibrium case B_1.

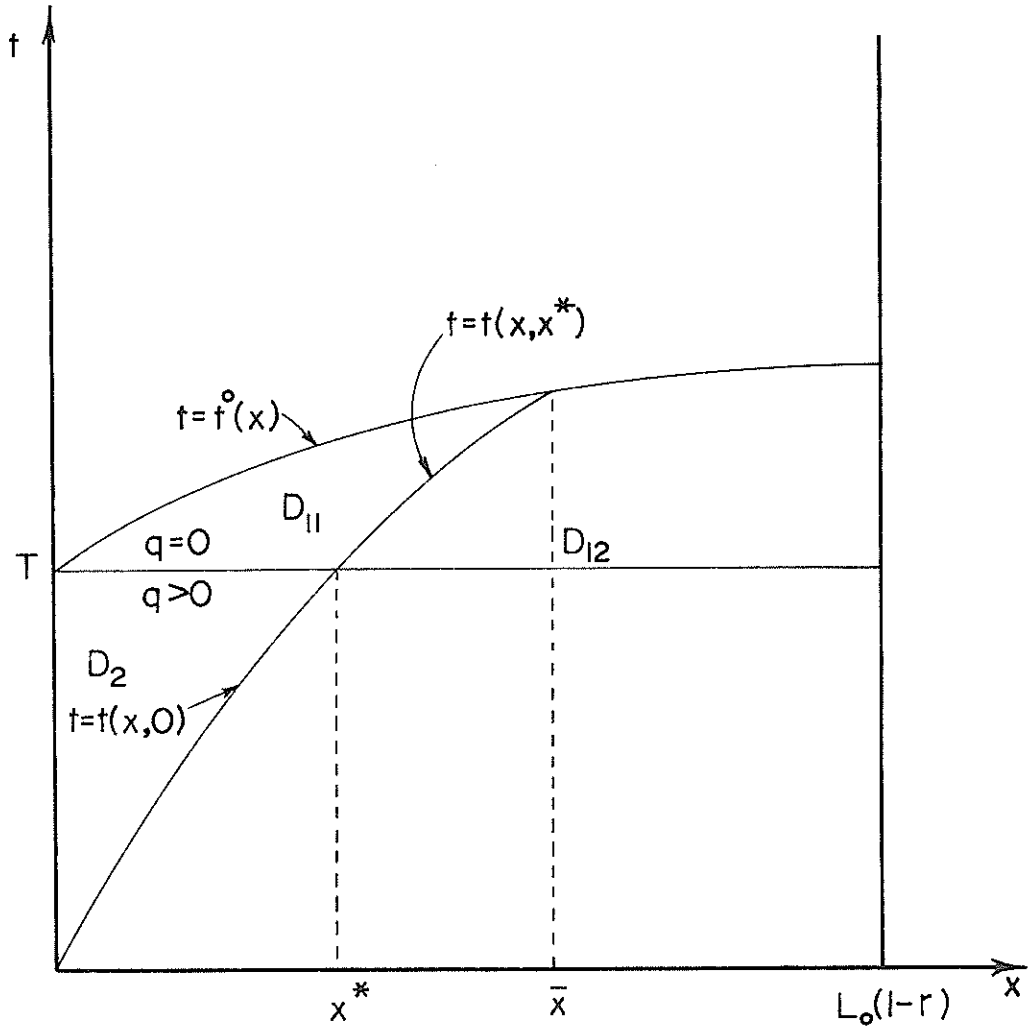

Fig. 3-4. Solution domain for partial equilibrium case B_2.

$$\gamma^* = \frac{1}{n}\left(\frac{2}{q^*}\right)^{\frac{n-1}{n}}$$

Then in domain D_2 the solution is given by Eqs. (2-12) and (2-13) with q replaced by $(q - f)$:

$$h(x,t_o) = \beta^* \left[\frac{L_o^2 - (L_o - x)^2}{\alpha(x)\ (L_o - x)}\right]^{\frac{1}{n}} \tag{3-9}$$

$$t(x,t_o) = t_o + \gamma^* \int_o^x \left(\frac{1}{\alpha(\eta)}\right)^{\frac{1}{n}} \left[\frac{L_o - \eta}{L_o^2 - (L_o - \eta)^2}\right]^{\frac{n-1}{n}} d\eta \tag{3-10}$$

If $\alpha(x) = \alpha$, a constant, then we have:

$$h(x,t_o) = \beta^* \left(\frac{1}{\alpha}\right)^{\frac{1}{n}} \left\{\frac{L_o^2 - (L_o - x)^2}{(L_o - x)}\right\}^{\frac{1}{n}} \tag{3-11}$$

$$t(x,t_o) = t_o + \gamma^* \left(\frac{1}{\alpha}\right)^{\frac{1}{n}} \int_o^x \left[\frac{L_o - \eta}{L_o^2 - (L_o - \eta)^2}\right]^{\frac{n-1}{n}} d\eta \tag{3-12}$$

The bracketed term in the intergrand can be expressed by an incomplete Beta function. Substituting $\xi = ((L_o - \eta)/L_o)^2$ in Eq. (3-12) we obtain:

$$t(x,t_o) = t_o + \frac{\gamma^*}{2}\left(\frac{1}{\alpha}\right)^{\frac{1}{n}} \left(L_o\right)^{\frac{1}{n}} \int_{\left(\frac{L_o - x}{L_o}\right)^2}^{1} \xi^{-\frac{1}{2n}} \left(1-\xi\right)^{\frac{1}{n}-1} d\xi$$

$$= t_o + \frac{\gamma^*}{2}\left(\frac{L_o}{\alpha}\right)^{\frac{1}{n}} \int_{\left(\frac{L_o - x}{L_o}\right)^2}^{1} \xi^{(1-\frac{1}{2n})-1} (1-\xi)^{\frac{1}{n}-1} d\xi$$

$$= t_o + \frac{\gamma^*}{2}\left(\frac{L_o}{\alpha}\right)^{\frac{1}{n}} \left\{ \int_o^1 \xi^{(1-\frac{1}{2n})-1} (1-\xi)^{\frac{1}{n}-1} d\xi - \int_o^{\left(\frac{L_o - x}{L_o}\right)^2} \xi^{(1-\frac{1}{2n})-1} (1-\xi)^{\frac{1}{n}-1} d\xi \right\}$$

$$= t_o + \frac{\gamma^*}{2}\left(\frac{L_o}{\alpha}\right)^{\frac{1}{n}} \left\{ \frac{\Gamma(1-\frac{1}{2n})\,\Gamma(\frac{1}{n})}{\Gamma(1+\frac{1}{2n})} - \frac{\left(\frac{L_o - x}{L_o}\right)^{2-\frac{1}{n}} \left\{1 - \left(\frac{L_o - x}{L_o}\right)^2\right\}^{\frac{1}{n}}}{(1-\frac{1}{2n})} \right.$$

$$\left. \left[1 + \sum_{j=o}^{\infty} \frac{\beta(2-\frac{1}{2n}\,;\, j+1)}{\beta(1+\frac{1}{2n}\,;\, j+1)} \left(\frac{L_o - x}{L_o}\right)^{2(j+1)} \right] \right\} \qquad (3\text{-}13)$$

In domain D_3 the solution is given by Eqs. (2-33) and (2-34) with q replaced by $(q - f)$:

$$h(x,t_o) = \beta^* \left[\frac{(L_o - x_o)^2 - (L_o - x)^2}{\alpha(x)\,(L_o - x)} \right]^{\frac{1}{n}} \qquad (3\text{-}14)$$

$$t(x,x_o) = \gamma^* \int_{x_o}^{x} \left(\frac{1}{\alpha(\eta)}\right)^{\frac{1}{n}} \left[\frac{(L_o - \eta)}{(L_o - x_o)^2 - (L_o - \eta)^2} \right]^{\frac{n-1}{n}} d\eta \qquad (3\text{-}15)$$

If $\alpha(x) = \alpha$, a constant, then we obtain:

$$h(x,x_o) = \beta^* \left(\frac{1}{\alpha}\right)^{\frac{1}{n}} \left[\frac{(L_o - x_o)^2 - (L_o - x)^2}{(L_o - x)}\right]^{\frac{1}{n}} \tag{3-16}$$

$$t(x,x_o) = \gamma^* \left(\frac{1}{\alpha}\right)^{\frac{1}{n}} \int_{x_o}^{x} \left[\frac{(L_o - \eta)}{(L_o - x_o)^2 - (L_o - \eta)^2}\right]^{\frac{n-1}{n}} d\eta \tag{3-17}$$

Substituting the transformation $\xi = ((L_o - \eta)/(L_o - x_o))^2$ and making proper algebraic manipulations we get:

$$t(x,x_o) = \frac{\gamma^*}{2} \left(\frac{L_o - x_o}{\alpha}\right)^{\frac{1}{n}} \int_{\left(\frac{L_o - x}{L_o - x_o}\right)^2}^{1} \xi^{(1-\frac{1}{2n})-1} (1 - \xi)^{\frac{1}{n}-1} d\eta$$

$$= \frac{\gamma^*}{2} \left(\frac{L_o - x_o}{\alpha}\right)^{\frac{1}{n}} \left\{\frac{\Gamma(1 - \frac{1}{2n})\ \Gamma(\frac{1}{n})}{\Gamma(1 + \frac{1}{2n})} - \left(\frac{L_o - x}{L_o - x_o}\right)^{2-\frac{1}{n}} \left\{1 - \left(\frac{L_o - x}{L_o - x_o}\right)^2\right\}^{\frac{1}{n}} \right.$$

$$\left. \frac{1}{(1 - \frac{1}{2n})} \left[1 + \sum_{j=o}^{\infty} \frac{\beta(2 - \frac{1}{2n}\ ;\ j+1)}{\beta(1 + \frac{1}{2n}\ ;\ j+1)} \left(\frac{L_o - x}{L_o - x_o}\right)^{2(j+1)}\right]\right\} \tag{3-18}$$

In domain D_1 we solve Eqs. (3-5) and (3-6), with $q(x,t) = o$ and $f(x,t) = f$, subject to:

$$t(x_o^*) = T$$

$$h(x_o^*) = \beta^* \left[\frac{L_o^{\,2} - (L_o - x_o^*)^2}{\alpha(x_o^*)\ (L_o - x_o^*)}\right]^{\frac{1}{n}}$$

Then the solution is (here $\rho = f/q$) :

$$h(x,x_o^*) = \beta \left[\frac{(1-\rho)\, L_o^2 - (L_o - x_o^*)^2 + \rho (L_o - x)^2}{2\,\alpha(x)\,(L_o - x)} \right]^{\frac{1}{n}} \tag{3-19}$$

$$t(x,x_o^*) = T + \gamma \int_{x_o^*}^{x} \left(\frac{1}{\alpha(\eta)} \right)^{\frac{1}{n}} \left[\frac{L_o - \eta}{(1-\rho)\, L_o^2 - (L_o - x_o^*)^2 + \rho (L_o - \eta)^2} \right]^{\frac{n-1}{n}} d\eta \tag{3-20}$$

If $\alpha(x) = \alpha$, we obtain:

$$h(x,x_o^*) = \beta \left(\frac{1}{\alpha} \right)^{\frac{1}{n}} \left[\frac{(1-\rho)\, L_o^2 - (L_o - x_o^*)^2 + \rho (L_o - x)^2}{2(L_o - x)} \right]^{\frac{1}{n}} \tag{3-21}$$

$$t(x,x_o^*) = T + \gamma \left(\frac{1}{\alpha} \right)^{\frac{1}{n}} \int_{x_o^*}^{x} \left[\frac{L_o - \eta}{(1-\rho)\, L_o^2 - (L_o - x_o^*)^2 + \rho (L_o - \eta)^2} \right]^{\frac{n-1}{n}} d\eta \tag{3-22}$$

Equation (3-22) can be expressed in terms of Beta functions.

Let

$$A = -(1-\rho)\, L_o^2 + (L_o - x_o^*)^2$$

$$\xi = \frac{\rho}{A} (L_o - \eta)^2$$

Then we can write:

$$t(x,x_o^*) = T + \gamma \left(\frac{1}{\alpha} \right)^{\frac{1}{n}} \int_{x_o^*}^{x} \left(\frac{1}{-A} \right)^{\frac{n-1}{n}} \left[\frac{L_o - \eta}{1 - \frac{\rho}{A} (L_o - \eta)^2} \right]^{\frac{n-1}{n}}$$

$$= T + \gamma \left(\frac{1}{\alpha} \right)^{\frac{1}{n}} \left(\frac{-1}{A} \right)^{\frac{n-1}{n}} \int_{\frac{\rho}{A}(L_o - x)}^{\frac{\rho}{A}(L_o - x_o^*)} \left[\frac{(\xi A/\rho)^{\frac{1}{2}}}{(1-\xi)} \right]^{\frac{n-1}{n}} \frac{d\xi}{2\xi^{\frac{1}{2}}}$$

$$= T + \gamma \left(\frac{1}{\alpha}\right)^{\frac{1}{n}} \left(\frac{1}{A\rho}\right)^{\frac{1}{2}(\frac{n-1}{n})} (-1)^{\frac{n-1}{n}} \int_{\frac{\rho(L_o-x)}{A}}^{\frac{\rho}{A}(L_o-x_o^*)} \xi^{(1-\frac{1}{n})-1} (1-\xi)^{\frac{1}{n}-1} d\xi$$

$$= T + \gamma \left(\frac{1}{\alpha}\right)^{\frac{1}{n}} \left(\frac{1}{A\rho}\right)^{\frac{1}{2}(n-1)} (-1)^{\frac{n-1}{n}} \left\{ \int_{o}^{\frac{\rho}{A}(L_o-x_o^*)} \xi^{(1-\frac{1}{n})-1} (1-\xi)^{\frac{1}{n}-1} d\xi \right.$$

$$\left. - \int_{o}^{\frac{\rho(L_o-x)}{A}} \xi^{(1-\frac{1}{n})-1} (1-\xi)^{\frac{1}{n}-1} d\xi \right\}$$

$$= T + \gamma \left(\frac{1}{\alpha}\right)^{\frac{1}{n}} \left(\frac{1}{A\rho}\right)^{\frac{1}{2}(n-1)} (-1)^{\frac{n-1}{n}} \left\{ \beta_{\psi}(1-\frac{1}{n} ; \frac{1}{n}) - \beta_{\phi}(1-\frac{1}{n} ; \frac{1}{n}) \right\} \qquad (3\text{-}23)$$

where $\psi = \frac{\rho}{A}(L_o - x_o^*)$ and $\phi = \frac{\rho(L_o - x)}{A}$

The curves $t = t(x,x_o^*)$ do not intersect in domain D_1 ; the curves $t = t(x,t_o)$ do not intersect in domain D_2 ; and on the assumption

$$\frac{d}{dx}\left(\frac{L_o - x}{\alpha(x)}\right) < o \qquad (3\text{-}24)$$

the curves $t = t(x,x_o)$ do not intersect in domain D_3 (appendix B). The free boundary $t = t^o(x)$ is now determined by

$$(1 - \rho) L_o^2 - (L_o - x_o^*)^2 + \rho (L_o - x)^2 = o \qquad (3\text{-}25)$$

and (3-20). Eliminating x_o^* between Eqs. (3-20) and (3-25) we get (here $\omega = \frac{1}{n}\left(\frac{2}{f}\right)^{\frac{n-1}{n}}$) we obtain:

$$t^{o}(x) = T + \omega \int_{\psi(x)}^{x} \left(\frac{1}{\alpha(\eta)}\right)^{\frac{1}{n}} \left[\frac{(L_o - \eta)}{(L_o - \eta)^2 - (L_o - x)^2}\right]^{\frac{n-1}{n}} d\eta \qquad (3\text{-}26)$$

where $\psi(x) = L_o - [(1 - \rho)\, L_o^{\,2} + \rho(L_o - x)^2]^{\frac{1}{2}}$

As in chapter 2, for fixed x, $h(x,t)$ is an increasing function of t in domain D_3, independent of t in domain D_2, and a decreasing function of t in domain D_1 (see Fig. 3-5).

The criterion to distinguish between case A and cases B_1 and B_2, as in chapter 2, is obtained from:

$$t = \gamma^* \int_{o}^{x} \left(\frac{1}{\alpha(\eta)}\right)^{\frac{1}{n}} \left[\frac{L_o - \eta}{L_o^{\,2} - (L_o - \eta)^2}\right]^{\frac{n-1}{n}} d\eta \qquad (3\text{-}27)$$

If $\alpha(x) = \alpha$, then we obtain:

$$t = \gamma^* \left(\frac{1}{\alpha}\right)^{n} \int_{o}^{x} \left[\frac{L_o - \eta}{L_o^{\,2} - (L_o - \eta)^2}\right]^{\frac{n-1}{n}} d\eta$$

This can be further simplified and written as:

$$T = \frac{\gamma^*}{2} \left(\frac{L_o}{\alpha}\right)^{\frac{1}{n}} \int_{\left(\frac{L_o - x}{L_o}\right)^2}^{1} \eta^{(1-\frac{1}{2n})-1} (1-\eta)^{\frac{1}{n}-1}\, d\eta$$

$$= \frac{\gamma^*}{2} \left(\frac{L_o}{\alpha}\right)^{\frac{1}{n}} \left[\int_{o}^{1} \eta^{(1-\frac{1}{2n})-1} (1-\eta)^{\frac{1}{n}-1}\, d\eta - \int_{o}^{\left(\frac{L_o - x}{L_o}\right)^2} \eta^{(1-\frac{1}{2n})-1} (1-\eta)^{\frac{1}{n}-1}\, d\eta\right]$$

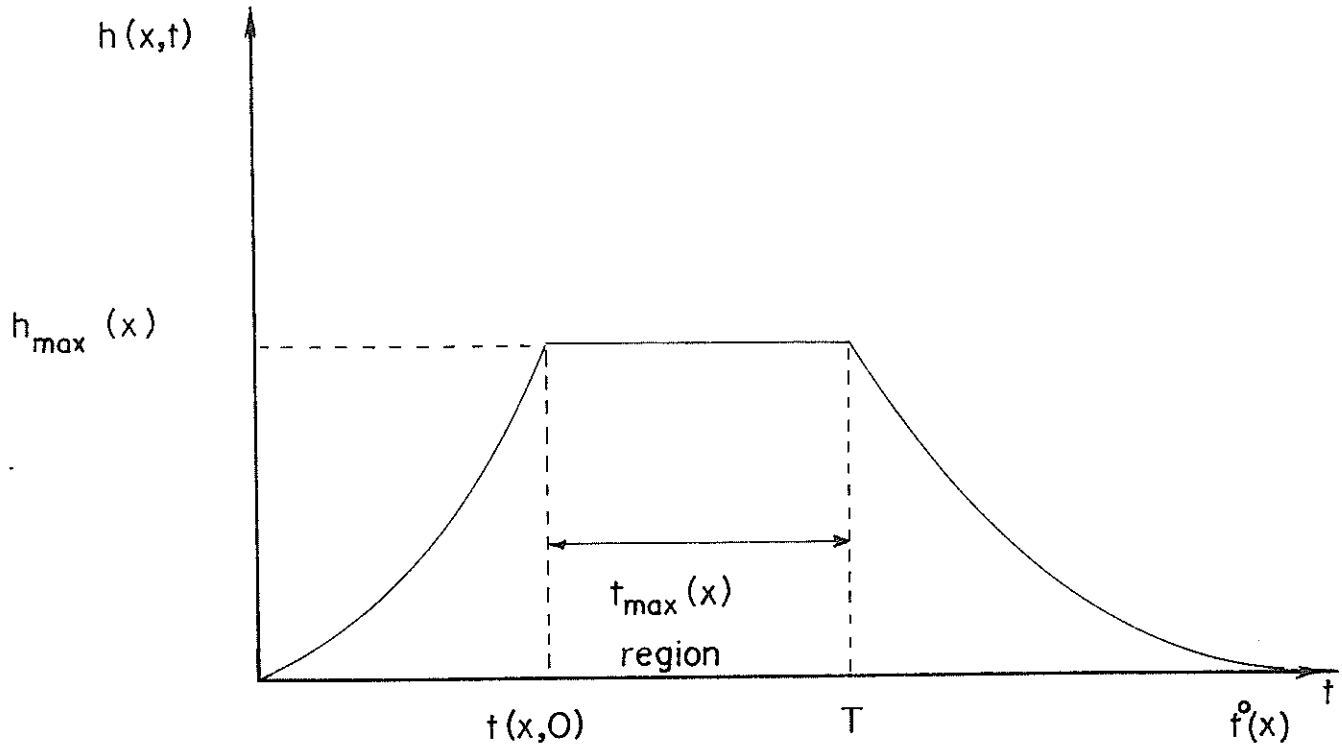

(a) Case A $\quad o < x < L_o(1 - r)$

(b) Cases B_1 and B_2 $\quad o < x < x^*$

Fig. 3-5. Depth of flow h(x,t) as a function of t for fixed x.

$$= -\frac{\gamma^*}{2}\left(\frac{L_o}{\alpha}\right)^{\frac{1}{n}}\left\{\frac{\Gamma\left(1-\frac{1}{2n}\right)\Gamma\left(\frac{1}{n}\right)}{\Gamma\left(1+\frac{1}{2n}\right)} - \frac{\left(\frac{L_o-x}{L_o}\right)^{2-\frac{1}{n}}\left(1-\left(\frac{L_o-x}{L_o}\right)^2\right)^{\frac{1}{n}}}{\left(1-\frac{1}{2n}\right)}\left[1+\sum_{j=o}^{\infty}\right.\right.$$

$$\left.\left.\frac{\beta\left(2-\frac{1}{2n}\,;\,j+1\right)}{\bar{\beta}\left(1+\frac{1}{2n}\,;\,j+1\right)}\left(\frac{L_o-x}{L_o}\right)^{2(j+1)}\right]\right\} \qquad (3\text{-}28)$$

If Eq. (3-27) does not have a root between o and $L_o(1-r)$ then we are in case A; if there is such a root x^* then we are in case B_1 or B_2. If $f(x)$ is the right side of Eq. (3-27) then case A occurs if and only if $f(L_o(1-r)) \leq T$, and case B_1 or B_2 occurs if and only if $f(L_o(1-r)) > T$. To distinguish between cases B_1 and B_2 we note, referring to Eq. (3-19), that:

$$(1-\rho)\,L_o^2 - (L_o - x^*)^2 + \rho(L_o - \eta)^2 = o \qquad (3\text{-}29)$$

does not have a root between o and $L_o(1-r)$ in case B_1 and does have such a root $\bar{x}$ in case B_2. Such a root exists if and only if

$$L_o^2 r^2 < \frac{1}{\rho}(L_o - x^*)^2 - \left(\frac{1}{\rho} - 1\right) L_o^2$$

or

$$1 - \rho(1-r^2) < \left[\frac{L_o - x^*}{L_o}\right]^2 \qquad (3\text{-}30)$$

Thus if Eq. (3-30) is true, we are in case B_2; otherwise we are in case B_1. In case B_2 the intersection of the curves $t = t(x,x^*)$ and $t = t^o(x)$ occurs at

$$\bar{x} = L_o - \left[\frac{1}{\rho}(L_o - x^*)^2 - \left(\frac{1}{\rho} - 1\right) L_o^2\right]^{\frac{1}{2}} \qquad (3\text{-}31)$$

$$\bar{t} = T + \omega \int_{x^*}^{\bar{x}} \left(\frac{1}{\alpha(\eta)}\right)^{\frac{1}{n}} \left\{\frac{(L_o - \eta)}{(L_o-\eta)^2 - (L_o-\bar{x})^2}\right\} d\eta \qquad (3\text{-}32)$$

We now discuss the solution in cases B_1 and B_2.

3.2.2 Cases B_1 and B_2: Partial Equilibrium Situation

In both cases the solution in domain D_{11} is given by Eqs. (3-19) and (3-20), in domain D_2 by Eqs. (3-9) and (3-10), and in domain D_3 by Eqs. (3-14) and (3-15). It remains to determine the solution in domain D_{12}. As in chapter 2, we define x_o^* by $T = t(x_o^*, x_o)$; here $x^* \leq x_o^* \leq L_o(1-r)$. Thus from Eqs. (3-15) we get:

$$T = \gamma^* \int_{x_o}^{x_o^*} \left(\frac{1}{\alpha(\eta)}\right)^{\frac{1}{n}} \left[\frac{L_o - \eta}{(L_o - x_o)^2 - (L_o - \eta)^2}\right]^{\frac{n-1}{n}} d\eta \qquad (3\text{-}33)$$

If $\alpha(x) = \alpha$, we get:

$$T = \gamma^* \left(\frac{1}{\alpha}\right)^n \int_{x_o}^{x_o^*} \left\{\frac{L_o - \eta}{(L_o - x_o)^2 - (L_o - \eta)^2}\right\}^{\frac{n-1}{n}} d\eta \qquad (3\text{-}34)$$

Then from Eqs. (2-33) and (2-34) of chapter 2 we get:

$$h(x;\, x_o^*,\, x_o) = \beta \left[\frac{(1-\rho)(L_o - x_o)^2 - (L_o - x_o^*)^2 + \rho(L_o - x)^2}{\alpha(x)\,(L_o - x)}\right]^{\frac{1}{n}} \qquad (3\text{-}35)$$

$$t(x;\, x_o^*,\, x_o) = T + \gamma \int_{x_o^*}^{x} \left(\frac{1}{\alpha(\eta)}\right)^n \left[\frac{(L_o - \eta)}{(1-\rho)(L_o - x_o)^2 - (L_o - x_o^*)^2 + \rho(L_o - \eta)^2}\right]^{\frac{n-1}{n}} \qquad (3\text{-}36)$$

It is proved in appendix E that the curves defined by Eqs. (3-34) and (3-36) do not, on condition given by Eq. (3-24), intersect in domain D_{12}.

In case B_2 part of the boundary of D_{12} is $t = t^o(x)$. This is

obtained by eliminating x_o and x_o^* between Eqs. (3-33) and (3-36), and from Eq. (3-35),

$$(1 - \rho)\ (L_o - x_o)^2 - (L_o - x_o^*)^2 + \rho(L_o - x)^2 = o \qquad (3\text{-}37)$$

From Eq. (3-37) we get $x_o^* = \psi(x,x_o)$, where

$$\psi(x,x_o) = L_o - [(1 - \rho)\ (L_o - x_o)^2 + \rho(L_o - x)^2]^{\frac{1}{2}} \qquad (3\text{-}38)$$

Thus $t = t^o(x)$ is defined by

$$T = \gamma^* \int_{x_o}^{\psi(x,x_o)} \left(\frac{1}{\alpha(\eta)}\right)^{\frac{1}{n}} \left[\frac{(L_o - \eta)}{(L_o - x_o)^2 - (L_o - \eta)^2}\right]^{\frac{n-1}{n}} d\eta \qquad (3\text{-}39)$$

$$t(x,x_o) = T + \omega \int_{\psi(x,x_o)}^{x} \left(\frac{1}{\alpha(\eta)}\right)^{\frac{1}{n}} \left[\frac{(L_o - \eta)}{(L_o - \eta)^2 - (L_o - x)^2}\right]^{\frac{n-1}{n}} d\eta \qquad (3\text{-}40)$$

In Eqs. (3-39) and (3-40) $\bar{x} \leq x \leq L_o(1-r)$; when $o \leq x < \bar{x}$, $t^o(x)$ is defined by Eq. (3-25).

The behavior of $h(x,t)$ as a function of t for fixed x, $o < x < x^*$, is the same in cases B_1 and B_2, as in case A (see Fig. 3-5). In cases B_1 and B_2, $h_t(x,t) > o$ when $(x,t) \in D_3$ and $h_t(x,t) < o$ when $(x,t) \in D_{11}$; the arguments are the same as in case A. The maximum of $h(x,t)$ occurs therefore when $(x,t) \in D_{12}$ (Figs. 3-6 and 3-7), but it can occur on the boundary of D_{12} as chapter 2 ($\rho = o$). Figures 3-8 - 3-10 illustrate the possibilities. Appendix F provides further details.

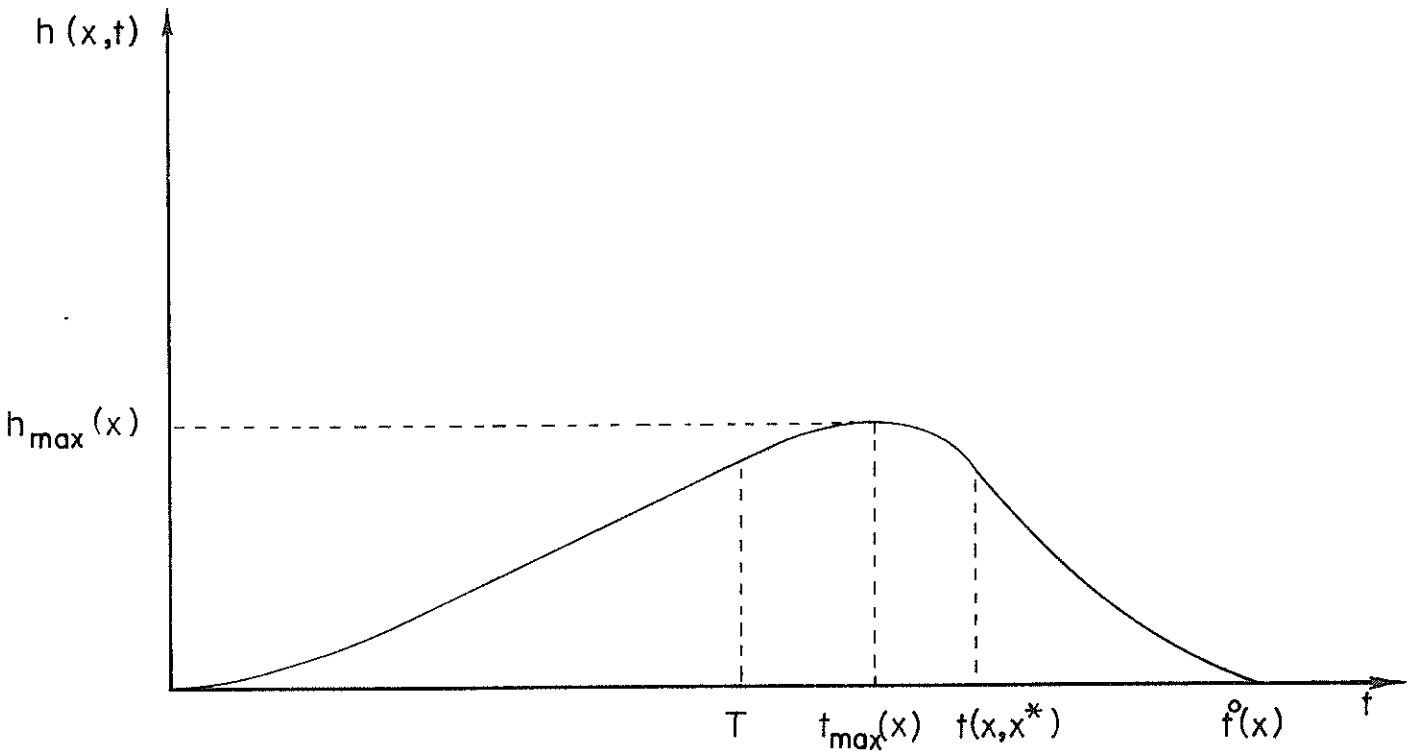

(a) Case B_1 $\quad x^* \leq x \leq L_o(1 - r)$

(b) Case B_2 $\quad x^* \leq x \leq \bar{x}$

Fig. 3-6. The depth of flow, h(x,t), as a function of t for fixed x.

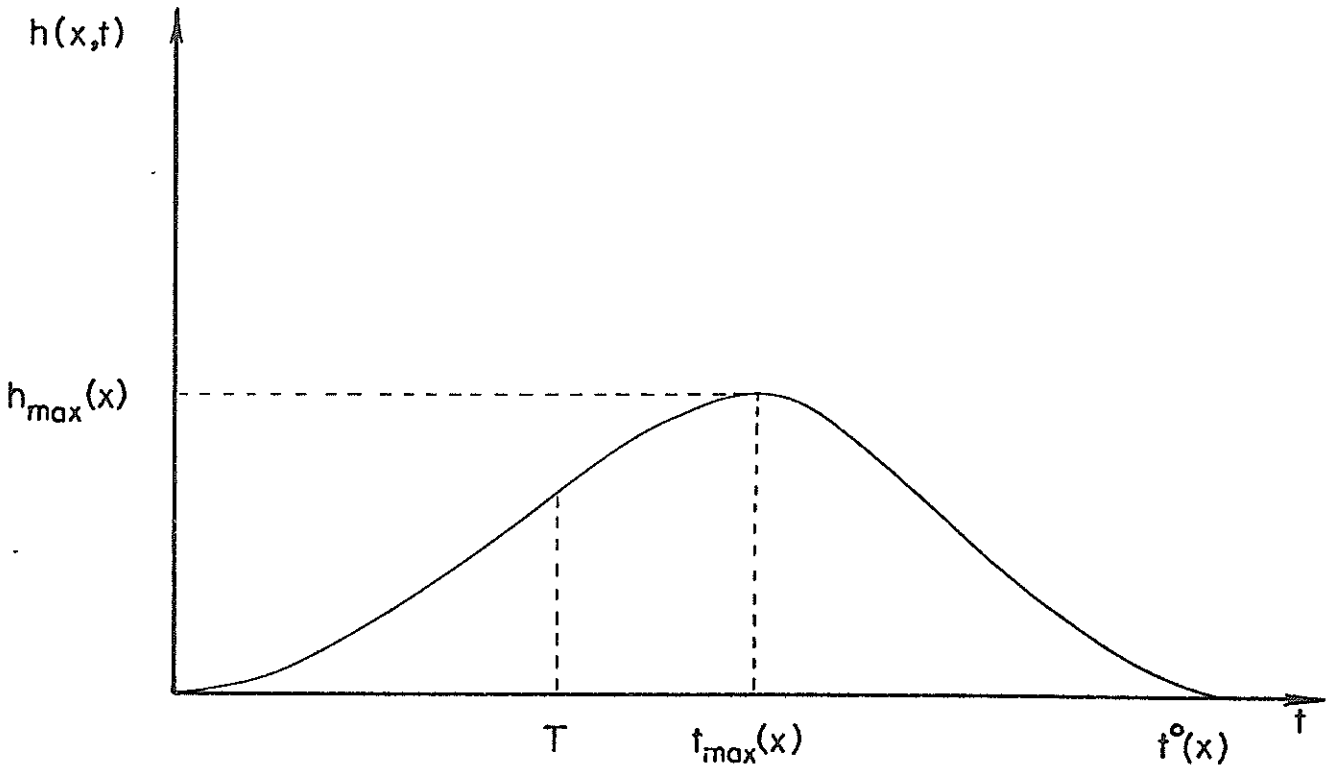

Case B_2 $\quad \bar{x} < x \leq L_o(1 - r)$

Fig. 3-7. The depth of flow, h(x,t), as a function of t for fixed x.

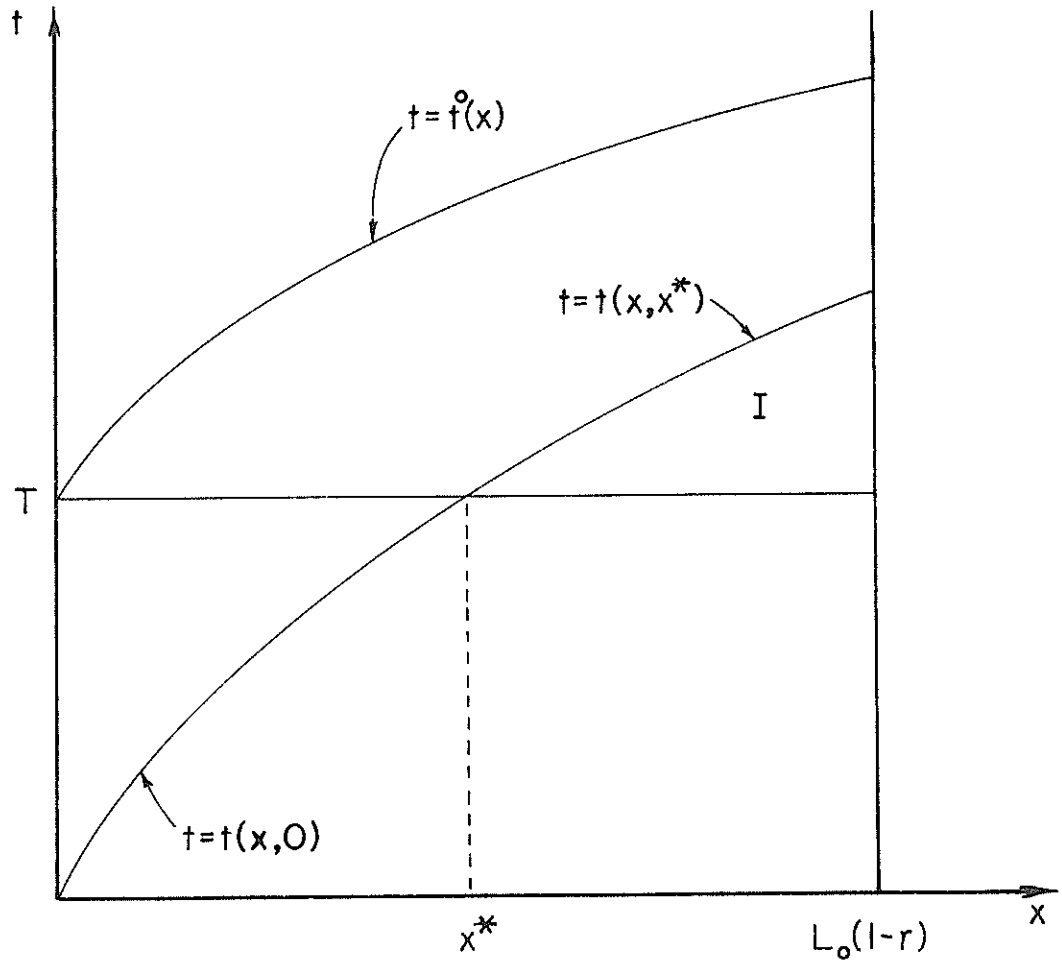

Case B_1: ρ small; $\alpha(x) = \alpha$; I = region where $h_t(x,t) > o$

Fig. 3-8. The behavior of h(x,t) as a function of t for fixed x in domain D_{12}.

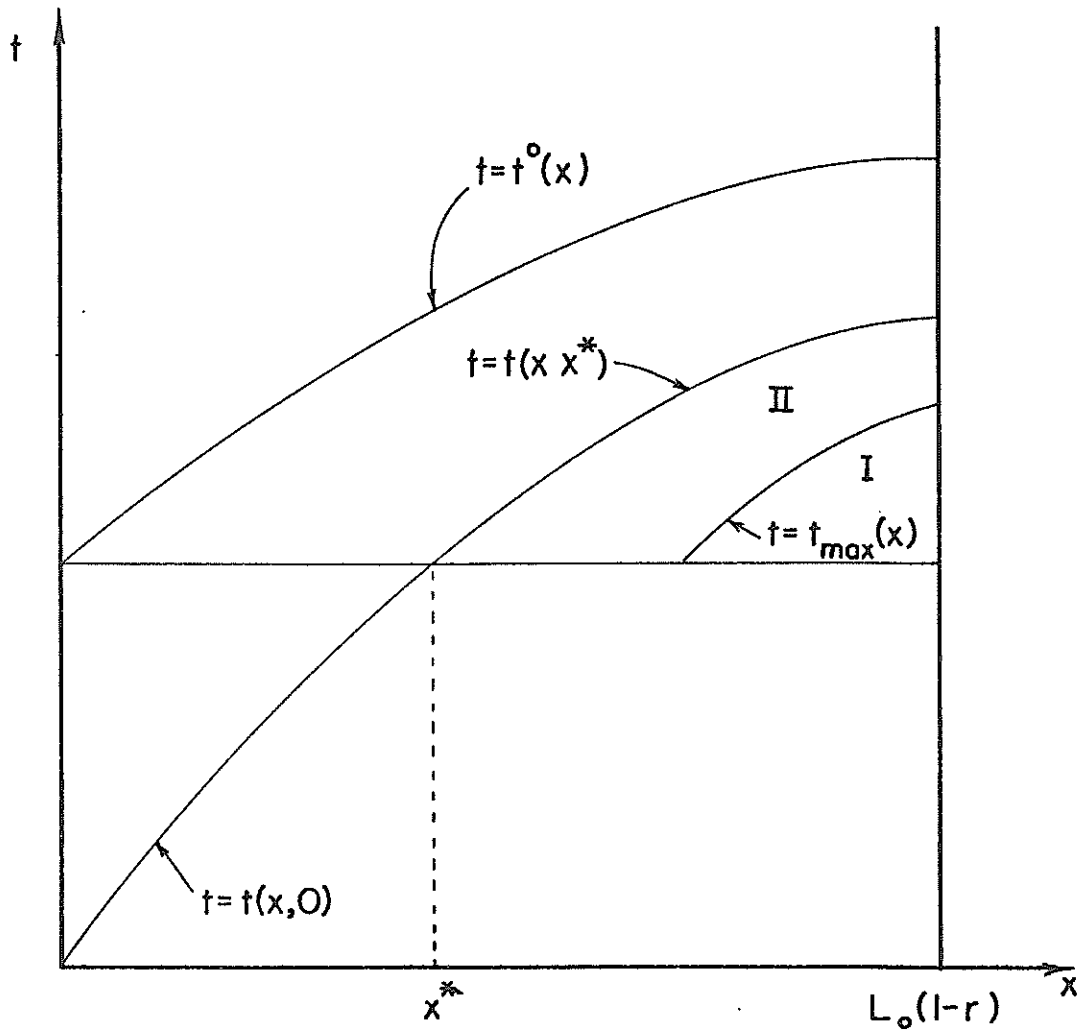

Case B_1: ρ intermediate; $\alpha(x) = \alpha$; I = region where $h_t(x,t) > o$; II = region where $h_t(x,t) < o$.

Fig. 3-9. The behavior of $h(x,t)$ as a function of t for fixed x in domain D_{12}.

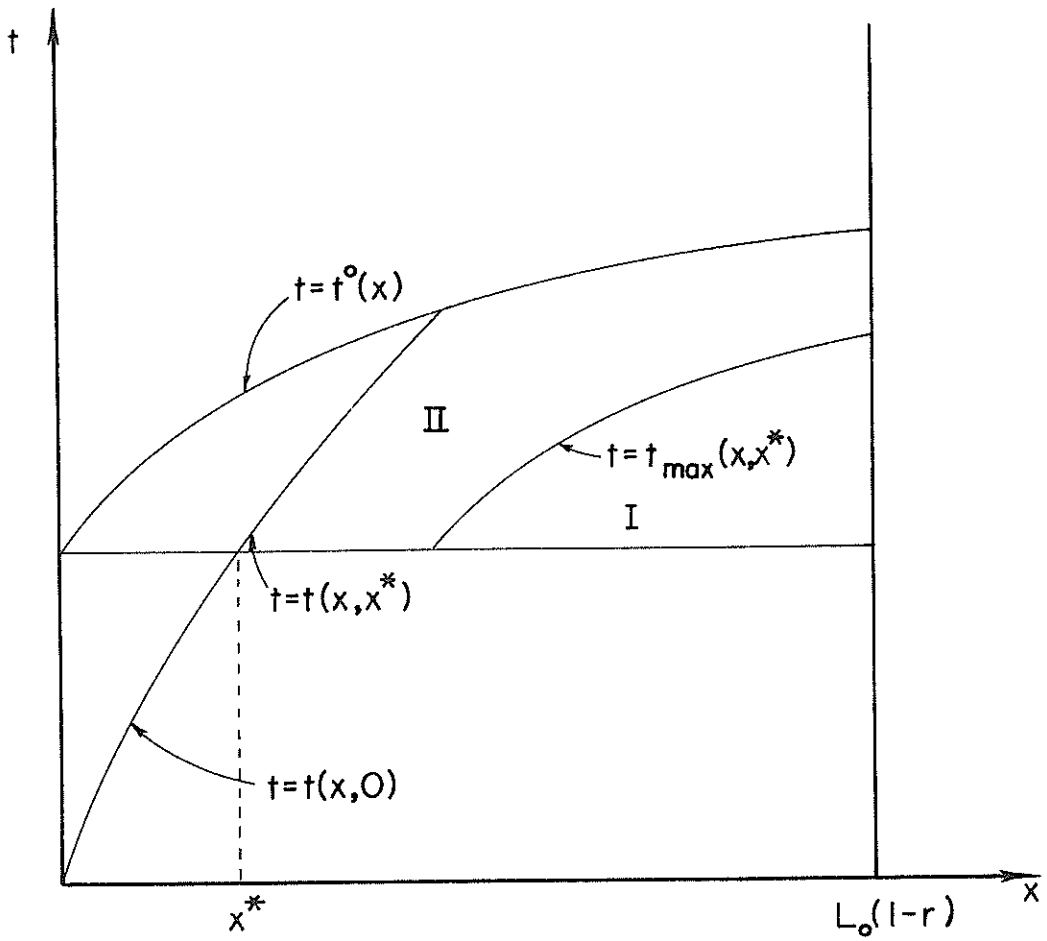

Case B_2: $\alpha(x) = \alpha$; I = region where $h_t(x,t) > o$; II = region where $h_t(x,t) < o$.

Fig. 3-10. The behavior of $h(x,t)$ as a function of t for fixed x in domain D_{12}.

CHAPTER 4

PARAMETER ESTIMATION AND OPTIMIZATION

4.1 CHOICE OF OBJECTIVE FUNCTION

The concept of automatically determining optimum model parameters requires that the objective function be compatible with the intended use. However, there is difficulty in defining an error criterion that, upon minimization, will produce optimum parameter values without an undesirable bias.

Several objective functions are available. A brief examination of each of them will be appropriate at this point.

4.1.1 Sum of Squares of Deviations

For the surface runoff problem the objective function based on the sum of squares of deviations may be defined as:

$$F = \sum_{i=1}^{M} [Q_o(i\Delta t) - Q_e(i\Delta t)]^2 \qquad (4\text{-}1)$$

where F = index of disagreement, or error, $Q_o(t)$ = observed runoff at a given time t, $Q_e(t)$ = estimated runoff at a given time t, and $M\Delta t$ = duration of runoff event. This F is analogous to the residual variance of a regression analysis. The minimization of the function F is designed to match the entire hydrograph even though greater weight is given to higher values of runoff. In the course of matching the entire hydrograph, it is likely that too great a weight is placed on small discharge values because of their sheer large number resulting in poor hydrograph peak matching. One weakness of this objective function is that it is strongly affected by poor time synchronization between the measured rainfall and runoff.

The value of F may be computed for each rainfall-runoff event

if the fitting for an individual event is desired. If the model parameters are to be optimized over a set of events, F needs to be computed over the set. In that case F will be a very poor index of measuring disagreement because the event having the least weight may be the most important of all. This is a rather severe limitation for flood studies.

4.1.2 Sum of Squares of Peak Deviations

This can be expressed as:

$$F = \sum_{j=1}^{N} (Q_{p_o}(j) - Q_{p_e}(j))^2 \qquad (4\text{-}2)$$

where $Q_{p_o}(j)$ = observed hydrograph peak for the j^{th} event, $Q_{p_e}(j)$ = estimated hydrograph peak for the j^{th} event, and N = number of runoff events in optimization set. This is particularly suitable in flood studies and seems to have some attractive features. Obviously, among peaks greater weight is placed on higher peaks. Implicitly, it assumes that from a risk viewpoint loss increases quadratically with the peak runoff. If F is divided by the number of events, the mean squared error will result. This shows, on the average, how much error occurs as the optimization is performed over a set of events. Because it requires only the hydrograph peak from each event, it is efficient computationally. However, its use is not recommended where hydrograph peak is not an important consideration, e.g., low flow studies.

4.1.3 Sum of Squares of Logarithmic Deviations of Hydrograph Peak and Volume

The objective function comprises two components:

$$F_1 = \sum_{j=1}^{N} (\ell nQ_{p_o}(j) - \ell nQ_{p_e}(j))^2 \qquad (4\text{-}3)$$

$$F_2 = \sum_{j=1}^{N} (\ell nVol_o(j) - \ell nVol_e(j))^2 \qquad (4\text{-}4)$$

Then

$$F = aF_1 + (1 - a)F_2 \qquad (4\text{-}5)$$

where $Vol_o(j)$ = observed runoff volume for j^{th} event, $Vol_e(j)$ = estimated runoff volume for j^{th} event, and a = a weighting factor chosen arbitrarily. It is evident from the equations that this objective function gives weight to both the volume and shape characteristics of the runoff hydrograph. The error between observed and estimated values is computed in terms of logarithmic deviations rather than natural units to prevent the parameters from being biased to fit only large magnitude events. To make it even more flexible, an arbitrary constant a is introduced as shown in Eq. (4-5). This constant can be chosen in accordance with the emphasis intended to be placed on a particular error component. For example, should the hydrograph peak be emphasized a should be greater than 0.5.

4.1.4 Sum of Squares of Logarithmic Deviations of Normalizing Time

This is defined as:

$$F = \sum_{j=1}^{N} (\ell nT_{o_o}(j) - \ell nT_{o_e}(j))^2 \qquad (4\text{-}6)$$

where $T_{o_o}(j)$ = observed normalizing time for event j, and $T_{o_e}(j)$ = estimated normalizing time for event j. The normalizing time is defined in appendix G. It is specifically designed for kinematic wave models. Because of its specialized nature it is not usable in

all runoff model optimization problems.

An attractive feature of this objective function is that the parameters can be solved analytically as shown in appendix H. Computation of F is performed over a set of events chosen for optimization. A least squares procedure is invoked to derive explicit, analytical expressions for the parameters. This feature makes it computationally more efficient than any other objective function. Hence, the optimization set of events can be as large as desirable. Implicitly it reflects somewhat on the physical adequacy of model structure. In other words, if the hydrograph matching is good using this objection function, it is implied that the model structure adequately represents the dynamics of runoff process.

It must also be pointed out that for each event, parameters n and α will have to be determined to compute the "observed" normalizing time. This will require that the parameter determination should be based on matching of, say, hydrograph peak. This operation is carried out for each event in an optimization set.

4.1.5 Sum of Relative Differences Raised to Power K

This can be written as:

$$F = \sum_{i=1}^{M} \left(\frac{Q_o(i\Delta t) - Q_e(i\Delta t)}{Q_o(i\Delta t)^K} \right)^K \quad ; \; K \geq 1 \tag{4-7}$$

For $K = 1$, this objective function places equal emphasis on all the ordinates. This, in fact, is a normalized version of Eq. (4-1). For $K > 1$, the effect will be to fit the smaller ordinates better. This may be more appropriate for fitting drought models.

It may be useful to point out that all the foregoing objective functions share some common properties. They include:

1. For certain classes of problems (linear models) the contours of F become quadratic surfaces which are amenable to very powerful optimization techniques.

2. For linear models F has statistical significance since F/(N - 1) (where N = number of data points) is the variance and can be used to place confidence limits upon the optimized parameter values.

3. For flood forecasting, greater emphasis is placed on matching the flood peak of a hydrograph. Peak ordinates are often an order of magnitude greater than the average ordinates and, therefore, near equal absolute errors mean proportional errors in the large ordinates.

The following objective functions are also useful but have limited general applicability.

4.1.6 Sum of Absolute Differences

This can be expressed as:

$$F = \sum_{i=0}^{M} (Q_o(i\Delta t) - Q_e(i\Delta t)) \qquad (4\text{-}8)$$

This objective function is stable in the sense that reduction of F quarantees a reduction in the area between the two curves. It places less emphasis on large ordinates of the hydrograph.

4.1.7 Sum of Squares of Deviations Raised to Power K

We can write as:

$$F = \sum_{i=0}^{M} [Q_o(i\Delta t) - Q_e(i\Delta t)]^K \qquad (4\text{-}9)$$

$K = 1, 2, \ldots$

By increasing K the emphasis of fitting is increasingly placed on the larger ordinates.

4.1.8 Absolute Differences of Peak and Its Time

This is expressed as:

$$F_1 = \left| \frac{Q_{p_o}(j) - Q_{p_e}(j)}{Q_{p_o}(j)} \right| \tag{4-10}$$

$$F_2 = \left| \frac{t_{p_o}(j) - t_{p_e}(j)}{t_{p_o}(j)} \right| \tag{4-11}$$

$$F = aF_1 + (1 - a)F_2 \tag{4-12}$$

where $t_{p_o}(j)$ = observed hydrograph peak time, and $t_{p_e}(j)$ = estimated hydrograph peak time. If equal emphasis is placed on both F_1 and F_2 then a should be 0.5. This function can be used in fitting only one point on the hydrograph for each event, e.g., the peak and its time.

4.1.9 Absolute Difference between Observed and Computed Peaks

$$F = \left| \frac{Q_{p_o}(j) - Q_{p_e}(j)}{Q_{p_o}(j)} \right| \tag{4-13}$$

This will be frequently utilized in fitting only the hydrograph peak due to an event. It will be seen in the next chapter that this will be used in estimating the parameter α of one-parameter kinematic wave model. F will be chosen to be less than or equal to 0.01.

4.2 OPTIMIZATION TECHNIQUES

An optimization technique is an algorithm to find the optimum value of the objective function, F (as defined in the preceding

section), for a given problem. In context of the present study, the optimum value of F will be its minimum. Consider the functional representation,

$$F = f(X_1, X_2 \ldots\ldots X_N) \tag{4-14}$$

Equation (4-14) shows dependence of the objective function, F , or quantity whose optimum is required, upon a set of control variables, or more appropriately parameters, X_1, X_2, ... X_N . For objective functions that are dependent upon only two parameters the distribution of F values for different parameter values can be plotted as shown in Fig. 4-1. For objective functions controlled by many parameters, the region in which the F values lie is a multi-dimensional vector space of which the plane is the two-dimensional example.

The procedure of optimization requires the assignment of a reference frame by which to define positions of objective function values. The origin of this reference frame is normally taken as the point at which all parameters have zero value while reference directions are a set of mutually perpendicular axes that span the full vector space, i.e. that allow any point within the vector space to be referenced.

By altering the values of the parameters, different points within the vector space can be referenced and the corresponding value of the objective function F evaluated. A comparison of each new value of F with the previous best value allows a decision to be made as to whether the new point is better than the old one. As the search causes the value of F to be evaluated at many points, an impression of the shape of the response surface can be gained. This impression may not be comprehensive but can show such things as surface

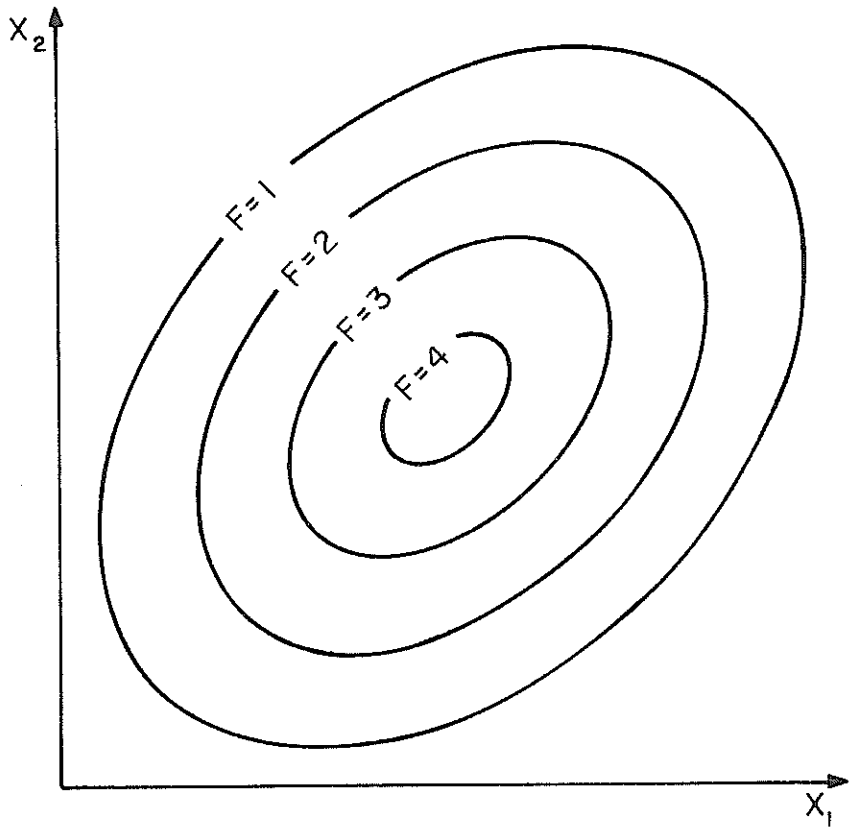

Fig. 4-1. A typical response surface (after Ibbit, 1970).

discontinuities, surface steepness, presence of more than one optimum F value, persistence of surface characteristics, etc. By utilizing this information it may be possible to make assumptions about the response surface that allow future searches to be made more rapidly and easily or place confidence limits upon the final optimum parameter values found.

4.3 PROBLEMS INVOLVED IN OPTIMIZATION TECHNIQUES

There are four main types of structure in a model response surface that can confound an optimization routine.

4.3.1 Local and Global Optimum

In maximization problems the global point is the point which has the highest value of the objective function, F , and vice-versa for minimization problems. Figure 4-2 shows a two-dimensional response surface on which there is more than one closed contour for a given value of F . The "peak" at the center of the righthand closed contour for F = 2 is a local optimum while the "peak" inside the contour F = 3 is the global optimum. This poses the problem of defining if the true optimum has been found when the technique is said to have converged.

If the optimization routine starts at point A in Fig. 4-2, it will, in all probability, find a nearby local optimum such as P_2 . Once at the local optimum, the technique will be able to satisfy its built-in test for convergence. For example, it will find that for small perturbations about its present point only worse points can be found. The optimizing program has no means to move to a higher peak from a lower one since it finds only one peak.

Local optima have all the properties of the global optimum except the value of the objective function F . If the optimal F were

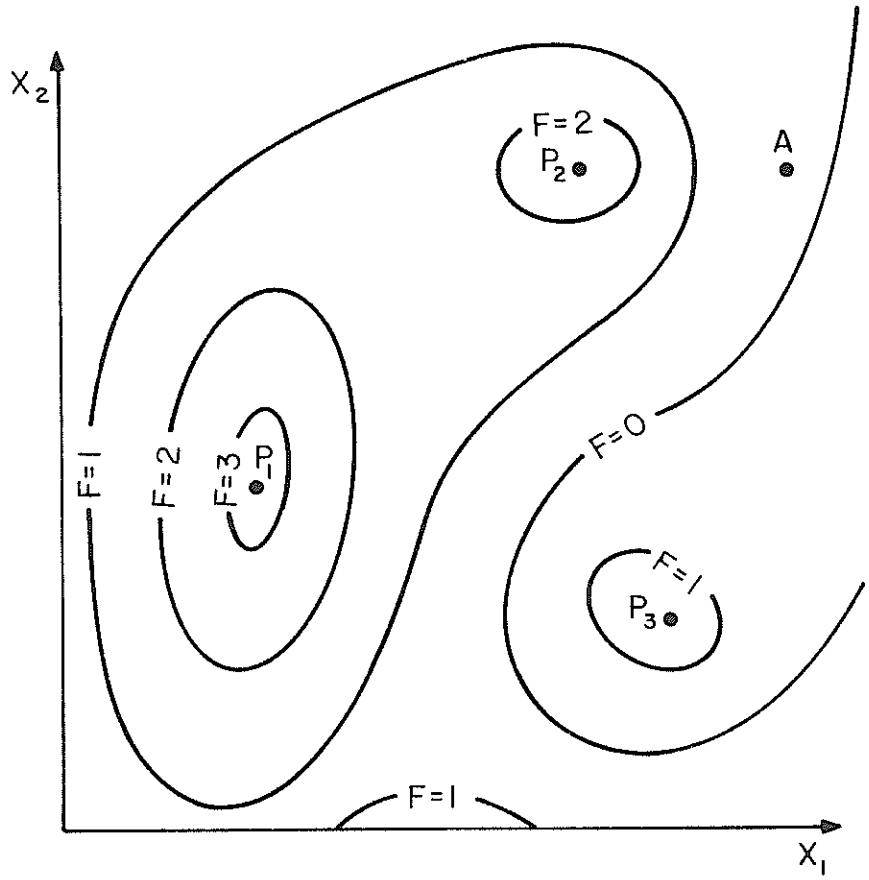

Fig. 4-2. Existence of multiple optima (after Ibbit, 1970).

known a priori, an assessment could be made as to whether or not the global peak has been achieved. Normally F is unknown a priori. Knowledge about the global optimum a priori can enable the decision to be made about the attainment of global optimum. Even though the global F value is unable in itself to furnish any information about its location. Consequently, the only thing to do if an attained optimum has an F value less than a known global F is to re-optimize the problem from different starting points on the response surface and hope that the global optimum will be found during a sufficient number of attempts. It is worth noting that when there is more than one optimum a saddle point must be present.

4.3.2 Saddle Points

For two-dimensional problems saddle points manifest themselves having a maximum (A-A) along one direction and a minimum (B-B) along another direction. This is shown in Fig. 4-3. This structure is less troublesome than local optima, since directions in which further progress can be made are available. Unfortunately, if next directions are defined as C-C and D-D in Fig. 4-3, both these directions have maxima along them, and then convergence will have been declared at such points.

4.3.3 Constraints and Feasible Regions

From a physical consideration of the problem being tackled, certain constraints may be imposed on parameter values, e.g. runoff cannot be negative. Imposition of limits on the parameters means searching directions with parameter increments that do not violate the constraints. This is satisfactory until the best valid point gets too close to a constraint value. When this occurs step sizes

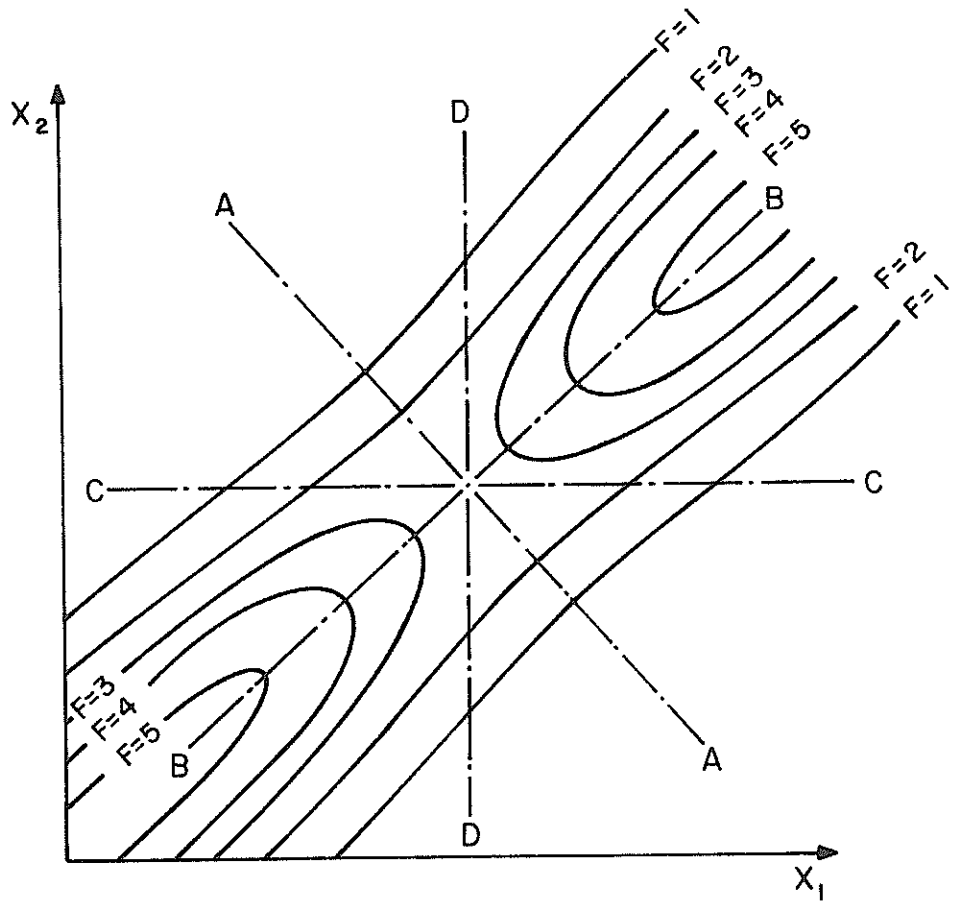

Fig. 4-3. Existence of a saddle point (after Ibbit, 1970).

shrink and the amount of information that the optimizing routine receives about the shape of the response surface decreases. Eventually the point is reached at which no information is obtained and the optimizing routine is unable to continue the search. This problem not only causes premature convergence on to a constraint value but is wasteful since many functional evaluations at very small parameter increments are needed to define what is effectively a false optimum.

When constraints are applied to a problem, the region in which the points that satisfy the constraints lie is known as the feasible region and all points within the region are known as feasible points. Conversely, the region of points that violate the constraints is known as infeasible region and contains all the invalid or infeasible points. The shape of the feasible region depends entirely on the constraints, and is important. This is depicted in Fig. 4.4.

If the response surface function is convex and if the constraints are convex then there is only one optimum, the global optimum. It may well be that in a constrained problem, the global optimum lies in the infeasible region. This leads to the best feasible point being at a position on one or more of the constraints. In this case the optimum is known as the constrained optimum. The latter is global only if the conditions of convexity are met.

Constrained optima always occur for linear problems subject to constraints since the response surface is a straight inclined plane that stretches to infinity. In this case constraints are vital to convergence and functional evaluations are made only at points on the boundary of the feasible region.

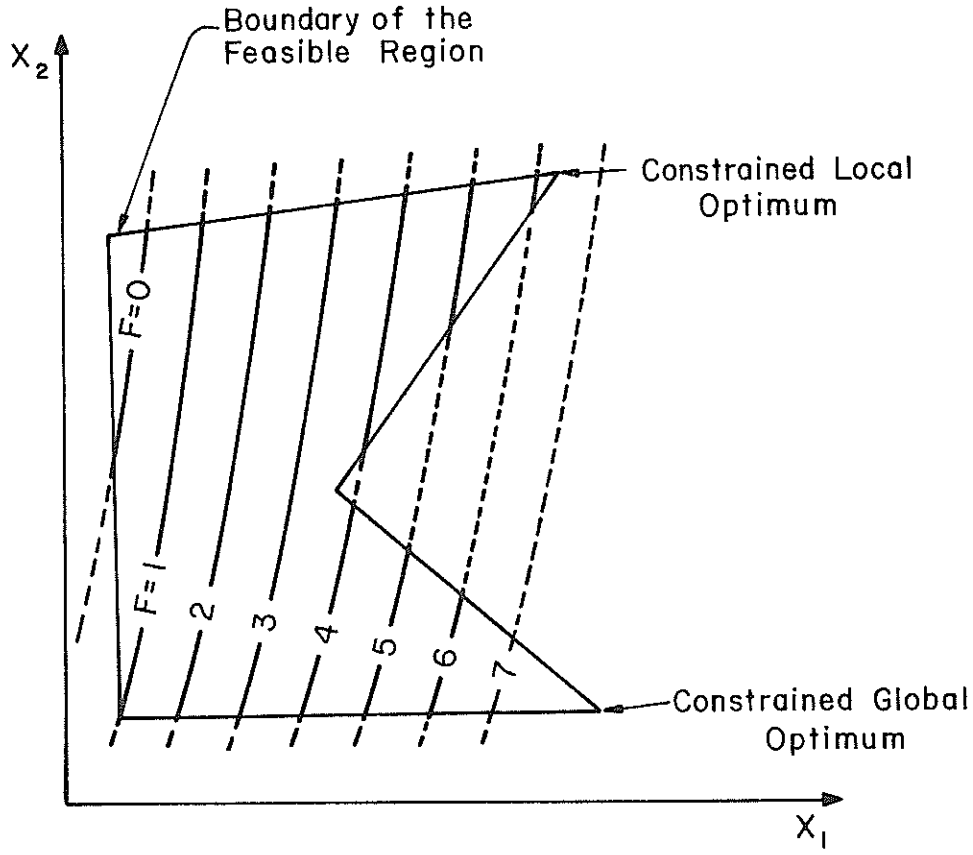

Fig. 4-4. Non-convex regions (after Ibbit, 1970).

4.3.4 Insensitive Directions and Parameter Correlations

Insensitive directions usually occur when a given parameter completely fails to enter the evaluation of F. This problem can, to a certain extent, be minimized by a judicious choice of constraints. If the optimizing technique is stable, insensitive directions reveal themselves as zero progress and this can cause a collapse of the vector search space. See Fig. 4-5.

Correlations between parameters exhibit themselves as ridges in the response surface that are inclined to the parameter axes. If the parameters are linearly correlated, the axis of the ridge will be straight as shown in Fig. 4-6. The inclination of the axis of ridge denotes the degree of correlation or dependence between the parameters. This dependence may be caused by the model structure in which case it will be a persistent feature for different data sets or it may be caused by the data to which the model is being fitted. When the correlation is nonlinear, the ridge becomes curved.

When correlation between parameters is present, simple one-parameter-at-a-time optimization techniques, in which search directions always remain parallel to the parameter axes, are very slow and may converge prematurely simply because the search directions get astride the ridge in much the same way as D-D and C-C in Fig. 4-3. Techniques that can overcome this difficulty use the information gained from a search cycle to define the axis of the ridge and then use this as a good new search direction in the next search cycle.

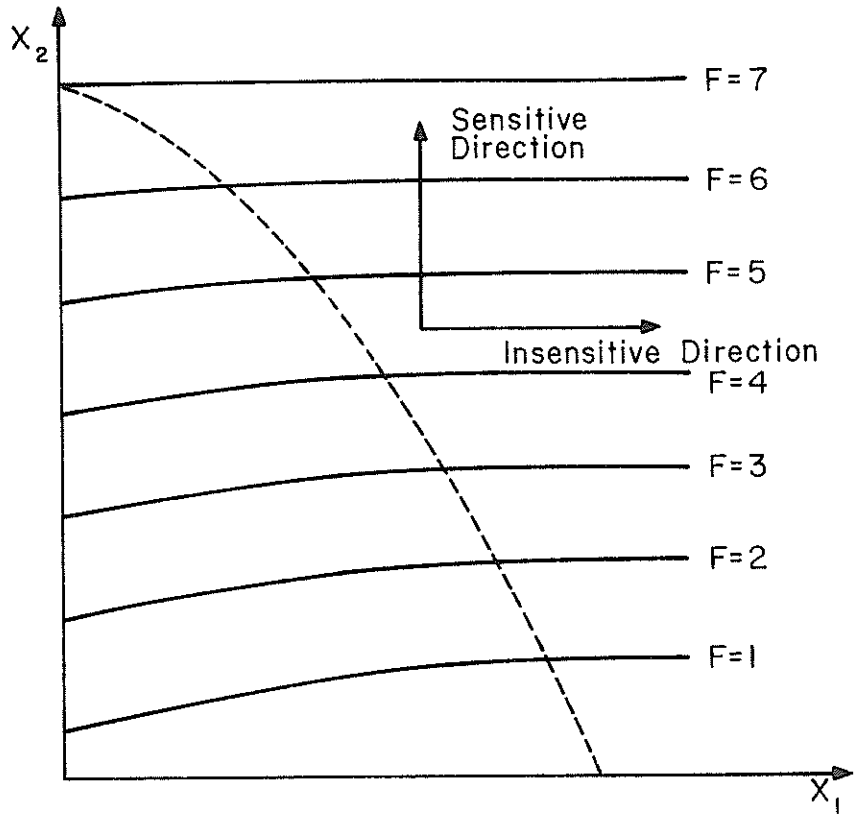

Fig. 4-5. Insensitive directions (after Ibbit, 1970).

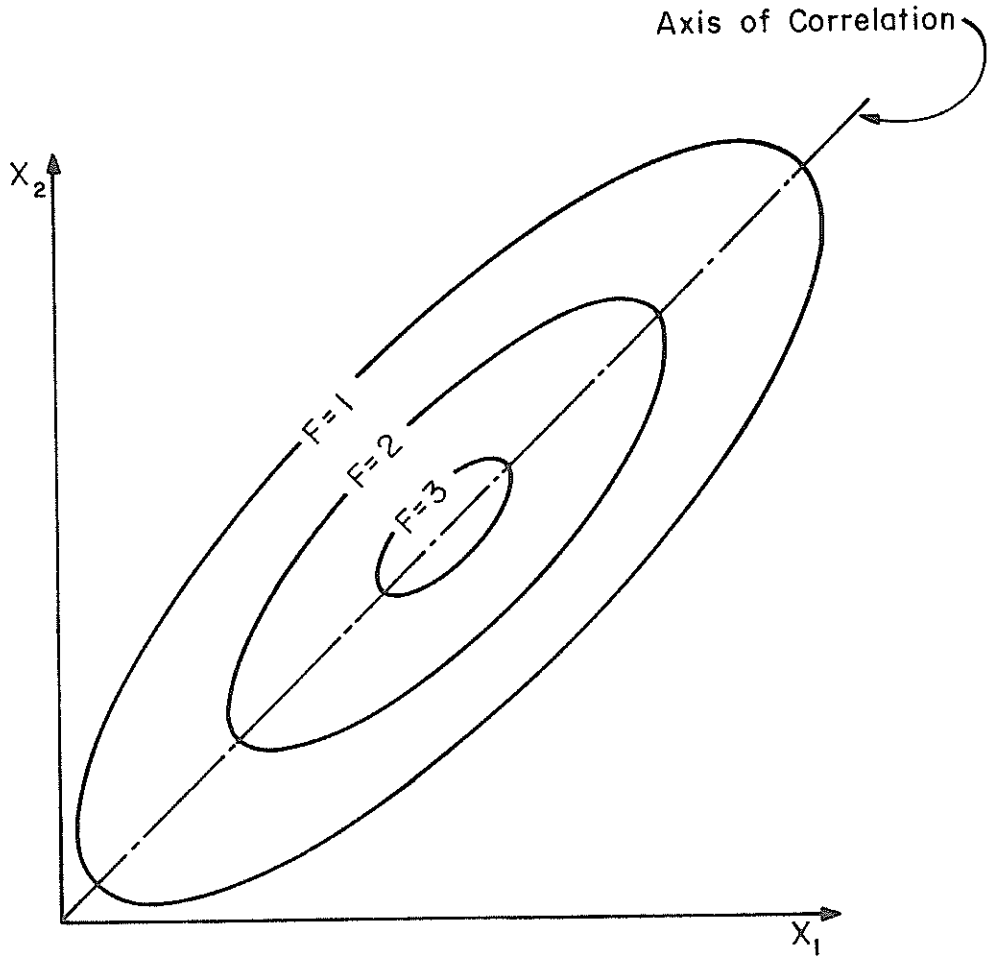

Fig. 4-6. Parameter correlation (after Ibbit, 1970).

CHAPTER 5

A LABORATORY INVESTIGATION OF CONVERGING OVERLAND FLOW

5.1 GENERAL REMARKS

Laboratory watershed models offer opportunities to study unsteady flow in a number of geometrically different systems. They are a powerful tool in testing purely mathematical models of watershed hydraulics and also in testing the applicability of lumped system models (linear or nonlinear) over the range of proto type sizes that can be accomodated. Studies of surface runoff on small prototypes without small variation in rainfall will unquestionably answer some interesting hydraulic and hydrologic questions. When used in conjunction with mathematical models they aid in understanding and predicting watershed behavior.

Experiments on a natural watershed are time-consuming, and there is no control over the input. The physical size of the system is also a problem; so for practical reasons, some investigators attempted to model hydrologic systems utilizing a change in scale (Chery, 1966). They found that this was not a viable approach. Grace and Eagleson (1966) demonstrated that scale models were feasible only in very special cases.

An important consideration, however, is that a laboratory model must duplicate the most important features of the complex system. If it does not, it cannot give insight into real system behavior. Realizing the significance of laboratory watershed models in hydrologic research, several investigators have carried out experiments on surface runoff process (Izzard, 1943; Woo and Brater, 1962; Robertson et al, 1966; Chow, 1967; Yen and Chow, 1969; Dass and Huggins, 1970; Kundu,

1971; Woolhiser et al, 1971; Langford and Turner, 1973; Muzik, 1973; Singh, 1974). For a detailed discussion and review of laboratory experiments see the reference by Singh (1975g).

5.2 ANALYSIS OF EXPERIMENTAL DATA

This chapter includes an analysis of data obtained on the rainfall-runoff experimental facility at the Colorado State University Engineering Research Center, Foothills Campus, Fort Collins, Colorado. A detailed description of the experimental facility can be found elsewhere (Woolhiser et al, 1971; Woolhiser and Schulz, 1973; and Holland, 1969), and will not be repeated here. The plan view of the experimental facility is given in Fig. 5-1. The data considered here are from the upstream, converging section portion of the facility. Data include pulse rainfall and runoff hydrograph observations for various configurations. Each configuration represents a unique type of surface composition or geometry as indicated in appendix I. A detailed treatment of data acquisition on various types of surfaces is given by Holland (1969). Data are available for 50 configurations and can be grouped into seven categories for analysis purposes.

In this study parameters were estimated in two different ways; by single storm estimation, and by optimization over a set of events. The term parameter estimation is used for the operation when the parameters are determined by fitting an individual event. For example, in this study parameters n and α were estimated for each event by fitting the hydrograph peak and its time (Eq. 4-12). When n was kept fixed, parameter α was estimated for each individual event by fitting its hydrograph peak (Eq. 4-13).

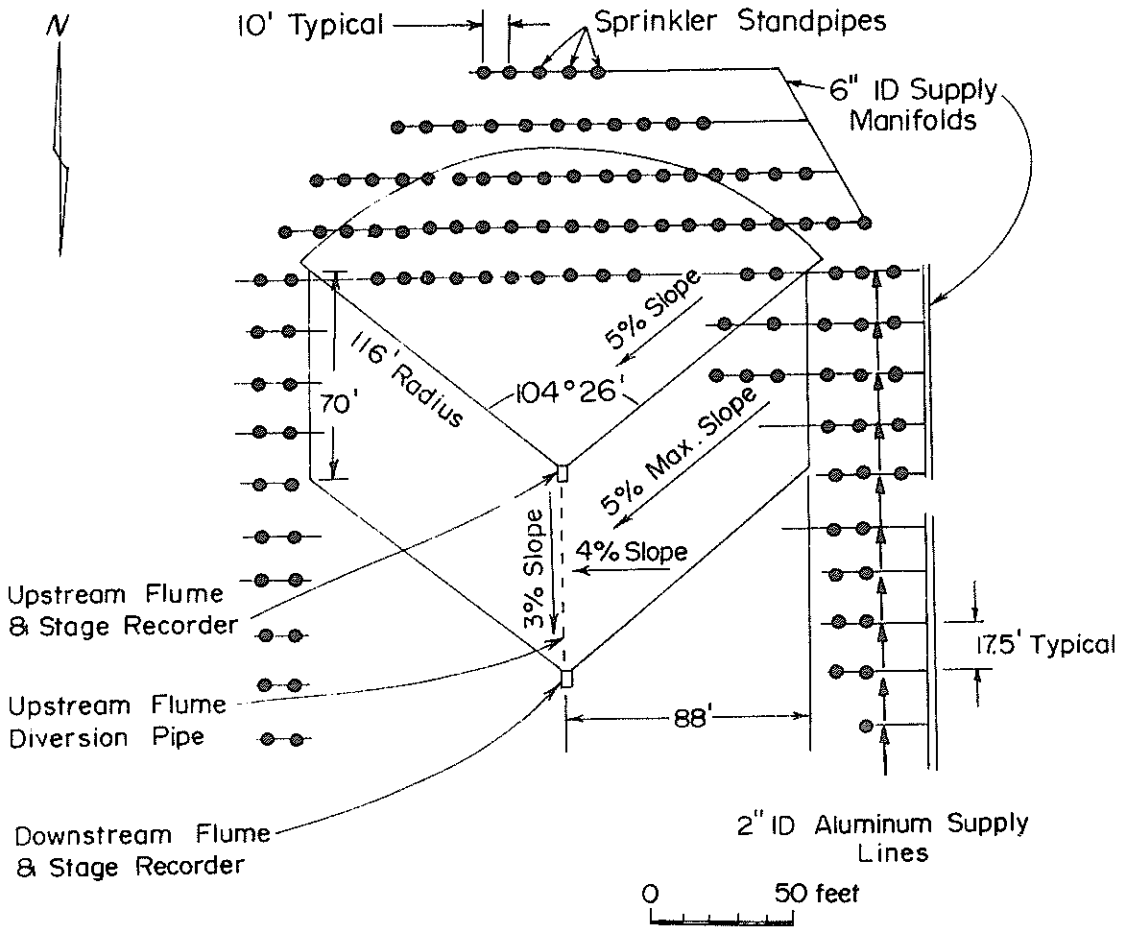

Area of Impervious Surface

Upstream Conic Sector	= 12,700 sq ft
Two Planes	= 12,300 sq ft.
Total	= 25,000 sq ft.

Fig. 5-1. Plan view of CSU Rainfall-Runoff Experimental Facility.

The term parameter optimization is used for the operation when parameters are optimized over a set of events utilizing a specified objective function. The parameters so obtained will form an optimum set for that set of events. For example, in this study, parameters are optimized over a set of events utilizing one of the two objective functions: either Eq. (4-2) or Eq. (4-6).

5.2.1 Identification of Model Parameters

In the event that there is a one-to-one correspondence between the geometric configuration of the watershed and the model, and there is no infiltration, the kinematic wave model contains only two parameters (Eq. (1-2)). When dealing with many events it is important to have a method of parameter estimation that is simple and fast.

Parameter Estimation

A basic property of the kinematic wave theory suggests that for a given rainfall there is a unique pair of the parameters n and α such that the computed peak runoff is exactly the same as the observed peak runoff at that point in time. In view of the objectives of this study, the criterion of Eq. (4-12) was used for parameter estimation. It was found that this peak matching technique led to predicted hydrographs that agreed quite well with the observed hydrographs at all times.

Graphical and numerical peak matching procedures were developed. The error criterion was chosen to be 0.05 for graphical procedure and 0.01 for numerical procedures. The numerical procedures were based on Newton's algorithm for a system of nonlinear equations (Conte, 1965). The graphical procedure is illustrated in appendix H.

Runoff hydrographs were reproduced for several rainfall events for which the parameters were estimated. They were compared with the observed runoff hydrographs, and were found to be in good agreement. A sample comparison is shown in Fig. 5-2. It is clear from the comparison that not only the hydrograph peak and its time are well matched but the entire hydrograph is well reproduced. This indicates that the model has the potential for adequately representing the runoff hydrograph generation process.

Parameter Optimization

A statistical least squares technique was utilized in developing an optimization program for optimizing the parameters n and α (Eq. (4-6)). Its development is detailed in Appendix H. Twenty rainfall events were selected for the butyl surface and light gravel surface of the experimental facility. The parameters n and α were determined for each event by the numerical procedures using the objective function of Eq. (4-12). Optimization of the parameters was performed. Optimized values of the parameters were found to be $n = 1.29$, and $\alpha = 1.91$ for that set of selected events.

Utilizing the optimized values of the parameters n and α as obtained above, hydrograph predictions were performed for four rainfall events on the light gravel surface of the experimental facility. Comparisons were made with observed runoff hydrograph peaks and their timing, and were found to be in good agreement. Figs. 5-3 and 5-4 demonstrate sample comparisons. Table 5-1 gives statistics of comparisons.

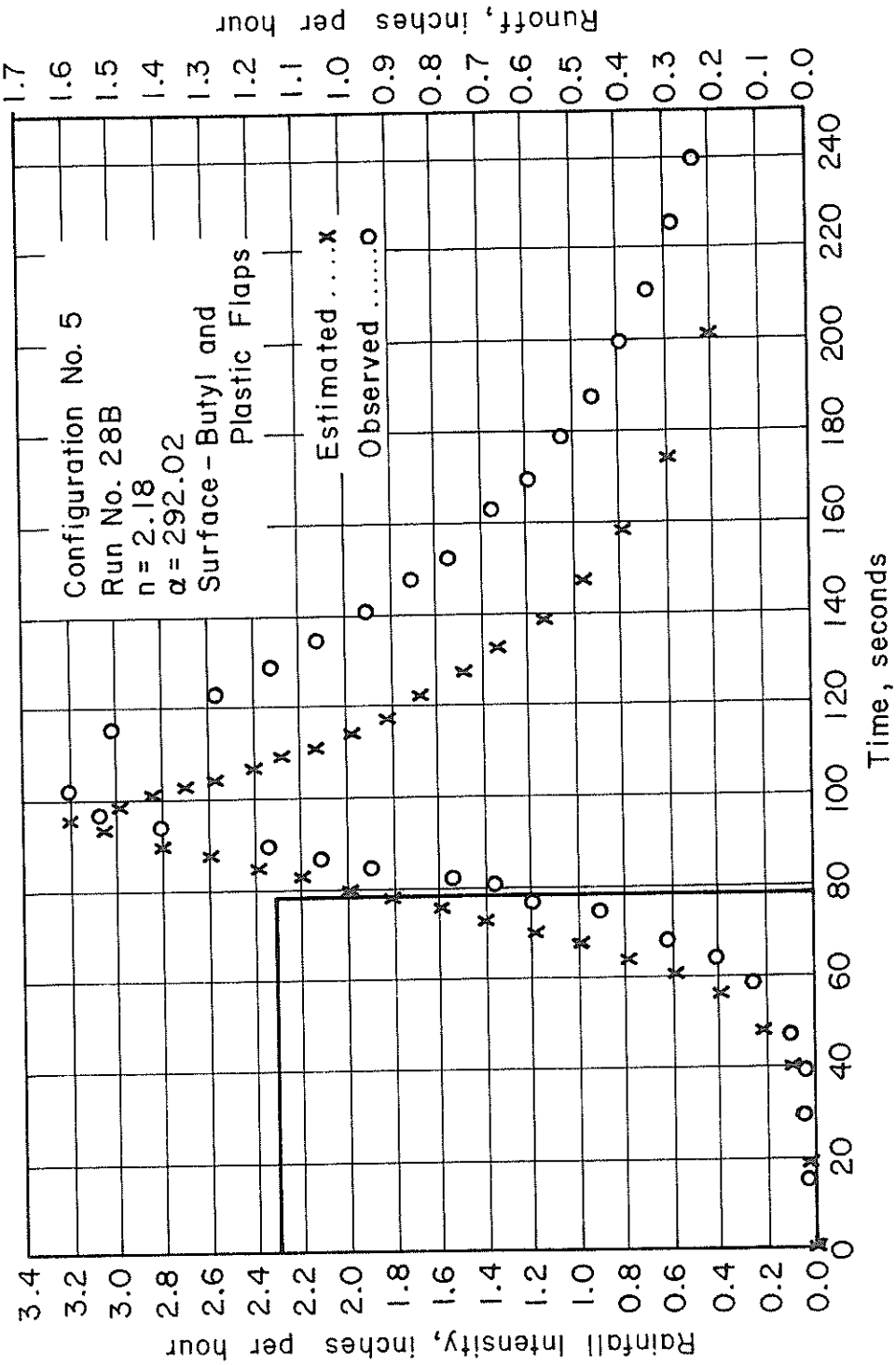

Fig. 5-2. Hydrograph reproduction on rainfall-runoff experimental facility using peak matching technique for parameter estimation.

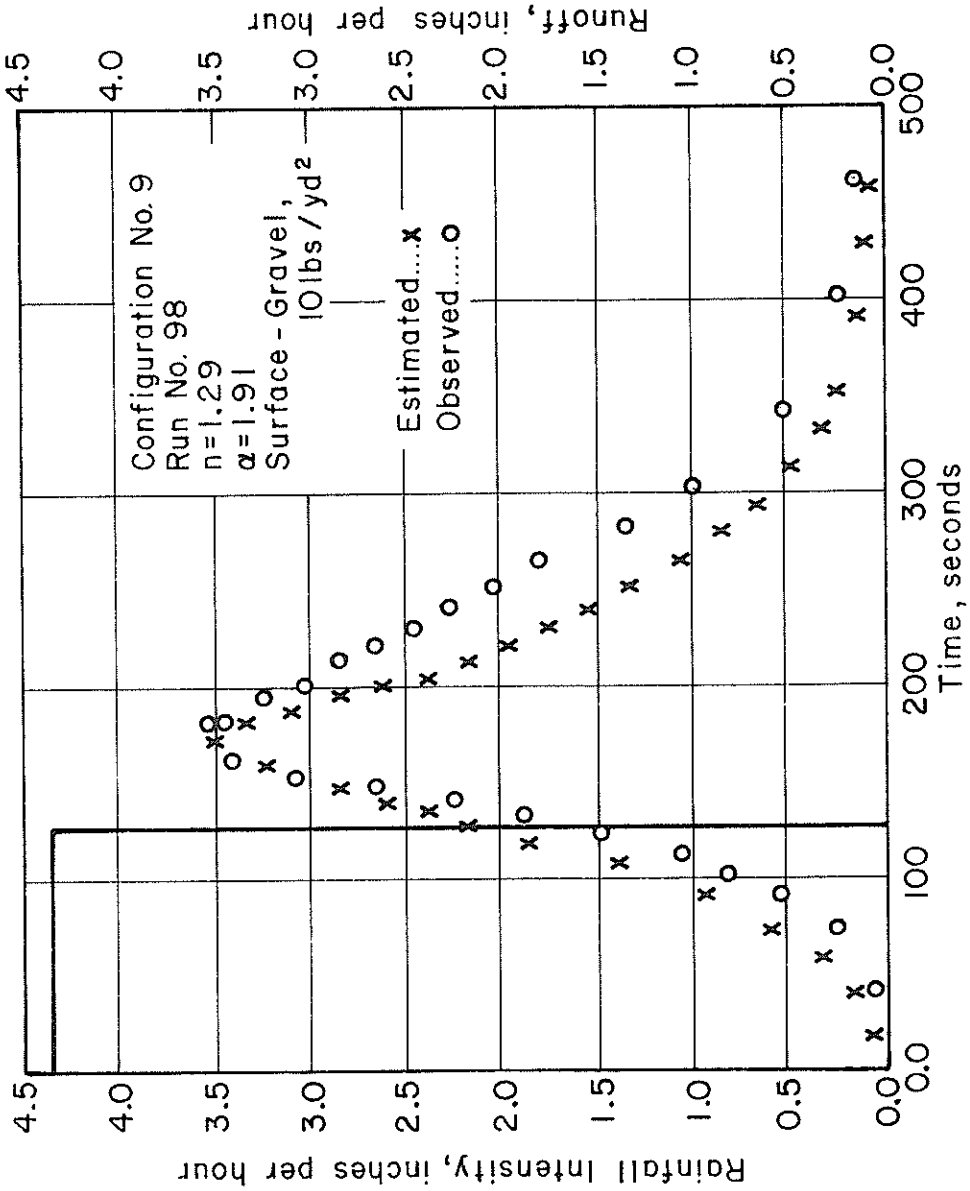

Fig. 5-3. Hydrograph prediction on rainfall-runoff experimental facility.

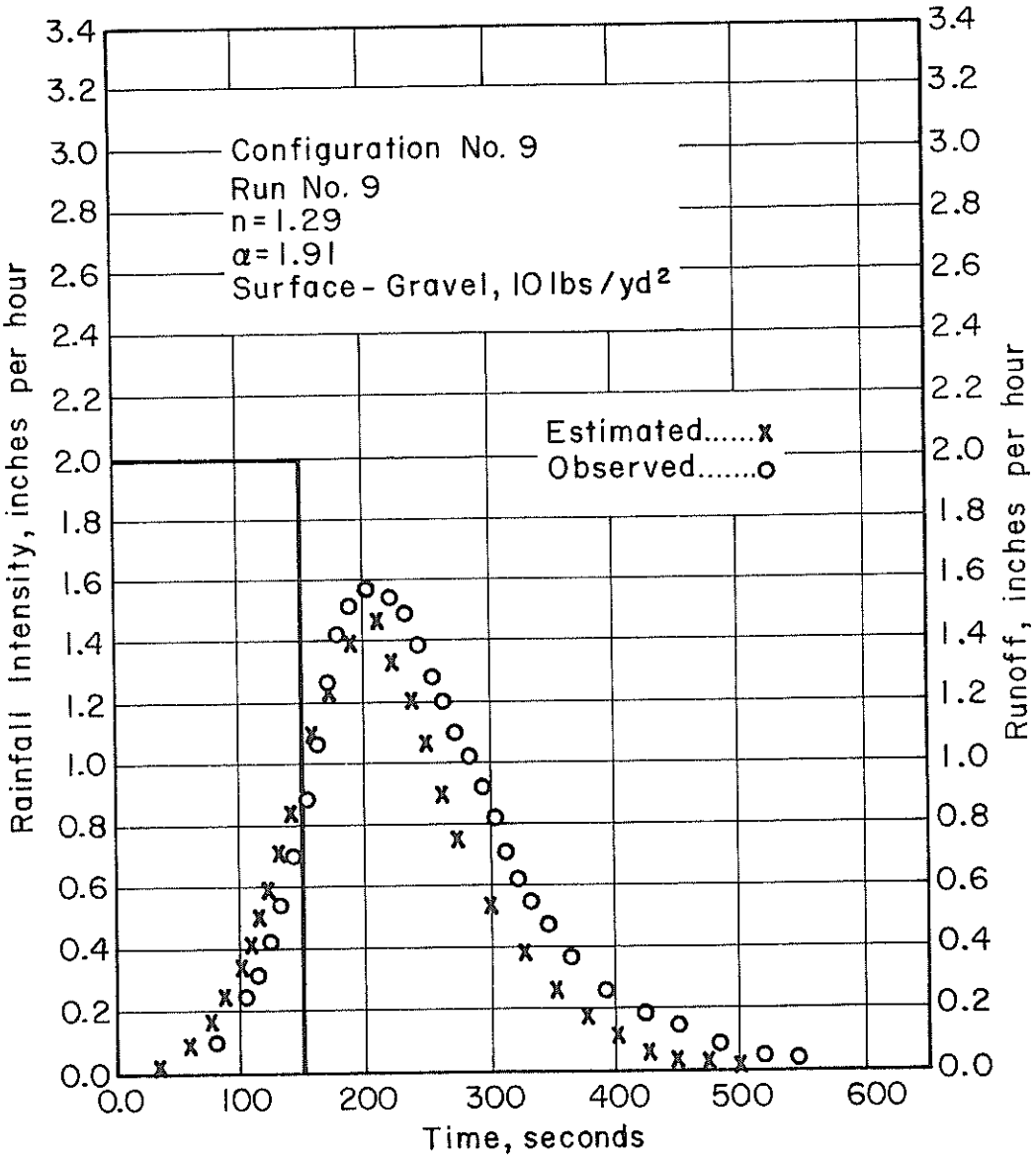

Fig. 5-4. Hydrograph prediction on rainfall-runoff experimental facility.

Table 5-1. Comparison of observed and predicted hydrograph peak and its timing on light gravel surface of CSU Rainfall-Runoff Experimental Facility, Fort Collins, Colorado.

Optimized Values of Parameters: $n = 1.29$; $\alpha = 1.91$

Code*	Rainfall intensity (in/hr)	Rainfall duration (sec)	Observed hydrograph peak (in/hr)	Predicted hydrograph peak (in/hr)	Absolute[1] relative error (%)	Observed hydrograph peak time (sec)	Predicted hydrograph peak time (sec)	Absolute[1] relative error (%)
1-9-82	0.884	26.76	0.057	0.12	110.896	308.80	272.00	11.917
2-9-91	1.978	149.64	1.569	1.57	0.057	213.60	210.00	1.685
3-9-98	4.370	128.13	3.502	3.50	0.049	169.10	170.00	0.532
4-9-99	4.370	149.64	3.876	3.95	1.901	166.30	180.00	8.238

*Serial number, configuration number and run number appear sequentially in Code, e.g., Code 1-9-82 consists of serial number as 1, configuration number as 9 and run number as 82.

[1]Absolute Relative Error = $\frac{\text{Observed Quantity} - \text{Predicted Quantity}}{\text{Observed Quantity}}$

Relationship between Q_p/q and t_p/D

Twenty-five rainfall-runoff events were selected for analysis on the butyl and gravel surfaces of the experimental facility. The dimensionless quantities Q_p/q (hydrograph peak divided by the rainfall intensity), t_p/D (time to hydrograph peak divided by rainfall duration) were computed for each event. Q_p/q was found to be correlated with the logarithm of t_p/D. A remarkably high correlation coefficient, 0.9423, with a standard error of estimate = 0.0929, was obtained. The relationship can be expressed as follows:

$$\frac{Q_p}{q} = 0.86557 - 0.94709 \log (t_p/D) \qquad (5\text{-}1)$$

with standard error 0.07017. A graphical display is shown in Fig. 5-5. This relationship will be useful in hydrograph analysis.

Relationship between Q_p/q and D/T_o

For the same set of 25 rainfall events on butyl and gravel surfaces, the parameters n and α were estimated by the graphical procedure, utilizing the objective function of Eq. (4-10). A least squares analysis was performed to provide optimum values of the parameters n and α for these events. Employing these optimized values of n and α, the normalizing times, T_o, were computed for each rainfall event using the defining equation presented in appendix G. The quantities Q_p/q and D/T_o were then computed, and a linear regression analysis was performed to relate them. The correlation coefficient was found to be as high as 0.9545 with a standard error of estimate = 0.0688. The relationship is shown in Fig. 5-6, and expressed quantitatively as

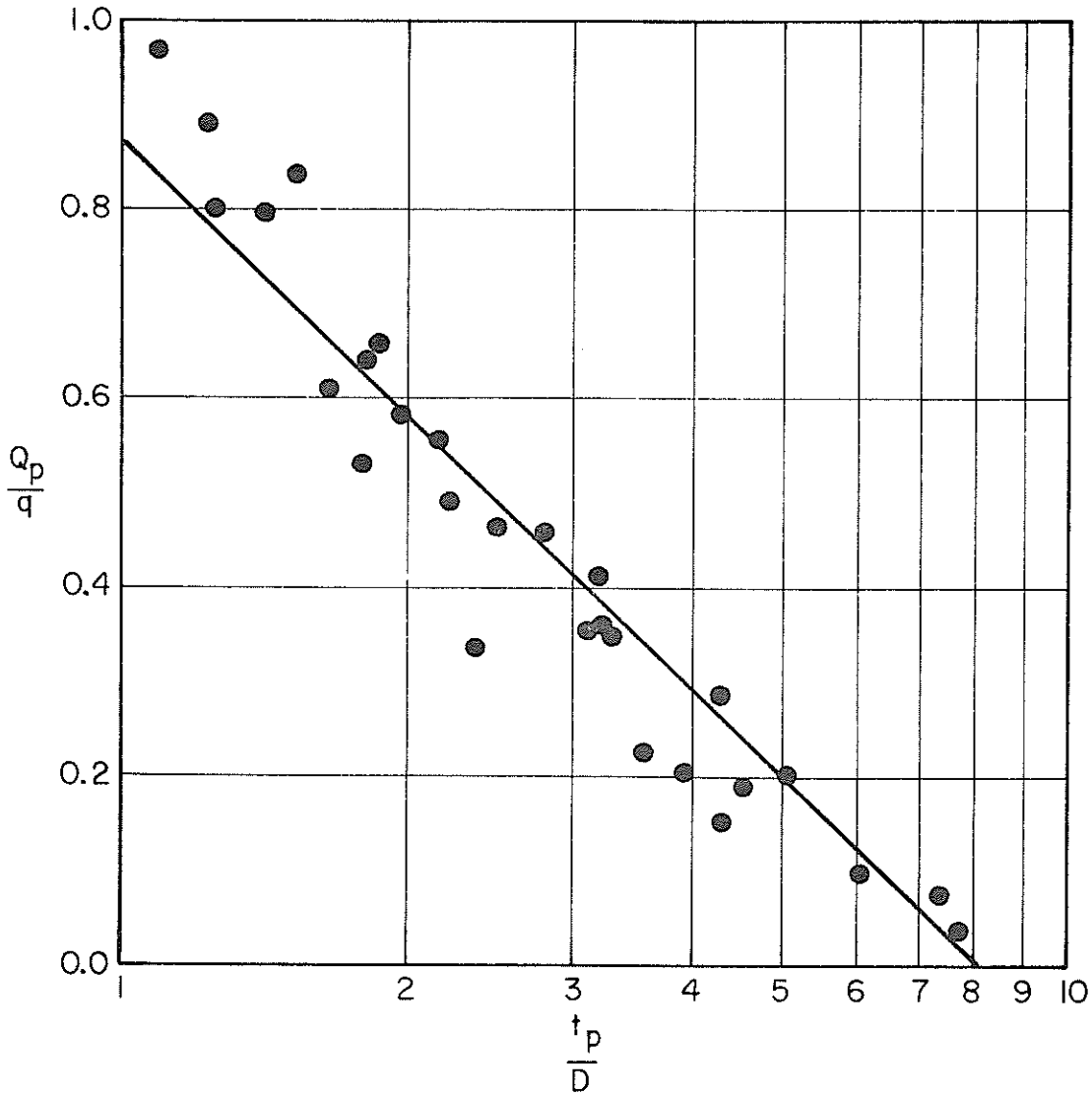

Fig. 5-5. Relationship between Q_p/q and t_p/D for hydrographs from the butyl and gravel surfaces of rainfall-runoff experimental facility.

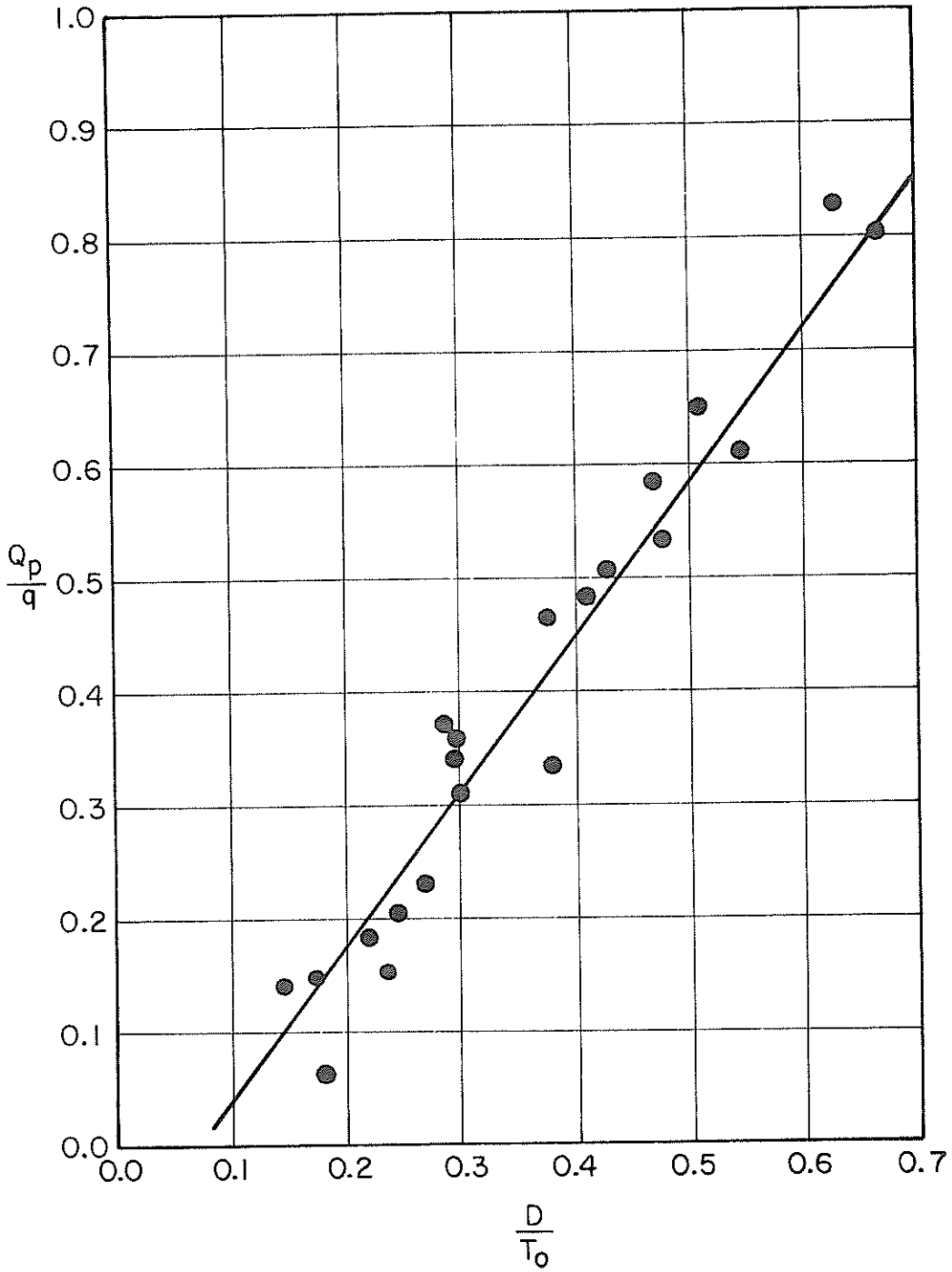

Fig. 5-6. Relationship between Q_p/q and D/T_o for hydrographs from the butyl and gravel surfaces of rainfall-runoff experimental facility.

$$Q_p/q = - 0.08600 + 1.31778\ D/T_o \qquad (5\text{-}2)$$

This relationship can be useful in numerous applications-hydrograph analysis and parameter estimation, to name but a few.

Parameter Variability and Interrelationship

As mentioned before, experimental facility runoff data were available for 50 geometric configurations of varying surface characteristics. These geometric configurations were divided into seven groups according to surface characteristics. Configurations having similar surface characteristics were placed in one group. The last group was formed by lumping together all the surfaces.

Two hundred and ten experimental runs were analyzed and parameters were determined by mathematical procedures utilizing the objective function of Eq. (4-12) as shown in appendix J. It was found that the parameter n was quite stable, while the parameter α was extremely sensitive to rainfall characteristics, surface composition and their interaction. The parameters were also found to be conspicuously correlated. For each group of surface characteristics, a simple statistical analysis based on regression and correlation techniques was performed. In all cases the correlation coefficient between n and $\log \alpha$ was greater than 0.91. A relation of the form

$$\alpha = 10^{a+bn} \qquad (5\text{-}3)$$

was found to exist between them, where a and b are regression constants. Statistics of the parameters and results of regression and correlation analysis are given in Table 5-2. The relationships between the parameters for each of the surfaces of the experimental facility are shown in Figs. 5-7 - 5-13.

Table 5-2. Correlation between the parameters n and α for different surfaces of CSU Rainfall-Runoff Experimental Facility, Fort Collins, Colorado.

Surface Characteristics	Number of Observations	Statistics of Parameter n		Statistics of Parameter α		Regression Constants		Correlation Coefficient between n and Log α	Standard Error of Estimate
		Mean	Standard Deviation	Mean	Standard Deviation	α	b		
Butyl	50	1.82	0.352	211.69	353.287	-2.435	2.311	0.967	0.217
Butyl & Dam	11	1.50	0.349	25.64	50.868	-3.116	2.533	0.999	0.042
Gravel, 20 lbs/yd^2	20	1.57	0.301	11.14	14.341	-2.312	1.911	0.960	0.172
Gravel, 50 lbs/yd^2	22	1.87	0.425	34.42	59.480	-2.214	1.701	0.969	0.188
Gravel & Butyl	24	1.84	0.305	87.68	121.666	-2.419	2.105	0.979	0.138
Brick & Random Plots of Gravel & Butyl	83	1.73	0.383	77.81	202.58	-2.185	1.973	0.953	0.241
Surfaces Lumped Together	210	1.75	0.375	97.19	228.429	-2.348	2.069	0.917	0.339

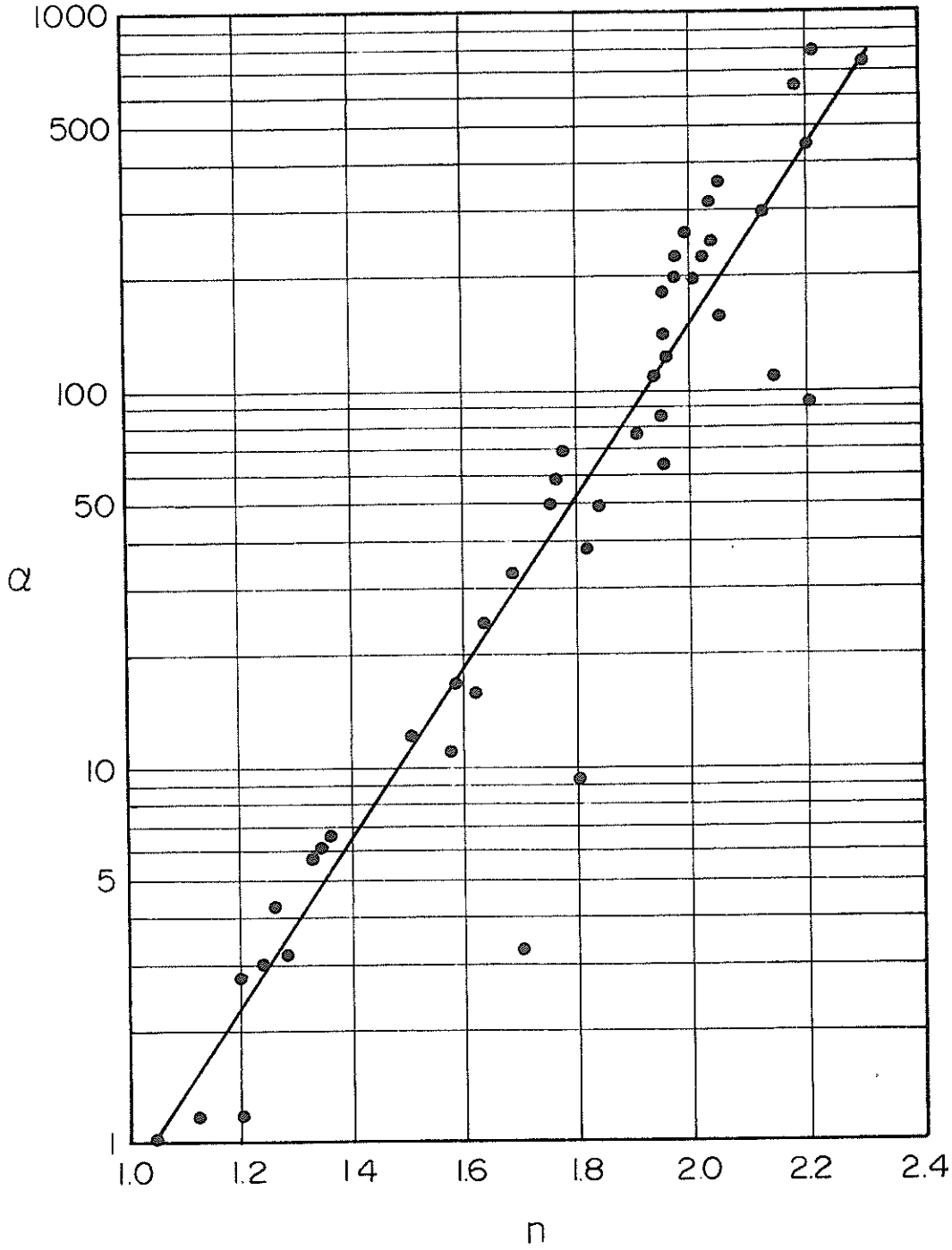

Fig. 5-7. Relationship between parameters n and α for butyl surface of rainfall-runoff experimental facility.

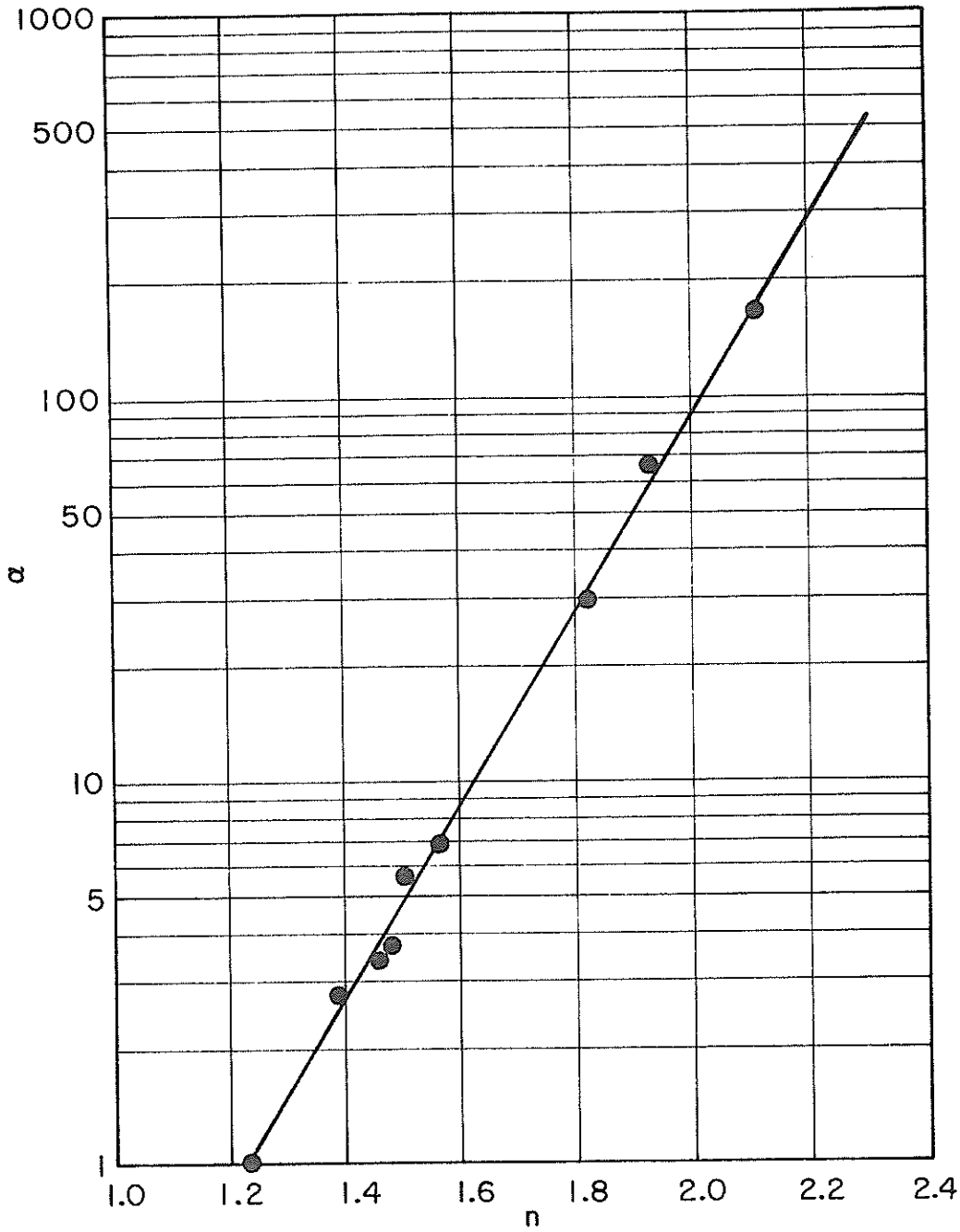

Fig. 5-8. Relationship between parameters n and α for butyl surface and dam of rainfall-runoff experimental facility.

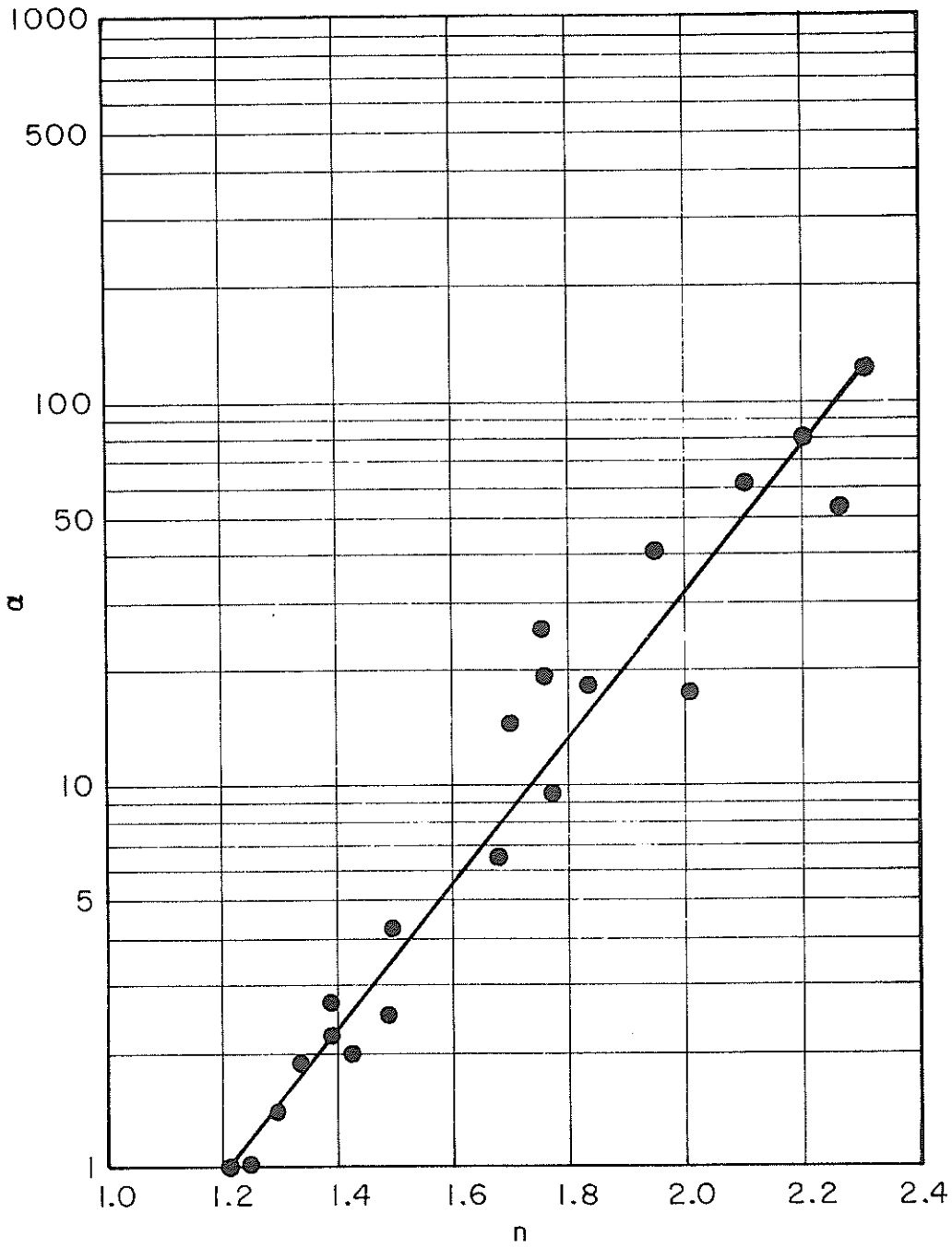

Fig. 5-9. Relationship between parameters n and α for gravel surface (20 lbs./yd.^{2}) of rainfall-runoff experimental facility.

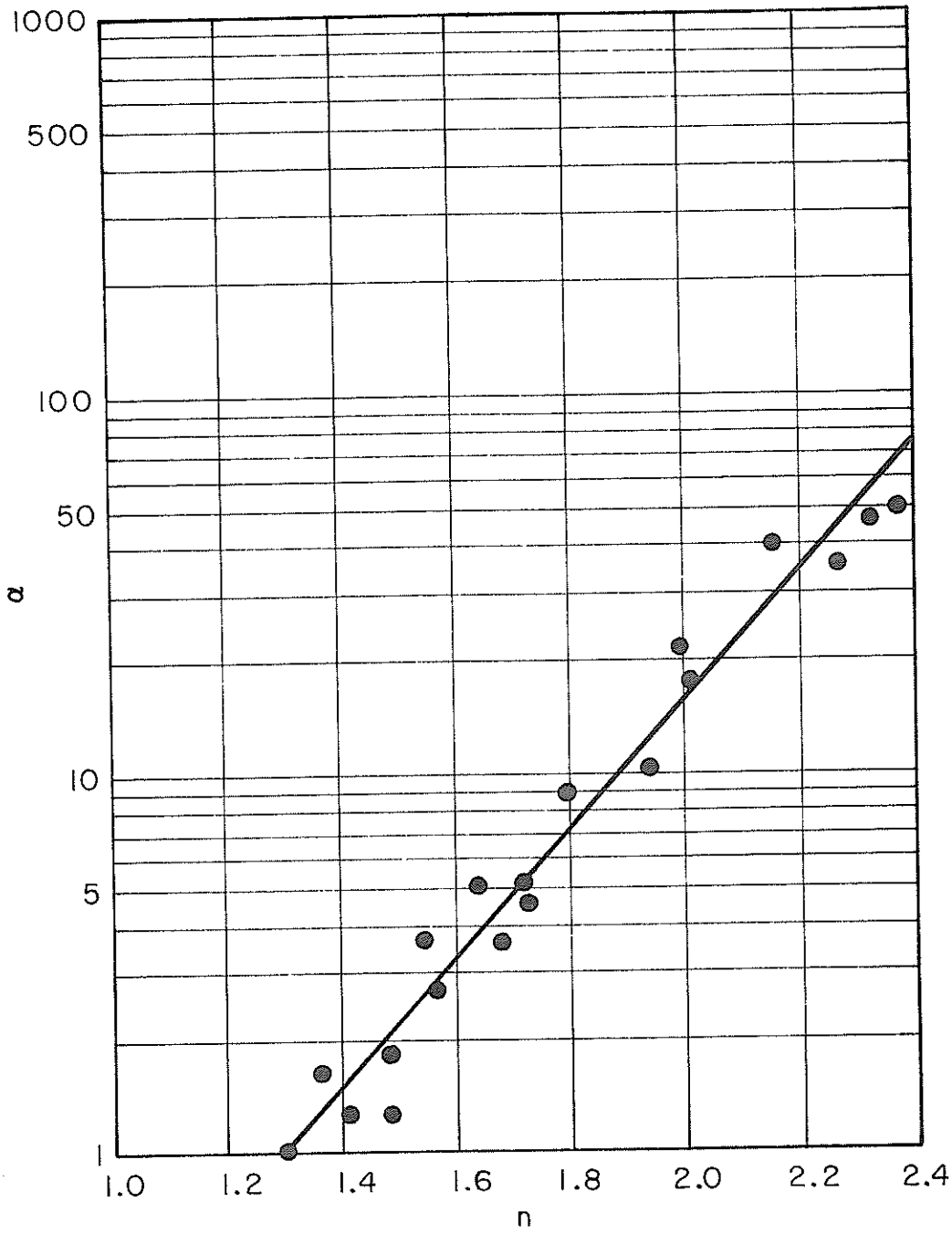

Fig. 5-10. Relationship between parameters n and α for gravel surface (50 lbs./yd.^{2}) of rainfall-runoff experimental facility.

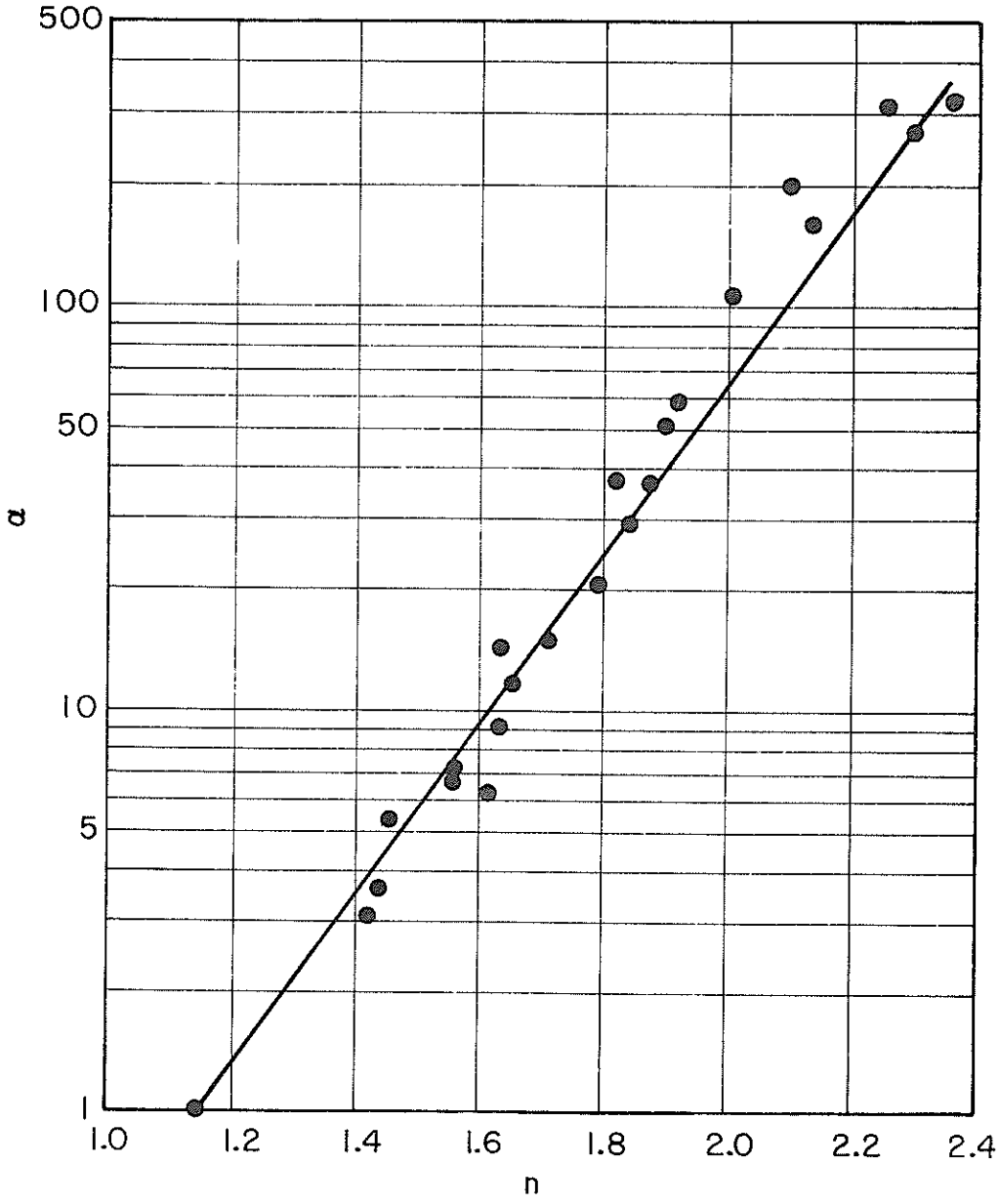

Fig. 5-11. Relationship between parameters n and α for gravel + butyl + random gravel pattern, surface of rainfall-runoff experimental facility.

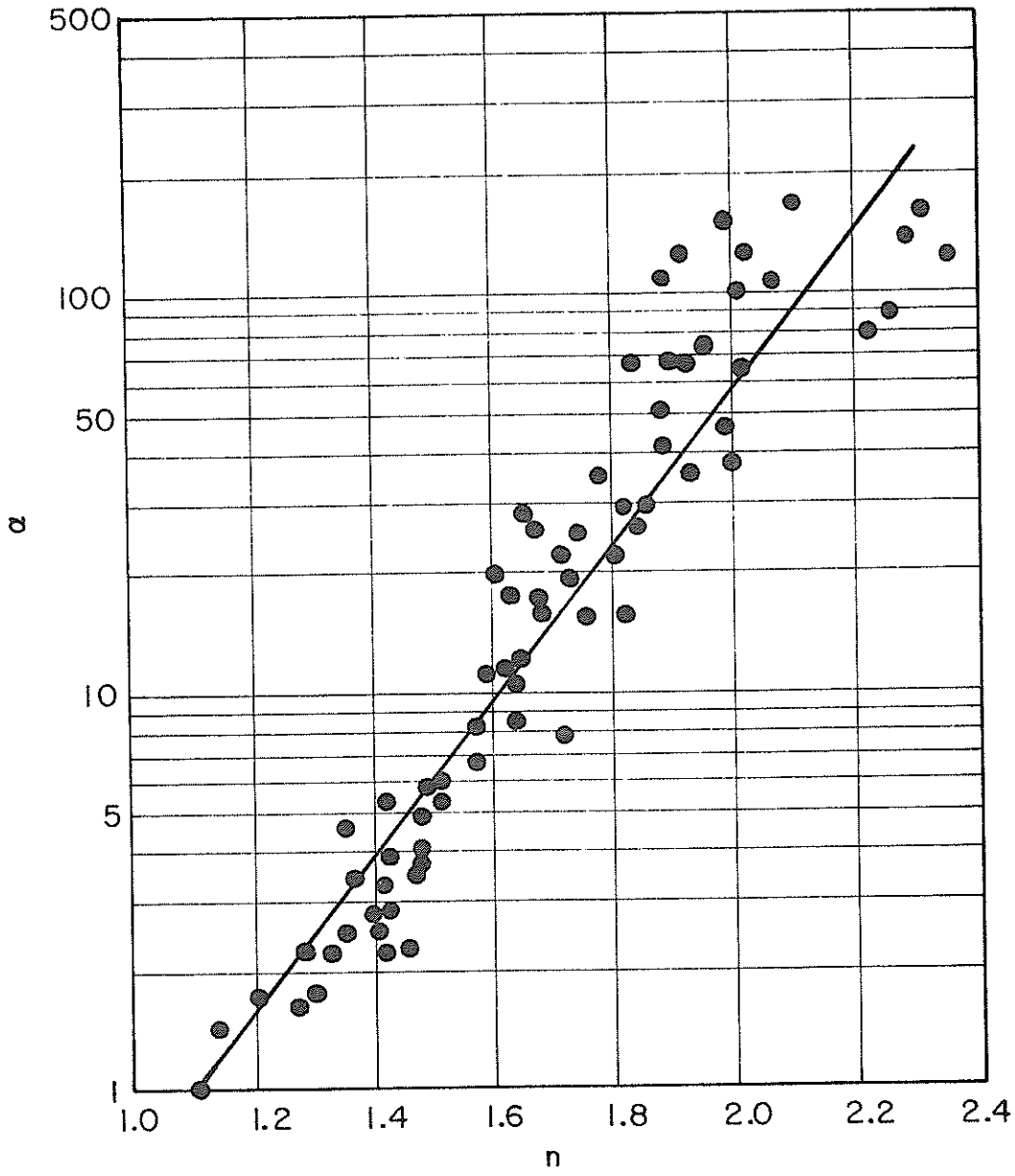

Fig. 5-12. Relationship between parameters n and α for gravel + butyl + bricks surface of rainfall-runoff experimental facility.

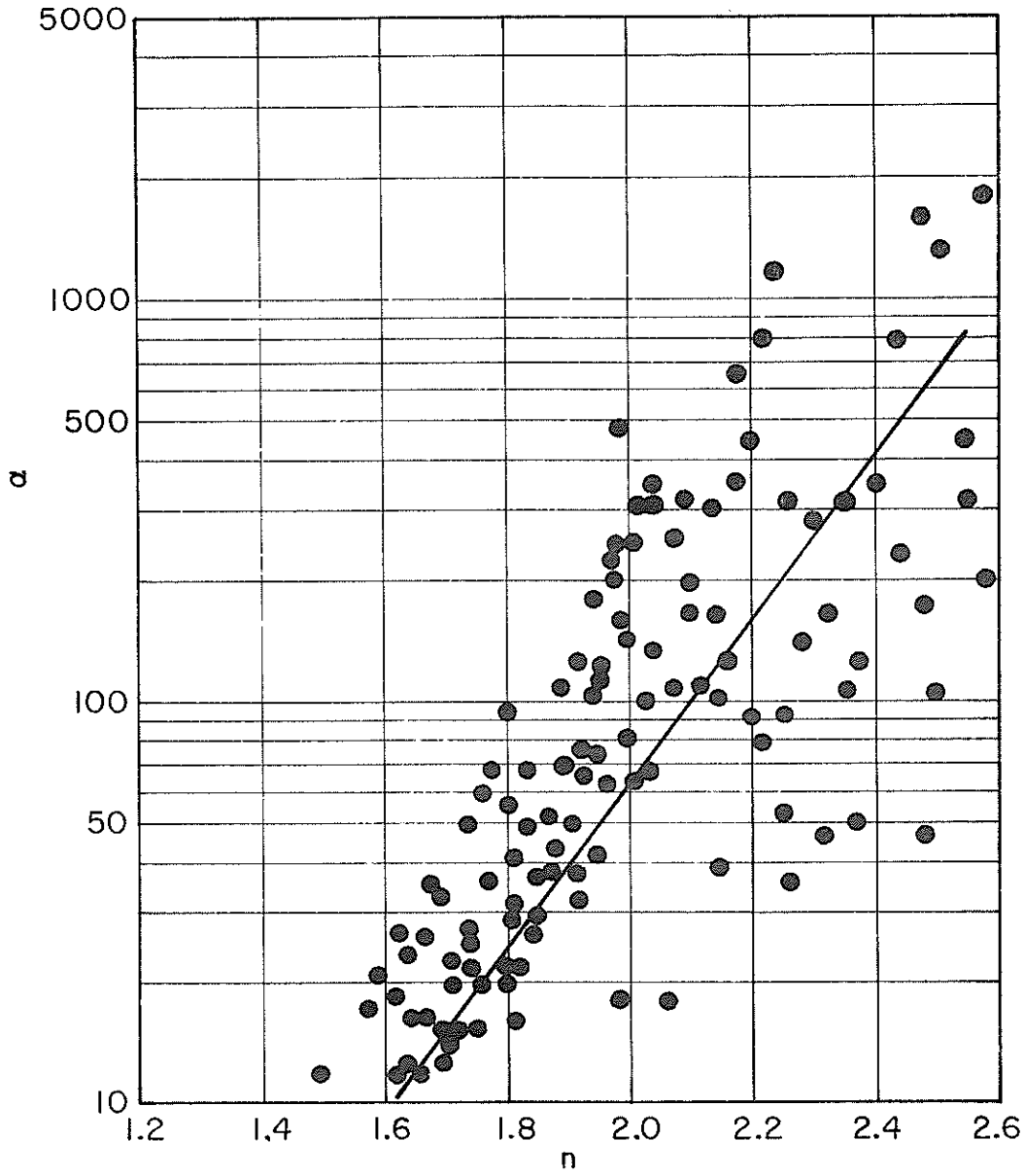

Fig. 5-13. Relationship between parameters n and α for mixture of surfaces of rainfall-runoff experimental facility.

The strong interaction between the parameters n and α suggested that one parameter could be expressed in terms of the other and, therefore, the two-parameter model could be reduced to a one-parameter model. Parameter statistics in Table 5-2, show that the parameter n has much less variance than the parameter α. It was, therefore, decided to keep the parameter n fixed and allow the parameter α to vary. At this point, two questions arise:

1. What should be the value of n ?
2. How much reduction in the variability of α can be achieved by keeping n fixed at a given value?

Based on the statistics in Table 5-2, the only requirement for the parameter, n , is that it must have a value somewhere between 1 and 3 inclusive. Within this range the parameter n may be assigned the value that may have physical justification or interpretation. The parameter n may also be chosen to have the value corresponding to the minimum variance of the parameter, α . These two criteria may not necessarily be complementary. Nevertheless, a value assigned to n on this basis may be a better choice than an arbitrarily chosen one. Keeping this in view, the parameter n was fixed at 1.5; this is physically justifiable in light of Chezy's friction law.

In answering the second question, it must be pointed out that by keeping n fixed at 1.5, the model reduces to a one-parameter model. The objective function of Eq. (4-13) was used to find a unique value of the parameter α corresponding to the matching of computed and observed hydrograph peaks. Based on this objective function, 210 experimental runs covering all the surfaces of the experimental

facility were analyzed. The parameter α was computed for each rainstorm corresponding to the parameter $n = 1.25, 1.50, 1.75, 2.00, 2.25, 2.50, 2.75$, and 3.00 as shown in appendix K. For a selected number of experimental runs, the variability of α with n is shown in Table 5-3. The interaction between the parameters n and α can also be demonstrated by considering the expression for the normalizing time. Rewriting the normalizing time expression,

$$T_o = (1/q_{max})^{(n-1)/n} \left[\frac{L_o(1 - r)}{\alpha}\right]^{1/n} \qquad (5\text{-}4)$$

For a given storm every term in Eq. (5-4) will be constant except n and α. Taking the logarithmic transformation, Eq. (5-4) becomes

$$\ell n T_o = ((n-1)/n)\ell n(1/q_{max}) + (1/n)\ \ell n[L_o(1 - r)] - (1/n)\ \ell n\alpha \qquad (5\text{-}5)$$

Upon rearranging the terms, Eq. (5-5) can be written as:

$$\ell n\alpha = \{\ell n\ q_{max} + \ell n[L_o(1 - r)]\} - n\{\ell n\ T_o + \ell n\ q_{max}\}$$

Let $\eta_1 = \{q_{max}\ L_o(1 - r)\}$

$$\eta_2 = \{\ell n\ T_o + \ell n\ q_{max}\}$$

Then $\alpha = \eta_1 e^{-n\eta_2}$ (5-6)

Equation (5-6) shows the high sensitivity of the parameter α to small changes in the parameter n for a given storm, given the matching of hydrograph peak.

It appears that an n value of 1.5 will also lead to a small variance of α. Therefore the model will now have only one parameter, α.

5.2.2 One-Parameter Model Study

The model now contains only one parameter, that is α. So the questions of estimating the parameter α, and the suitability of the objective function in Eq. (4-13) are considered first.

Table 5-3. Variability in parameter α with parameter n on CSU Rainfall-Runoff Experimental Facility, Fort Collins, Colorado.

Code	Rainfall Intensity (in/hr)	Rainfall Duration (sec)	Hydrograph Peak (in/hr)	Parameter α			
				n=1.25	n=1.50	n=2.25	n=2.75
1-1-8A2	4.19	33.95	1.556	2.80	11.40	814.75	14072.50
2-1-11B	1.08	85.09	0.590	1.94	8.84	880.57	18579.60
3-2-18B	1.03	69.59	0.405	1.13	5.45	649.27	15770.88
4-2-20B	3.36	42.21	1.516	1.68	6.74	454.75	7609.00
5-3-21B	0.90	65.59	0.354	0.63	3.21	442.75	11874.79
6-3-23B	4.39	52.98	2.066	0.65	2.36	115.53	1559.52
7-4-24B	0.98	353.33	0.863	0.65	2.07	73.56	795.70
8-5-27B	1.09	80.78	0.472	1.57	7.24	737.65	16208.44
9-6-30B	1.04	77.79	0.418	1.54	7.21	786.47	18011.11
10-6-32B	4.42	32.69	1.057	1.81	7.30	520.62	8953.37

Parameter Estimation for Individual Events

The parameter α was estimated for a given rainstorm on the experimental facility analytically and numerically. The numerical scheme was based on Newton's method (Conte, 1965). The analytical scheme is described in Appendix H. The estimation of the parameter α was based on the objective function in Eq. (4-13).

In order to check the suitability of objective function in Eq. (4-13), runoff hydrographs were generated for some selected rainfall storms for which the parameter α was estimated a priori. Comparison of computed hydrographs with observed ones displayed remarkably well the suitability of the objective function as shown in sample Fig. 5-14 . It may be fair to say that matching the hydrograph peak leads to an acceptable match of the entire hydrograph, a remarkable feature of the model.

Parameter Optimization for a Set of Events

Two optimization schemes--one based on the statistical least squares principle, and the other on parabolic interpolation--were developed for optimizing the parameter α . Ten rainfall events were selected on the butyl surface of the experimental facility, and the parameter α was optimized.

The scheme based on the statistical least squares principle is described in Appendix H. The objective function for this scheme was based on Eq. (4-6). The parameter α was estimated for each event using Eq. (4-13). The main advantage of this technique is that it lends itself to analytical solution. That is, the parameter can be analytically expressed in terms of other known quantities. This feature has a tremendous time-saving advantage. Utilizing this

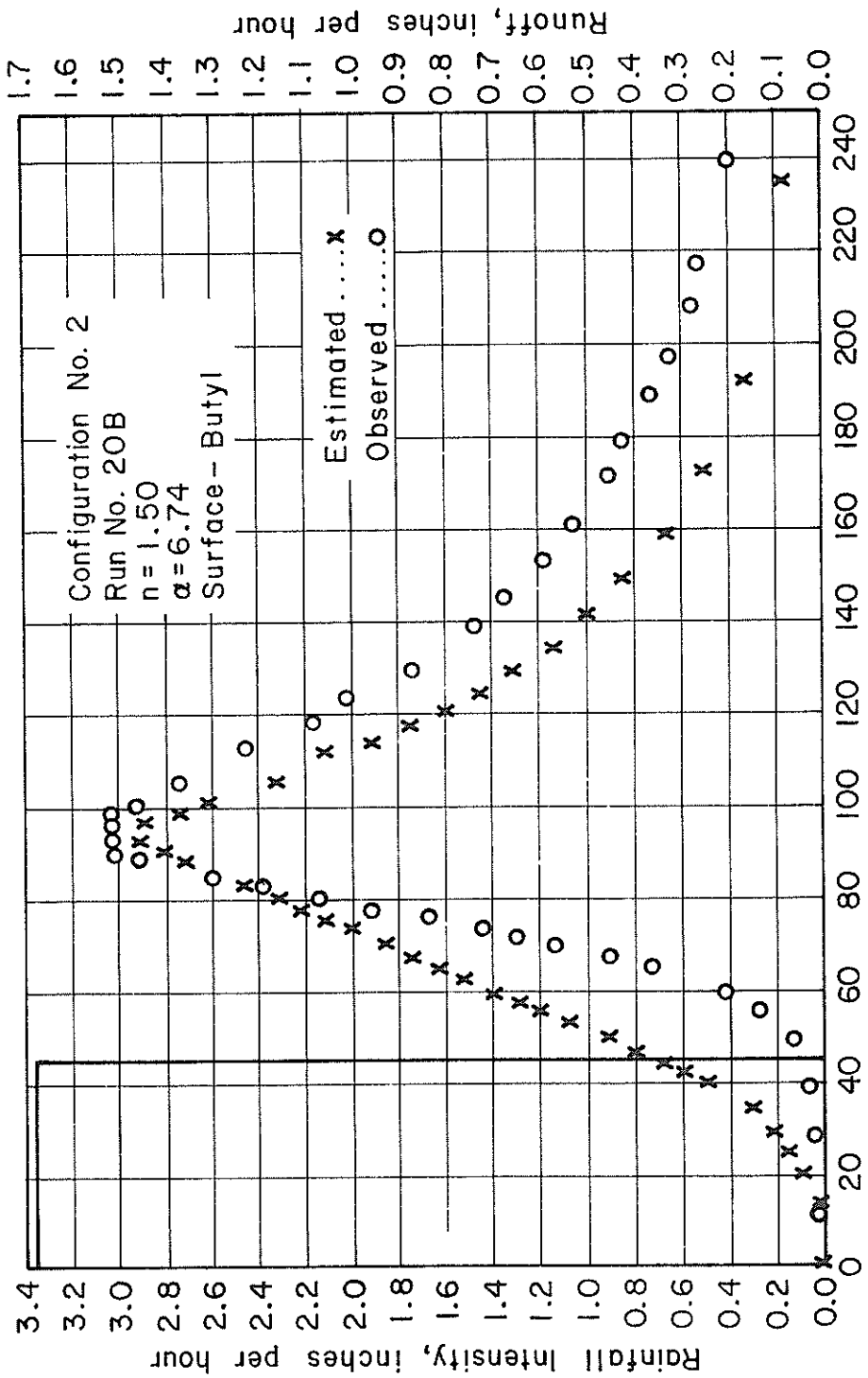

Fig. 5-14. Hydrograph reproduction by converging overland flow model on rainfall-runoff experimental facility.

scheme, the optimal value of the parameter α was found to be 7.34 for the set of selected events. Before leaving this section, it must be pointed out that the objective of matching the hydrograph is well served by concocting the optimization scheme on Eq. (4-6)--a remarkable feature of the kinematic wave model--even though the runoff peak is not explicitly involved in Eq. (4-6).

The other scheme was based on parabolic interpolation. The objective function for the scheme was Eq. (4-2). In this scheme the hydrograph peak appears explicitly. Unlike the previous scheme, the parameter α cannot be determined explicitly, and a search needs to be made for the parameter satisfying Eq. (4-2). The optimum value of the parameter α was found to be 8.70 for that same set of rainfall events by the search technique of parabolic interpolation.

Utilizing the optimized value of the parameter α obtained from both optimization schemes, hydrograph predictions were made for another set of events, not included in the optimization set. The predicted hydrographs are depicted in Figs. 5-15 to 5-18. The agreement between the predicted and observed hydrographs is remarkably good for both schemes. However, the scheme based on Eq. (4-2) appears to be a little better. The prediction performance of the model is shown further in Table 5-4.

Relating Hydrograph Peak to Rainfall and the Parameter α

It was considered worthwhile to attempt to relate directly the hydrograph peak to rainfall intensity and its duration, and the friction parameter α, keeping the parameter $n = 1.5$. Should this be done, it would be of immediate use in estimating hydrograph peak, given the rainfall intensity, duration, and the parameter α. Also a quick

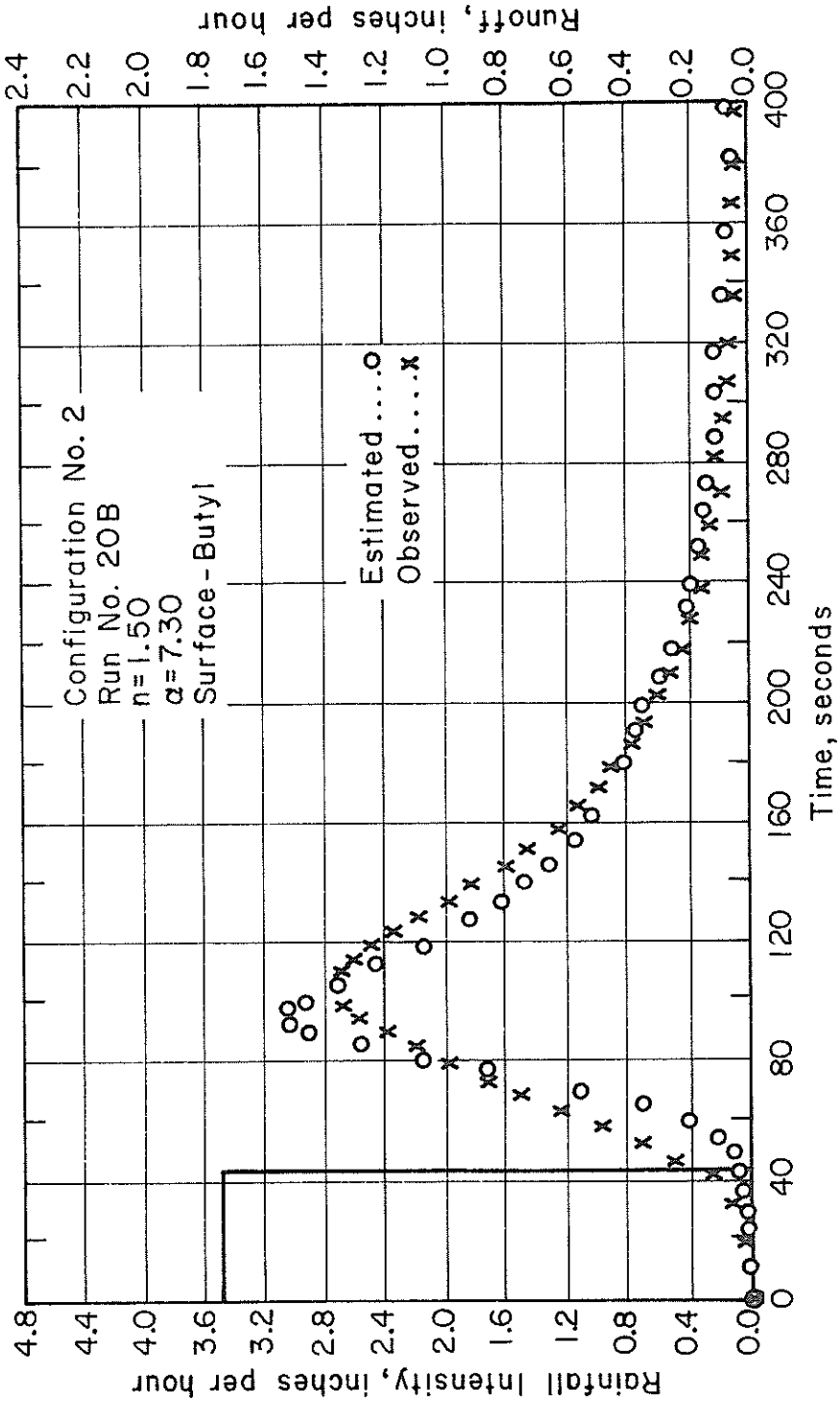

Fig. 5-15. Hydrograph prediction by converging overland flow model on rainfall-runoff experimental facility.

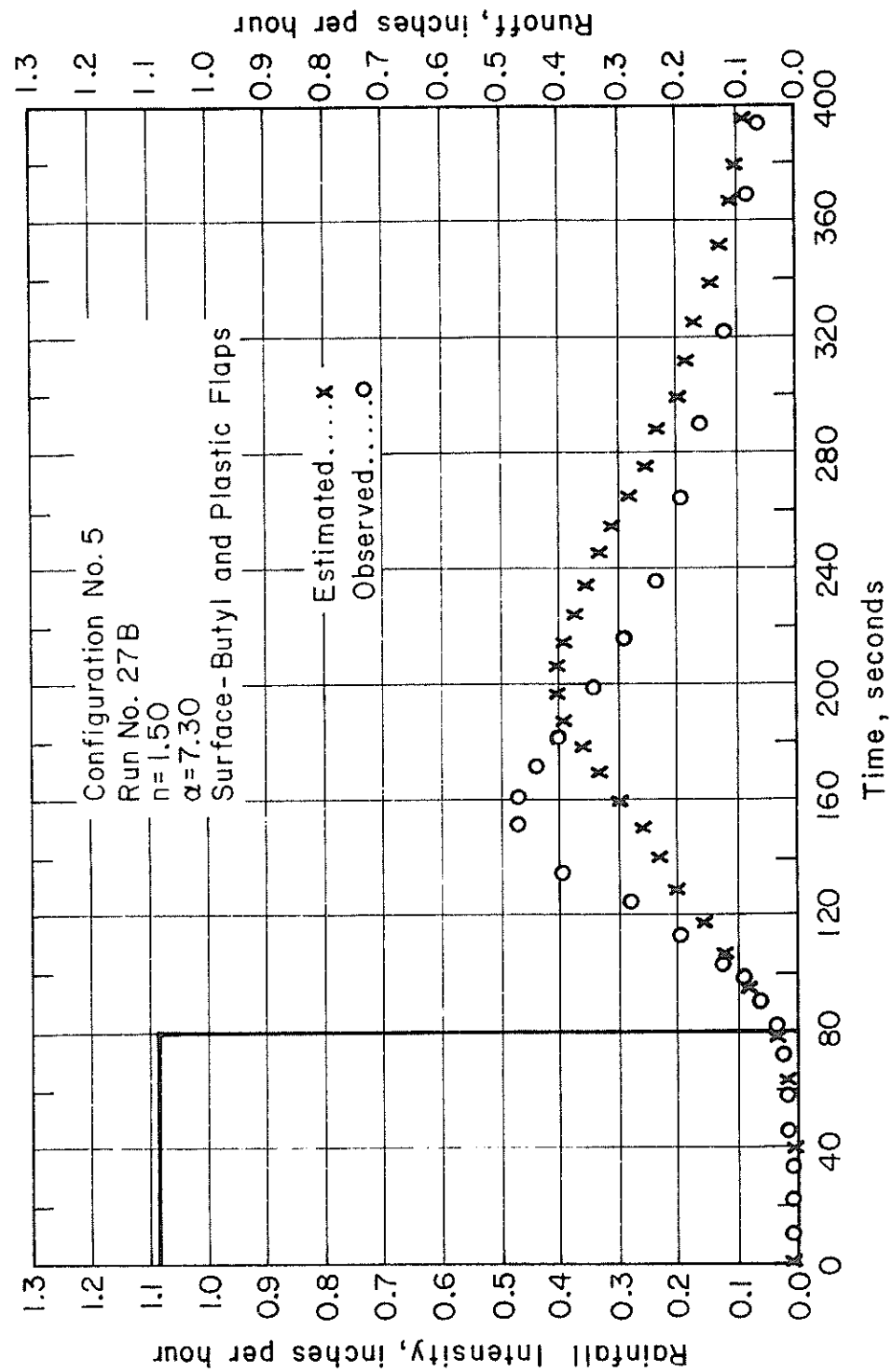

Fig. 5-16. Hydrograph prediction by converging overland flow model on rainfall-runoff experimental facility.

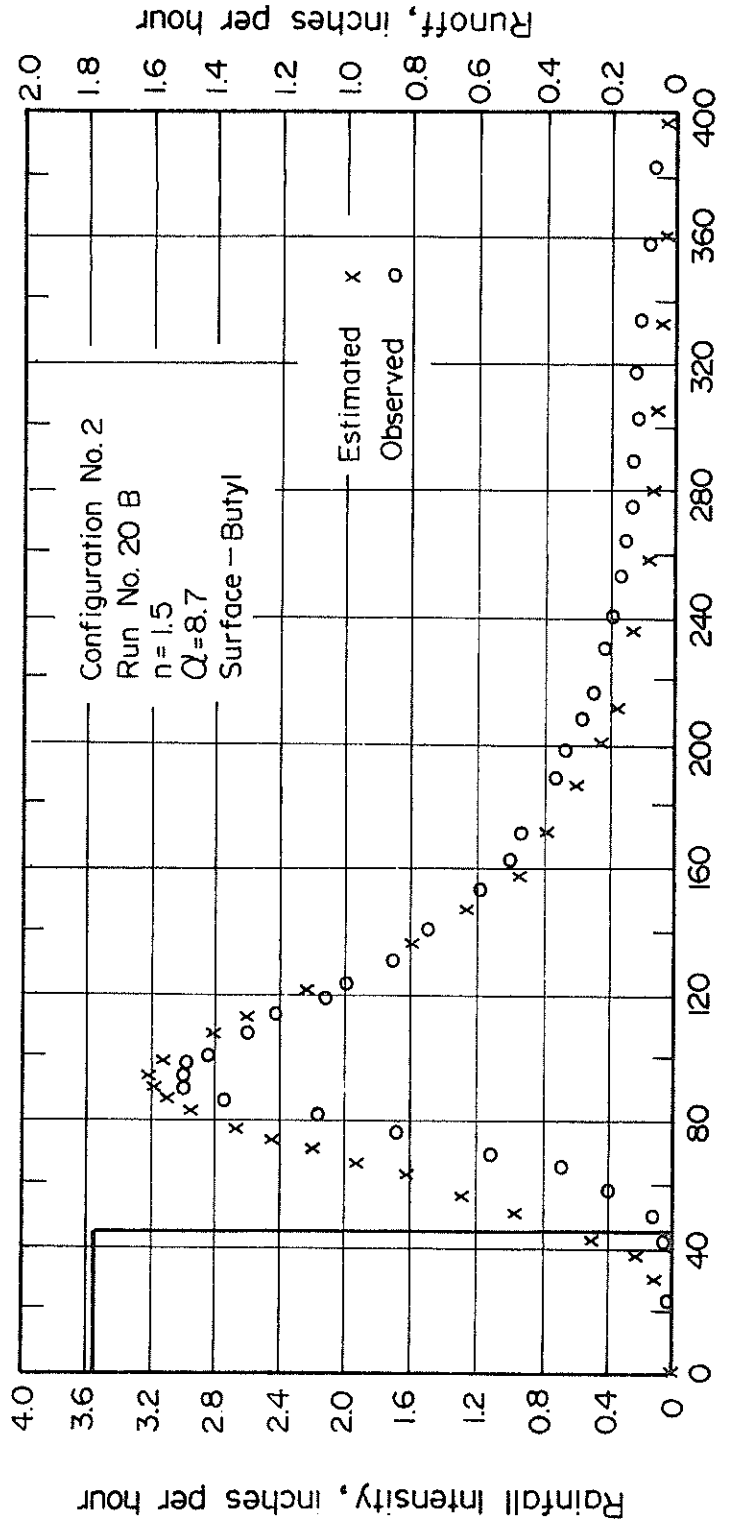

Fig. 5-17. Hydrograph prediction by converging overland flow model on rainfall-runoff experimental facility.

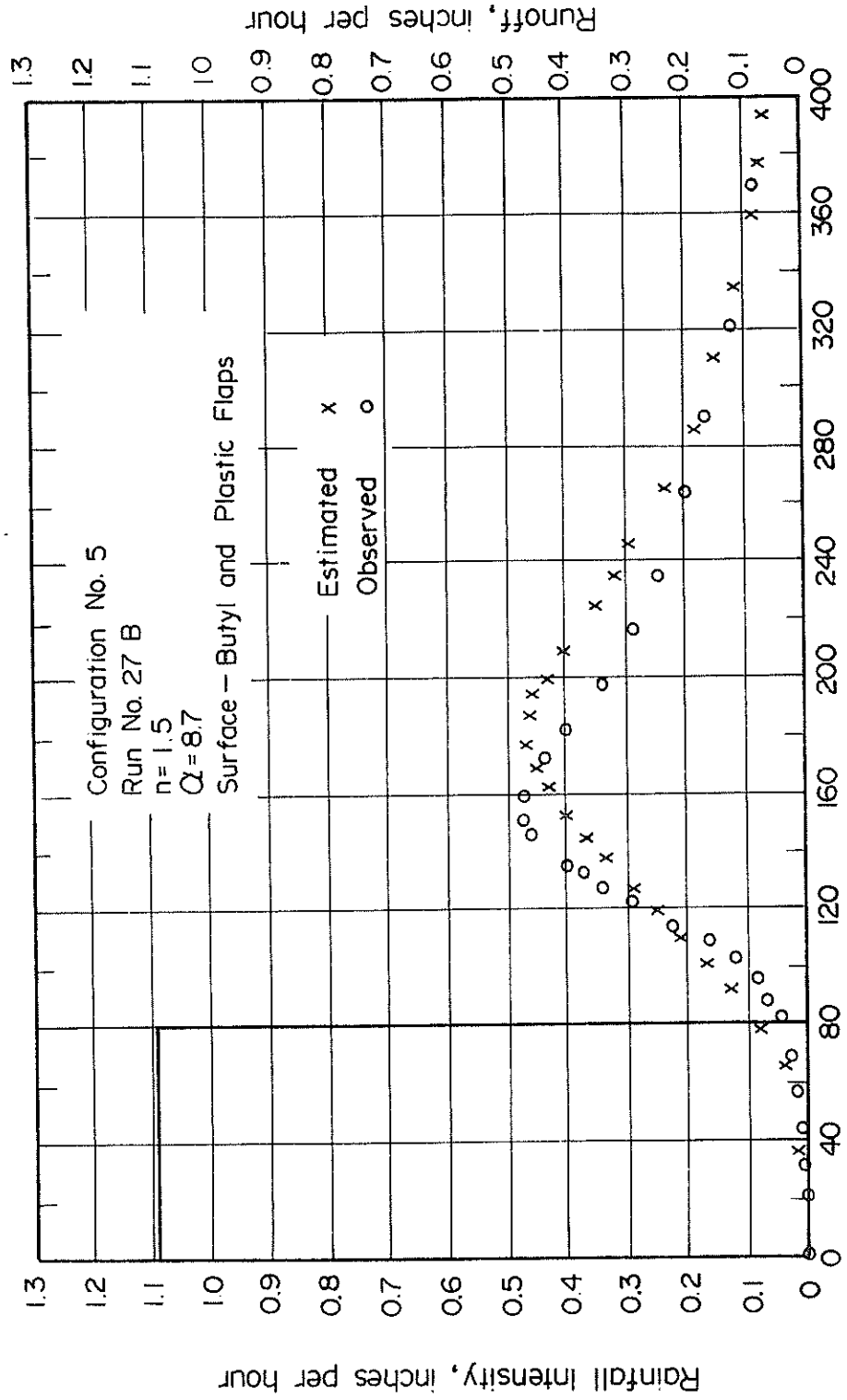

Fig. 5-18. Hydrograph prediction by converging overland flow model on rainfall-runoff experimental facility.

Table 5-4. Predictive performance of converging overland flow model on CSU Rainfall-Runoff Experimental Facility, Fort Collins, Colorado.

Code	Rainfall Intensity (in/hr)	Rainfall Duration (sec)	Hydrograph Peak (in/hr)	Predictive Performance of Converging Overland Flow Model	
				Predicted Hydrograph Peak (in/hr)	Absolute Relative Error (%)
1-1-11B	1.075	85.10	0.590	0.490	16.88
2-2-20B	3.358	45.20	1.516	1.598	5.46
3-2-19B	2.130	51.70	0.803	0.991	23.38
4-5-27B	1.088	80.8	0.472	0.464	1.69
5-6-30B	1.038	77.8	0.418	0.410	1.79
6-17-118	0.890	102.5	0.575	0.478	16.78
7-28-341	0.415	144.2	0.287	0.239	16.79
8-28-343	0.814	65.6	0.245	0.213	12.98
9-28-346	2.035	38.7	0.450	0.381	15.30
9-27-317	2.035	142.6	1.921	1.988	3.52

graphical nomograph solution could be developed to serve as a valuable practical tool. Keeping this notion in perspective, 71 rainfall events on the butyl surface of the experimental facility were analyzed. By matching the hydrograph peak only the parameter α was estimated for each rainfall event. In order to relate hydrograph peak Q_p to the rainfall characteristics, q and D, and the parameter α, a multiple linear regression analysis was performed. In the regression analysis, input variables were logarithmically transformed in various combinations. A large correlation coefficient was obtained in each case. The results can be quantitatively summarized as follows:

$$Q_p = (10)^{-3.16876} q^{1.50274} D^{1.25960} \alpha^{0.45} \tag{5-7}$$

The correlation coefficient in this case was 0.9874 with standard error of estimate = 0.0807.

$$Q_p = (10)^{-1.07673 + 0.00458D + 0.0338\alpha} q^{1.35752} \tag{5-8}$$

The correlation coefficient was 0.9388 with the standard error of estimate = 0.1759.

$$Q_p = (10)^{-2.97890 + 0.03012\alpha} q^{1.47184} D^{1.23955} \tag{5-9}$$

The correlation coefficient was found to ba a 0.9870 with standard error of estimate = 0.0822.

Finally,

$$Q_p = (10)^{-1.28287 + 0.00475\ D} q^{1.39355} \alpha^{0.52896} \tag{5-10}$$

The correlation coefficient was found to be 0.9404 with standard error of estimate = 0.1737. Note that in all cases the relationship $Q_p \leq q$ must hold. These relationships can be very useful in the development of flood frequency distribution and associated relationships.

CHAPTER 6

APPLICATION OF LUMPED PARAMETER MODEL TO NATURAL WATERSHEDS

6.1 GENERAL REMARKS

This chapter includes testing and a rather extensive study of lumped parameter converging overland flow model on uncontrolled, agricultural watersheds. Twenty-one watersheds were selected for this study. They are from two regions: 1. Hastings, Nebraska, and 2. Riesel (Waco), Texas, and have been discussed at some length in the USDA publications entitled "Hydrologic Data for Experimental Agricultural Watersheds in the United States" for various years. Table 6-1 entails brief information on these watersheds. It should be indicated that the physiographic characteristics of the two regions are quite different; within the same region, watershed areas vary from about 2 acres to 4,500 acres.

Deep, fine-textured, granular, slowly permeable, alkaline throughout, and slow internal drainage are typical characteristics of soils of watersheds near Riesel (Waco), Texas. The dominance of Houston black clay is notable. These soils are also noted for the formation of large extensive cracks upon drying. Surface drainage is, by and large, good, but no well-defined drainageways exist on the watersheds. Usually, water is drained by rills and poorly defined field gullies.

Most of the time these watersheds are covered with an agricultural crop. Because of low permeability of the soils the watersheds respond rapidly to rainfall and produce quickly rising hydrographs. For the events under consideration the major part of rainfall was observed as surface runoff; the infiltration losses did not dominate (see Table 6-5).

Table 6-1. Characteristics of experimental agricultural watersheds.

Watershed identification	Area (Acres)	Weighted average slope (%)	Soil characteristics	Surface drainage
Riesel (Waco) Texas				
Watershed C	579.00	2.1100	Soils of varying texture and structure; slow internal drainage; deep, fine textured, slowly permeable soils noteworthy; cracks upon drying	Good, few well-defined waterways, much of drainage by field gullies and rills
Watershed D	1,110.00	2.1750	-do-	-do-
Watershed G	4,380.00	2.1500	-do-	-do-
Watershed W-1	176.00	2.2400	Deep, fine textured, granular, slowly permeable, alkaline throughout, slow internal drainage; Houston black clay notable; extensive cracks upon drying	-do-
Watershed W-2	130.00	2.4750	-do-	-do-
Watershed W-6	42.30	2.0250	-do-	-do-
Watershed W-10	19.70	1.7550	-do-	-do-
Watershed Y	303.00	2.4200	-do-	-do-
Watershed Y-2	132.00	2.6150	-do-	-do-
Watershed Y-4	79.90	2.8700	-do-	-do-

Table 6-1. (continued)

Watershed identification	Area (Acres)	Weighted average slope (%)	Soil characteristics	Surface drainage
Watershed Y-6	16.30	3.2750	-do-	-do-
Watershed Y-7	40.00	1.9100	-do-	-do-
Watershed Y-8	20.80	2.0550	-do-	-do-
Watershed Y-10	18.60	2.3750	-do-	-do-
Watershed SW-12	2.97	3.8100	-do-	-do-
Watershed SW-17	2.99	1.8300	-do-	-do-
Hastings, Nebraska				
Watershed 2-H	3.40	9.9250	Loessial; internal drainage medium; silt loam predominant; permeability moderate	Good; overland flow deominant
Watershed 4-H	3.64	5.9600	Loessial; moderate internal drainage; mixture of silt loam and clay; permeability moderate	Good; surface flow to a well-defined waterway
Watershed W-3	481.00	7.1250	-do-	Good; arterial flow to a central drainageway; channel meandering present
Watershed W-8	2,086.0	5.5000	-do-	-do-
Watershed W-11	3,490.0	5.0950	-do-	-do-

The watersheds near Hastings, Nebraska, have Loessial soils. The top soil is normally a mixture of silt loam and silt clay. The internal drainage is medium, and the permeability of subsoil is moderately slow. Surface drainage is good. The watersheds develop arterial flow toward a central drainageway. Channel meandering is noticeable and leads to impounding some water.

These are also agricultural watersheds and have agricultural cover on the surface. A major part of the rainwater seeps into the ground as shown in Table 6-2, thus infiltration losses are predominant. Their response to rainfall input is not as fast as that of watersheds near Riesel (Waco), Texas, especially for the events under consideration.

Rainfall-runoff data for the aforementioned watersheds were obtained from two sources: 1. USDA publications on hydrologic data, and 2. the USDA Hydrologic Data Center, USDA-ARS, Beltsville, Maryland. Rainfall-runoff data for watersheds near Riesel (Waco), Texas, were obtained directly from the USDA publications on hydrologic data. These publications are released almost every year and consist of about one rainfall-runoff event per year for a watershed.

For watersheds near Hastings, Nebraska, the data were obtained from the USDA Hydrologic Data Center. They are for a longer period of time and consist of all rainfall-runoff events for a year on a watershed. The dates of the rainfall-runoff events used in this analysis are given in Table 6-3.

Although a watershed has more than one raingage, data are normally available in the USDA publications for a centrally located raingage only, indicating that this has been taken to represent the mean areal rainfall.

Table 6-2. Summary of rainfall, infiltration, and runoff for selected storms on watershed 2-H, Hastings, Nebraska.

Serial number	Date of rainfall runoff event	Rainfall volume (in)	Runoff volume (in)	Infiltration loss (in)	Loss coefficient (loss/rainfall volume)	Runoff coefficient (runoff volume/ rainfall volume)
1	8-11-1939	0.770	0.156	0.615	0.798	0.202
2	5-20-1949	0.670	0.041	0.630	0.940	0.060
3	6-16-1950	2.570	0.580	1.991	0.775	0.226
4	5-20-1954	2.510	0.461	2.049	0.816	0.184
5	6-12-1958	1.720	0.180	1.540	0.895	0.105
6	7- 3-1959	2.620	1.414	1.206	0.460	0.540
7	5-15-1960	2.150	0.586	1.564	0.727	0.273
8	8-11-1961	1.543	0.160	1.384	0.897	0.103
9	8-23-1962	1.860	0.432	1.428	0.768	0.232
10	6-21-1964	1.020	0.107	0.913	0.895	0.105

Table 6-3. Dates of selected runoff events.

Serial number	Watershed	Runoff event number					
		1	2	3	4	5	6
1	Watershed C	6-10-41	4-24-57	5- 9-57	5-13-57	6-23-59	7- 9-61
2	Watershed D	5- 6-55	5- 3-57	6-23-59	12-31-59	7-16-61	7-23-61
3	Watershed G	7-14-41	2-14-59	8-23-59	11- 4-59	12-13-59	7-16-61
4	Watershed W-1	3-12-53	5-13-57	6- 4-57	6-23-59	6-15-61	7-16-61
5	Watershed W-2	5-22-51	3-12-53	4-24-57	5-13-57	6-23-57	6-25-61
6	Watershed W-6	4-27-49	4-24-57	5-13-57	6-23-57	6-18-57	6-25-61
7	Watershed W-10	3-12-53	4-24-57	6- 4-57	6-23-59	5-22-61	6-25-61
8	Watershed Y	4-27-49	3-31-57	4-24-57	6- 4-57	6-23-59	7-16-61
9	Watershed Y-2	3-26-46	4-24-57	5-13-57	6- 4-57	6-23-59	7-16-61
10	Watershed Y-4	3-12-53	4-24-57	5-13-57	6- 4-57	6-23-59	6-25-61
11	Watershed Y-6	5- 6-55	4-24-57	5-13-57	6- 4-57	6-23-59	5-25-61
12	Watershed Y-7	5- 6-55	4-24-57	5-13-57	6- 4-57	6-23-59	5-22-61
13	Watershed Y-8	3-12-53	4-24-57	5-13-57	6- 4-57	6-23-59	6-18-61
14	Watershed Y-10	5- 6-55	4-24-57	5-13-57	6- 4-57	6-23-59	5-25-61
15	Watershed SW-12	3-12-53	6- 4-57	6-23-59	6- 9-62	3-29-65	
16	Watershed SW-17	3-12-53	3-31-57	4-24-57	5-13-57	6-23-59	6-26-61
17	Watershed 2-H	8-13-39	6-22-42	8- 7-42	9- 7-42	8-23-44	8- 7-47
18	Watershed 4-H	8-11-39	6-20-42	8- 7-42	9- 7-42	8-29-44	8- 7-46
19	Watershed W-3	6-10-42	9- 5-46	5-20-49	6- 5-49	9-19-50	6-25-51
20	Watershed W-8	6- 5-48	6-14-43	5-11-44	6- 5-45	7-16-45	9-19-50
21	Watershed W-11	5-11-44	9-19-50	6- 1-51	7-10-51	6-26-52	7-13-52

Table 6-3. (continued)

Serial number	Watershed	Runoff event number					
		7	8	9	10	11	12
1	Watershed C	7-16-61	6- 4-62	5-10-65			
2	Watershed D	6- 4-62	5-10-65				
3	Watershed G	7-23-61	6- 9-61	3-29-65			
4	Watershed W-1	6- 9-62	3-29-65				
5	Watershed W-2	6- 9-61	3-29-65				
6	Watershed W-6	6- 9-62	3-29-65				
7	Watershed W-10	6- 9-62	3-29-65				
8	Watershed Y	6-26-61	6- 9-62	3-29-65			
9	Watershed Y-2	6-25-61	6- 9-62	3-29-65			
10	Watershed Y-4	7-16-61	6- 9-62	3-29-65			
11	Watershed Y-6	6-15-61	6- 9-62	3-29-65			
12	Watershed Y-7	7-16-61	6- 9-62	3-29-65			
13	Watershed Y-8	6- 9-62	3-29-65				
14	Watershed Y-10	6-21-61	6- 9-62	3-29-65			
15	Watershed SW-12						
16	Watershed SW-17	7-16-61	6- 9-62	3-29-65			
17	Watershed 2-H	9- 5-46	5-20-49	6-16-50	6- 1-51	6-26-52	7-13-52
18	Watershed 4-H	9- 5-46	5-20-49	6-16-50	6- 1-51	6-26-52	7-13-52
19	Watershed W-3	7-10-51	5-21-52	6-26-52	7-13-52	6- 7-53	6-15-57
20	Watershed W-8	6- 1-51	7-10-51	6-26-52	6-29-52	7- 6-52	6- 7-53
21	Watershed W-11	5-22-54	6-16-57	6-14-61	5-21-65		

Table 6-3. (continued)

Serial number	Watershed	Runoff event number 13	14	15	16	17	18
17	Watershed 2-H	5-22-54	6-12-58	7- 3-59	5-15-60	3-23-62	6-12-65
18	Watershed 4-H	5-22-54	6-12-58	5-15-60	8-23-62	6-12-65	6-12-65
19	Watershed W-3	6-15-57	6-16-57	7- 3-59			
20	Watershed W-8	6-16-57	6-16-57	7- 3-59			
21	Watershed W-11						

Table 6-3 (continued)

Serial number	Watershed	Runoff event number 19	20
17	Watershed 2-H	6-12-65	6-29-65
18	Watershed 4-H	6-19-65	
19	Watershed W-3		
20	Watershed W-8		
21	Watershed W-11		

In order to be consistent throughout, this practice has been followed on each watershed.

6.1.1 Determination of Rainfall-Excess

Rainfall-excess forms the input to the model. Estimating infiltration is essential for determining rainfall-excess. Infiltration was estimated by two methods:

1. ϕ - Index,

2. Philip's Infiltration Equation.

In the ϕ - Index method the infiltration capacity is assumed constant throughout a storm. It is the rate above which rainfall volume equals the runoff volume, thus preserving the continuity of flow over the surface of the ground. The ϕ - Index will always lie between zero and maximum rainfall intensity. It will vary from storm to storm. It was estimated by a numerical scheme called the method of "Regula Falsi" or the method of false position (Conte, 1965).

Philip's infiltration equation is written as

$$f = A + st^{\frac{1}{2}} \quad ,$$

or

$$F = At + 2st^{\frac{1}{2}} \qquad (6\text{-}1)$$

where A = a parameter dependent on soil characteristics and initial moisture conditions, s = a parameter dependent on soil characteristics and initial soil moisture conditions, t = time, f = infiltration rate, and F = accumulated infiltration.

The parameters A and s have the dimensions L/T and $L/\sqrt{T}$ respectively; L denotes the length dimension and T time dimension. Note that the parameter A has the same dimension as f.

Theoretically, the parameters A and s will vary from storm to storm on the same watershed and from watershed to watershed for the same storm. The parameter A was considered roughly identical to steady infiltration, thus rendered amendable to determination from physical characteristics of the soil. It could also be considered roughly equivalent to saturated hydraulic conductivity. In the absence of information on steady infiltration it was taken roughly equal to 50% to 80% of the lowest ϕ - Index estimated for given storms on the watershed under consideration. The parameter A determined for each watershed is given in Table 6-4.

The parameter s was allowed to vary with each rainfall episode, thus accounting for soil moisture conditions existing prior to its occurrence. It was estimated for each storm by Newton's Algorithm subject to preserving the mass continuity. The parameter s was found sensitive to antecedent soil moisture conditions and relatively less sensitive to the parameter A. This is clearly evidenced by Table 6-5.

6.1.2 Geometric Representation

An important question is how to represent the watershed geometry in a simple manner that would preserve some important hydrograph characteristics and yet not so simple as to sacrifice important details affecting the dynamics of overland and channel flow. This question was considered in choosing converging geometry. In the representation of a natural watershed geometry by a linearly converging section of a cone, two parameters ought to be determined, namely, 1) length of flow, $L_o(1 - r)$, and 2) degree of convergence, r, where L_o represents the total length of the converging section. Given the area of the watershed, the angle, θ, can be determined, and thus the converging section geometry can be completely characterized.

Table 6-4. Parameter A of Philip's equation for agricultural watersheds.

Serial number	Watershed identification	Parameter A	Serial number	Watershed identification	Parameter A
	Riesel (Waco) Texas		11	Watershed Y-6	0.050
1	Watershed C	0.100	12	Watershed Y-7	0.025
2	Watershed D	0.100	13	Watershed Y-8	0.025
3	Watershed G	0.100	14	Watershed Y-10	0.025
4	Watershed W-1	0.050	15	Watershed SW-12	0.050
5	Watershed W-2	0.050	16	Watershed SW-17	0.010
6	Watershed W-6	0.060		Hastings, Nebraska	
7	Watershed W-10	0.100	17	Watershed 2-H	0.200
8	Watershed Y	0.100	18	Watershed 4-H	0.050
9	Watershed Y-1	0.025	19	Watershed W-3	0.050
10	Watershed Y-4	0.025	20	Watershed W-8	0.125
			21	Watershed W-11	0.010

Table 6-5. Philip's infiltration model parameters and their statistics for Watershed SW-17, Riesel (Waco), Texas

Serial number		Rainfall volume (in)	Runoff volume (in)	Infiltration loss (in)	Loss coefficient (loss/rainfall)	Parameter s for			
						A=0.03	A=0.05	A=0.06	A=0.09
1	3-12-1953	0.830	0.695	0.135	0.162	0.249	0.206	0.200	0.157
2	3-31-1957	0.590	0.240	0.350	0.593	0.951	0.941	0.936	0.921
3	5-13-1957	1.620	1.360	0.260	0.161	0.138	0.106	0.090	0.041
4	6-23-1959	1.990	1.520	0.470	0.236	0.507	0.485	0.473	0.439
5	6-25-1961	1.380	0.350	1.030	0.746	3.976	3.917	3.888	3.800
6	7-16-1961	1.080	0.280	0.800	0.741	1.085	1.070	1.063	1.040
7	6- 9-1962	2.080	1.670	0.410	0.197	0.498	0.473	0.461	0.425

Parameter Statistics

Parameter A	Average s	Standard deviation of s	Coefficient of variation of s
0.03	1.058	1.332	1.260
0.05	1.028	1.322	1.286
0.06	1.016	1.315	1.295
0.09	0.975	1.298	1.332

The geometric parameters $L_o(1 - r)$ and r were determined for a watershed from its physiographic map. The parameter $L_o(1-r)$ was estimated by measuring the longest horizontal projection; that is, the horizontal distance from the outlet to the most remote point of the watershed. The parameter r was fixed at 0.01. On the basis of experience this value of r was found adequate for all the watersheds considered for this study. The converging geometry for respective watersheds is given in Table 6-6.

6.2 MODEL TESTING

In the quantification of the goodness of model performance an objective criterion of evaluation must be delineated. Two aspects must be incorporated in any such criterion. One pertains to hydrodynamic adequacy and the other computational efficiency. The former implies that the hypothesized model should represent or encompass in some way those physical details that affect the overland flow dynamics and hence be able to reproduce the overland flow process as closely as possible. The latter must include: 1. efficiency of computation, 2. ease of programming, and 3. storage (computer) requirement. This same objective criterion can be utilized in comparison of one model with another. In that case it is quite likely that one model may be better than the other but only in some respects and not necessarily uniformly. To choose amongst models under such circumstances some kind of trade-off seems to be the only plausible alternative. It must, however, be emphasized that hydrodynamic adequacy must form a necessary requirement. The requirement of sufficiency may be met by satisfying the computational requirement. These two aspects, therefore, form necessary and sufficient conditions which, upon satisfaction, will quantify the goodness of a model.

Table 6-6. Converging section geometry representing natural watersheds.

Serial number	Watershed identification	Area (acres)	Length of flow (ft)	Degree of convergence r
	Riesel (Waco), Texas			
1	Watershed C	579.00	8,000	0.01
2	Watershed D	1,110.00	12,000	0.01
3	Watershed G	4,380.00	22,000	0.01
4	Watershed W-1	176.00	3,500	0.01
5	Watershed W-2	130.00	2,100	0.01
6	Watershed W-6	42.30	1,200	0.01
7	Watershed W-10	19.70	800	0.01
8	Watershed Y	309.00	4,800	0.01
9	Watershed Y-2	132.00	3,200	0.01
10	Watershed Y-4	79.80	2,400	0.01
11	Watershed Y-6	16.30	1,200	0.01
12	Watershed Y-7	40.00	1,800	0.01
13	Watershed Y-8	20.80	1,000	0.01
14	Watershed Y-10	18.60	1,000	0.01
15	Watershed SW-12	2.97	450	0.01
16	Watershed SW-17	2.99	400	0.01
	Hastings, Nebraska			
17	Watershed 2-H	3.40	600	0.01
18	Watershed 4-H	3.64	500	0.01
19	Watershed W-3	481.00	7,540	0.01
20	Watershed W-8	2,086.00	17,348	0.01
21	Watershed W-11	3,490.00	27,154	0.01

Nineteen rainfall-runoff events were selected on watershed 2-H, Hastings, Nebraska. These were randomly divided into two sets: one was the optimization set consisting of 10 events and the other the prediction set consisting of 9 events. These two sets did not have any event in common. The model parameter α was optimized over the optimization set by parabolic interpolation scheme utilizing the objective function of Eq. (4-2). Infiltration was estimated by Philip's equation. The optimum value of α was 4.75. Utilizing the optimized parameter value hydrograph predictions were made for another set of events — the prediction set. Upon examining the hydrographs predicted by the model and comparing them with observed hydrographs it was clear that the model performed fairly well in predicting the hydrograph peak in particular and the entire hydrograph in general. An examination of the events for which the model predictions were relatively poor revealed that in most cases these were the complex events with two or more peaks and that the rainfall excess pattern as computed was not consistent with the relative magnitude of the observed peaks. A sample display of hydrographs predicted by the model is shown in Table 6-7 and Figs. 6-1 through 6-3.

6.3 DETAILED STUDY OF THE MODEL

After preliminary model testing several questions arise that may require further perusal. One question is to enumerate the effect of infiltration on the model performance and its parameters. The other is to test its adequacy on watersheds in different geographical regions. Another is with regard to the parameter α and its estimation a priori from information ordinarily available on a watershed. These questions will be addressed in the ensuing discussion.

Table 6-7. Predictive performance of converging overland flow model on watershed 2-H, Hastings, Nebraska.

Serial numbers	Date of Rainfall event	Observed Hydrograph Peak (In/hr)	Predicted Hydrograph Peak (In/hr)
1	6-20-1942	0.572	0.491
2	6-23-1944	0.493	0.311
3	6-26-1952	0.849	1.232
4	7-13-1952	1.860	1.959
5	5-22-1954	1.890	1.632
6	6-12-1958	0.849	0.804
7	7- 3-1959	2.520	4.065
8	5-15-1960	1.550	2.124
9	3-23-1962	1.230	1.751
	Mean	1.313	1.597
	Variance	0.476	1.270
	Standard deviation	0.690	1.127
	Coefficient of variation	0.525	0.704

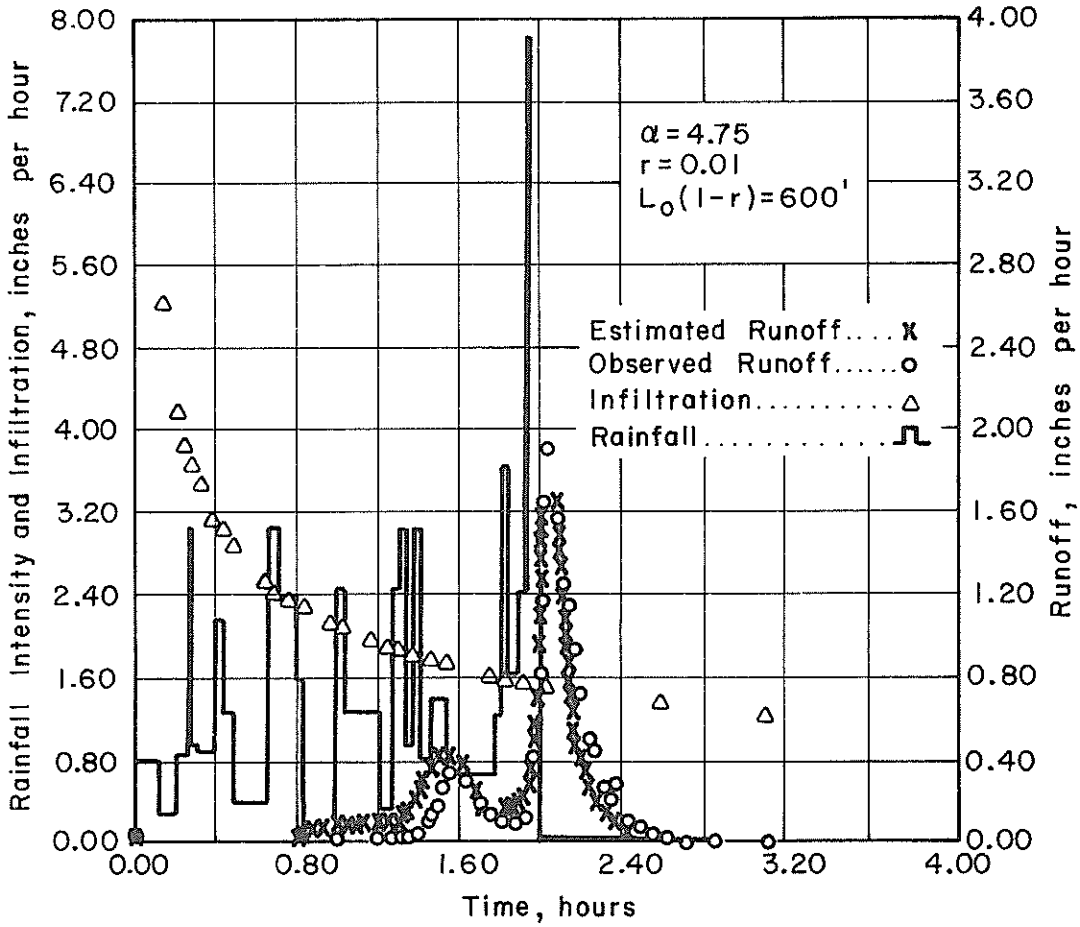

Fig. 6-1. Hydrograph prediction by converging overland flow model for rainfall event of 5-22-1954 on watershed 2-H, Hastings, Nebraska.

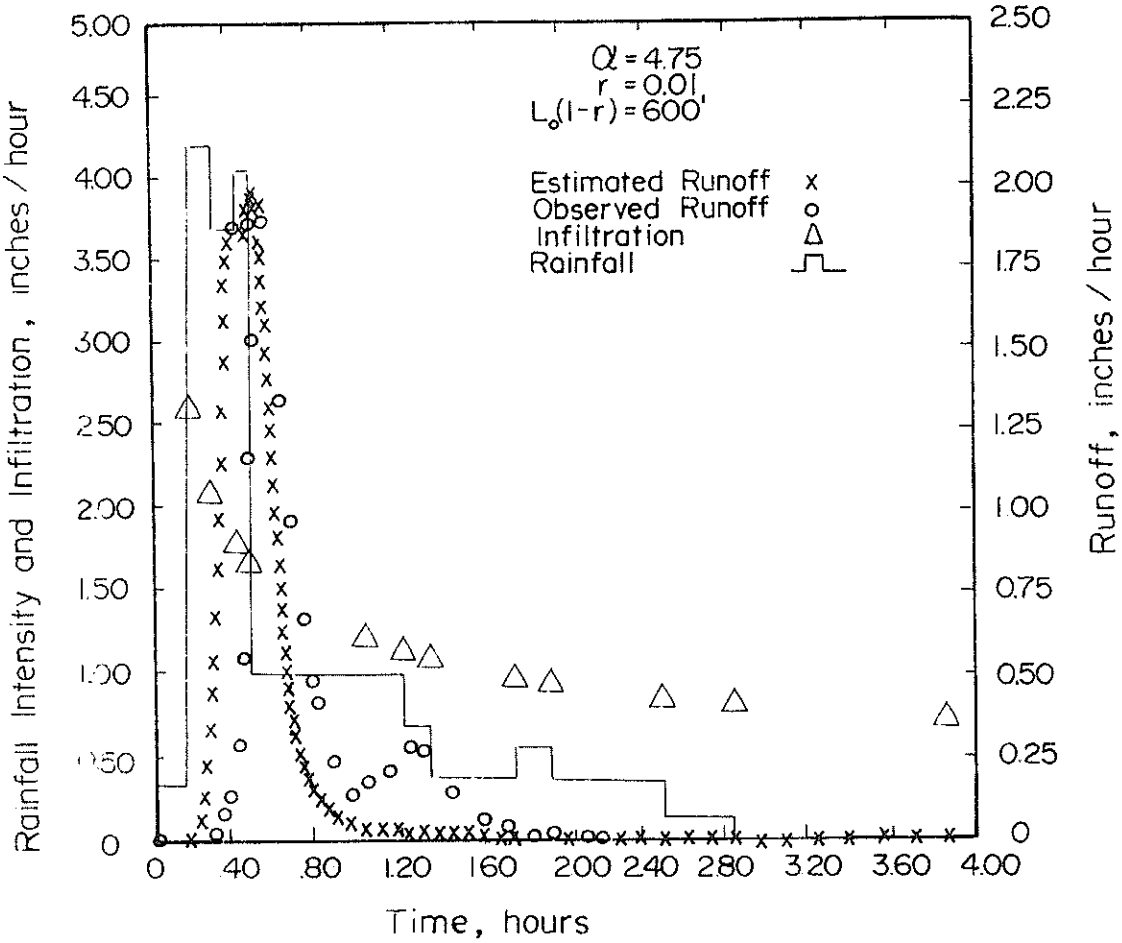

Fig. 6-2. Hydrograph prediction by converging overland flow model for rainfall event of 7-13-1952 on watershed 2-H, Hastings, Nebraska.

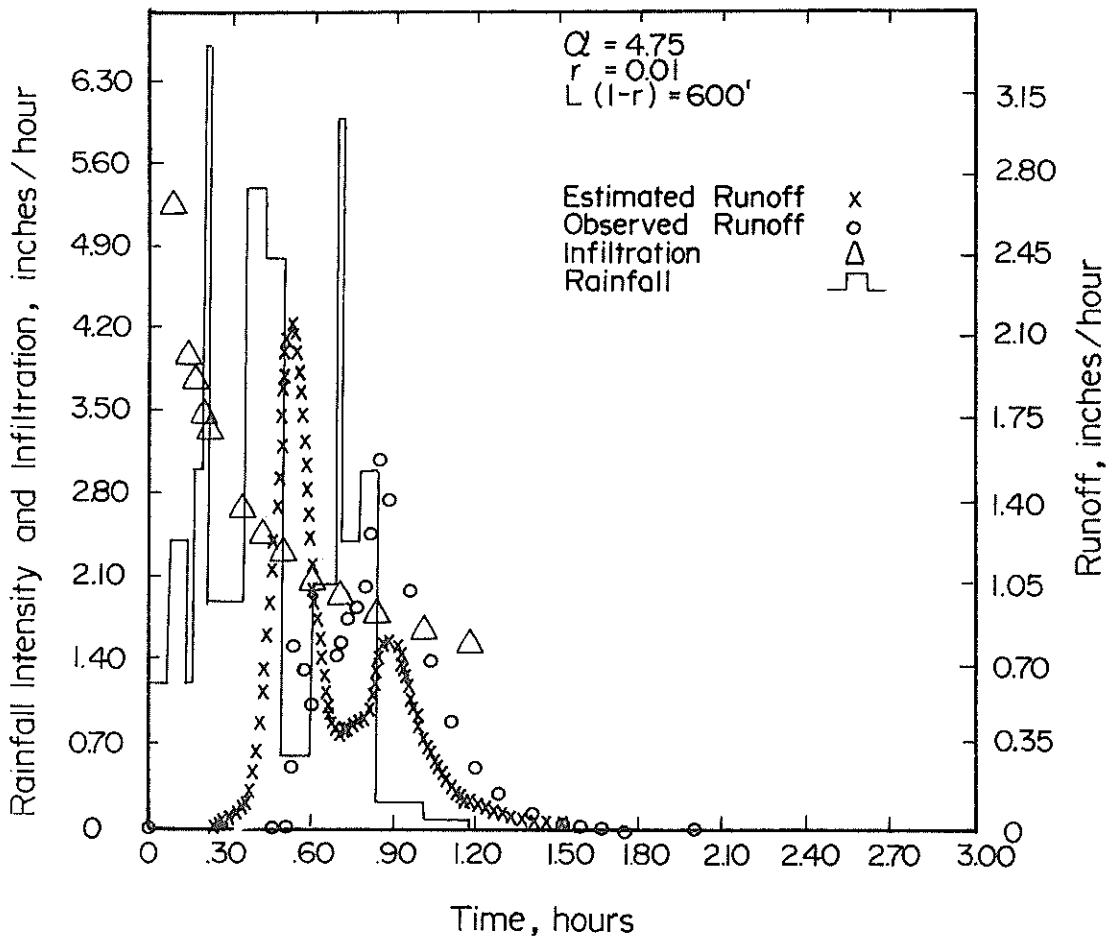

Fig. 6-3. Hydrograph prediction by converging overland flow model for rainfall event of 5-15-1960 on watershed 2-H, Hastings, Nebraska.

6.3.1 Effect of Infiltration on Model Performance and Parameter Estimation

Determining the effect of infiltration estimating scheme on the model performance and its parameters is essential to assess its adequacy. One infiltration method may be better than the other, but only under limited circumstances. The effect of the mechanics of infiltration estimation on the model performance will be very much governed by the rainfall characteristics, soil characteristics, antecedent conditions, and physiography of the watershed. Short duration, high intensity rainstorms ordinarily produce sharply rising, short duration hydrographs. Under such circumstances, a simpler method like ϕ - Index may not be wholly unacceptable. In fact, it may work nearly as good as a realatively complex method. Such situations seem to exist on some of the watersheds near Riesel (Waco), Texas, where the combination of climatology with watershed physiography makes a simple method like ϕ - Index work quite well.

The parameter α was estimated for a number of rainfall events on watershed SW-17 near Riesel (Waco), Texas, by matching the hydrograph peak (Eq. (4-13)) utilizing ϕ - Index and Philip's equation for infiltration. Table 6-8 provides the parameter α obtained by matching the hydrograph peak for a number of rainfall events. It is evident that for these cases the parameter α is not very sensitive to the mechanics of infiltration estimation.

To observe the effect of infiltration methods on model results, five rainfall-runoff events were selected on that same watershed SW-17, and the parameter α was optimized (objective function, Eq. (4-2)) by the method of parabolic interpolation. The optimum value of α was found to be 0.900 for both methods of infiltration. Hydrograph predictions were performed

Table 6-8. Effect of infiltration on the model parameter α for Watershed SW-17, Riesel (Waco), Texas.

Serial number	Date of rainfall-runoff event	Hydrograph peak (in/hr)	Parameter α	
			ϕ - Index	Philip's Equation
1	3-12-1953	1.610	0.870	0.858
2	3-31-1957	0.441	0.965	0.962
3	4-24-1957	2.900	0.711	0.709
4	5-13-1957	1.740	0.493	0.529
5	6-24-1957	2.170	1.395	0.928
6	6-25-1961	0.604	2.026	1.720
7	7-16-1961	0.348	0.618	0.640
8	6- 9-1962	3.790	1.398	1.381
9	3-29-1965	2.440	0.346	0.342
Mean		1.783	1.060	0.897
Variance		1.392	0.264	0.183
Standard Deviation		1.180	0.513	0.428
Coefficient of Variation		0.662	0.485	0.477

for another set of rainfall events and comparisons made. Both methods fared nearly equally well in representing the dynamics of overland flow. Statistics of hydrograph predictions are included in Table 6-9. Sample predicted hydrographs are shown in Figs. 6-4 & 6-5.

However, the situation peculiar to the watershed SW-17 may not always hold on the same watershed or on others. To further investigate the effect of infiltration methods watershed 2-H, Hastings, Nebraska, was chosen. It was decided to include the length of flow $L_o(1 - r)$, and degree of convergence r also as parameters besides the parameter α in the model. A set of 10 rainfall events were selected for optimization. In contrast to the watershed SW-17, Riesel (Waco), Texas, the parameters were found to be extremely sensitive to the method of computing infiltration.

Using ϕ - Index, optimized parameter values were found to be $L_o(1 - r) = 756$ ft, $r = 0.1954$, $\alpha = 2.3223$ and using Philip's equation, optimized parameter values were $L_o(1 - r) = 480$ ft, $r = 0.005$, and $\alpha = 3.7323$. The objective function of Eq. (4-2) was utilized for parameter optimization by the TVA optimization scheme based on differential algorithm and principle component analysis. Another set of 10 events were selected for hydrograph prediction on the same watershed 2-H, Hastings, Nebraska. Utilizing the optimized values of the parameters obtained for both methods hydrographs were predicted. The results and their statistics are shown in Table 6-10. Philip's equation appears to be superior to the simple ϕ - Index on this watershed. On the basis of these results, Philip's equation was considered to be superior to ϕ - Index.

As mentioned previously, hydrograph predictions were made for 10 rainfall events on Watershed 2-H, Hastings, Nebraska. The model geometry

Table 6-9. Effect of infiltration on the model performance on Watershed SW-17, Riesel (Waco), Texas.

Serial number	Date of rainfall event	Observed hydrograph peak (in/hr)	Predicted hydrograph peak (in/hr)	
			ϕ - Index	Philip's Equation
1	4-24-1957	2.900	3.216	3.212
2	5-13-1957	1.740	2.268	2.185
3	6- 9-1962	3.790	3.355	3.361
4	3-29-1965	2.440	2.282	3.258
Mean		2.717	3.030	2.642
Variance		0.739	0.262	1.200
Standard Deviation		0.860	0.512	1.095
Coefficient of Variation		0.717	0.169	0.415

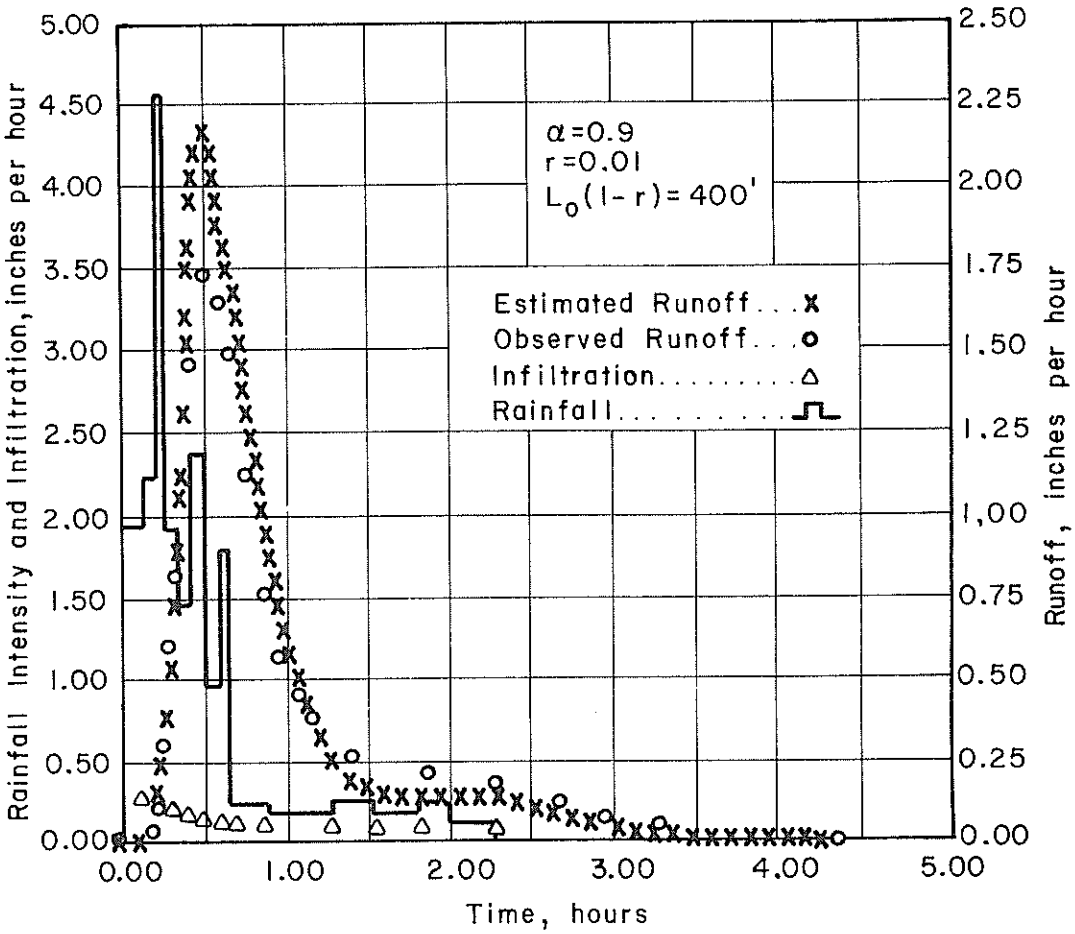

Fig. 6-4. Hydrograph prediction by converging overland flow model, using Philip's equation, for rainfall event of 5-13-1957 on watershed SW-17, Riesel (Waco), Texas.

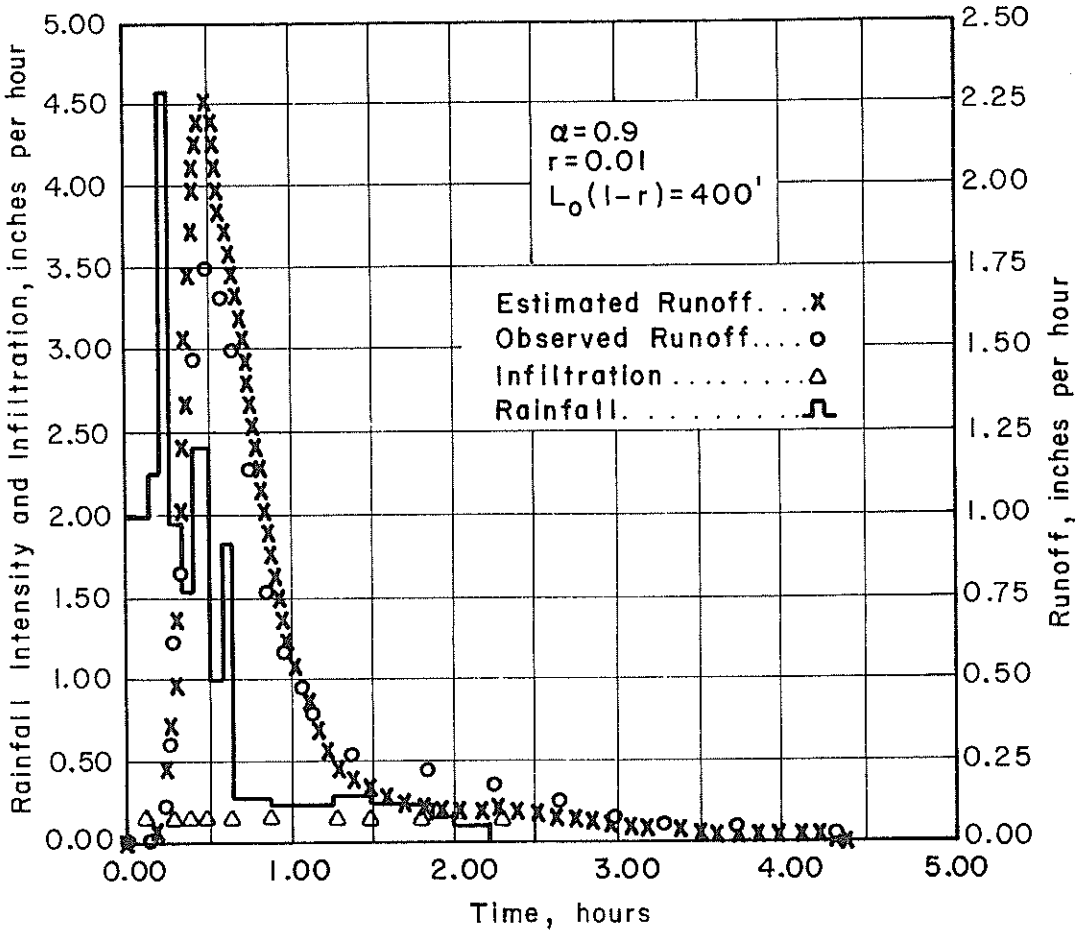

Fig. 6-5. Hydrograph prediction by converging overland flow model, using ϕ-index, for rainfall event of 5-13-57 on watershed SW-17, Riesel (Waco), Texas.

Table 6-10. Influence of infiltration on predictive performance of the model on Watershed 2-H, Hastings, Nebraska.

Serial number	Date of rainfall storm	Observed hydrograph peak (in/hr)	Predicted peak (in/hr)	
			ϕ - Index	Philip's equation
1	7-13-1952	1.860	1.630	1.959
2	5-22-1954	1.890	0.539	1.632
3	5-15-1960	1.550	1.175	2.124
4	6- 1-1951	1.170	0.599	1.354
5	6-26-1952	0.849	0.472	1.232
6	8-23-1962	1.230	1.116	1.751
7	6-20-1942	0.572	0.192	0.491
8	8-23-1944	0.493	0.522	0.311
9	6-12-1958	0.849	0.330	0.804
Mean		1.163	0.731	1.295
Variance		0.271	0.221	0.414
Standard Deviation		0.520	0.470	0.644
Coefficient of Variation		0.447	0.644	0.497

was determined from watershed physiography as indicated in the preceding section, keeping r = 0.01 for each watershed. In Table 6-11 relative and absolute prediction errors are given. Figs. 6-6 through 6-9 display some predicted hydrographs. From these figures, it is quite clear that the predicted hydrographs compare well with the observed ones. This further supports the earlier conclusion that matching the hydrograph peak is sufficient to match the entire hydrograph — a remarkable characteristic of the model. The average relative percentage error (ignoring the algebraic sign) stays within the limit 30%. This, however, is for a small sample considered in the study, and more exhaustive testing needs to be done. Nevertheless, it does indicate that the model has the potential for adequate representation of runoff dynamics.

To test the model on another watershed in a different geographical region, some prediction runs were made on watershed SW-17, Riesel (Waco), Texas. Prediction errors are listed in Table 6-12, and predicted hydrographs are compared with observed ones in Figs. 6-10 through 6-12. The predictive capability of the model is further demonstrated.

6.4 INVESTIGATION OF MODEL PARAMETER α

In investigating the significance of the parameter α three questions naturally arise:

1. How does the parameter vary on a watershed from one rainfall event to another?
2. What can be concluded with regard to the physical significance of the parameter?
3. Can the parameter be related to what is ordinarily known a priori about a watershed?

Table 6-11. Predictive performance of the model on Watershed 2-H, Hastings, Nebraska.

Serial number	Date of rainfall event	Observed hydrograph peak (in/hr)	Computed hydrograph peak (in/hr)	Absolute error of prediction[1] (in/hr)	Relative error of prediction[2] (%)
1	6-20-1942	0.572	0.491	0.081	14.161
2	8-23-1944	0.493	0.311	0.182	36.978
3	6- 1-1951	1.170	1.355	-0.185	15.778
4	7-13-1952	1.860	1.959	-0.099	5.296
5	5-22-1954	1.890	1.632	0.258	13.651
6	6-25-1952	0.849	1.232	-0.383	45.065
7	6-12-1958	0.849	0.804	0.045	5.253
8	7- 3-1959	2.520	4.065	-1.545	61.310
9	5-15-1960	1.550	2.124	-0.574	37.058
10	3-23-1962	1.230	1.751	-0.521	42.358

Mean of Relative Error = 27.691

[1]Absolute Error of Prediction = $(Q_{p_o} - Q_{p_e})$

[2]Relative Error of Prediction = $\left|\frac{Q_{p_o} - Q_{p_o}}{Q_{p_o}}\right|$

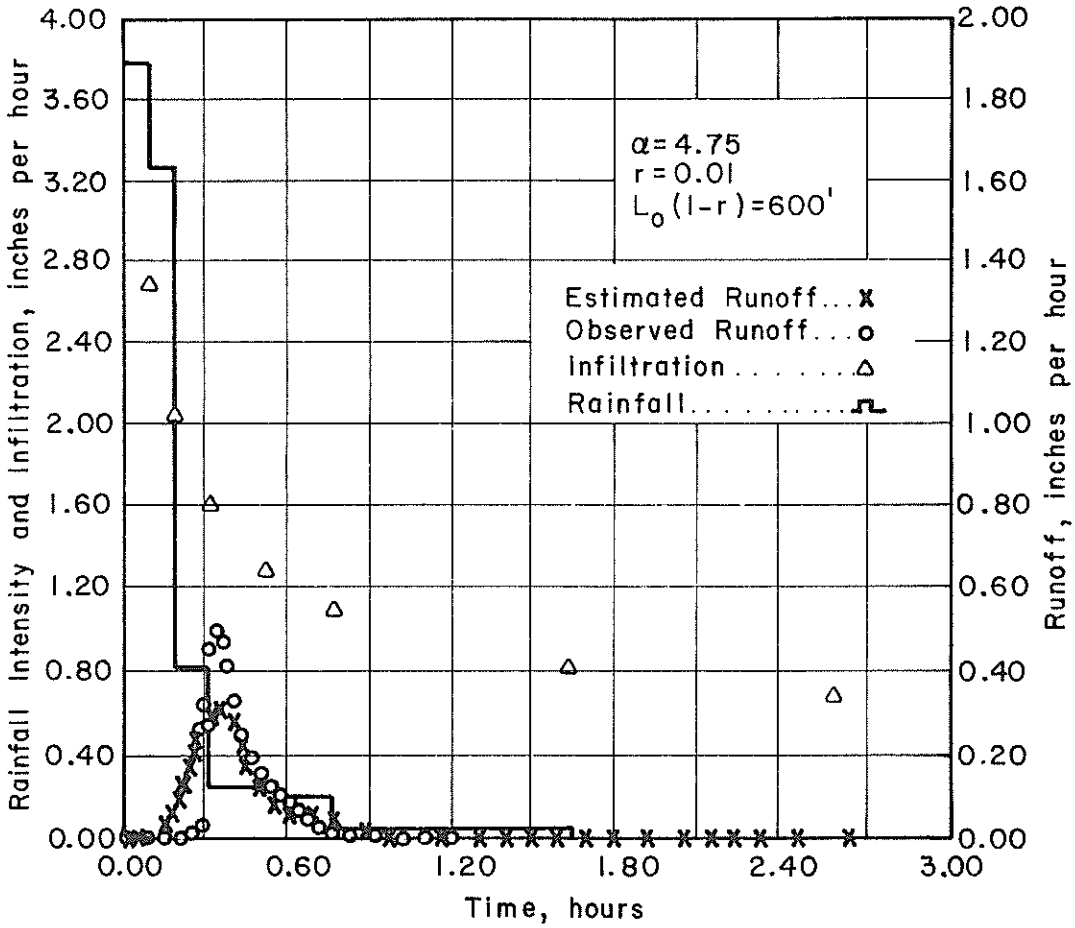

Fig. 6-6. Hydrograph prediction by converging overland flow model for rainfall event of 8-29-1944 on watershed 2-H, Hastings, Nebraska.

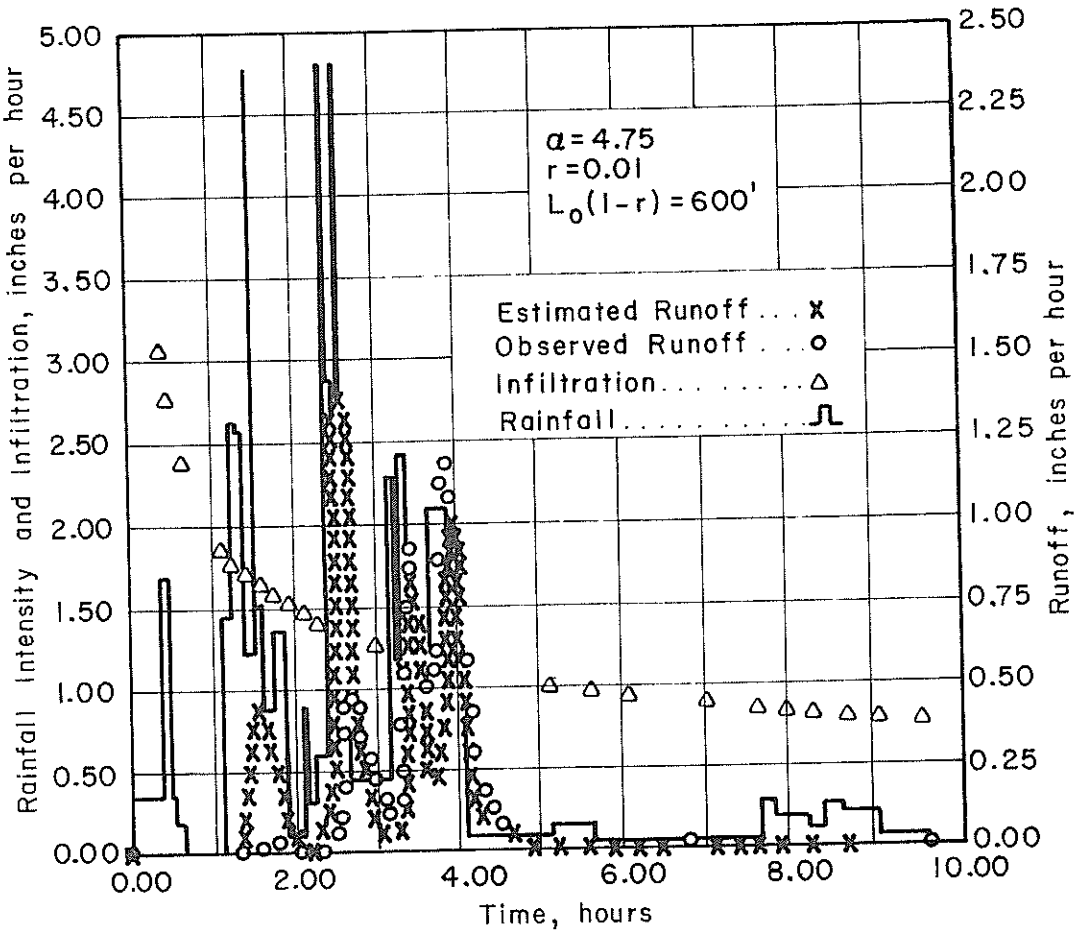

Fig. 6-7. Hydrograph prediction by converging overland flow model for rainfall event of 6-1-1951 on watershed 2-H, Hastings, Nebraska.

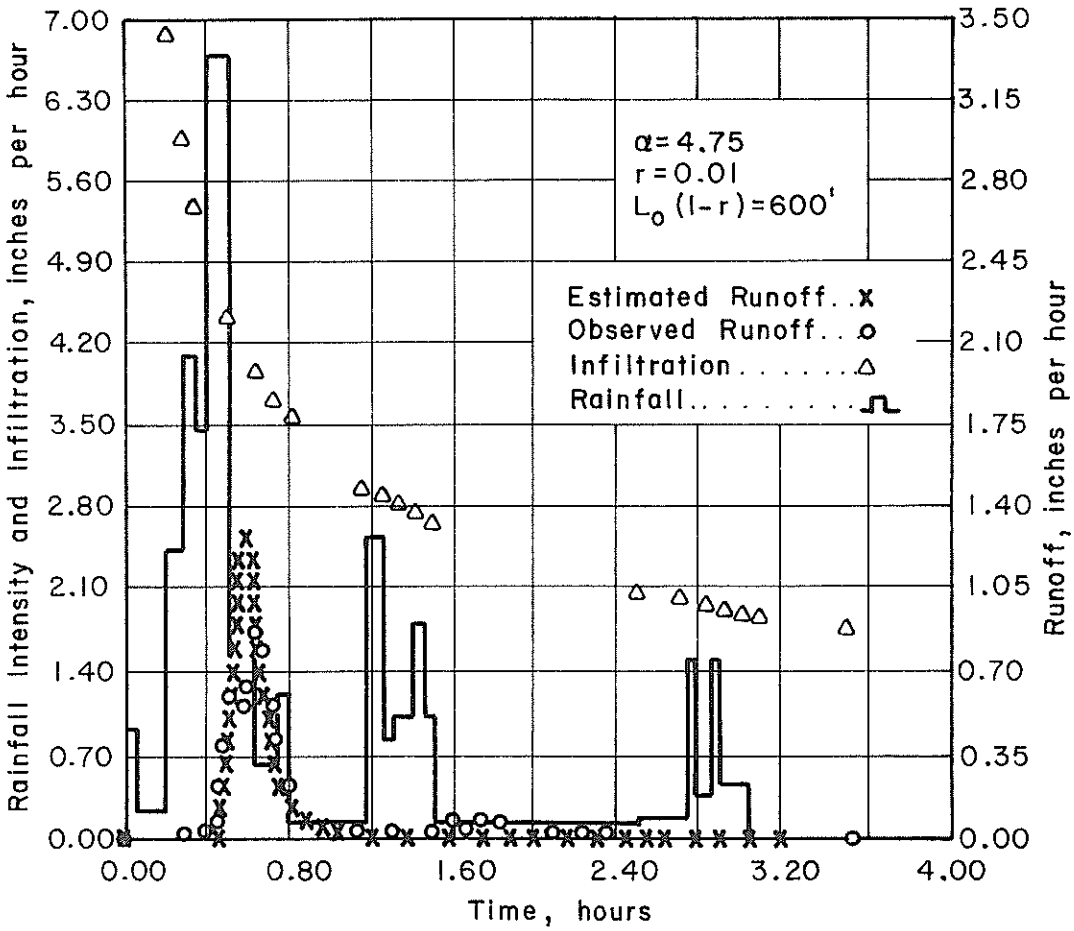

Fig. 6-8. Hydrograph prediction by converging overland flow model for rainfall event of 6-26-1952 on watershed 2-H, Hastings, Nebraska.

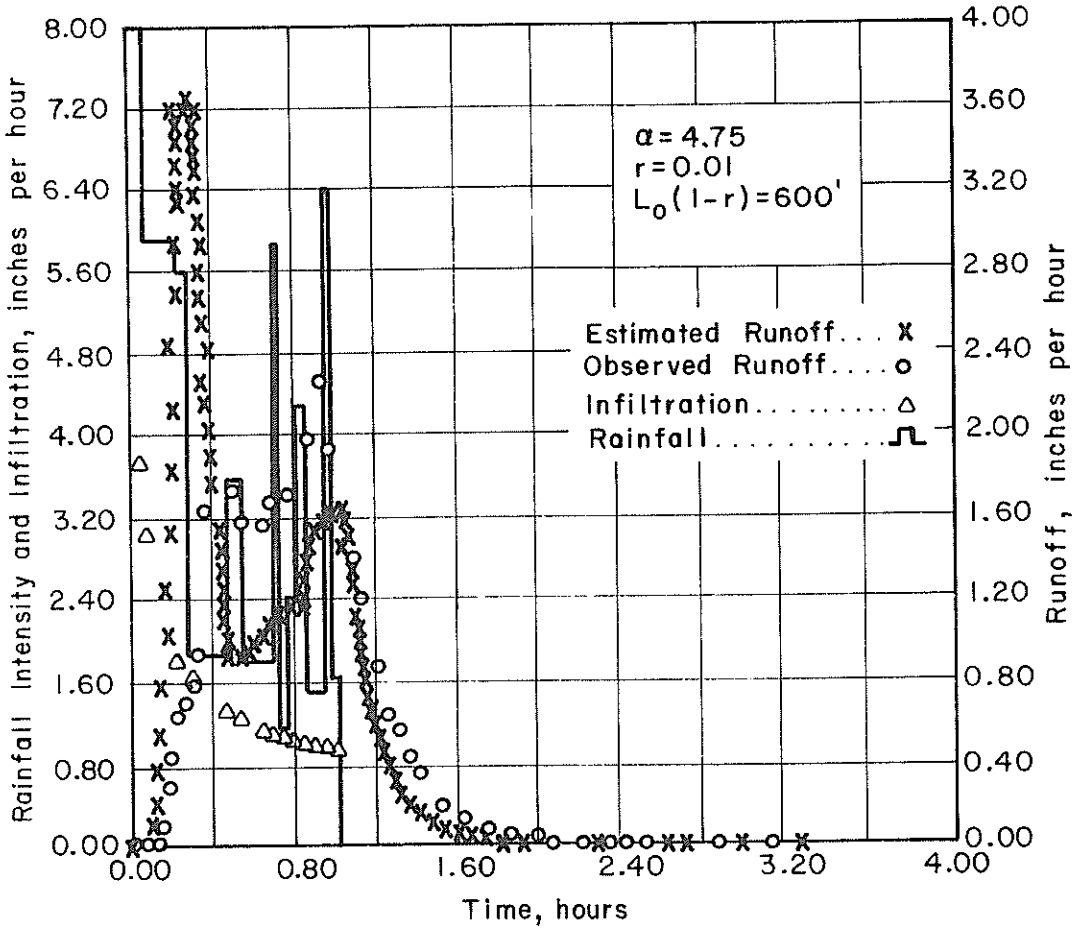

Fig. 6-9. Hydrograph prediction by converging overland flow model for rainfall event of 7-13-59 on watershed 2-H, Hastings, Nebraska.

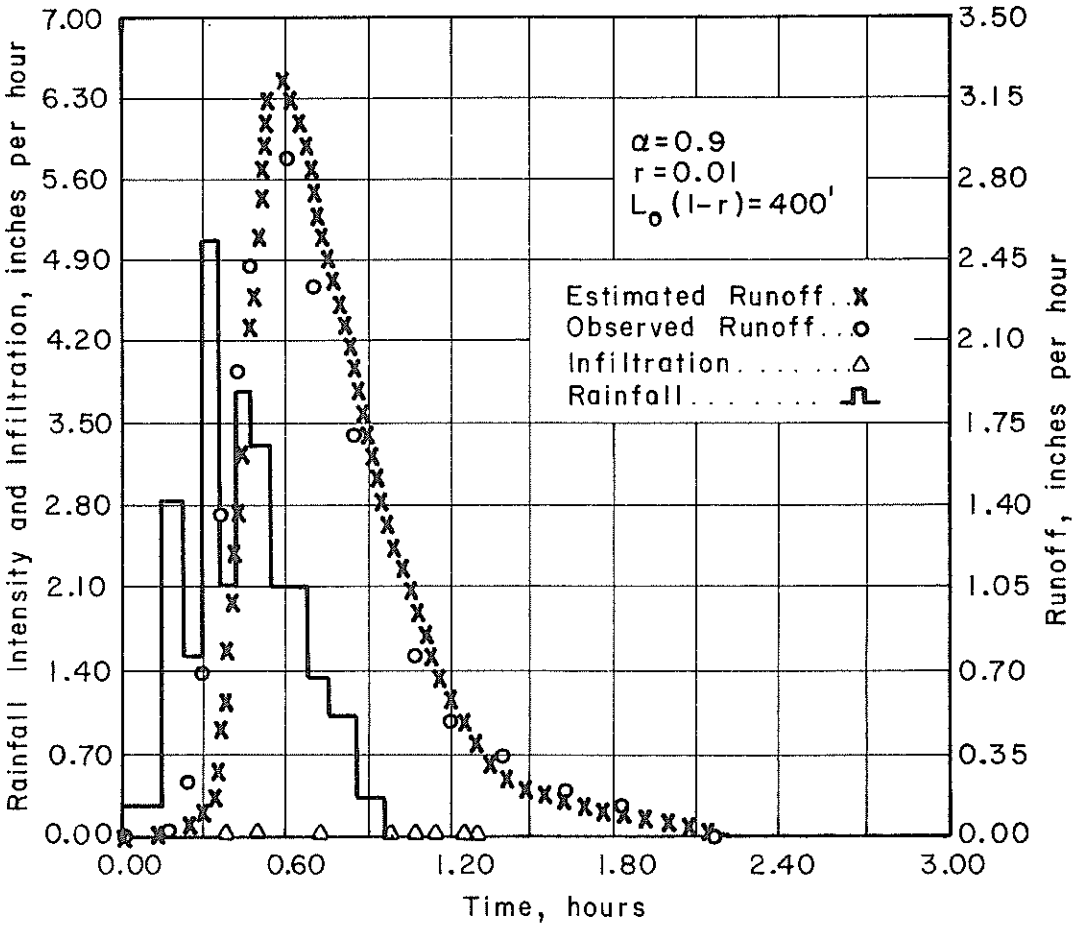

Fig. 6-10. Hydrograph prediction by converging overland flow model for rainfall event of 4-24-1957 on watershed SW-17, Riesel (Waco), Texas.

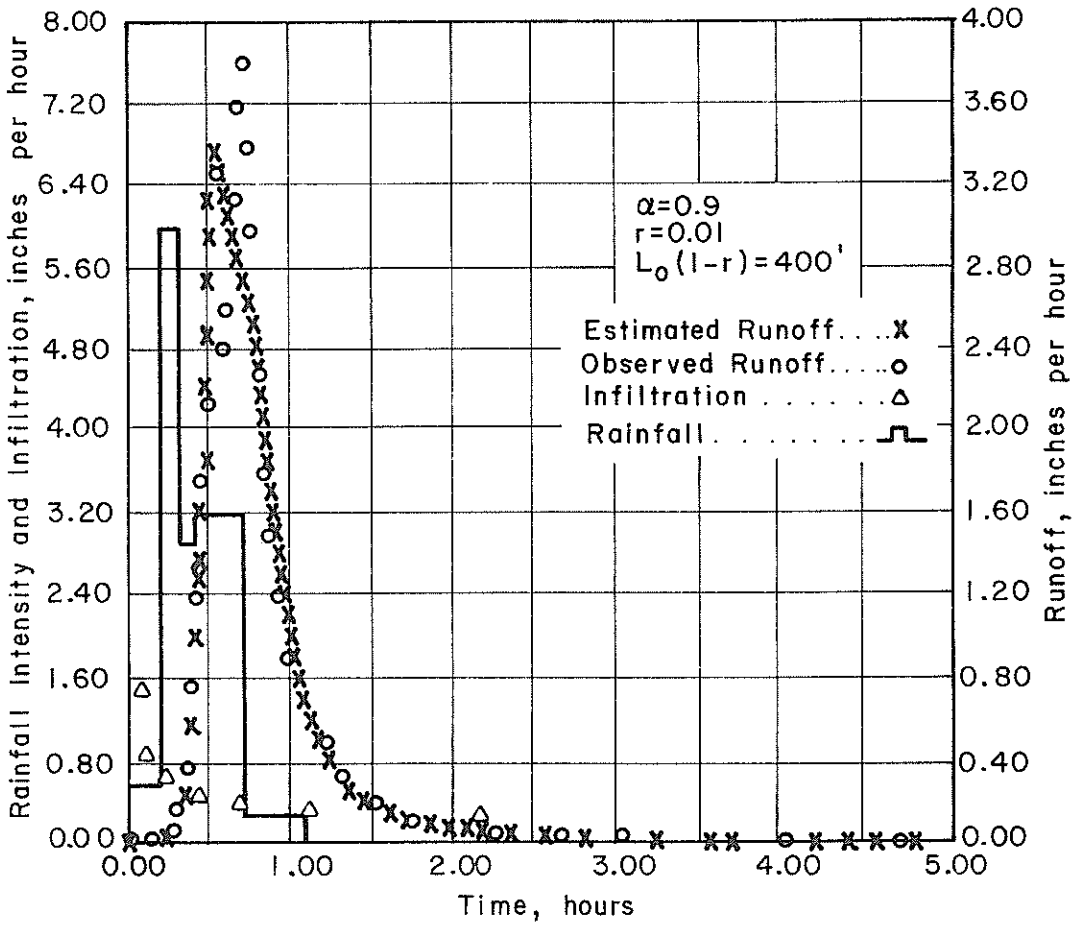

Fig. 6-11. Hydrograph prediction by converging overland flow model for rainfall event of 6-9-1962 on watershed SW-17, Riesel (Waco), Texas.

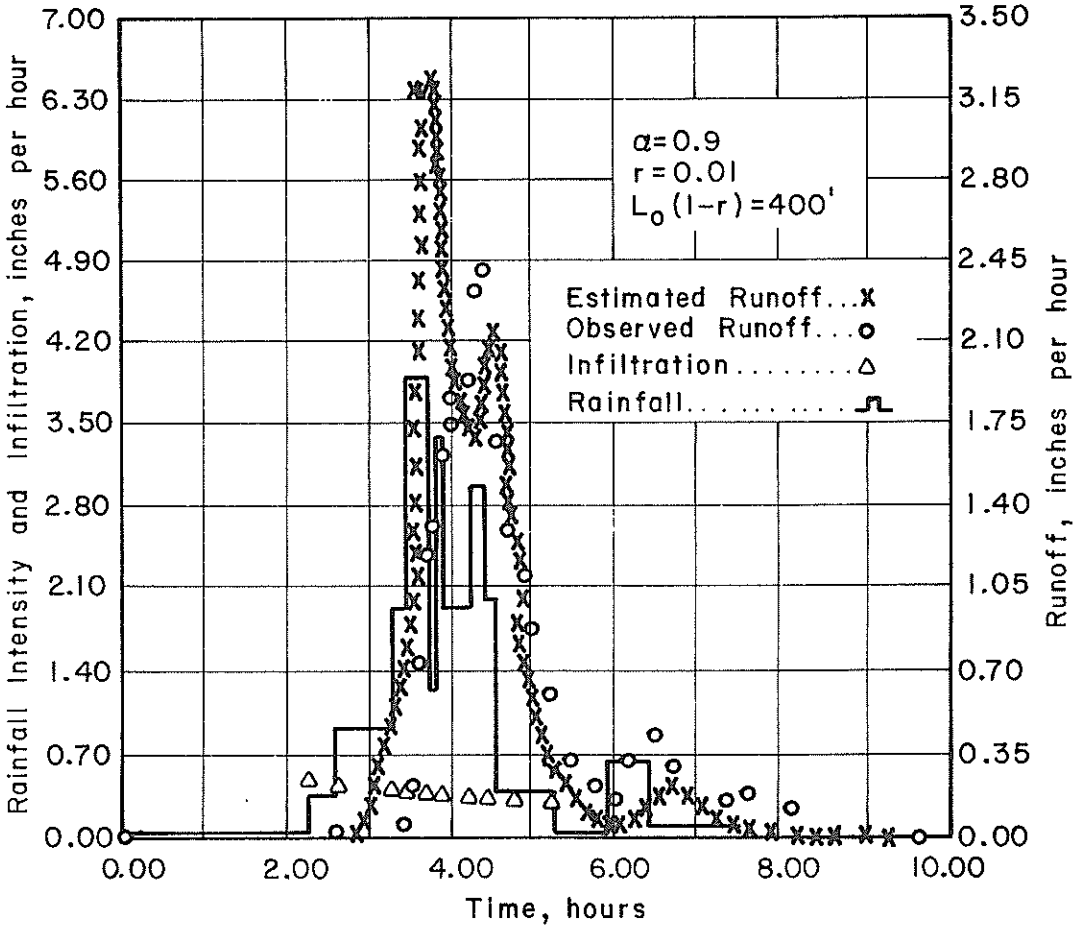

Fig. 6-12. Hydrograph prediction by converging overland flow model for rainfall event of 3-29-1965 on watershed SW-17, Riesel (Waco), Texas.

Table 6-12. Predictive performance of the model on Watershed SW-17, Riesel (Waco), Texas.

Serial number	Date of rainfall event	Observed hydrograph peak (in/hr)	Predicted hydrograph peak (in/hr)	Error	
				Absolute[1] (in/hr)	Relative[2] (%)
1	4-24-1957	2.900	3.212	-0.312	10.766
2	5-13-1957	1.740	2.185	-0.445	25.552
3	6- 9-1962	3.790	3.361	0.429	11.314
4	3-29-1965	2.440	3.258	-0.819	41.151

Mean of Relative Error 22.195

[1]Absolute Error = $(Q_{p_o} - Q_{p_e})$

[2]Relative Error = $\left|\frac{Q_{p_o} - Q_{p_e}}{Q_{p_o}}\right|$

To study the parameter variability on a watershed from rainfall event to rainfall event, the parameter was estimated for a number of rainfall events on 16 watersheds in Riesel (Waco), Texas. For these watersheds — small to medium to large size — the parameter is listed in Tables M-1 through M-16 of appendix M. The parameter estimation was performed by the method of linear interpolation of errors (see appendix H) utilizing the objective function of Eq. (4-13). It is apparent from the tables that the parameter does vary from one rainfall event to another, but not violently. This suggests that the parameter α can be expressed for a given rainfall event on a given watershed as follows:

$$\alpha = \bar{\alpha} + \Delta\alpha \qquad (6\text{-}2)$$

where the component $\bar{\alpha}$ is the value of the parameter α that will be fixed for a given watershed by its physiographic characteristics that are usually known or readily obtainable. The value $\bar{\alpha}$ will, henceforth, be called as the fixed component of the parameter α. The variable component $\Delta\alpha$ may take positive or negative values. Its negative value will be bounded by the fixed component $\bar{\alpha}$; that is, the variable component $\Delta\alpha$ will always be less than $\bar{\alpha}$. The variable component $\Delta\alpha$ will depend upon rainfall characteristics and their interaction with watershed physiography and may reflect errors in the infiltration model. In a statistical sense, should the parameter α be regarded as a random variable, then its fixed component $\bar{\alpha}$ may be regarded as its expected value or mean to be obtainable from its probability density function. The pursuance of a statistical approach lies beyond the scope of present study.

At this point, it was considered worthwhile to examine the variability of the parameter on a larger scale. So, it was estimated for a number of rainfall events available on each of 16 watersheds near Riesel (Waco), Texas.

The parameter statistics — average, variance, standard deviation, and coefficient of variation — along with the number of rainfall events utilized in their estimation are listed in Table 6-13. The table reflects remarkably on relatively small variability in the parameter about its average value for most of the watersheds. There is, in fact, only one watershed Y-7 for which the coefficient of variation goes as high as 1.5583. For two watersheds it gets to be about 0.91, but for the remaining 13 watersheds it stays around 0.5. The cause for its going so high for the other three watersheds is unwieldly at the moment. One point that needs to be brought out along this line is the size of the sample used in evaluating the statistics. One bad data point might make a substantial difference in the statistical results. Therefore, the cause of high coefficient of variation of α may be attributable to small size of the sample, bad data, the watershed itself, and a combination of them all.

Table 6-14 shows the variability in α on watershed SW-17 with its length of flow. It is apparent that the parameter increases with an increase in the length of flow, which is reasonable from physical considerations. Statistics of α are also given there corresponding to each $L_o(1 - r)$. It should be emphasized that the coefficient of variation in α is the least for $L_o(1 - r) = 400'$, the length of flow measured from the topographic map as indicated previously. This is a statistical confirmation of the propriety of taking the longest horizontal projection as the length of flow. In Tables 6-15 and 6-16 the effect of the degrees of convergence on the model parameter is elucidated. It is interesting to note that the parameter α is not very sensitive to the parameter r. It is, therefore, reasonable to keep r fixed at a small value because in most natural watersheds r is small, indeed.

Table 6-13. Statistics of model parameter α on various watersheds.

Serial number	Watershed identification	Number of rainfall-runoff events	Parameter α			
			Average	Variance	Standard deviation	Coefficient of variation
	Riesel (Waco), Texas					
1	Watershed C	8	4.044	4.044	2.115	0.523
2	Watershed D	6	9.589	75.625	8.696	0.907
3	Watershed G	8	4.048	1.750	1.323	0.327
4	Watershed W-1	8	6.953	22.414	4.734	0.681
5	Watershed W-2	8	2.199	0.515	0.717	0.325
6	Watershed W-6	6	1.044	0.218	0.467	0.448
7	Watershed W-10	8	2.298	0.873	0.934	0.407
8	Watershed Y	8	3.531	1.662	1.289	0.365
9	Watershed Y-2	9	2.781	0.373	0.610	0.219
10	Watershed Y-4	9	2.609	2.184	1.478	0.566
11	Watershed Y-6	8	5.164	22.125	4.704	0.911
12	Watershed Y-7	9	13.749	459.032	21.425	1.558
13	Watershed Y-8	7	2.014	1.033	1.016	0.505
14	Watershed Y-10	8	2.487	2.619	1.618	0.651
15	Watershed SW-12	5	1.977	0.513	0.716	0.362
16	Watershed SW-17	9	0.898	0.184	0.429	0.479

Table 6-14. Variability of parameter α with length of flow, $L_o(1-r)$, on Watershed Sw-17, Riesel (Waco), Texas.

Serial number	Date of rainfall event	Observed hydrograph peak (in/hr)	Parameter α		
			$L_o(1-r)=200'$	$L_o(1-r)=300'$	$L_o(1-r)=400'$
1	3-12-1953	1.610	0.433	0.651	0.858
2	3-31-1957	0.441	0.481	0.717	0.962
3	4-24-1957	2.900	0.352	0.528	0.709
4	5-13-1957	1.740	0.265	0.397	0.528
5	6-24-1959	2.170	0.464	0.693	0.928
6	6-25-1961	0.604	0.864	1.295	1.727
7	7-16-1961	0.348	0.320	0.480	0.640
8	6- 9-1962	3.790	0.691	1.037	1.381
9	3-29-1965	2.440	1.710	0.256	0.342
		Statistics of Parameter α			
Mean			0.620	0.673	0.897
Variance			0.202	0.104	0.184
Standard Deviation			0.450	0.322	0.429
Coefficient of Variation			0.725	0.479	0.479

Table 6-14. (continued)

Serial number	Parameter α		
	$L_o(1-r)=500'$	$L_o(1-r)=600'$	$L_o(1-r)=800'$
1	1.069	1.282	1.710
2	1.201	1.442	1.922
3	0.881	1.057	1.409
4	0.661	0.794	1.054
5	1.159	1.391	1.855
6	2.159	2.591	3.454
7	0.801	0.961	1.281
8	1.728	2.073	2.764
9	0.427	0.513	0.684
	Statistics of Parameter α		
Mean	1.121	1.345	1.793
Variance	0.289	0.416	0.740
Standard Deviation	0.537	0.645	0.860
Coefficient of Variation	0.480	0.480	0.480

Table 6-15. Effect of the degree of convergence, r, on model parameter, α, on Watershed SW-17, Riesel (Waco), Texas.

Infiltration by Philip Model

Serial number	Date of event	Observed hydrograph peak (in/hr)	Parameter α for select values of r				
			0.01	0.05	0.1	0.25	0.5
1	3-12-1953	1.610	0.858	0.859	0.895	0.956	0.976
2	3-31-1957	0.441	0.962	0.972	1.000	1.074	1.177
3	4-24-1957	2.900	0.709	0.711	0.715	0.740	1.110
4	5-12-1957	1.740	0.529	0.528	0.539	0.560	0.590
5	6-24-1959	2.170	0.928	0.937	0.960	1.016	1.008
6	6-25-1961	0.604	1.727	1.764	1.804	1.954	2.192
7	7-16-1961	0.348	0.640	0.646	0.661	0.711	0.134
8	6- 9-1962	3.790	1.381	1.405	1.421	1.500	1.655
9	3-29-1965	2.440	0.342	0.389	0.351	0.386	0.420

Table 6-16. Effect of the degree of convergence, r, on model parameter, α, on Watershed SW-17, Riesel (Waco), Texas.

Infiltration by ϕ - Index

Serial number	Date of event	Observed hydrograph peak (in/hr)	Parameter α for select values of r				
			0.01	0.05	0.1	0.25	0.50
1	3-12-1953	1.610	0.870	0.885	0.900	0.957	0.975
2	3-31-1957	0.441	0.965	0.973	1.000	1.073	1.178
3	4-24-1957	2.900	0.711	0.712	0.705	1.073	1.178
4	5-12-1957	1.740	0.493	0.498	0.505	0.525	0.547
5	6-24-1959	2.170	1.395	1.412	1.452	1.481	1.640
6	6-25-1961	0.604	2.026	2.060	2.106	2.272	2.500
7	7-16-1961	0.348	0.622	0.631	0.645	0.694	0.783
8	6- 9-1962	3.790	1.398	1.276	1.300	1.362	1.533
9	3-29-1965	2.440	0.346	0.345	0.354	0.384	0.416

The answers to the second and third questions are related. Therefore it was decided to optimize the parameter α on each of the 21 watersheds near Riesel (Waco), Texas and Hastings, Nebraska. A set of events were selected on each watershed. Utilizing the objective function (Eq. 4-2), the parameter α was optimized by the parabolic interpolation scheme. Optimized parameter values are listed in Table 6-17. It is notable that in spite of a wide spectrum of conditions on the watersheds α does not change drastically from one watershed to another. In order to relate α to physically measurable quantities on a watershed, a simple regression and correlation analysis was made. Weighted slope, area, and length of flow were considered as independent variables. Slope alone afforded the highest correlation coefficient for α. It was 0.5732. Next came area which improved the correlation coefficient to 0.666. The remaining variable did not add much to the correlation coefficient. It must be pointed out here that slope was transformed to $(\text{slope})^{\frac{1}{2}}$, and area to log area before running the analysis. The regression equation can be written as

$$\alpha = 0.98165 + 2.27996\ S^{\frac{1}{2}} + 1.37141 \log A - 1.36830 \log (L_o(1 - r))$$

where A = area in acres, and S = weighted average slope.

The correlation coefficient was 0.6678 with standard error of estimate of 1.4351. An attempt was also made to relate α with various other combinations of S, A, and $L_o(1 - r)$, but the correlation coefficient did not improve. Nevertheless, this suggests that the fixed component of α may be determined for a watershed from its slope and area. The variable component must be determined by consideration of rainfall characteristics and their interaction with watershed surface characteristics.

Table 6-17. Optimized values of parameter α for various watersheds.

Serial number	Watershed identification	Watershed area (acres)	Weighted average slope (%)	Length of flow (ft)	Optimized α
1	Watershed C	579.00	2.110	8,000	2.800
2	Watershed D	1,110.00	2.175	12,000	5.971
3	Watershed G	4,380.00	2.150	22,000	3.000
4	Watershed W-1	176.00	2.240	3,500	4.968
5	Watershed W-2	130.00	2.475	2,100	2.100
6	Watershed W-6	42.30	2.025	1,200	1.524
7	Watershed W-10	19.70	1.755	8,000	2.449
8	Watershed Y	309.00	2.420	4,800	2.342
9	Watershed Y-2	132.00	2.615	3,200	2.500
10	Watershed Y-4	79.80	2.870	2,400	2.297
11	Watershed Y-6	16.30	3.275	1,200	0.750
12	Watershed Y-7	40.00	1.910	1,800	1.969
13	Watershed Y-8	20.80	2.055	1,000	1.471
14	Watershed Y-10	18.60	2.375	1,000	1.559
15	Watershed SW-12	2.97	3.810	450	1.750
16	Watershed SW-17	2.99	1.830	400	0.900
17	Watershed 2-H	3.40	3.925	600	4.750
18	Watershed 4-H	3.64	5.960	500	6.313
19	Watershed W-3	481.00	7.125	7,540	6.184
20	Watershed W-8	2,086.00	5.500	17,348	5.260
21	Watershed W-11	3,490.00	5.095	27,154	2.560

Even though slope and area are correlated with α with a correlation coefficient of 0.666, this correlation may be improved by incorporating in the analysis the watersheds having a wide range of slopes. In the present analysis, the variability in slope is not much. Besides that, all watersheds could be clustered in two groups according to slope. Riesel (Waco), Texas watersheds may form one group having slope from 1.7% to 3.3%; watersheds near Hastings, Nebraska may form another group having slope from 3.9% to 7.22%. The former group contains the majority of the watersheds. The small sample size coupled with low variability in slope of watersheds might have contributed to the low correlation coefficient.

The above analysis indicates that the parameter α is a slopefriction parameter as postulated in the beginning when developing the kinematic wave theory. Relating α to Chezy's friction coefficient,

$$\alpha = C\sqrt{S}$$

where C = Chezy's friction coefficient. Thus the parameter α is amendable to physical interpretation.

CHAPTER 7

APPLICATION OF DISTRIBUTED PARAMETER MODEL TO NATURAL WATERSHEDS

7.1 GENERAL REMARKS

In the previous chapters we dealt with analytical mathematics of nonlinear watershed runoff dynamics by the method of characteristic domains in that conditions were pointed out regarding the feasibility of explicit, analytical solutions. In this chapter our objective is to apply the proposed distributed converging overland flow model to predict surface runoff from natural agricultural watersheds, examine its performance and reflect on its potential in simulating watershed surface runoff response.

When analytical solutions are not feasible use is made of hybrid solutions which combine advantages of numerical and analytical solutions. For a complete discussion on hybrid solutions see the reference by Singh (1974, 1975a, 1976). We will only give numerical solutions here (see appendix L for derivation and stability analysis). The coupling of continuity equation and kinematic approximation to momentum equation (Singh, 1974) yields:

$$\frac{\partial h}{\partial t} + n\alpha(x)\, h^{n-1} \frac{\partial h}{\partial x} + h^n \frac{\partial \alpha(x)}{\partial x} = q(x,t) + \frac{\alpha(x)\, h^n}{(L_o - x)} \tag{7-1}$$

The Lax-Wendroff scheme (Houghton and Kasahara, 1960), which has been successfully used in many investigations on kinematic wave modeling of watershed runoff (Kibler and Woolhiser, 1970; Singh, 1974, 1975a, 1976) is formulated to solve Eq. (7-1). We can write:

$$\frac{\partial h}{\partial t} = -\alpha(x) n h^{n-1} \frac{\partial h}{\partial x} - h^n \frac{\partial \alpha(x)}{\partial x} + q(x,t) + \frac{\alpha(x)\, h^n}{(L_o - x)} \tag{7-2}$$

Expanding $h(x,t + \Delta t)$ by Taylor series,

$$h(x,t + \Delta t) = h(x,t) + \Delta t \frac{\partial h}{\partial t} + \frac{(\Delta t)^2}{2} \frac{\partial^2 h}{\partial t^2} + \text{HOT} \tag{7-3}$$

where HOT denotes higher order terms. Differentiating Eq. (7-2) with respect to t,

$$\frac{\partial^2 h}{\partial t^2} = -\alpha(x) \frac{\partial}{\partial x} \left(nh^{n-1} \frac{\partial h}{\partial t} \right) - \frac{\partial \alpha(x)}{\partial x} nh^{n-1} \frac{\partial h}{\partial t} + \frac{\partial q(x,t)}{\partial t} + \frac{\alpha(x) nh^{n-1}}{(L_o - x)} \frac{\partial h}{\partial t} \tag{7-4}$$

Inserting Eqs. (7-2) and (7-4) into Eq. (7-3) and neglecting HOT we obtain:

$$h(x,t + \Delta t) = h(x,t) + \Delta t \left\{ -n\alpha(x) h^{n-1} \frac{\partial h}{\partial x} - h^n \frac{\partial \alpha(x)}{\partial x} + q(x,t) + \frac{\alpha(x) h^n}{(L_o - x)} \right\} + \frac{(\Delta t)^2}{2} \left\{ -\alpha(x) \frac{\partial}{\partial x} \left(nh^{n-1} \frac{\partial h}{\partial t} \right) - \frac{\partial \alpha(x)}{\partial x} nh^{n-1} \frac{\partial h}{\partial t} + \frac{\partial q(x,t)}{\partial t} + \frac{\alpha(x) nh^{n-1}}{(L_o - x)} \frac{\partial h}{\partial t} \right\} \tag{7-5}$$

Writing Eq. (7-5) in a compact form,

$$h(x,t + \Delta t) = h(x,t) + \left\{ -\alpha(x) \frac{\partial h^n}{\partial x} - h^n \frac{\partial \alpha(x)}{\partial x} + q(x,t) + \frac{\alpha(x)\, h^n}{(L_o - x)} \right\} \left\{ \Delta t + (\Delta t)^2 \frac{n}{2} h^{n-1} \left(- \frac{\partial \alpha(x)}{\partial x} + \frac{\alpha(x)}{(L_o - x)} \right) \right\} + \frac{(\Delta t)^2}{2} \left\{ \frac{\partial q(x,t)}{\partial t} - \alpha(x) \frac{\partial}{\partial x} \left[nh^{n-1} \left(-\alpha(x) \frac{\partial h^n}{\partial x} - h^n \frac{\partial \alpha(x)}{\partial x} + q(x,t) + \frac{\alpha(x)\, h^n}{(L_o - x)} \right) \right] \right\} \tag{7-6}$$

Following the notation in Fig. 7-1 we can write Eq. (7-6) in finite difference form as:

$$h_j^{i+1} = h_j^i + \left\{ -\alpha_j^i \left(\frac{h_{j+1}^{i\,n} - h_{j-1}^{i\,n}}{2\Delta x} \right) - h_j^{i\,n} \left(\frac{\alpha_{j+1}^i - \alpha_{j-1}^i}{2\Delta x} \right) + q_j^i + \frac{\alpha_j^i\, h_j^{i\,n}}{(L_o - x_j^i)} \right\}$$

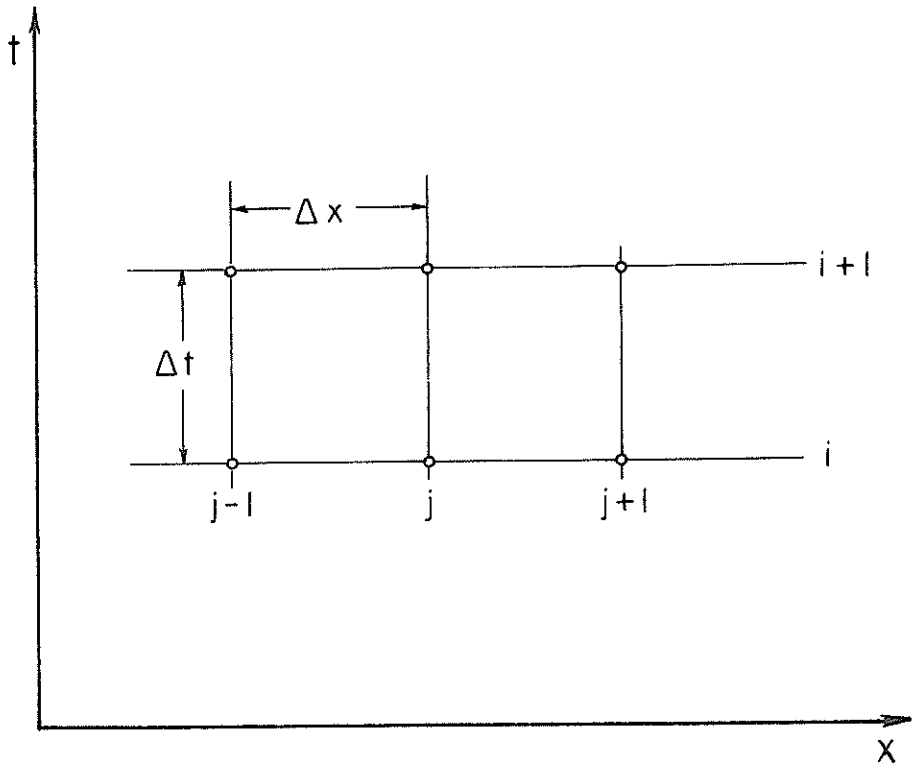

Fig. 7-1. Notation for finite different scheme.

$$\left\{\Delta t + \frac{(\Delta t)^2}{2} n h_j^{i\,n-1} \left[- \frac{\alpha_{j+1}^i - \alpha_{j-1}^i}{2\Delta x} + \frac{\alpha_j^i}{(L_o - x_j^i)} \right] \right\} + \frac{(\Delta t)^2}{2}$$

$$\left[\left[\frac{q_j^{i+1} - q_j^i}{\Delta t} \right] - \left\{ \alpha_j^i \frac{n}{\Delta x} \left[\frac{h_{j+1}^{i\,(n-1)} + h_j^{i\,(n-1)}}{2} \right] \left[- \left[\frac{\alpha_{j+1}^i + \alpha_j^i}{2} \right] \right. \right. \right.$$

$$\left[\frac{h_{j+1}^{i\,n} - h_j^{i\,n}}{\Delta x} \right] - \left[\frac{h_{j+1}^{i\,n} + h_j^{i\,n}}{2} \right] \left[\frac{\alpha_{j+1}^i - \alpha_j^i}{\Delta x} \right] + \left[\frac{q_{j+1}^i + q_j^i}{2} \right] +$$

$$\left. \left[\frac{\alpha_{j+1}^i + \alpha_j^i}{2} \right] \left[\frac{h_{j+1}^{i\,n} + h_j^{i\,n}}{2} \right] \frac{2}{\left[2L_o - \left(x_{j+1}^i + x_j^i \right) \right]} \right] - \alpha_j^i \frac{n}{\Delta x}$$

$$\left[\frac{h_j^{i\,(n-1)} + h_{j-1}^{i\,(n-1)}}{2} \right] \left[- \left[\frac{\alpha_j^i + \alpha_{j-1}^i}{2} \right] \left[\frac{h_j^{i\,n} - h_{j-1}^{i\,n}}{\Delta x} \right] - \right.$$

$$\left[\frac{h_j^{i\,n} + h_{j-1}^{i\,n}}{2} \right] \left[\frac{\alpha_j^i - \alpha_{j-1}^i}{\Delta x} \right] + \left[\frac{q_j^i + q_{j-1}^i}{2} \right] + \left[\frac{\alpha_j^i + \alpha_{j-1}^i}{2} \right]$$

$$\left. \left. \left. \left[\frac{h_j^{i\,n} + h_{j-1}^{i\,n}}{2} \right] \frac{2}{\left[2L_o - \left(x_j^i + x_{j-1}^i \right) \right]} \right] \right\} \right] \right] \qquad (7\text{-}7)$$

Assume that the depth of flow is to be determined at N nodal points. Then the depth of flow at nodal points j = 1, 2, ... (N-1) will be computed by the scheme in Eq. (7-7) in conjunction with the following boundary conditions:

$$h(o,t) = 0$$

$$h(x,t) = 0 \qquad (7\text{-}8)$$

Equation (7-8) represents an initially dry surface. The finite-difference scheme of Eq. (7-7) is explicit, second order, and single step. The depth of flow at the downstream boundary (j = N) can be computed by the first order scheme. That is,

$$h(x,t + \Delta t) = h(x,t) + \Delta t \frac{\partial h}{\partial t} \tag{7-9}$$

Substituting Eq. (7-2) into Eq. (7-9),

$$h(x,t + \Delta t) = h(x,t) + \Delta t \left\{-\alpha(x) \frac{\partial h^n}{\partial x} - h^n \frac{\partial \alpha(x)}{\partial x} + q(x,t) + \frac{\alpha(x) h^n}{(L_o - x)}\right\} \tag{7-10}$$

Writing the difference form of Eq. (7-10),

$$h_N^{i+1} = h_N^i + \Delta t \left\{-\alpha_N^i \left(\frac{h_N^{i^n} - h_{N-1}^{i^n}}{\Delta x}\right) - h_N^{i^n} \left(\frac{\alpha_N^i - \alpha_{N-1}^i}{\Delta x}\right) + q_n^i + \frac{\alpha_N^i h_N^{i^n}}{(L_o - x_N^i)}\right\} \tag{7-11}$$

These numerical schemes can be combined with analytical solutions in an appropriate manner to yield hybrid solutions (Singh, 1974, 1975b, 1975c, 1976).

7.2 APPLICATION TO NATURAL WATERSHEDS

The distributed converging overland flow model was applied to three natural agricultural watersheds near Riesel (Waco), Texas. They include watershed W-2 of 132 acres in area as shown in Fig. 7-2; watershed W-6, 42.3 acres in area as shown in Fig. 7-3; and watershed G, 4380 acres in area as shown in Fig. 7-4. Deep, fine-textured, granular, slowly permeable, alkaline throughout, and slow internal drainage are typical characteristics of soils of these watersheds. The dominance of Houston black clay is notable. These soils are also noted for the formation of large extensive cracks upon drying. Surface drainage is usually good but no well-defined drainage-ways exist on these watersheds. Normally, water is drained by rills and poorly defined field gullies.

Most of the time these watersheds are covered with agricultural crops. Because of low permeability of the soils, these watersheds respond rapidly to rainfall, and produce quickly rising hydrographs. For rainfall events, that were considered in this study, the major portion

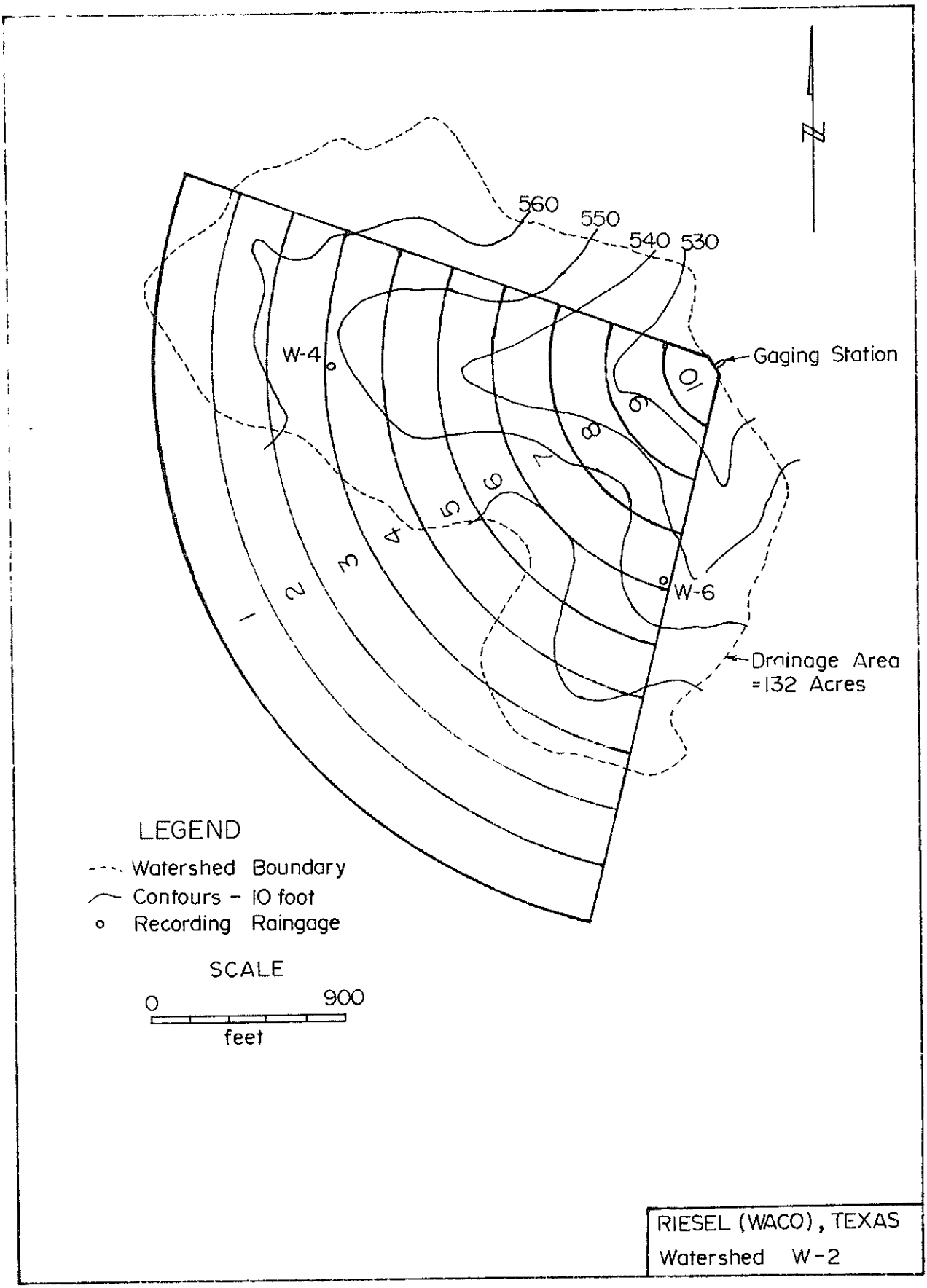

Fig. 7-2. Watershed W-2, Riesel (Waco), Texas.

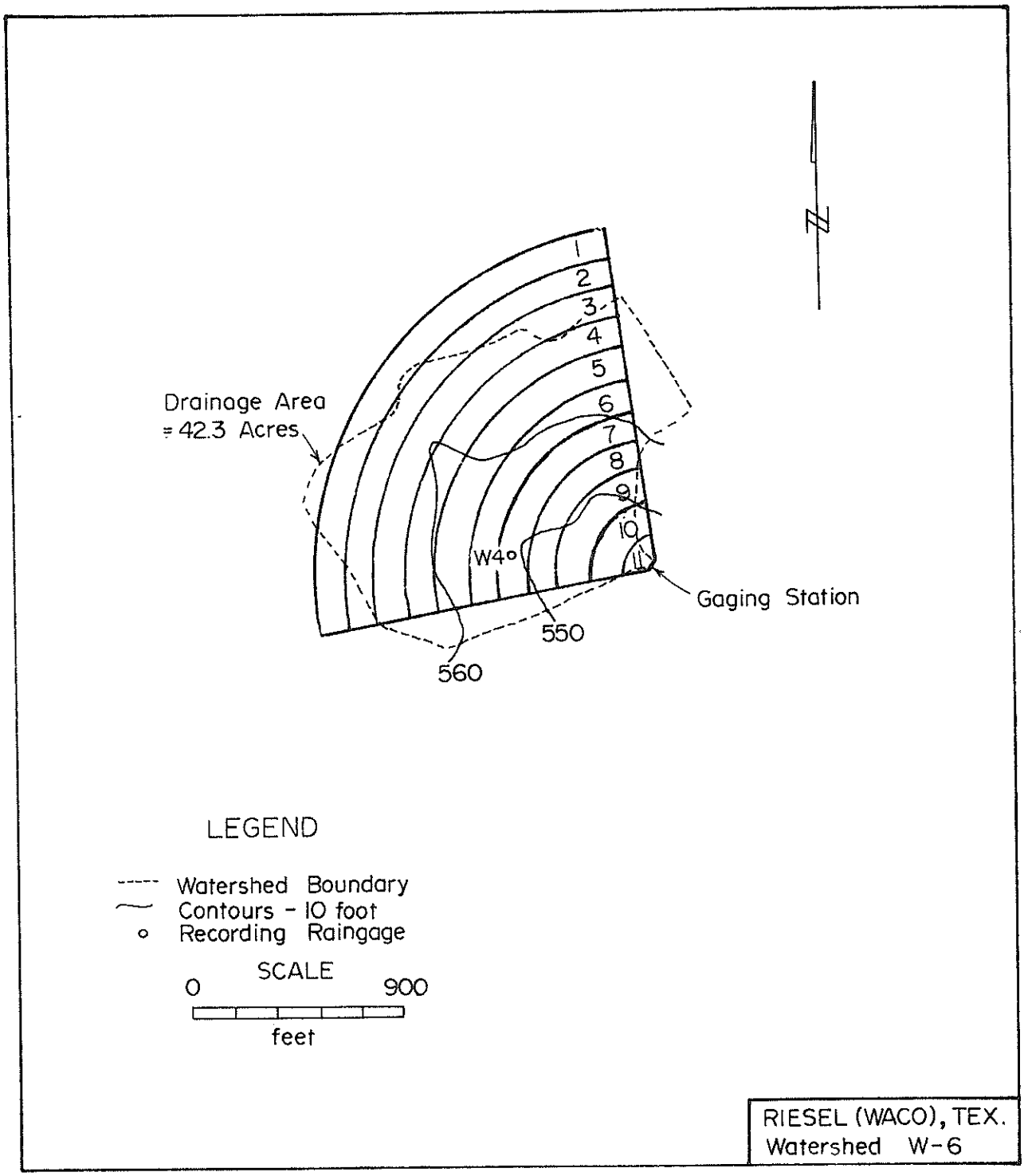

Fig. 7-3. Watershed W-6, Riesel (Waco), Texas.

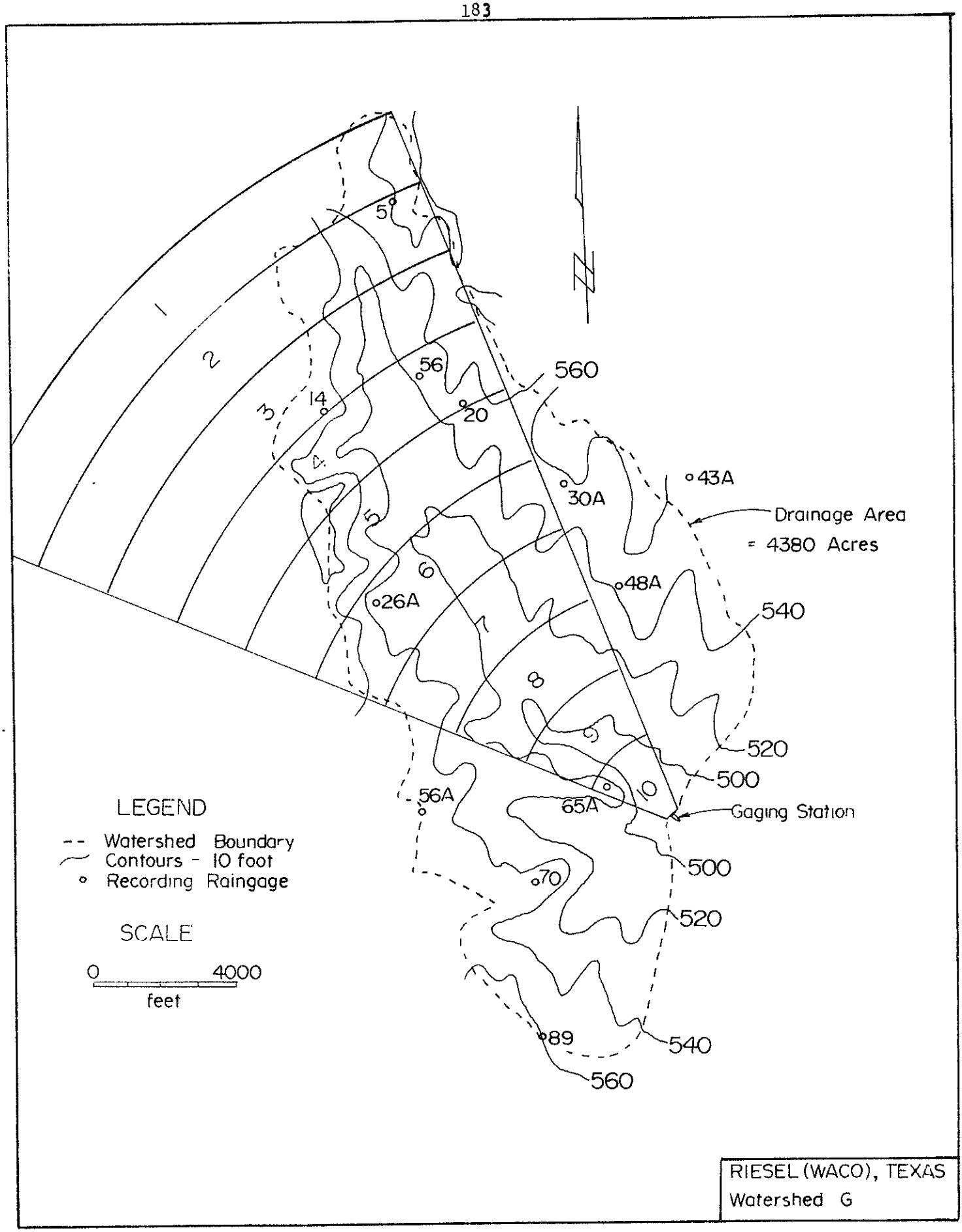

Fig. 7-4. Watershed G, Riesel (Waco), Texas.

of rainfall was observed as surface runoff; and infiltration was only minor. For a more complete discussion of these watersheds and rainfall-runoff data thereon see the USDA publications entitled "Hydrologic Data for Experimental Agricultural Watersheds in the United States." These publications appear almost every year and contain, on the average, one event per watershed.

7.2.1 Determination of Rainfall-Excess.

Rainfall-excess forms input to the model. We do recognize that the concept of rainfall-excess is more of an artifice than a reality. The processes of rainfall, infiltration, and runoff occur concurrently in nature. Simultaneous consideration of these distinct processes injects intractable complexity in runoff modeling. It is, therefore, not surprising that despite this recognition, a great many investigators have utilized this artificial notion of rainfall-excess in their investigations on rainfall-runoff modeling, and a great many continue to do so even today; in addition, very little attention has been paid to this fundamental problem.

For simplicity we ourselves adhered to the traditional practice. Infiltration was determined by Philip's equation (Philip, 1957). In a recent study (Singh, 1974) the parameters of Philip's equation were specified for all available events on these watersheds. We utilized these results in the present study.

7.2.2 Geometric Representation

The objective is to transform the geometry of a natural watershed into a simpler geometry having a similar hydrologic response. The only perfect representation of a watershed is, of course, the watershed itself. In studies of the response characteristics of the linearly converging

section (Woolhiser, 1969) it was suggested that such a geometry might be a useful abstraction of a watershed regardless of its complexity. This hypothesis was later incorporated in a study by Singh (1974, 1975a, 1975b, 1975c, 1976) and found promising. Therefore the linearly converging section of a cone, as shown in Fig. 1-1, was utilized to represent the geometry of a natural watershed. From this figure, it is apparent that the converging section geometry has four geometric parameters including $L_o(1-r)$, r, θ and S_o where $L_o(1-r)$ is the length of flow, S_o is the slope, r the parameter related to the degree of convergence, and θ the interior angle. Because of the radial symmetry, θ does not affect the relative response characteristics. It is necessary only to preserve the watershed area and is, therefore, dependent on L_o and r. The converging section geometry possesses some interesting properties:

1. Its discrete analog is, from a systems viewpoint, a system composed of a cascade of unequal nonlinear reservoirs.

2. Its response is similar to that of a cascade of planes of decreasing size.

3. The convergence may account for the concentration of runoff at the mouth of a natural watershed.

The converging section geometry has 3 geometric parameters $L_o(1-r)$, r, and θ that need to be specified. With the area of a watershed usually known only two parameters need to be estimated. The study (Singh, 1974) showed that for a watershed under consideration, the parameter $L_o(1-r)$ could be taken to be equal to the longest horizontal projection from the most remote portion of the watershed to the outlet, and the parameter r to be equal to 0.01. Thus the topographic map of a watershed suffices to transform the natural geometry into a simpler geometry.

7.2.3 Choice of Objective Function

The objective function, based on hydrograph peak of Eq. (4-2), was used in the present study. The choice of this objective function is based on the finding of Kibler and Woolhiser (1970) and Singh (1974, 1975a, 1975b, 1975c, 1975f, 1976). Besides its usefulness in flood studies and some statistical properties that it possesses, it has an advantage that it does not suffer from timing errors that result from improper synchronization between rainfall and runoff observations.

7.2.4 Parameter Optimization.

A simple relation between the parameter α and topographic slope was considered:

$$\alpha(x) = C_1 + C_2\sqrt{S(x)} \tag{7-12}$$

where $S(x)$ = topographic slope varying in space, and C_1 and C_2 are parameters. These parameters will supposedly vary from one watershed to another. At present we can only hope to obtain them by the technique of optimization. The topographic slope varies in space and so does the parameter α correspondingly. The choice of this relation is based on recent studies conducted by Singh (1974, 1975f, 1976).

For computational purposes the converging section geometry was decomposed into several segments, for example, 10 segments for watershed W-2, 10 segments for W-6 and 10 segments for watershed G as shown in Figs. 7-2 through 7-4 respectively. For each segment weighted slope is known from the topographic map. Two sets of rainfall-runoff events were selected on each of the three watersheds; one set was called as optimization set implying that the events in this set were used for optimization only, and the other set was named as the prediction set implying that the events were used for hydrograph predictions only. These two sets were mutally

exclusive implying that they did not have any events in common. The optimization sets consisted of a set of 5 events on watershed G, a set of 5 events on watershed W-2, and a set of 5 events on watershed W-6. The prediction sets consisted of a set of 3 events on watershed G, a set of 3 events on watershed W-2, and a set of 3 events on watershed W-6. The constants were obtained by optimization over the optimization set for each watershed. The optimization was performed by the Rosinbrock-Palmer algorithm (Rosenbrock, 1970; Himmelblau, 1972) utilizing the objective function of Eq. (4-2) The optimized values of the constants C_1 and C_2 were respectively 3.3 and 4.95 for watershed G, 3.6 and 5.0 for watershed W-2, and 1.5 and 2.94 for watershed W-6.

7.2.5 Hydrograph Prediction

Utilizing optimized values of the constants C_1 and C_2 hydrograph predictions were made for the events in the prediction set of each watershed. Sample predicted hydrographs are shown in Figs. 7-5 through 7-7 On comparing predicted runoff peaks with observed runoff peaks we found that they were in reasonable agreement. Hydrograph time and shape characteristics were predicted quite well by the model, especially for its simplicity. However, a few points prompt discussion:

(1) In some cases the error in the prediction of hydrograph peak was so high as about 50%; although in most cases it remained well below 20%. There might be several reasons for high prediction error. Of all the two appear to be most prominant:

(a) The size of the optimization set is very small and, therefore, we cannot hope to obtain representative values of the constants C_1 and C_2. This is even more true when we see that the rainfall-runoff events for each watershed under consideration represent a long stretch

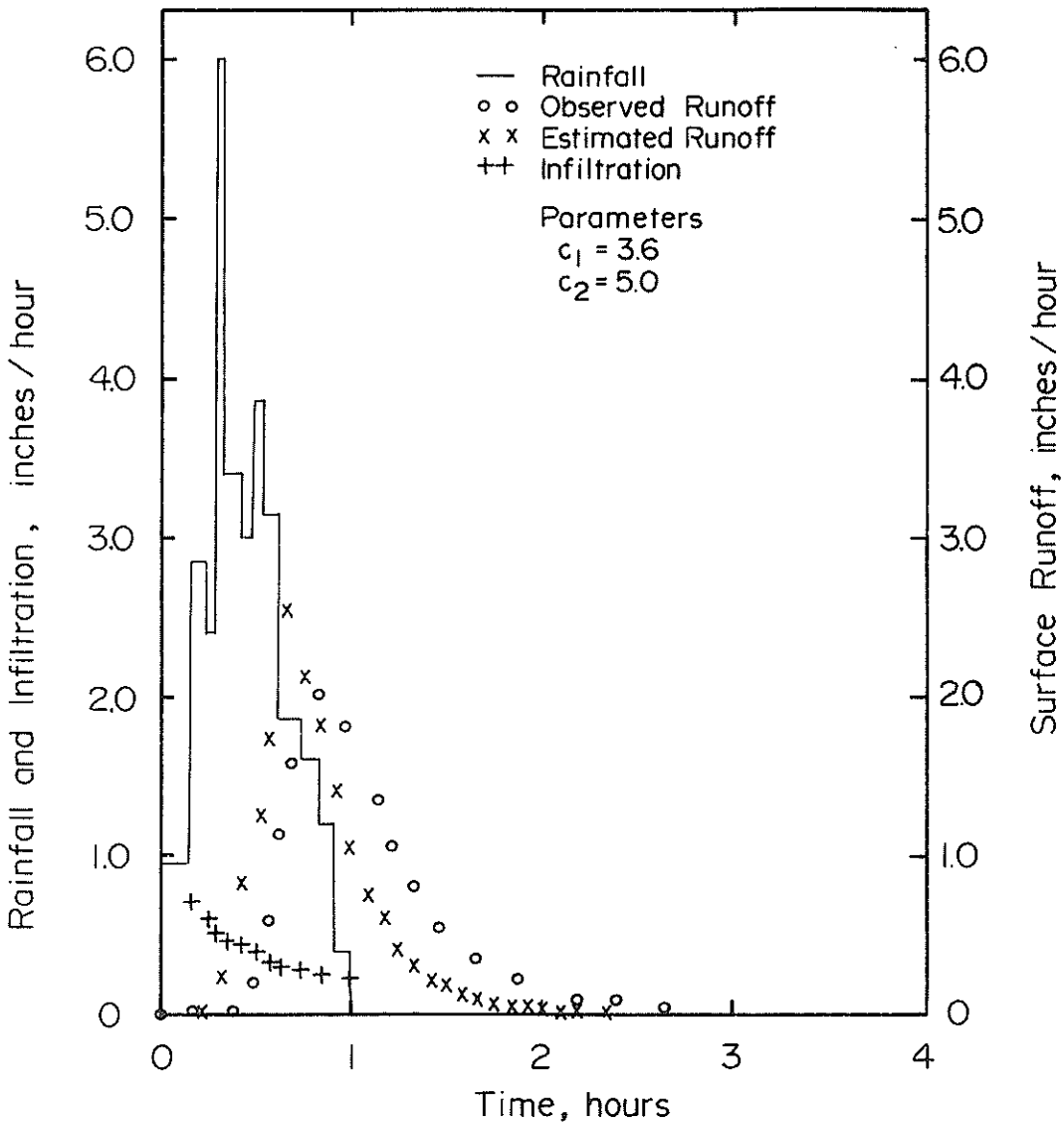

Fig. 7-5. Prediction of surface runoff hydrograph for rainfall event of 4-24-1957 on Watershed SW-17, Riesel (Waco), Texas.

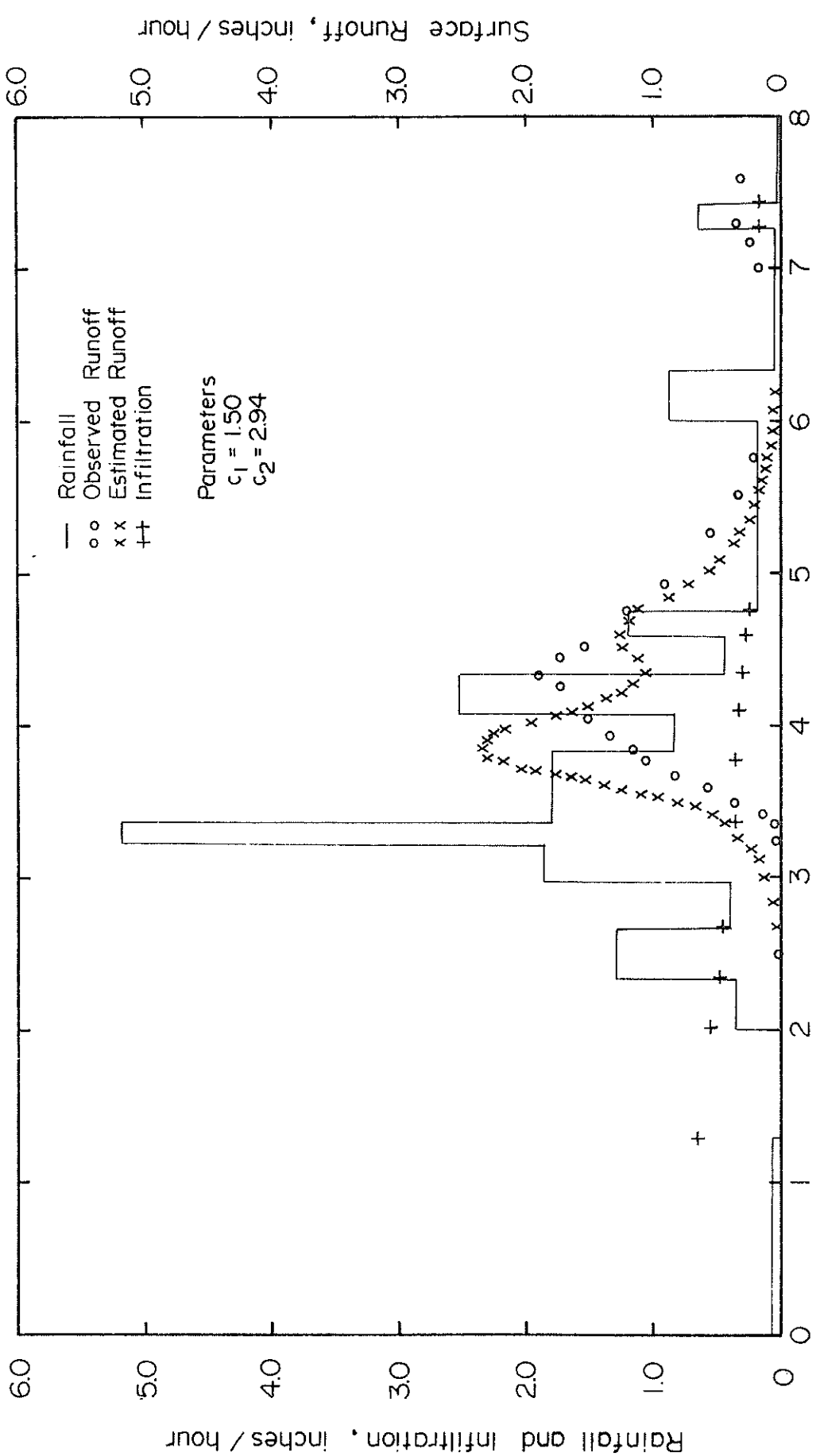

Fig. 7-6. Prediction of surface runoff hydrograph for rainfall event of 3-29-1965 on watershed W-6, Riesel (Waco), Texas.

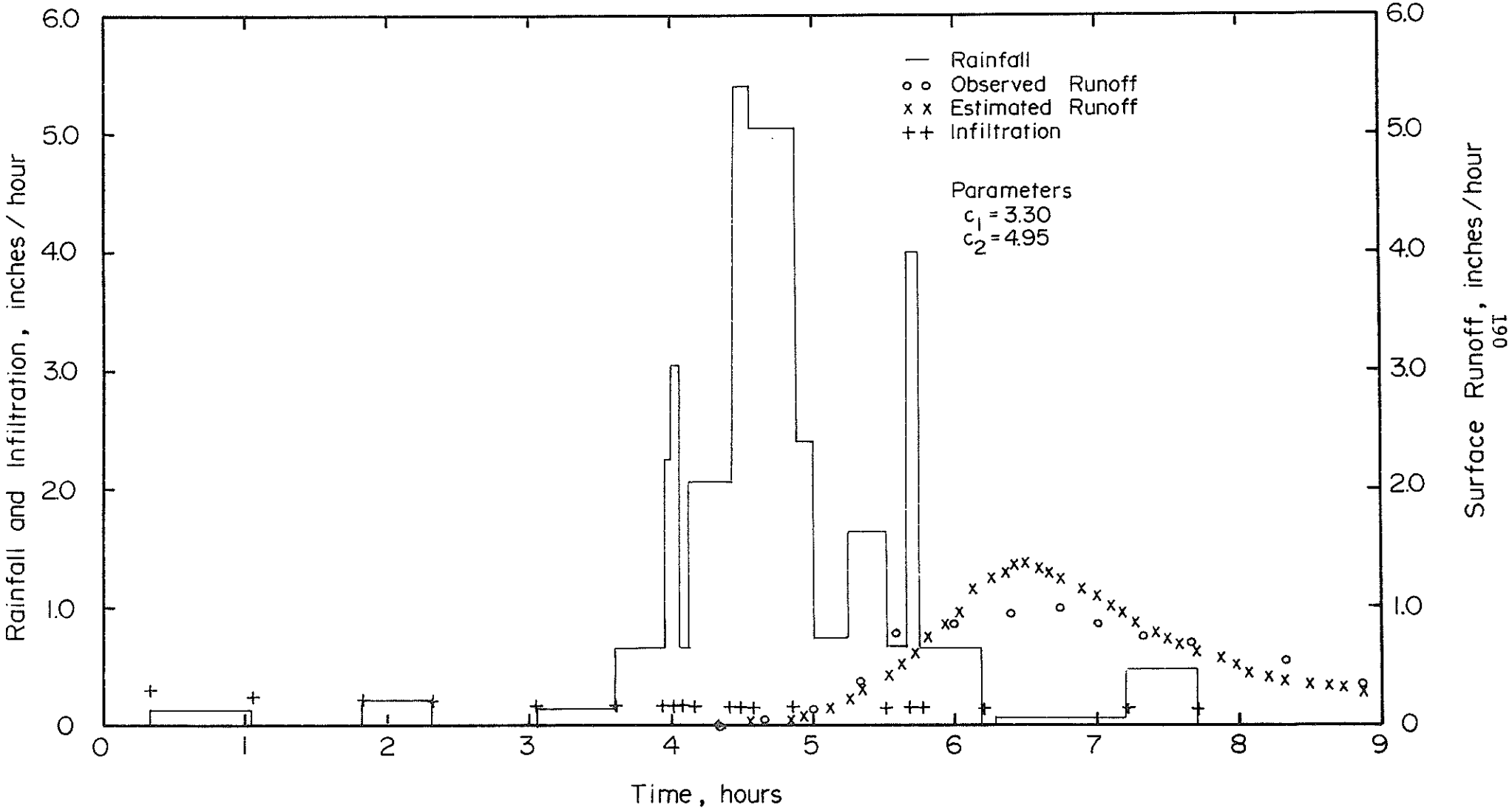

Fig. 7-7. Prediction of surface runoff hydrograph for rainfall event of 3-29-1965 on watershed G, Riesel (Waco), Texas.

of time, often 15 years or more. During this period of time several changes in land management and cropping pattern must have taken place on these watersheds. These changes can, in no way, be represented by such small samples as we have considered.

(b) There is difficulty in determining rainfall-excess which, in fact, generated observed runoff. The determination of true rainfall-excess seems to be the major problem in most rainfall-runoff models, and our model is no exception. Philip's equation, utilized in this study, is too simple to accurately predict time-distribution of infiltration, and then there is the difficulty of estimating its parameters. It was used primarily for its simplicity.

(2) Figures 7-5 through 7-7 illustrate that the model predicts time distribution of runoff quite well. We must note that the optimization of parameters C_1 and C_2 employed an objective function that was based on hydrograph peak only. There was no consideration given explicitly to the runoff timing, yet the hydrograph shape and time characteristics are well predicted. It seems to us that if the model structure is sound it might suffice to perform optimization of parameters on some prominent characteristics of runoff hydrograph even for the prediction of the entire hydrograph; and there is no need to consider the entire hydrograph explicitly in the optimization.

For its simplicity the distributed converging overland flow model appears to be a promising tool. There is, however, a need for an exhaustive testing of the proposed model and a number of natural watersheds in a variety of physiographic and climatic settings. Another aspect would be to investigate into the problem of determining the constants C_1 and C_2 from physically measurable watershed characteristics. If the problem of

a priori estimation of the parameters C_1 and C_2 can be tackled the utility of the proposed model will be greatly enhanced.

LITERATURE CITED

Brakensiek, D. L.: A simulated watershed flow system for hydrograph prediction: a kinematic application. Proc. Int'l Hydrology Symposium, pp. 18-24, Fort Collins, Colorado, 1967.

Chery, D. L.: Design and tests of a physical watershed model. J. Hydrology, Vol. 4, pp. 224-235, 1966.

Chow, V. T.: Laboratory study of watershed hydrology. Proc. Int'l Hydrology Symposium, pp. 194-202, Fort Collins, Colorado, 1967.

Conte, S. D.: Elementary numerical analysis: an algorithm approach. 278 p., McGraw-Hill Book Company, 1965.

Dass, K. C. and L. F. Huggins: Laboratory modeling and overland flow analysis. Water Resources Research Center, Purdue University, Lafayette, Indiana, 1970.

Eagleson, P. S.: Dynamics of flood frequency. Water Resources Research, Vol. 8, No. 4, pp. 878-894, 1972.

Grace, R. A. and P. S. Eagleson: Similarity criteria in surface runoff process. Hydrodynamics Lab Report No. 77, 6-23 p., MIT, Cambridge, Massachusetts, July 1965.

Hanks, R. J. and S. A. Bowers: Numerical solution of the moisture flow equation for infiltration into layered soil. Soil Sci. Soc. Amer. Proc., Vol. 26, No. 6, pp. 530-534, 1962.

Henderson, F. M. and R. A. Wooding: Overland flow and groundwater flow from a steady rainfall of finite duration. J. Geophysical Research, Vol. 69, No. 8, pp. 1531-1540, 1964.

Himmelblan, D. M.: Applied nonlinear programming. pp. 158-167, McGraw-Hill Book Company, 1972.

Holland, M. E.: Colorado State University Experimental Rainfall-Runoff Facility: design and testing of rainfall systems. Colorado State University Experiment Station, Fort Collins, Colorado, 1969.

Houghton, D. D. and A. Kasahara: Nonlinear shallow fluid flow over an isolated ridge. Communications in Pure and Applied Mathematics, Vol. XXI, pp. 1-23, 1968.

Ibbit, R. P.: Systematic parameter fitting for conceptual models of catchment hydrology. Ph.D. dissertation, 400 p., University of London, England, 1970.

Izzard, C. F. and M. T. Augustine: Preliminary report on analysis of runoff resulting from simulated rainfall on a paved plot. Trans. AGU, Part 2, pp. 500-509, January 1943.

Kibler, D. F. and D. A. Woolhiser: The kinematic cascade as a hydrologic model. Colorado State University Hydrology Paper No. 39, pp. 1-27, Fort Collins, Colorado, 1970.

Kundu, P. A.: Mechanics of flow over very rough surfaces. Ph.D. dissertation, 254 p., Purdue University, Lafayette, Indiana, August 1971.

Lane, L. J.: Influence of simplifications of watershed geometry in simulation of surface runoff. Ph.D. dissertation, 198 p., Colorado State University, Fort Collins, Colorado, April 1975.

Langford, D. J. and A. K. Turner: An experimental study of the application of kinematic wave theory to overland flow. J. Hydrology, Vol. 18, pp. 125-1245, 1973.

Li, R. M.: Mathematical modeling of response from small watersheds. Ph.D. dissertation, 212 p., Colorado State University, Fort Collins, Colorado, August 1974.

Lighthill, M. J. and G. B. Whitham: On kinematic waves: flood movement in long rivers. Proc. Royal Society (London), Series A., Vol. 229, pp. 281-316, 1955.

Muzik, I.: State variable model of surface runoff from a laboratory catchment. Ph.D. dissertation, University of Alberta, Edmonton, Alberta, Canada, 1973.

Philip, J. R.: The theory of infiltration: 4. sorptivity and algebraic equations. Soil Science, Vol. 84, No. 3, pp. 257-264, 1957.

Robertson, A. F., et al: Runoff from impervious surfaces under conditions of simulated rainfall. Trans. ASAE, Vol. 9, No. 3, pp. 343-346, 1966.

Rosenbrock, H. H.: An automatic method for finding the greatest or least value of a function. Computer Journal, Vol. 4, pp. 175-184, 1960.

Rovey, E. W.: A kinematic model of upland watersheds. M. S. thesis, 113 p., Colorado State University, Fort Collins, Colorado, September 1974.

Rubin, J.: Theory of rainfall uptake by soils initially drier than their field capacity and its application. Water Resources Research, Vol. 2, No. 4, pp. 739-749, 1966.

Singh, V. P.: A nonlinear kinematic wave model of surface runoff. Ph.D. dissertation, 282 p., Colorado State University, Fort Collins, Colorado, May 1974.

Singh, V. P.: A laboratory investigation of surface runoff. J. Hydrology, Vol. 25, No. 2, pp. 187-200, 1975a.

Singh, V. P.: Hybrid formulation of kinematic wave models of watershed runoff. J. Hydrology, Vol. 27, pp. 33-40, 1975b.

Singh, V. P.: Kinematic wave modeling of watershed surface runoff: a hybrid approach. Proc. Int'l Symposium on the Hydrological Characteristics of River Basins and the Effect on these Characteristics of Better Water Management, Tokyo, Japan, 1975c.

Singh, V. P.: Estimation and optimization of kinematic wave parameters. Water Resources Bulletin, Vol. 11, No. 6, pp. 1091-1102, 1975d.

Singh, V. P.: Derivation of surface water lag time for converging overland flow. Water Resources Bulletin, Vol. 11, No. 3, pp. 505-513, 1975e.

Singh, V. P.: A distributed approach to kinematic wave modeling of watershed runoff. Proc. Nat'l Symposium on Urban Hydrology and Sediment Control, University of Kentucky, Lexington, Kentucky, July 1975f.

Singh, V. P.: Studies on rainfall-runoff modeling: 2. a distributed kinematic wave model of watershed surface runoff. New Mexico Water Resources Research Institute Report No. 065, 1976.

Smith, R. E.: Mathematical simulation of infiltrating watersheds. Ph.D. dissertation, Colorado State University, Fort Collins, Colorado, June 1970.

Smith, R. E. and D. A. Woolhiser: Mathematical simulation of infiltrating watersheds. Colorado State University Hydrology Paper No. 47, pp. 1-44, Fort Collins, Colorado, 1971.

Whisler, F. D. and A. Klute: The numerical analysis of infiltration, considering hysteresis, into vertical soil column of equilibrium under gravity. Soil Sci. Soc. Amer. Proc., Vol. 29, No. 5, pp. 489-494, 1965.

Woo, D. C. and E. F. Brater: Spatially varied flow from controlled rainfall. J. Hydraulics Div., Proc. ASCE, Vol. 88, No. HY6, pp. 31-56, 1962.

Wooding, R. A.: A hydraulic model for the catchment stream problem: 1. kinematic wave theory. J. Hydrology, Vol. 3, No. 3, pp. 254-264, 1965a.

Wooding, R. A.: A hydraulic model for the catchment problem: 2. numerical solutions. J. Hydrology, Vol. 3, No. 3, pp. 268-282, 1965b.

Wooding, R. A.: A hydraulic model for the catchment stream problem: 3. comparison with runoff observations. J. Hydrology, Vol. 4, pp. 21-37, 1966.

Woolhiser, D. A. and J. A. Ligget: Unsteady, one dimensional flow over a plane - the rising hydrograph. Water Resources Research, Vol. 3, No. 3, pp. 753-771, 1967.

Woolhiser, D. A.: Overland flow on a converging surface. Trans. ASAE, Vol. 12, No. 4, pp. 460-462, 1969.

Woolhiser, D. A., et al: Overland flow on rangeland watersheds. J. Hydrology (N.Z.), Vol. 9, No. 2, pp. 336-356, 1970.

Woolhiser, D. A., et al: Experimental investigation of converging overland flow. Trans. ASAE, Vol. 14, No. 4, pp. 684-687, 1971.

Woolhiser, D. A. and E. F. Schulz: Large material models on watershed hydrology research. Int'l Symposium on River Mechanics, IAHR, Bangkok, Thailand, 1973.

Yen, D. C. and V. T. Chow: A laboratory study of surface runoff due to moving rainstorms. Water Resources Research, Vol. 5, No. 5, pp. 989-1006, 1969.

APPENDIX A

DERIVATION OF EQUATIONS OF FLOW FOR A CONVERGING SECTION

This derivation of flow equations requires the following simplifying assumptions:

1. The slope of land surface is so small that the sine of the slope angle may be taken to be equal to the tangent, and the cosine equal to unity.
2. The friction slope for uniform steady flow may be applied to nonuniform, unsteady flow of the same depth and average velocity.
3. The streamlines of flow have negligible curvature, ensuring hydrostatic vertical pressure distribution at all time.
4. The flow velocity in any cross-section is constant.
5. The flow is gradually varied so that vertical components of velocity and acceleration are negligible in comparison with the components along the direction of flow.
6. The energy and momentum coefficients, used as corrections to nonuniform velocity distributions, are equal to one.
7. The channel geometry is prismatic.
8. The transverse water surface profile is horizontal.
9. Surface tension forces are negligible.
10. The x-component of momentum flux due to the distributed lateral inflow is negligible.

Because of the radial symmetry, only a small element in one sector of the flow region need be considered for deriving the flow equations. The flow element is shown in Fig. A-1 (a).

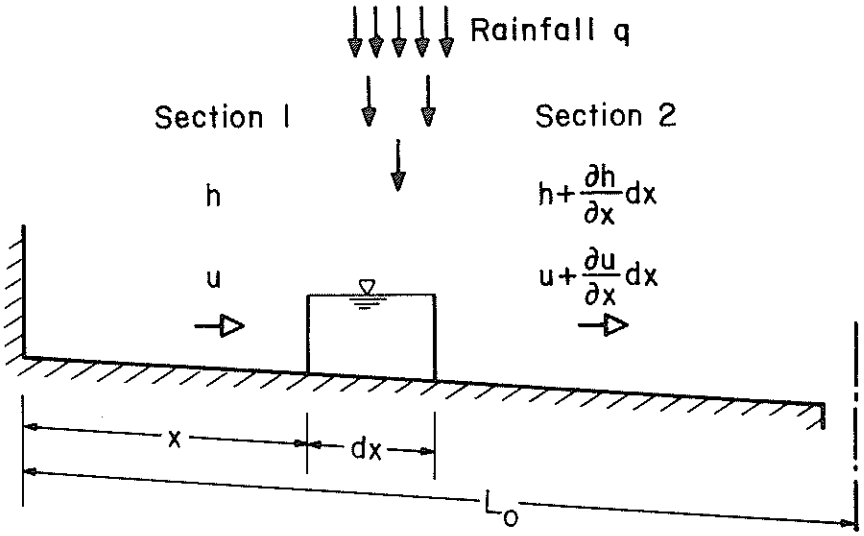

Fig. A-1(a). Sectional element of flow element.

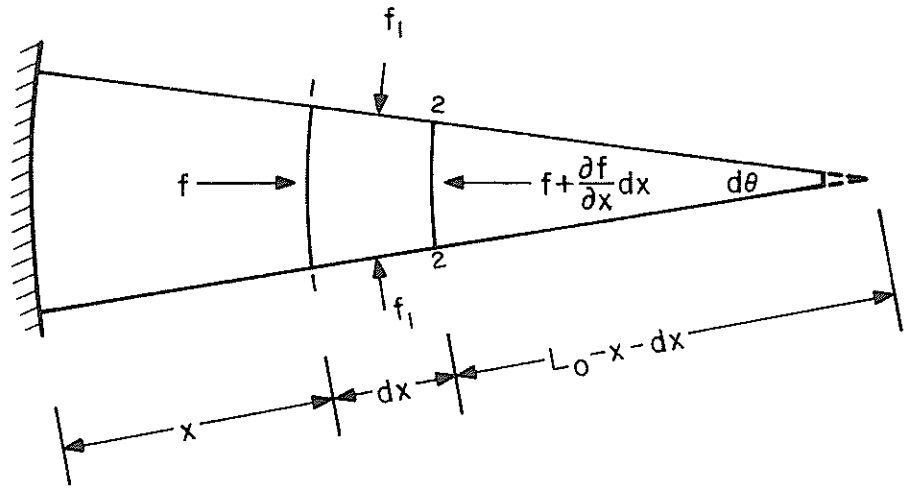

Fig. A-1(b). Plan sketch of flow element showing hydrostatic forces.

Consider two points, 1 and 2, corresponding to the upstream and downstream sections of the flow element with respect to the upstream boundary. The velocities and depths at the sections are u and $(u + \frac{\partial h}{\partial x} dx)$, and h and $(h + \frac{\partial h}{\partial x} dx)$ as indicated in the Fig. A-1 (a). The lateral inflow, rainfall is denoted by q and has dimensions of volume per unit area per unit time. The radius of the flow region is L_o(length).

A.1 CONTINUITY EQUATION

The continuity equation states that the net flow rate into the element under consideration must equal the outflow from the element and the rate of change in its storage. That is, the difference between inflow and outflow for a small time interval, dt, is equal to change in storage during that time.

The inflow consists of two components: the flow at section 1 and the rainfall or lateral inflow, and is equal to:

$$uh(L_o - x)\, d\theta dt + q(L_o - x)\, dx d\theta dt$$

The outflow comprises the flow at section 2, and is equal to:

$$(u + \frac{\partial u}{\partial x} dx)\ (h + \frac{\partial h}{\partial x} dx)\ (L_o - x - dx)\, d\theta dt$$

The change in storage equals the rate of change of the volume of the element multiplied by dt, that is:

$$\frac{\partial h}{\partial t}\ (L_o - x)\, d\theta dx dt$$

Upon combining these terms the continuity relation becomes:

$$uh\ (L_o - x)\, d\theta dt + q(L_o - x)\, dx d\theta dt - (u + \frac{\partial u}{\partial x} dx)\ (h + \frac{\partial h}{\partial x} dx)$$

$$(L_o - x - dx)\, d\theta dt = \frac{\partial h}{\partial t}\ (L_o - x)\, d\theta dx dt$$

Upon simplification,

$$uh(L_o - x) + q(L_o - x)\, dx - (u + \frac{\partial u}{\partial x} dx)\ (h + \frac{\partial h}{\partial x} dx)\ (L_o - x - dx) = \frac{\partial h}{\partial t}\ (L_o - x)\, dx$$

upon further simplification,

$$q + \frac{uh}{(L_o - x)} - u\frac{\partial h}{\partial x} + u\frac{\partial h}{\partial x}\frac{dx}{(L_o - x)} - h\frac{\partial u}{\partial x} + h\frac{\partial u}{\partial x}\frac{dx}{(L_o - x)} - \frac{\partial u}{\partial x}\frac{\partial h}{\partial x}dx$$

$$\frac{(L_o - x - dx)}{(L_o - x)} = \frac{\partial h}{\partial t}$$

Neglecting the terms of higher order and rearranging the remaining terms yields:

$$\frac{\partial h}{\partial t} + u\frac{\partial h}{\partial x} + h\frac{\partial u}{\partial x} = q + \frac{uh}{(L_o - x)} \qquad \text{(A-1)}$$

This is the continuity equation for a converging surface.

A.2 MOMENTUM EQUATION

The momentum principle states that the rate of change of momentum is equal to the sum of the forces acting on that element. The forces are depicted in Fig. A-1 (b).

The hydrostatic force at section 1, acting downstream, is:

$$f = \gamma\frac{h^2}{2}(L_o - x)\,d\theta$$

The hydrostatic force at Section 2, acting upstream, is:

$$f + \frac{\partial f}{\partial x}dx = f + \gamma h(L_o - x)\frac{\partial h}{\partial x}d\theta dx - \tfrac{1}{2}\gamma h^2 d\theta dx$$

where γ = weight density of the fluid.

A further hydrostatic force acts on each of the converging sides of the element as shown in Fig. A-1 (b). That is:

$$f_1 = \tfrac{1}{2}\gamma h^2 dx$$

The resultant component of side forces in the direction of flow is:

$$f_{1c} = 2\tfrac{1}{2}\gamma h^2 dx\frac{d\theta}{2}$$

$$= \tfrac{1}{2}\gamma h^2 dx d\theta$$

acting in the direction opposing the motion. The force due to gravity, acting downstream, is:

$$f_G = \gamma h(L_o - x)\, d\theta dx \sin \phi$$

where ϕ = bed slope.

The frictional force opposing the motion is:

$$f_F = \gamma h(L_o - x)\, d\theta dx \frac{\zeta}{\gamma h}$$

where ζ = shear stress. The force resulting from the momentum exchange with the lateral inflow or rainfall is:

$$f_q = \rho q(L_o - x)\, d\theta dx\, (u - v)$$

where ρ = mass density of the fluid, and v = component of lateral inflow velocity in the direction of flow.

The force, f_q, tends to retard the flow. The rate of change of momentum of the element of fluid is:

$$\frac{d}{dt}(mu) = \rho h(L_o - x)\, dx d\theta \frac{du}{dt}$$

It can be written that:

$$\frac{du}{dt} = \frac{\partial u}{\partial x}\frac{dx}{dt} + \frac{\partial u}{\partial t}$$

$$= u\frac{\partial u}{\partial x} + \frac{\partial u}{\partial t}$$

Hence,

$$\frac{d}{dt}(mu) = \rho h(L_o - x)\, dx d\theta \left(u\frac{\partial u}{\partial x} + \frac{\partial u}{\partial t}\right)$$

The equation of motion can now be written as:

$$f - \left(f + \frac{\partial f}{\partial x} dx\right) - f_{lc} + f_G - f_F - f_q = \frac{d}{dt}(mu)$$

Substitution of terms leads to the following:

$$f - \left(f + \gamma h(L_o - x)\frac{\partial h}{\partial x} d\theta dx - \tfrac{1}{2}\gamma h^2 d\theta dx\right) - \tfrac{1}{2}\gamma h^2 d\theta dx + \gamma h(L_o - x)\, d\theta dx \sin \phi$$

$$- \gamma h(L_o - x)\, d\theta dx \frac{\zeta}{\gamma h} - \rho q(L_o - x)\, d\theta dx\, (u - v) = \rho h(L_o - x)\, dx d\theta \left(u\frac{\partial u}{\partial x} + \frac{\partial u}{\partial t}\right)$$

Simplification and re-arrangement of the terms give:

$$\frac{\partial u}{\partial t} + u\,\frac{\partial u}{\partial x} + g\,\frac{\partial h}{\partial x} = g\left(\sin\phi - \frac{\zeta}{\gamma h}\right) - \frac{g}{h}(u - v) \qquad \text{(A-2)}$$

This is the equation of momentum for a converging section.

A.3 KINEMATIC MOMENTUM EQUATION

Consider that the inflow, free surface slope, and inertia terms of Eq. (A-2) are all negligible as compared with those of bottom slope and friction. Equation (A-2) then reduces to:

$$\zeta = \gamma h \sin\phi \qquad \text{(A-3)}$$

This is a well-known relation for steady, uniform flow in a wide rectangular channel.

Define

$$\zeta = C_f \gamma \frac{u^2}{2g} \qquad \text{(A-4)}$$

where C_f is a function of Reynolds Number and the relative surface roughness.

From Eqs. (A-3) and (A-4), u can be written as

$$u = \left(\frac{2gh \sin\phi}{C_f}\right)^{1/2} = C(h \sin\phi)^{1/2} \qquad \text{(A-5)}$$

where $C = (2g/C_f)^{1/2}$, Chezy's coefficient. Assuming C to be constant (as a first approximation), Eq. (A-5) can be used to write:

$$Q = uh = ah^{3/2}$$

where

$$\alpha = C(\sin\phi)^{1/2} = \left(\frac{2g \sin\phi}{C_f}\right)^{1/2}$$

More accurately, of course, because of the variability of C_f

$$Q = \alpha h^n \qquad \text{(A-6)}$$

Hence

$$u = \alpha h^{n-1} \tag{A-7}$$

Equations (A-6) and (A-7) are equations of motion for the kinematic case.

APPENDIX B

We will show that the curves $t = t(x,t_o)$, $o \leq t_o \leq T$, fill out all of S above $t = t(x,o)$. For this purpose it is sufficient to prove that, for fixed $x > o$, $t(x,t_o) \to \infty$ as $t_o \to T$. Together with our assumption that the curves $t = t(x,t_o)$ do not intersect in S for distinct values of t_o, this implies that $h(x,t)$ is defined throughout S.

We make the following assumptions on $q(x,t)$, $\alpha(x)$ and n:

$n > 1$; $\alpha_1 \leq \alpha(x) \leq \alpha_2$, $\alpha_1 > o$

$o < q(x,t) \leq q$ if $t \leq T$, $q(x,t) = o$ if $t > T$

From Eq. (2-10) we get:

$$o < h(x,t_o) < \left[\frac{1}{L_o r\alpha_1}\int_o^x qL_o d\xi\right]^{\frac{1}{n}} = \left(\frac{qx}{r\alpha_1}\right)^{\frac{1}{n}} \tag{B-1}$$

From Eq. (2-7)

$$\frac{dt}{dx} > \frac{1}{n\alpha_2}\left(\frac{qx}{r\alpha_1}\right)^{-\left(\frac{n-1}{n}\right)} = \frac{C_1}{n}\, x^{-1+\frac{1}{n}} \tag{B-2}$$

where

$$C_1 = \frac{1}{\alpha_2}\left(\frac{q}{r\alpha_1}\right)^{-1+\frac{1}{n}}$$

Integrating Eq. (B-2) between o and x

$$t(x,t_o) > t_o + C_1\, x^{\frac{1}{n}} \tag{B-3}$$

Let $x^*(t_o)$ be the solution of $T = t(x^*,t_o)$. Then, from Eq. (B-3),

$$x^*(t_o) < \left(\frac{T - t_o}{C_1}\right)^n$$

We have, referring to Eq. (2-11),

$$\int_o^{\eta} (L_o - \xi)\, q(\xi, t\,(\xi,t_o))\, d\xi < \int_o^{x^*(t_o)} qL_o d\xi = qL_o x^*(t_o) < qL_o \left(\frac{T - t_o}{C_1}\right)^n$$

Then we have:

$$t(x,t_o) > t_o + \int_o^x \frac{(L_o r)^{\frac{n-1}{n}}}{n\alpha_2^{\frac{1}{n}}} \left\{qL_o \left(\frac{T - t_o}{C_1}\right)^n\right\}^{-\left(\frac{n-1}{n}\right)} d\eta = t_o + \frac{C_2 x}{(T - t_o)^{n-1}} \qquad \text{(B-4)}$$

It follows from Eq. (B-4) that $t(x,t_o) \to \infty$ as $t_o \to T$ for fixed $x > o$.

It follows from Eq. (B-1) that

$$o < h(x,t) < \left(\frac{qx}{r\alpha_1}\right)^{\frac{1}{n}} \qquad \text{(B-5)}$$

Equation (B-5) implies that $h(o,t) = o$ for $t > T$.

APPENDIX C

When $q(x,t) = q$ the curves $t = t(x,t_o)$ do not, for distinct values of t_o, intersect in S. This implies from Eqs. (2-11) and (2-53); the curves of Eq. (2-53) are the prolongation beyond $t = T$ of the curves (Eq. 2-11). Equation (2-11) implies that $t(x,t_o)$ is, for fixed x, an increasing function of t_o, and Eq. (2-53) implies that $t(x,x_o^*)$ is, fixed x, a decreasing function of x_o^*.

To prove that the curves $t = t(x,x_o)$ do not intersect in domain D_3 we impose the condition that $(L_o - x)/\alpha(x)$ is a decreasing function of x; we retain the condition $q(x,t) = q$. Under these conditions we show that Eq. (2-34) is, for fixed x, a decreasing function of x_o. We write the integral in Eq. (2-34) as the difference of two integrals, one from x_o to L_o and the other from x to L_o; we extend the definition of $\alpha(x)$ to $L_o < x \leq L_o$ by $\alpha(x) = \alpha(L_o(1-r))$. The integral from x to L_o is an increasing function of x_o, so its negative is a decreasing function x_o. In the integral from x_o to L_o we introduce the change of variable $\xi = (L_o - \eta)/(L_o - x_o)$. Then it becomes

$$\int_o^1 \left[\frac{L_o - x_o}{\alpha(L_o - \xi\,(L_o - x_o))}\right]^{\frac{1}{n}} \left(\frac{\xi}{1 - \xi^2}\right)^{\frac{n-1}{n}} d\xi \qquad \text{(C-1)}$$

Now if $x = L_o - \xi\,(L_o - x_o) = (1 - \xi)\,L_o + \xi x_o$

then

$$\frac{L_o - x_o}{\alpha(L_o - \xi\,(L_o - x_o))} = \frac{L_o - x}{\xi\alpha(x)}$$

It is clear from Eq. (C-1) that for fixed ξ the bracketed term is a decreasing function of x_o. Thus Eq. (C-1) is a decreasing function of

x_o and, therefore, $t(x,x_o)$ is a decreasing function of x_o in domain D_3.

To conclude the discussion we need to prove that the curves $t = t(x; x_o^*, x_o)$ do not intersect in domain D_{12}. We will show that $t(x; x_o^*, x_o)$ is, for fixed x, a decreasing function of x_o. In Eq. (2-97) we introduce, as above, the change of variables:

$$T = \alpha \int_{\left(\frac{L_o - x_o^*}{L_o - x_o}\right)}^{1} \left[\frac{L_o - x_o}{\alpha(L_o - \xi\,(L_o - x_o))}\right]^{\frac{1}{n}} \left(\frac{\xi}{1-\xi^2}\right)^{\frac{n-1}{n}} d\xi \qquad (C\text{-}2)$$

The bracketed term in Eq. (C-2) is a decreasing function of x_o for fixed ξ, so $(L_o - x_o^*)/(L_o - x_o)$ is a decreasing function of x_o. Introducing ξ in Eq. (2-96) we get

$$t(x; x_o^*, x_o) = T + \frac{1}{n} \frac{\left(\frac{q}{2}\right)^{\frac{1-n}{n}}}{\left[1 - \left(\frac{L_o - x_o^*}{L_o - x_o}\right)^2\right]^{\frac{n-1}{n}}} \int_{\frac{L_o - x}{L_o - x_o}}^{\frac{L_o - x_o^*}{L_o - x_o}} \left[\frac{L_o - x_o}{\alpha(L_o - \xi\,(L_o - x_o))}\right]^{\frac{1}{n}} \xi^{\frac{n-1}{n}}\, d\xi$$

since

$$\frac{1}{1 - \left(\frac{L_o - x_o^*}{L_o - x_o}\right)^2}\ ;\ \frac{L_o - x_o^*}{L_o - x_o}\ ;\ \frac{L_o - x_o}{\alpha(L_o - \xi\,(L_o - x_o))}$$

are decreasing functions of x_o and $(L_o - x)/(L_o - x_o)$ is an increasing function of x_o, $t(x; x_o^*, x_o)$ is a decreasing function of x_o.

APPENDIX D

We investigate the behavior of $h(x,t)$ for fixed x in domain D_{12}. We assume that $q(x,t) = q$ and $(L_o - x)/\alpha(x)$ is a decreasing function of x. It is sufficient, from Eq. (2-99), to consider

$$(L_o - x_o)^2 - (L_o - x_o^*)^2 \tag{D-1}$$

as a function of t for fixed x. We may write Eq. (D-1) as:

$$G(x_o,Z) = (L_o - x_o)^2(1 - Z^2) \quad , \quad Z = \frac{L_o - x_o^*}{L_o - x_o} \quad , \quad o < Z < 1 \tag{D-2}$$

where, by Eq. (C-2),

$$T = \frac{1}{n}\left(\frac{q}{2}\right)^{\frac{1-n}{n}} \int_Z^1 \left[\frac{L_o - x_o}{\alpha(L_o - \xi\,(L_o - x_o))}\right]^{\frac{1}{n}} \left(\frac{\xi}{1 - \xi^2}\right)^{\frac{n-1}{n}} d\xi \tag{D-3}$$

We have

$$\frac{\partial G}{\partial t} = \frac{dG}{dZ}\,\frac{dZ}{dx_o}\,\frac{\partial x_o}{\partial t} \tag{D-4}$$

where, on the left of Eq. (D-4), G is a function of x and t, and on the right a function of Z. Since $\frac{dZ}{dx_o} < o$ and $\partial x_o/\partial t < o$ it is clear from Eq. (D-4) that the sign of $\partial G/\partial t$, and therefore the sign of $\partial h/\partial t$ agrees with the sign of dG/dZ.

We now specialize the hypothesis on $\alpha(x)$ still further: $\alpha(x) = \alpha$ when $x^* < x \leq L_o(1-r)$. Then Eq. (D-3) becomes

$$\frac{nT\alpha^{\frac{1}{n}}}{\left(\frac{q}{2}\right)^{\frac{1-n}{n}}(L_o - x_o)^{\frac{1}{n}}} = \int_Z^1 \left(\frac{\xi}{L_o - \xi}\right)^{\frac{n-1}{n}} d\xi \tag{D-5}$$

Combining Eqs. (D-5) and D-2) we obtain:

$$G(x_o,Z) = g(Z) = \alpha^2 \left\{ \frac{nT}{\left(\frac{q}{2}\right)^{\frac{1-n}{n}}} \right\}^{2n} \frac{1 - Z^2}{\left[\int_Z^1 \left(\frac{\xi}{1 - \xi^2} \right)^{\frac{n-1}{n}} d\xi \right]^{2n}} \tag{D-6}$$

Calculating $g'(Z)$ we see that the sign of $g'(Z)$ is determined by

$$n(1 - Z^2)^{\frac{1}{n}} - Z^{\frac{1}{n}} \int_Z^1 \left(\frac{\xi}{1 - \xi^2} \right)^{\frac{n-1}{n}} d\xi \tag{D-7}$$

Since $\xi/(1 + \xi) \leq \frac{1}{2}$ when $o \leq \xi \leq 1$

$$\int_Z^1 \left(\frac{\xi}{1 - \xi^2} \right)^{\frac{n-1}{n}} d\xi < \left(\frac{1}{2} \right)^{\frac{n-1}{n}} n(1 - Z)^{\frac{1}{n}}$$

and therefore Eq. (D-7) is greater than

$$n \left\{ (1 - Z^2)^{\frac{1}{n}} - \left[\left(\frac{1}{2} \right)^{n-1} (Z - Z^2) \right]^{\frac{1}{n}} \right\} \tag{D-8}$$

Because of

$$a^n - b^n = (a - b)\ (a^{n-1} + a^{n-2}b + \ldots\ldots + b^{n-1})$$

the sign of Eq. (D-8) is the same as that of

$$1 - Z^2 - \frac{1}{2^{n-1}} (Z - Z^2) = (1 - Z) \left[1 + \left(1 - \frac{1}{2^{n-1}} \right) Z \right] \tag{D-9}$$

Since Eq. (D-9) is positive for $o < Z < 1$ we conclude that $g'(Z) > o$ for $o < Z < 1$, and finally that $\partial h/\partial t > o$. Thus, on the hypothesis $\alpha(x) = \alpha$ when $x^* < x \leq L_o(1-r)$, $h(x,t)$ is, for fixed x, an increasing function of t in domain D_{12}.

APPENDIX E

It follows from appendix C that the curves $t = t(x,t_o)$ do not intersect in domain D_2 and, on the assumption of Eq. (3-24), that the curves $t = t(x,x_o)$ do not intersect in domain D_3. It follows from Eq. (3-20) that $t_{x_o}^*(x,x_o^*) < o$, so the curves $t = t(x,x_o^*)$ do not intersect in domain D_1(case A) or in domain D_{11} (cases B_1 and B_2). We now prove, on the assumption of Eq. (3-24), that the curves $t = t(x;x_o^*,x_o)$ do not intersect in domain D_{12}. We introduce the change of variable $\xi = (L_o - \eta)/(L_o - x_o)$ in Eqs. (3-33) and (3-36):

$$T = \gamma^* \int_x^1 \left[\frac{L_o - x_o}{\alpha(L_o - \xi\,(L_o - x_o))}\right]^{\frac{1}{n}} \left(\frac{\xi}{1 - \xi^2}\right)^{\frac{n-1}{n}} d\xi \qquad \text{(E-1)}$$

$$t(x;x_o^*,x_o) = T + \frac{1}{n}\left(\frac{q}{2}\right)^{\frac{1-n}{n}} \int_{\frac{L_o - x}{L_o - x_o}}^{x} \left[\frac{L_o - x_o}{\alpha(L_o - \xi\,(L_o - x_o))}\right]^{\frac{1}{n}}$$

$$\left(\frac{\xi}{1 - \rho - Z^2 + \rho\xi^2}\right)^{\frac{n-1}{n}} d\xi \qquad \text{(E-2)}$$

where $Z = (L_o - x_o^*)/(L_o - x_o)$. As in appendix C, it follows from Eq. (E-1) that $dZ/dx_o < o$. We have, therefore, from Eq. (E-2), that $t_{x_o}(x;x_o^*(x_o),x_o) < o$.

APPENDIX F

In this appendix we discuss the behavior, when $\alpha(x) = \alpha$, of $h(x,t)$ for fixed x in domain D_{12}. The discussion is parallel to that of appendix D. From Eq. (E-1) we have:

$$T = \gamma^* \alpha^{-\frac{1}{n}} (L_o - x_o)^{\frac{1}{n}} \int_Z^1 \left(\frac{\xi}{1-\xi^2}\right)^{\frac{n-1}{n}} d\xi \tag{F-1}$$

From Eq. (3-35) it is clear that we need to be concerned only with

$$G(x_o,Z) = (1-\rho)(L_o - x_o)^2 = (L_o - x_o)^2 (1 - \rho - Z^2) \tag{F-2}$$

as a function of x and t. On eliminating x_o between Eqs. (F-1) and (F-2) we see that Eq. (F-2) is, except for a constant positive multiplier,

$$g(L) = \frac{1-\rho-Z^2}{\left[\int_L^1 \frac{\xi}{1-\xi^2} d\xi\right]^{\frac{n-1}{n}}} \tag{F-3}$$

The relationship between (x,t) and (x,Z) in domain D_{12} is obtained from Eq. (E-2):

$$t(x,L) = T + \frac{1}{n} \left(\frac{q}{2}\right)^{\frac{1-n}{n}} \alpha^{-\frac{1}{n}} (L_o - x_o)^{\frac{1}{n}} \int_{\frac{L_o-x}{L_o-x_o}}^{Z} \left[\frac{\xi}{1-\rho-Z^2+\rho\xi^2}\right]^{\frac{n-1}{n}} d\xi \tag{F-4}$$

Here x_o is a function of Z through Eq. (F-1). Since $Z'(x_o) < 0$ and $t_{x_o}(x;x_o^*(x_o),x_o) < 0$, $t_Z(x,Z) > 0$. The correspondence between (x,t) and (x,Z) in domain D_{12} is one to one. The curve $Z = Z_o$ coincides with $t = t(x; x_o^*, x_o)$ where x_o and x_o^* are determined by $(L_o - x_o^*)/(L_o - x_o) = Z_o$ and Eq. (F-1).

A simple calculation shows that the sign of $g'(Z)$ and therefore also the sign of $h_t(x,t)$ is determined by

$$K(Z) = n(1-\rho-Z^2) - \left[Z(1-Z^2)^{n-1}\right]^{\frac{1}{n}} \int_Z^1 \left(\frac{\xi}{1-\xi^2}\right)^{\frac{n-1}{n}} d\xi \tag{F-5}$$

For a fixed x, $T \leq t \leq t(x, x^*)$ in case B_1, and also in case B_2 when $x \leq \bar{x}$; when $x > \bar{x}$, $t \leq t \leq t^o(x)$. Correspondingly

$$\frac{L_o - x}{L_o - x_o} \leq Z \leq Z_o(x) \qquad \text{(F-6)}$$

where $Z_o(x) = (L_o - x^*)/L_o$ in case B_1 and also in case B_2 when $x \leq \bar{x}$; when $x < \bar{x}$ we determine $Z_o(x)$ from Eq. (F-4) by replacing the left side of Eq. (F-4) by $t^*(x)$ and then solving Eqs. (F-4) and (F-1) for Z. Thus the problem is to determine the sign of K(Z) in the interval of Eq. (F-6). If $K(Z_o) = 0$ and Z_o is in the interval of Eq. (F-6) then the maximum occurs on $Z = Z_o$; the corresponding value of t is determined from Eq. (F-4). Since the locus $Z = Z_o$ is one of the curves $t = t(x; x_o^*, x_o)$, the maximum of h(x,t), for fixed x, occurs on this curve when these maxima are interior to the t-interval corresponding to the given x. Various possibilities are indicated in Figs. 3-7 to 3-9.

APPENDIX G

DIMENSIONLESS EQUATIONS AND DERIVATION OF NORMALIZING QUANTITIES

There is an advantage in writing Eqs. (A-1), (A-6) and (A-7) in dimensionless form. Therefore, the following normalizing quantities are introduced:

H_o = normal depth for a discharge equal to the total steadystate outflow from the converging section divided by the mean width of the section.

$X_o = L_o(1-r)$

$T_o = \left(\frac{1}{q_{max}}\right)^{\frac{n-1}{n}} \left[\frac{L_o(1-r)}{\alpha}\right]^{\frac{1}{n}}$, the time required to traverse the distance x_o, at the velocity V_o, corresponding to the normalizing depth.

$V_o = \alpha H_o^{n-1}$

q_{max} = maximum spatially uniform lateral inflow

$$q_o = \frac{H_o V_o}{L_o(1-r)}$$

$$Q_o = \frac{H_o V_o (1+r)}{2r}$$

The parameter r defines the degree of convergence. The dimensionless variables, designated with asterisks, are thus given by:

$$h_* = \frac{h}{H_o} \; ; \; q_* = \frac{q}{q_o} \; ; \; t_* = \frac{t}{T_o} ; \; x_* = \frac{x}{x_o} \; ; \; u_* = \frac{u}{V_o} \; ; \; Q_* = \frac{Q}{Q_o}$$

The following equations are obtained when the dimensionless variables are substituted into Eqs. (A-1), (A-6) and (A-7):

$$\frac{\partial h_*}{\partial t_*} + \frac{\partial h_*^n}{\partial x_*} = q_* + \frac{(1-r)h_*^n}{[1-(1-r)x_*} \tag{G-1}$$

$$Q_* = h_*^n \tag{G-2}$$

$$u_* = h_*^{n-1} \tag{G-3}$$

These are dimensionless forms of Eqs. (A-1) and (A-6)-(A-7). Note that the parameter α no longer appears in the equations. We will now present the derivation of the above normalizing quantities.

G. 1 DEFINITION OF q_o

Write the equation of continuity in dimensionl form for a converging section as

$$\frac{\partial h}{\partial t} + u \frac{\partial h}{\partial x} + h \frac{\partial u}{\partial x} = q + \frac{uh}{(L_o - x)} \qquad (G\text{-}4)$$

All symbols retain their same meaning as explained in Chapter 2. Utilizing the normalizing quantities, write the Eq. (G-4) in dimensionless form as

$$\frac{\partial h_*}{\partial t_*} + u_* \frac{\partial h_*}{\partial x_*} + h_* \frac{\partial u_*}{\partial x_*} = \frac{q_o}{H_o} \frac{L_o}{V_o} (1-r) q_* + \frac{(1-r) u_* h_*}{[1-x_*(1-r)]} \qquad (G\text{-}5)$$

One of the objectives of normalization is to reduce the number of parameters. From Eq. (G-5) if q_o is chosen as $\frac{H_o V_o}{L_o(1-r)}$ the normalizing quantities will be eliminated.

G. 2 DEFINITION OF T_o

Area of the converging section,

$$A = \frac{\pi\theta}{360} (L_o^2 - r^2 L_o^2)$$

$$\text{Mean width} = \frac{\text{Area}}{\text{Length of flow}}$$

$$= \frac{\pi\theta(L_o^2 - r^2 L_o^2)}{360(1-r)L_o}$$

$$= \frac{\pi\theta L_o (1+r)}{360}$$

$$Q_o = \frac{\pi\theta L_o^2 (1-r^2) q_{max}/360}{2\pi\theta r L_o/360}$$

$$= \frac{L_o}{2} \frac{(1-r^2)}{r} q_{max}$$

= flow/unit width at $x_* = 1$.

Note $Q_o \neq H_o V_o$

$$H_o V_o = \frac{L_o(1-r^2)}{2r} q_{max} \frac{\frac{2\pi\theta r L_o}{360}}{\frac{\pi\theta L_o(1+r)}{360}} = L_o(1-r)q_{max} \qquad \text{(G-6)}$$

$$V_o = \alpha H_o^{n-1} \qquad \text{(G-7)}$$

$$H_o = (V_o/\alpha)^{1/(n-1)}$$

$$T_o = \frac{L_o(1-r)}{V_o} \qquad \text{(G-8)}$$

Combine Eqs. (G-6) and (G-7) to give

$$V_o = (\alpha)^{1/n}[L_o(1-r)q_{max}]^{(n-1)/n} \qquad \text{(G-9)}$$

Substitute Eq. (G-9) into Eq. (G-8) to obtain

$$T_o = \left(\frac{1}{q_{max}}\right)^{(n-1)/n} \left[\frac{L_o(1-r)}{\alpha}\right]^{1/n} \qquad \text{(G-10)}$$

G. 3 DEFINITION OF q_{max}

Since $$q_o = \frac{H_o V_o}{L_o(1-r)}$$, and

$$H_o V_o = L_o(1-r)q_{max}$$

These two terms can be combined to yield

$$q_o = \frac{H_o V_o}{L_o(1-r)} = \frac{L_o(1-r)q_{max}}{L_o(1-r)} = q_{max}$$

Hence $$q_{max} = q_o \qquad \text{(G-11)}$$

G. 4 DEFINITION OF Q_o

Since $$Q_o = \frac{L_o}{2} \frac{(1-r^2)}{r} q_{max}$$

Also, $$Q_o \neq H_o V_o$$

$$H_o V_o = L_o (1-r) q_{max}$$

Hence

$$Q_o = H_o V_o \frac{(1+r)}{2r} \qquad \text{(G-12)}$$

APPENDIX H

PARAMETER ESTIMATION AND OPTIMIZATION TECHNIQUES

This appendix briefly discusses those techniques of parameter estimation and optimization that were specifically developed for this study and may have limited applicability in other cases.

H. 1 PARAMETER ESTIMATION TECHNIQUES

H. 1. 1 Linear Interpolation of Errors

This scheme was utilized to estimate the watershed parameter α such that the observed and computed peak flow rates were equal for a complex rainstorm.

The method is based on linear interpolation of errors. Two initial approximations are chosen and corresponding errors[1] are computed. The directional derivative of error with respect to the approximation is determined, and the next iteration is enumerated accordingly. The algorithm is structured as follows:

Let Ψ_{i-1}, Ψ_i be the initial approximations, and E_{i-1}, E_i be the corresponding errors. Then successive iteration is computed from the following

(1) If $(E_{i-1}E_i) < 0$ then

$$\Psi_{i+1} = \frac{|E_{i-1}|\Psi_i + |E_i|\Psi_{i-1}}{E_{i-1} + E_i} \qquad \text{(H-1)}$$

(2) If $E_i < 0$, $E_{i-1} < 0$, $|E_i| > E_{i-1}|$, and $\Psi_i > \Psi_{i-1}$ or

$E_i > 0$, $E_{i-1} > 0$, $E_i > E_{i-1}$, and $\Psi_i > \Psi_{i-1}$ then

---

[1]Error E was defined as $E = (Q_{p_o} - Q_{p_e})/Q_{p_o}$ corresponding to a given α.

$$\Psi_{i+1} = \Psi_{i-1} - \frac{(\Psi_i - \Psi_{i-1})}{E_i - E_{i-1}} E_{i-1} \qquad \text{(H-2)}$$

(3) If $E_i < 0$, $E_{i-1} < 0$, $|E_i| > |E_{i-1}|$, and $\Psi_i < \Psi_{i-1}$, or

$E_i > 0$, $E_{i-1} > 0$, $E_i > E_{i-1}$, and $\Psi_i < \Psi_{i-1}$ then

$$\Psi_{i+1} = \Psi_{i-1} + \frac{\Psi_{i-1} - \Psi_i}{E_i - E_{i-1}} E_{i-1} \qquad \text{(H-3)}$$

(4) If $E_i < 0$, $E_{i-1} < 0$, $|E_i| < |E_{i-1}|$, and $\Psi_i > \Psi_{i-1}$ or

$E_i > 0$, $E_{i-1} > 0$, $E_i > 0$, $E_i > E_{i-1}$, and $\Psi_i > \Psi_{i-1}$ then

$$\Psi_{i+1} = \Psi_i + \frac{(\Psi_i - \Psi_{i-1})}{(E_{i-1} - E_i)} E_i \qquad \text{(H-4)}$$

(5) If $E_i < 0$, $E_{i-1} < 0$, $|E_i| < |E_{i-1}|$, and $\Psi_i < \Psi_{i-1}$, or

$E_i > 0$, $E_{i-1} > 0$, $E_i > E_{i-1}$, and $\Psi_i < \Psi_{i-1}$

Then

$$\Psi_{i+1} = \Psi_i - \frac{(\Psi_{i-1} - \Psi_i)}{E_{i-1} - E_i} E_i \qquad \text{(H-5)}$$

The convergence criterion was

$$|E_i| \leq \varepsilon$$

where ε was chosen to be 0.01. The scheme was found to converge invariably and the rate of convergence was almost quadratic. It must be noted here that the scheme is constrained by the fact that the parameter α cannot be negative. The starting values $\alpha_i = 2.50$ and $\alpha_{i+1} = 1.1\ \alpha_i$ were found to be good initial guesses.

H. 1. 2 Analytical Method

The analytical method was developed to estimate the parameter such that observed and estimated hydrograph peaks would be exactly the same due to a given pulsed rainstorm. The method was specifically useful on rainfall-runoff experimental facility. The recession hydrograph in dimensionless form can be written

as (from Chapter 2):

$$Q_* = \frac{x_*[2-(1-r)x_*]}{(1+r)} \tag{H-6}$$

Equation (H-6) will give the hydrograph peak also. Writing Eq. (H-6) for the hydrograph peak Q_{p*} as,

$$Q_{p*} = \frac{x_*[2-(1-r)x_*]}{(1+r)} \tag{H-7}$$

Writing Eq. (H-7) for x_* as

$$(1-r)x_*^2 - 2x_* + (1 + r)Q_{p*} = 0 \tag{H-8}$$

Equation (H-8) is quadratic x_*; solving for x_*yields

$$x_* = \frac{1 \pm (1-(1-r^2)Q_{p*})^{0.5}}{(1-r)} \tag{H-9}$$

Noting the fact that $x_* \varepsilon (0, 1)$; x_* must be given by

$$x_* = \frac{1 - (1-(1-r^2)Q_{p*})^{0.5}}{(1-r)} \tag{H-10}$$

This suggests that the hydrograph peak due to a given rainfall episode must uniquely correspond to x_* of Eq. (H-10). From Chapter 2, the recession time can be expressed as:

$$t_* = f(x_*) \tag{H-11}$$

But

$$t_* = \frac{D}{T_o} \tag{H-12}$$

where D = duration of rainfall.

Therefore,

$$T_o = \frac{D}{t_*}$$

$$= \eta \tag{H-13}$$

From the expression for T_o, the normalizing time, the parameter α can be found to be

$$\alpha = \left[\frac{1}{q_{max}}\right]^{(n-1)} \left[\frac{(L_o(1-r)}{\eta^n}\right] \qquad \text{(H-14)}$$

Equation (H-14) gives an explicit, analytic way of computing α. An interesting and a rather important implication of this procedure is that it can be used in detecting some of the errors in the rainfall-runoff observations. Assume, for example, that Eq. (H-10) is not satisfied, that is, the term under square root comes out to be imaginary. This suggests that the observed hydrograph peak does not, in fact, correspond to the rainfall event responsible for its generation. This will happen only when $Q_{p*} \geq \frac{1}{(1 - r^2)}$ when Q_{p*}, indeed, must always be less than 1 because of the partial equilibrium situation.

H. 1. 3 Graphical Procedure

A quick graphical procedure was devised for an exact estimation of the parameters n and α by matching the hydrograph peak (Q_{p*}) and its time (t_{p*}). It can be described in the following steps:

1. Generate theoretical equilibrium hydrographs for various values of n (i.e., n = 1, 1.25, ... 3.0), and plot them separately. See Fig. H-1.
2. Reduce the equilibrium hydrographs to partial equilibrium hydrographs for various values of $d_* = D/T_o$ (i.e., d_*= 0.1, 0.2, ... 1.0). The reduction procedure is explained in ensuing section. From the partial equilibrium hydrographs find out t_{p*}, Q_{p*}, and t_{p*}/d_*. A graphical display is provided in Fig. H-1.
3. Plot $t_{p*}|d_*$ versus d_* for various values of n as shown in Fig. H-2.
4. Plot Q_{p*} versus d_* for various values of n as shown in Fig. H-3.
5. Computer $(t_{p*}/d_*) = T_p/D)$ from the observed data, where T_p corresponds to the dimensional hydrograph peak time.

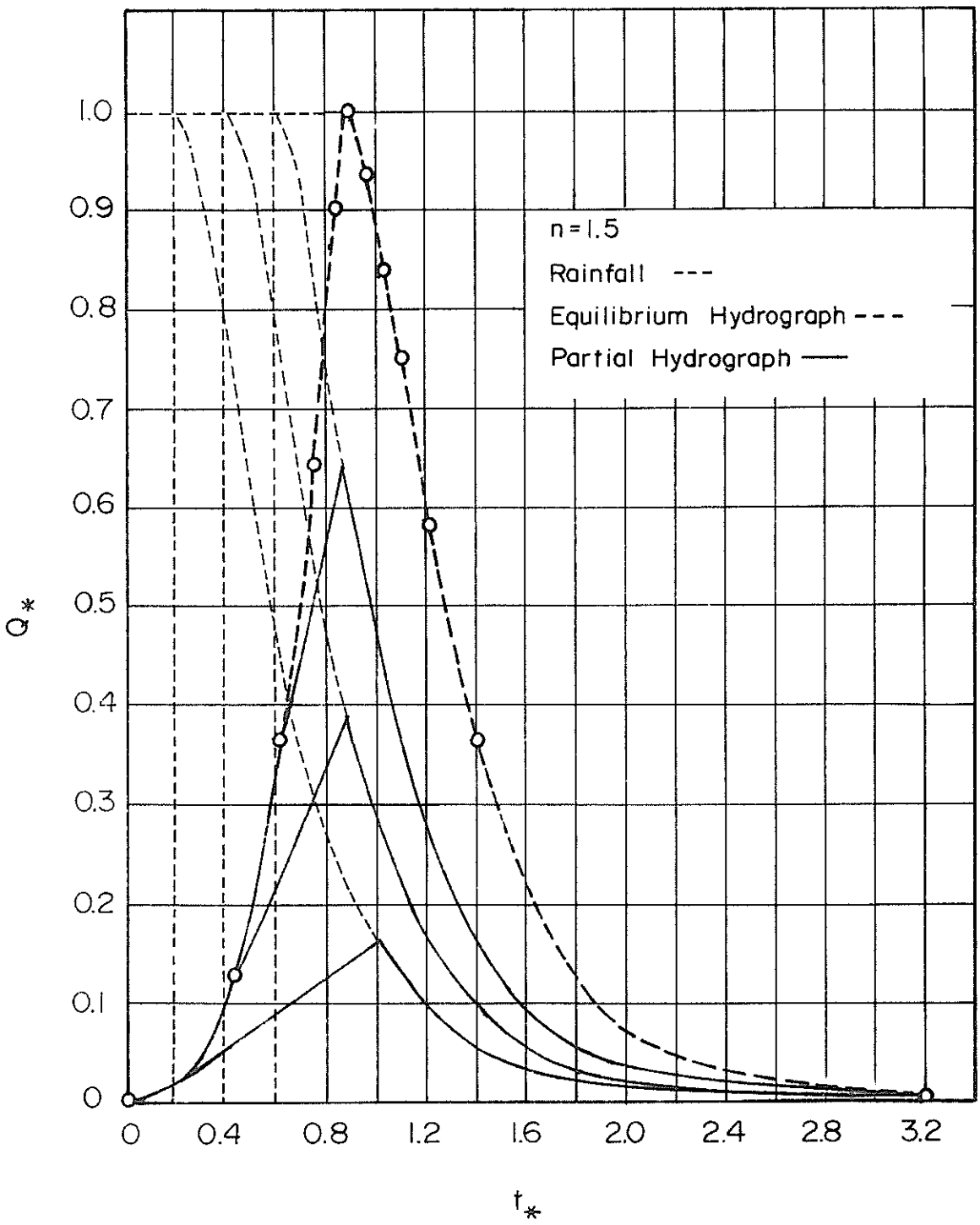

Fig. H-1. Equilibrium and partial equilibrium hydrographs for n = 1.5 corresponding to various values of d_*.

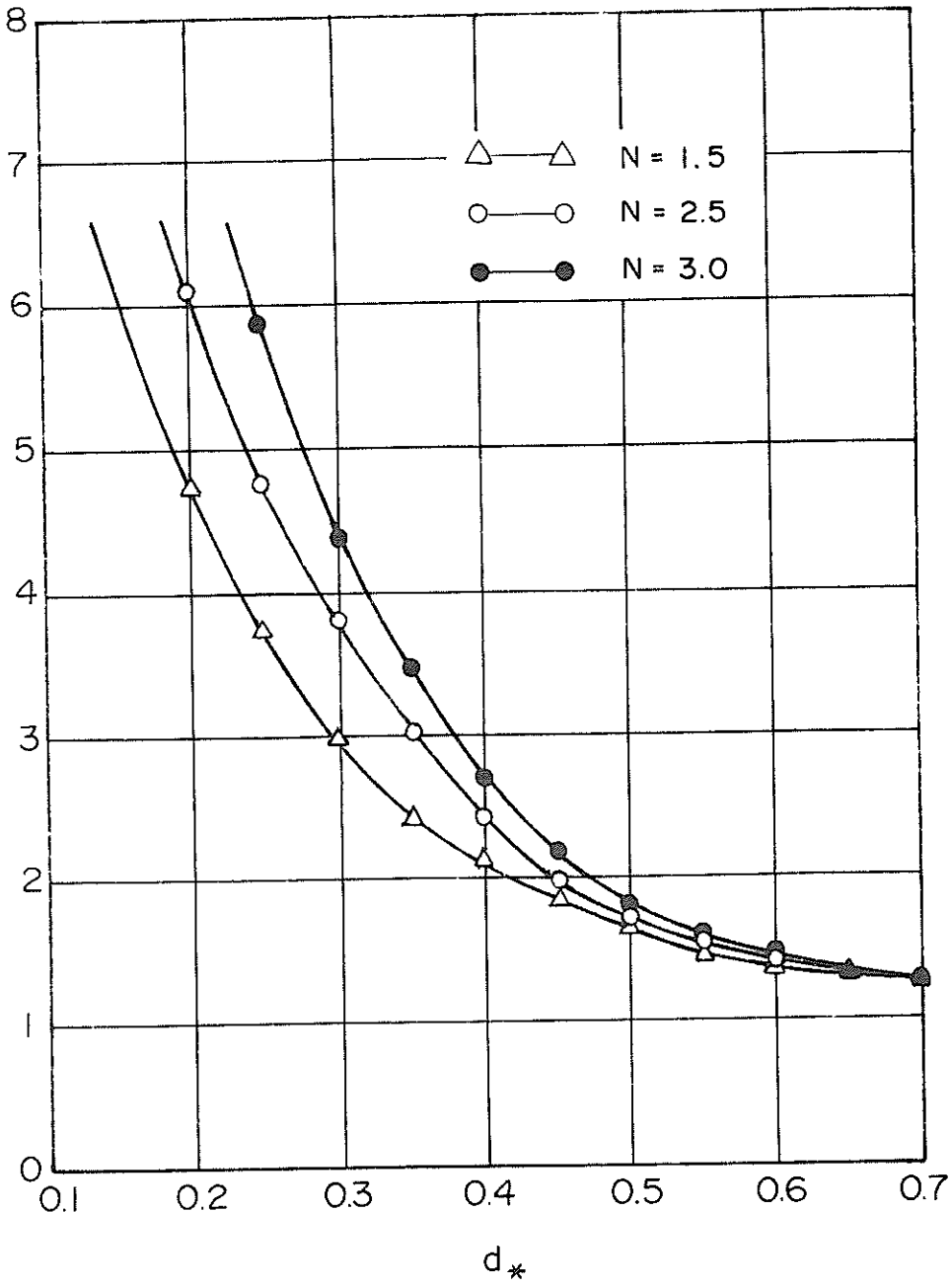

Fig. H-2. Relationship between t_{p*}/d_* and d_*.

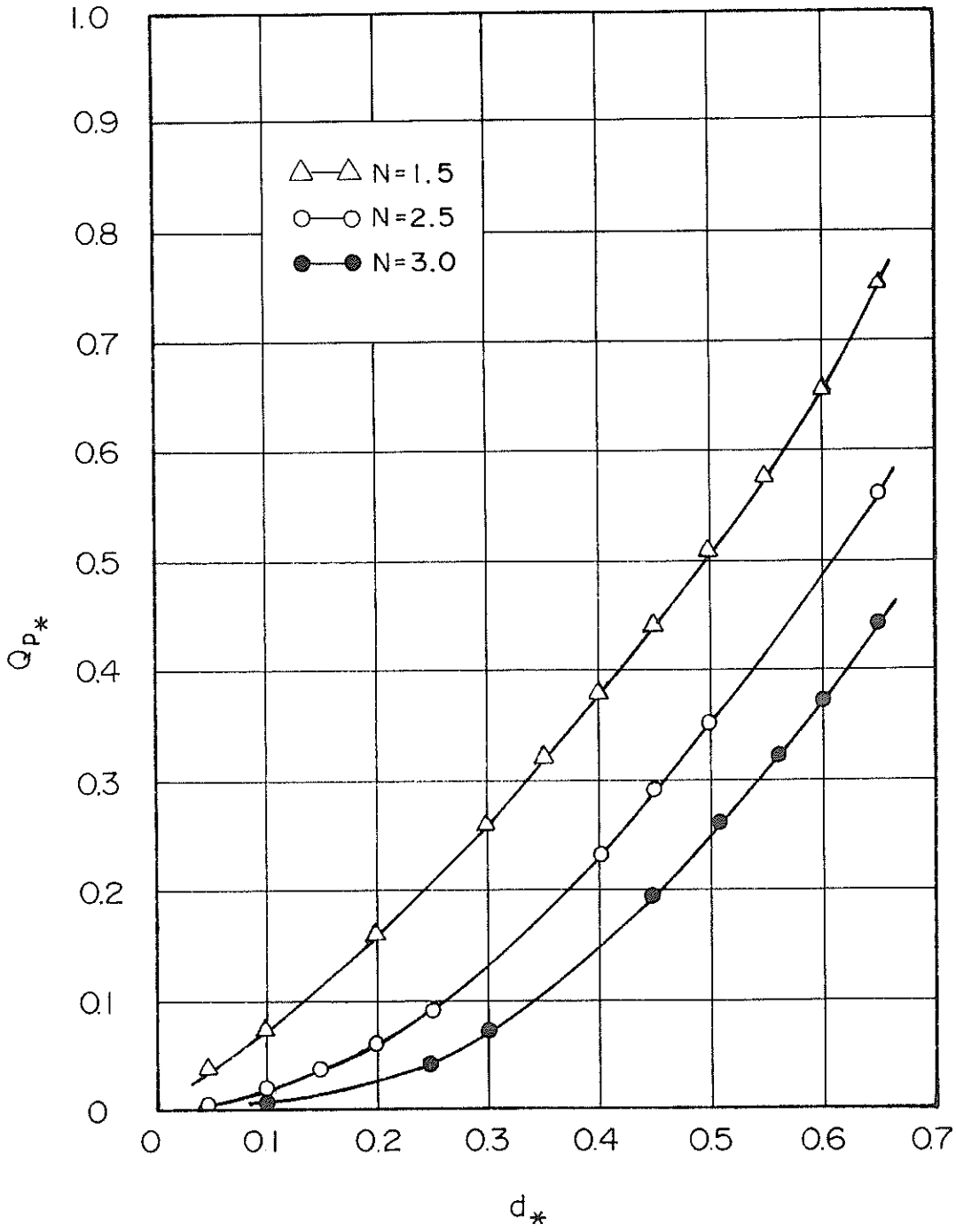

Fig. H-3. Relationship between Q_{p*} and d_*.

6. Obtain a set of d_* for various values of n from Step (3) corresponding to the quantity in Step (5).
7. Computer $Q_{p*} = Q_p/q_{max}$ from the observed data, where Q_p = observed hydrograph peak.
8. Obtain a set of d_* for various values of n from Step (4) corresponding to the quantity in Step (7).
9. Plot d_* (obtained in Step (6)) versus n, and d_* (obtained in Step (8)) versus n on one and the same graph. The intersection of the two plots must give n and d_*, as shown in Fig. H-4.
10. Now compute the normalizing time from

$$T_o = \frac{D}{d_*} \tag{H-15}$$

11. Compute α from the expression for T_o. That is

$$\alpha = \left(\frac{1}{q_{max}}\right)^{n-1}\left[\frac{L_o(1-r)}{T_o^n}\right] \tag{H-16}$$

This method of computing n and α can be carried out for each rainfall event under consideration.

H. 1. 4 Partial Equilibrium Hydrograph

A partial equilibrium hydrograph can be obtained from an equilibrium hydrograph in a simple graphical way which is illustrated in the following steps:

1. Plot the equilibrium hydrograph for a given rainfall intensity as shown in Fig. H-5(a).
2. Construct the graphs t versus x and t_{Re} versus x_R for a given value of n as shown in Fig. H-5(c) and (d), where t_{Re} = recession time and x_R = space parameter for recession.

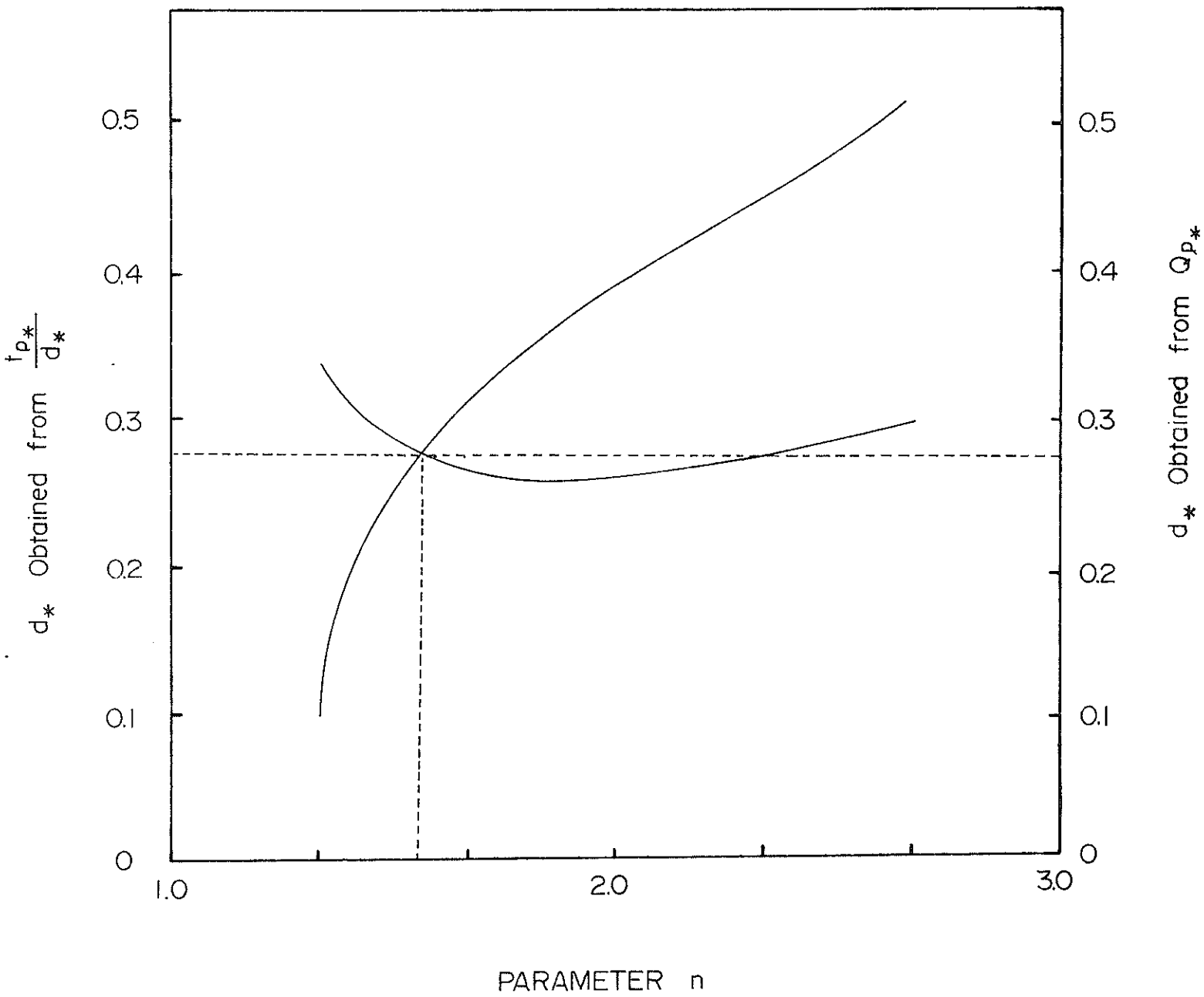

Fig. H-4. Determination of parameter n.

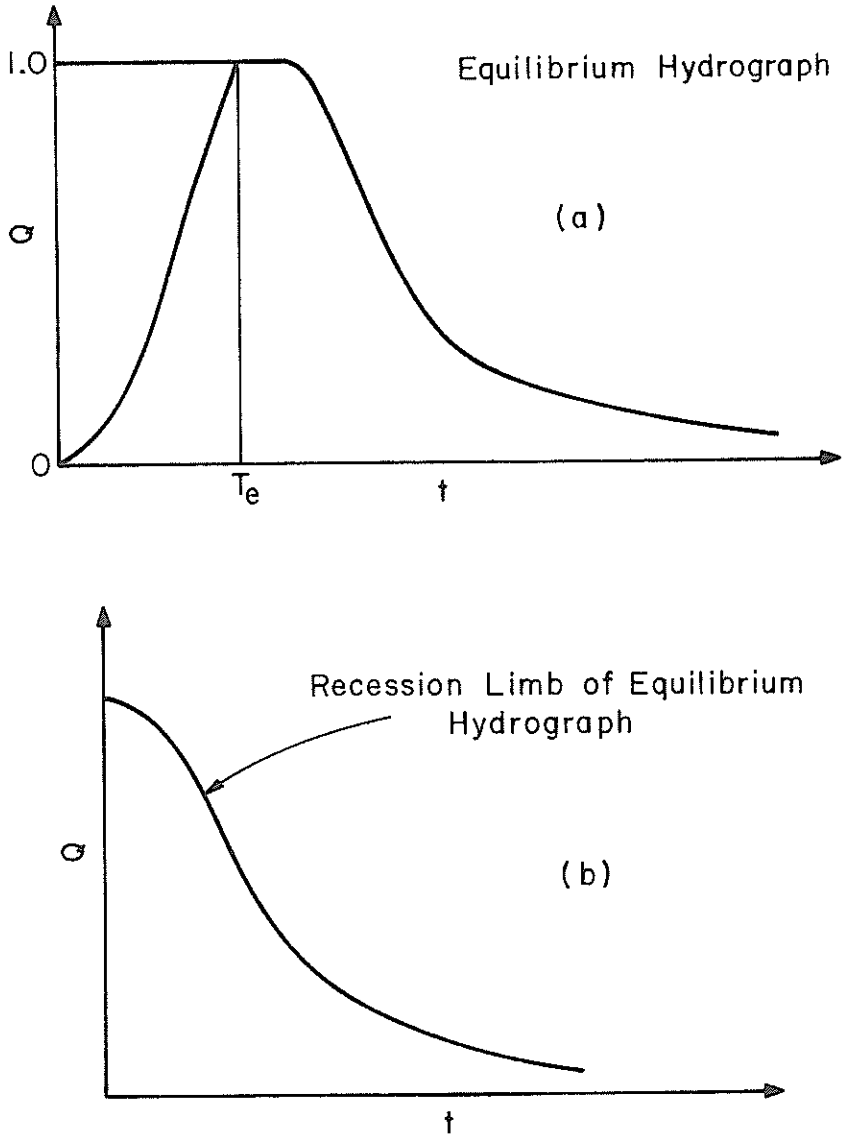

Fig. H-5. Graphical derivation of partial equilibrium hydrograph.

3. For a given rainfall duration compute x_o and t_{Re} from the above graphs (Fig. H-5(c) and (d)), where x_o = the value of x when t = d, rainfall duration.
4. Trace the recession limb of the equilibrium hydrograph on a separate sheet as shown in Fig. H-5(b).
5. Superimpose the recession limb on the equilibrium hydrograph from the point of rainfall ending as shown in Fig. H-5(e).
6. Compute t_p, time to hydrograph peak.
7. Draw a vertical line at t_p to mark the point B where it intersects the superimposed recession limb.
8. Draw a vertical line at D, and call the point A where it casts the equilibrium rising limb.
9. Join the points A and B with a straight line. Point B will give the dimensionless peak discharge as well as dimensionless time to the peak. The partial equilibrium hydrograph is completely defined.

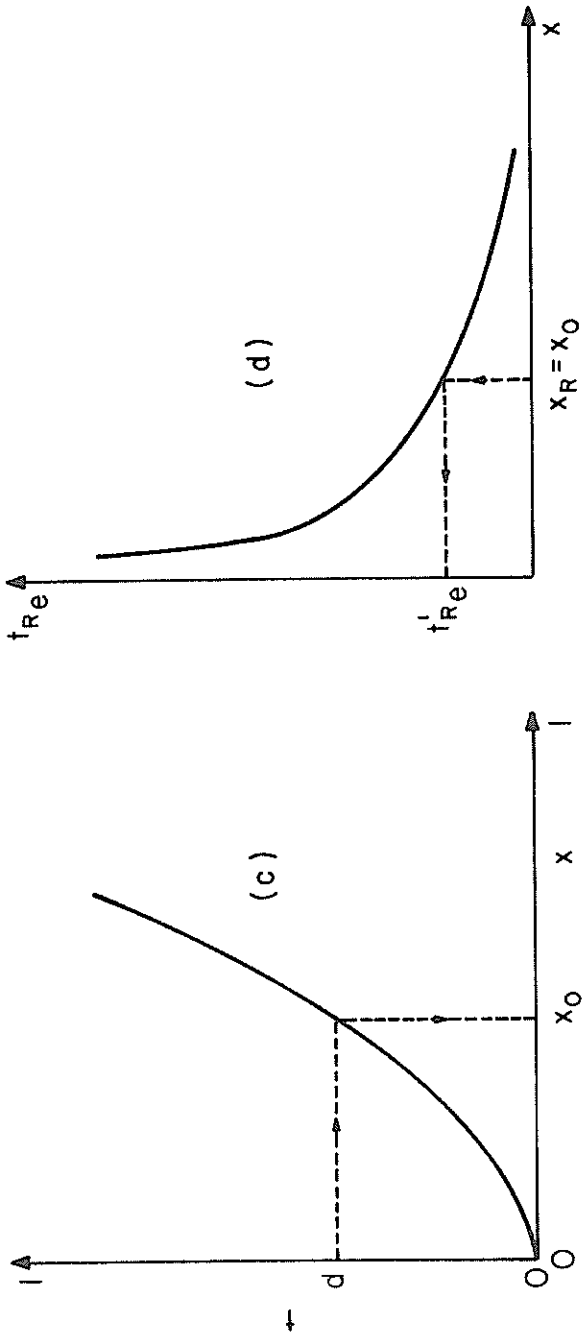

Fig. H-5. Graphical derivation of partial equilibrium hydrograph (contd.)

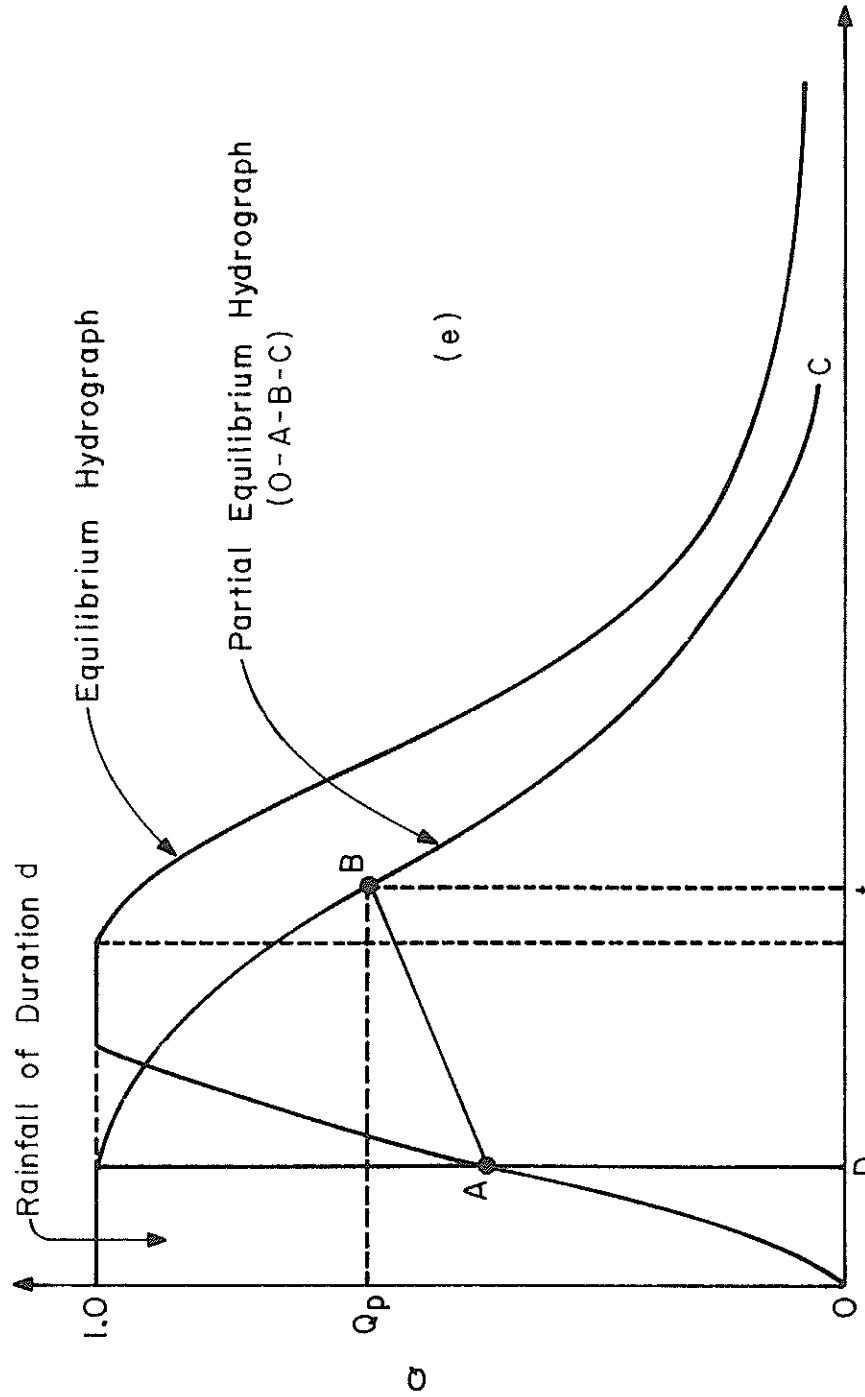

Fog. H-5. Graphical derivation of partial equilibrium hydrograph (contd).

H.2 LEAST SQUARES PROCEDURES FOR PARAMETER OPTIMIZATION

H. 2. 1 Two-Parameter Optimization

The parameters to be optimized in the two-parameter model include n and α. The optimization is performed on the objective function wich is derived from the expression for the normalizing time. As pointed out earlier, the objective function set forth is

$$\text{Min} \sum_{i=1}^{N} [\ell n\, T_{o_i} - \{((n-1)/n)\ell n(\frac{1}{q_{max_i}}) + (1/n)\ell n(L_o(1-r)/\alpha)\}]^2 \qquad \text{(H-17)}$$

subject to the constraints:

$T_o > 0$; $q_{max} = 0$; $n > 0$; and $\alpha > 0$.

Minimization of the sum of squares of deviations of estimated normalizing time from observed normalizing time would be accomplished by differentiating Eq. (H-17) with respect to the parameters and equating it to zero. This is the essence of the least squares procedure. The process of differentiation leads to two simultaneous equations which can be solved for the parameters to be optimized. Hence Eq. (H-17) can be written as:

$$\frac{\partial}{\partial n}, \frac{\partial}{\partial \alpha} \sum_{i=1}^{N} [\ell n\, T_{o_i} + ((n-1)/n)\ell n\, q_{max_i} - (1/n)\ell n\, L_o(1-r) + (1/n)\ell n\alpha]^2 = 0 \qquad \text{(H-18)}$$

Writing Eq. (H-18) as

$$\frac{\partial}{\partial n}, \frac{\partial}{\partial \alpha} \sum_{i=1}^{N} [n\ell n\, T_{o_i} + (n-1)\ell n\, q_{max_i} - \ell n\, L_o(1-r) + \ell n\alpha]^2 = 0 \qquad \text{(H-19)}$$

Differentiating Eq. (H-19) with respect to (w.r.t.) n leads to

$$2 \sum_{i=1}^{N} [n\, \ell\, n\, T_{o_i} + (n-1)\, \ell n\, q_{max_i} - \ell n\, L_o(1-r) + \ell n\alpha][\ell n\, T_{o_i} + \ell n\, q_{max_i}] = 0 \qquad \text{(H-20)}$$

Equation (H-20) can be rearranged and be written as

$$n\left[\sum_{i=1}^{N} (\ell n\, T_{o_i})^2 + 2\sum_{i=1}^{N} \ell n\, T_{o_i}\, \ell n\, q_{max_i} + \sum_{i=1}^{N} (\ell n\, q_{max_i})^2\right]$$

$$+ \ell n\alpha\left[\sum_{i=1}^{N} \ell n\, T_{o_i} + \sum_{i=1}^{N} \ell n\, q_{max_i}\right] = \sum_{i=1}^{N} \ell n\, q_{max_i}\, \ell n\, T_{o_i}$$

$$+ \sum_{i=1}^{N} \ell n\, L_o(1-r)\, \ell n\, T_{o_i} + \sum_{i=1}^{N} (\ell n\, q_{max_i})^2 + \sum_{i=1}^{N} \ell n\, L_o(1-r)\, \ell n\, q_{max_i})^2 \qquad \text{(H-21)}$$

Let $\eta_1 = \sum_{i=1}^{N} (\ell n\, T_{o_i})^2 + 2\sum_{i=1}^{N} \ell n\, T_{o_i}\, \ell n\, q_{max_i} + \sum_{i=1}^{N} (\ell n\, q_{max_i})^2$

$$\eta_2 = \sum_{i=1}^{N} \ell n\, T_{o_i} + \sum_{i=1}^{N} \ell n\, q_{max_i}$$

$$\eta_3 = \sum_{i=1}^{N} \ell n\, q_{max_i}\, \ell n\, T_{o_i} + \sum_{i=1}^{N} \ell n\, L_o(1-r)\, \ell n\, T_{o_i}$$

$$+ \sum_{i=1}^{N} (\ell n\, q_{max_i})^2 + \sum_{i=1}^{N} \ell n\, L_o(1-r)\, \ell n\, q_{max_i}$$

Equation (H-21) can then be written as

$$\eta_1 n + \eta_2 \ell n\alpha = \eta_3 \qquad \text{(H-22)}$$

Differentiating Eq. (H-19) w.r.t.α leads to:

$$2\sum_{i=1}^{N} [n\ \ell n\, T_{o_i} + (n-1)\, \ell n\, q_{max_i} - \ell n\, L_o(1-r) + \ell n\alpha][1/\alpha] = 0 \qquad \text{(H-23)}$$

Equation (H-23) can be written as

$$n\left[\sum_{i=1}^{N} \ell n\, T_{o_i} + \sum_{i=1}^{N} \ell n\, Q_{max_i}\right] + N\ell n\alpha = \sum_{i=1}^{N} \ell n\, q_{max_i} + \sum_{i=1}^{N} \ell n\, L_o(1-r)$$

Let $\xi_1 = \sum_{i=1}^{N} \ell n\, T_{o_i} + \sum_{i=1}^{N} \ell n\, q_{max_i}$

$$\xi_2 = N$$

$$\xi_3 = \sum_{i=1}^{N} \ell n\, q_{max_i} + \sum_{i=1}^{N} \ell n\, L_o(1-r)$$

Equation (H-22) can then be written as

$$\xi_1 n + \xi_2 \ln\alpha = \xi_3 \qquad \text{(H-24)}$$

The system of Eqs. (H-23) and (H-24) can be solved for n and α.

The solution yields

$$n = \frac{\xi_3}{\xi_1} - \frac{\xi_2}{\xi_1}\,\frac{[\eta_3\xi_1 - \xi_3\eta_1]}{[\xi_1\eta_2 - \xi_2\eta_1]} \qquad \text{(H-25)}$$

$$\text{and } \ln = \frac{\eta_3\xi_1 - \xi_3\eta_1}{\xi_1\eta_2 - \xi_2\eta_1} \qquad \text{(H-26)}$$

Equation (H-26) then follows

$$\alpha = e^{\left(\frac{\eta_3\xi_1 - \xi_3\eta_1}{\xi_1\eta_2 - \xi_2\eta_1}\right)} \qquad \text{(H-27)}$$

H. 2. 2 One-Parameter Optimization

The parameter to be optimized is α. The objective function is

$$\min \sum_{i=1}^{N} \{ \ln T_{o_i} - [((n-1)/n)\ln(1/q_{max_i}) + (1/n)\ln \frac{L_o(1-r)}{\alpha}\,]\}^2 \qquad \text{(H-28)}$$

s. t. the constraints

$T_o > 0$; $q_{max} > 0$; $\alpha > 0$; and $n > 0$.

Differentiate Eq. (H-28) w.r.t. α to obtain

$$\frac{\partial}{\partial\alpha} \sum_{i=1}^{N} [n\ln T_{o_i} + (n-1)\ln q_{max_i} - \ln L_o(1-r) + \ln\alpha]^2 = 0$$

$$2 \sum_{i=1}^{N} [n\ln T_{o_i} + (n-1)\ln q_{max_i} - \ln L_o(1-r) + \ln\alpha][1/\alpha] = 0 \qquad \text{(H-29)}$$

Upon rearranging the terms in Eq. (H-29) we obtain:

$$\ln = \frac{1}{N}\left[\sum_{i=1}^{N} L_o(1-r) - \sum_{i=1}^{N} (n-1)\ln q_{max_i} - \sum_{i=1}^{N} n \ln T_{o_i}\right]$$

or

$$\alpha = e^{\left[\sum_{i=1}^{N} L_o(1-r) - \sum_{i=1}^{N} (n-1) \ln q_{max_i} - \sum_{i=1}^{N} n \ln T_{o_i}\right]} \qquad \text{(H-30)}$$

APPENDIX I

GEOMETRIC AND PHYSICAL CHARACTERISTICS OF CSU R-R FACILITY

Table I-1. Geometric and physical characteristics of surface configurations of Rainfall-Runoff Experimental Facility at Colorado State University, Fort Collins, Colorado

erial umber	Configuration number	Length of section (L_o) (ft)	Degree of convergence (r)	Interior angle (θ) (degrees)	Area of section $(ft)^2$	Surface composition
1	1	110	0.0106	120	12,670	Butyl
2	2	72	0.0162	120	5,428	Butyl
3	3	36	0.0325	120	1,356	Butyl
4	4	110	0.0106	120	12,670	Butyl;triangular board ridges covered with butyl flap; openings in artificial ridges to allow flow
5	5	110	0.0106	120	12,670	Butyl; plastic flaps for ridges laid down.
6	6	110	0.0106	30	3,167	Butyl
7	7	110	0.0106	30	3,167	Butyl
8	8	110	0.0106	30	3,167	Upper 70' covered with gravel of 10 lbs/yd^2, lower 40' convered with butyl
9	9	110	0.0106	30	3,167	Upper 106' covered with gravel of 10 lbs/yd^2, lower 4' with butyl
10	10	110	0.0106	30	3,167	Alternate strips of gravel and butyl; each strip being 10' wide; gravel 20 lbs/yd^2
11	11	110	0.0106	30	3,167	Checker board pattern of gravel, 20 lbs/yd^2; alternate patches of butyl
12	12	110	0.0106	30	3,167	Random gravel patches of 20 lbs/yd^2, 10° sector of 30° sector
13	13	110	0.0106	30	3,167	Random gravel patches, 20 lbs/yd^2, 10° sector of 30° sector
14	14	110	0.0106	30	3,167	Gravel, 20 lbs/yd^2
15	15	110	0.0106	30	3,167	Gravel, 20 lbs/yd^2, with stream pattern cleared in
16	16	110	0.0106	113	11,931	Gravel, 10 lbs/yd^2, on one sector, butyl on the other (30°:83°)

Table I- 1. (continued)

rial mber	Configuration number	Length of section (L_o) (ft)	Degree of convergence (r)	Interior angle (θ) (degrees)	Area of section $(ft)^2$	Surface composition
17	17	110	0.0106	84	8,869	Butyl
18	18	110	0.0106	113	11,931	Butyl and gravel in two sectors; 1.5" gravel 20 lbs/yd^2; (83°:30°)
19	19					
20	20	110	0.0106	30	3,167	Gravel, 30 lbs/yd^2
21	21	110	0.0106	30	3,167	Gravel, 40 lbs/yd^2, 1.5"
22	22	110	0.0106	30	3,167	Gravel, 50 lbs/yd^2
23	23	110	0.0106	30	3,167	Gravel, 50 lbs/yd^2; streamlines carved in gravel surface
24	24	110	0.0106	30	3,167	Gravel, 50 lbs/yd^2; channels carved in gravel surface
25	25	110	0.0106	30	3,167	Upper 55' butyl, lower 55' gravel of 50 lbs/yd^2
26	26	116	0.0101	104	12,211	Butyl rubber; a portion of complex watershed configuration
27	27	116	0.0101	104	12,211	Butyl rubber; a portion of complex watershed surface configuration
28	28	116	0.0101	104	12,211	Butyl; a part of complex configuration.
29	29	116	0.0101	104	12,211	Butyl
30	30	116	0.0101	104	12,211	Butyl
31	31	116	0.0101	104	12,211	Butyl
32	32	116	0.0101	60	7,067	
33	33	116	0.0101	44	5,166	Butyl
34	34	116	0.0101	44	5,166	Butyl plus brick lines in a portion of the converging section
35	35	116	0.0101	44	5,166	Butyl + bricks put on at the spacing of one brick length
36	36	116	0.0101	44	5,166	Brick layout upto 102', bricks turned 45° by dice throw

Table I- 1.(continued)

urface umber	Configuration number	Length of section (L_o) (ft)	Degree of convergence (r)	Interior angle (θ) (degrees)	Area of section $(ft)^2$	a Surface composition
37	37	116	0.0101	60	7,045	Alternate strips of gravel in each sector of 20° each
38	38	116	0.0101	60	7,045	Alternate strips of gravel of 20 lbs/yd^2; each strip being 20' wide
39	39	116	0.0101	44	5,166	Bricks oriented at 45° from center line to converge flow; bricks upto 102' from the mouth
40	40	116	0.0101	60	7,045	Random plots of gravel, 20 lbs/ yd^2
41	41	116	0.0101	44	5,166	Three tiers of bricks simulating terraces; bricks tightly packed, but not sealed to the surface; water does leak through in places; soil is placed at corners to prevent flow along borders
.42	42	116	0.0101	60	7,045	Random plots of gravel with approximately the same total quantity as in configuration 3; each strip being 20'
43	43	116	0.0101	44	5,166	Three tiers of bricks simulating terraces; bricks are tightly packed, but not sealed to the surface; water does leak through in places; soil placed at corners to prevent flow along borders; terraces have formed a fairly good seal with the rubber because in most places soil has washed us against the bricks
44	44	116	0.0101	44	5,166	Bricks terraces with wide channels
45	45	116	0.0101	44	5,166	Terraces are 4 bricks wide, 20' apart and have grade 0.5%

Table I-1. (continued)

Serial number	Configuration number	Length of section (L_o) (ft)	Degree of convergence (r)	Interior angle ( ) (degrees)	Area of section a $(ft)^2$	Surface composition
46	46	116	0.0101	44	5,166	Brick terraces
47	47	116	0.0101	44	5,166	Terraces are 4 bricks wide, closely spaced with fairly good adhesion to the surface, grade 2%, spacing 20'
48	48	116	0.0101	104	12,211	1/3 covered by gravel, 20 lbs/yd^2
49	49	116	0.0101	104	12,211	1/3 gravel covered, 20 lbs/yd^2
50	50	116	0.0101	104	12,211	Butyl surface; gravel dam 6" high, 3' wide
51	51	116	0.0101	104	12,211	Butyl surface; gravel dam 6' high, 3' wide

APPENDIX J

ESTIMATION OF PARAMETERS BY HYDROGRAPH PEAK MATCHING

Table J-1. Parameters n and α obtained by matching peak discharge and its time for different events on butyl surface of CSU Rainfall-Runoff Facility, Fort Collins, Colorado.

Code	Rainfall duration (sec)	Rainfall intensity (In/hr)	Peak discharge (In/hr)	Time to peak discharge (Sec)	n	α
-1-8A2	33.95	4.189	1.556	90.8	1.504	11.92
-1-11B	85.09	1.075	0.590	139.9	1.952	138.26
-2-18B	60.69	1.032	0.405	151.9	1.915	77.94
-2-19B	51.68	2.130	0.803	103.9	1.948	84.51
-2-20B	45.21	3.358	1.516	91.4	1.816	39.98
-3-21B	65.59	0.898	0.354	140.5	1.952	63.82
-3-22B	66.00	2.135	1.073	110.3	2.141	105.31
-3-23B	52.98	4.389	2.006	93.8	2.200	89.48
-4-24B	352.33	0.976	0.863	463.6	1.236	0.607
-5-27B	80.78	1.088	0.472	159.9	1.956	121.95
-5-28B	77.64	2.321	1.614	102.9	2.139	292.02
-6-30B	77.79	1.038	0.418	143.3	1.948	107.10
-6-31B	70.75	2.390	1.307	121.0	1.835	49.29
-6-32B	32.69	4.420	1.057	94.1	2.044	159.02
-17-118	102.49	0.890	0.575	147.3	2.005	195.86
-17-120	88.80	1.860	1.401	110.3	2.200	439.99
-17-124	68.80	3.690	3.123	97.8	1.208	2.703
-26-326	134.72	0.390	0.238	194.8	2.029	304.082
-26-326A	126.60	0.415	0.238	188.5	2.049	337.67
-26-327	55.05	0.800	0.215	179.1	1.765	57.794
-26-327A	54.10	0.814	0.215	178.1	1.787	67.14
-26-328	113.28	0.800	0.543	155.8	2.036	241.05
-26-330	94.68	2.035	1.796	124.2	1.249	2.92
-26-332	53.30	4.135	3.149	87.5	1.335	5.66
-26-333	80.50	4.050	3.615	86.1	2.520	1,339.59
-26-333A	78.65	4.135	3.615	84.3	2.579	1,763.20
-27-311	49.92	4.039	2.591	78.7	1.687	34.95
-27-312	58.18	4.039	3.133	86.7	1.342	5.93
-27-318	45.59	0.799	0.152	182.4	1.976	247.64
-27-319	116.30	0.814	0.612	163.7	1.580	16.47
-27-322	71.40	0.390	0.109	217.6	1.809	93.03
-27-323	117.60	0.390	0.202	193.6	1.975	228.68
-27-323A	110.51	0.415	0.202	186.5	1.974	227.49

Table J - 1. (continued)

Code	Rainfall duration (sec)	Rainfall intensity (In/hr)	discharge (In/hr)	Time to peak discharge (Sec)	n	α
34-28-341	144.25	0.415	0.287	181.1	2.243	1,147.87
35-28-342	252.45	0.415	0.409	269.2	1.206	1.29
36-28-343	65.58	0.814	0.245	165.9	1.980	197.07
37-28-345	120.10	0.814	0.665	140.3	2.223	797.57
39-28-347	81.47	2.035	1.522	111.3	1.702	32.43
39-28-348	128.06	2.035	1.919	142.4	1.570	10.97
40-28-349	30.57	4.135	1.282	73.1	2.187	636.21
41-28-350	53.19	4.135	2.845	88.8	1.357	6.11
42-29-353	134.53	0.814	0.729	157.2	1.640	23.67
43-29-355	94.87	0.814	0.502	136.0	2.039	310.28
44-29-360	63.29	4.135	3.560	85.2	1.267	4.23
45-30-364	77.61	0.814	0.339	144.0	1.957	179.95
46-30-365	141.36	0.814	0.788	162.8	1.135	1.42
47-31-368	69.45	0.814	0.307	169.4	1.745	48.35
48-33-378	65.20	3.642	2.698	83.5	2.079	215.03
49-33-379	103.29	3.642	3.568	111.8	1.287	3.38
50-33-382	146.98	0.772	0.609	195.2	1.624	15.91

Table J-2. Parameters n and α obtained by matching peak discharge and its time for different events on butyl plus dam surface of CSU Rainfall-Runoff Experimental Facility, Fort Collins, Colorado.

Code	Rainfall duration (Sec)	Rainfall intensity (In/hr)	Peak discharge (In/hr)	Time to peak discharge (Sec)	n	α
1-50-631	163.70	0.515	0.233	326.9	1.820	29.78
2-50-632	229.21	0.515	0.386	325.1	1.567	6.78
3-50-633	295.58	0.515	9.480	374.6	1.106	0.51
4-50-635	88.66	1.082	0.310	233.7	2.102	166.42
5-50-636	162.70	1.082	0.759	264.2	1.396	2.74
6-50-637	234.02	1.082	0.96	319.2	1.153	0.69
7-50-638	294.62	1.082	1.032	363.6	1.045	0.375
8-50-641	193.96	2.086	1.976	217.1	1.471	3.70
9-51-645	273.34	0.512	0.444	343.8	1.463	3.50
10-51-647	83.24	1.026	0.277	230.5	1.928	66.64
11-51-648	259.15	1.026	0.863	350.3	1.229	0.873

Table J - 3. Parameters n and α obtained by matching peak discharge and its time for different events on gravel (20 lbs/yd^2) surface of CSU Rainfall-Runoff Experimental Facility, Fort Collins, Colorado.

Code	Rainfall duration (Sec)	Rainfall intensity (In/hr)	Peak discharge (In/hr)	Time to peak discharge (Sec)	n	α
1-14-61B	138.67	0.458	0.153	384.6	1.707	14.35
2-14-62B	132.71	1.099	0.428	338.0	1.636	6.47
3-14-63B	100.97	2.311	0.887	294.6	1.418	2.03
4-14-64B	86.97	4.490	1.702	310.7	1.205	0.70
5-14-149A	246.82	0.807	0.721	319.0	1.238	1.02
6-14-149A	246.82	0.807	0.718	319.0	1.238	1.02
7-14-150	67.73	0.807	0.166	284.9	1.747	25.50
8-14-151	215.49	1.871	1.562	264.3	1.760	3.51
9-14-151	225.13	1.871	1.592	287.7	1.481	2.56
10-14-152	57.53	1.871	0.481	270.3	1.330	1.89
11-14-152	56.48	1.871	0.479	254.8	1.379	2.58
12-14-153	207.48	2.886	2.330	252.5	2.003	17.89
13-14-153	57.64	2.686	0.718	270.7	1.292	1.40
14-14-155	204.58	3.782	3.486	219.5	2.268	52.18
15-14-156	53.72	3.782	0.989	236.0	1.386	2.24
16-15-65B	130.16	0.468	0.139	390.4	1.756	19.25
17-15-66B	123.56	1.127	0.418	219.1	1.947	40.49
18-15-67B	84.02	2.385	0.730	236.8	1.828	18.19

Table J - 4. Parameters n and α obtained by matching peak discharge and its time for different events on gravel surface (50 lbs/yd^2) of CSU Rainfall-Runoff Experimental Facility, Fort Collins, Colorado.

Code	Rainfall duration (Sec)	Rainfall intensity (In/hr)	Peak discharge (In/hr)	Time to Peak discharge (Sec)	n	α
1-20-169	258.51	0.860	0.635	374.5	1.550	3.55
2-20-170	67.83	1.850	0.440	334.8	1.358	1.65
3-20-171	254.54	1.850	1.446	309.5	2.166	39.31
4-20-172	51.41	3.85	0.766	301.4	1.365	1.58
5-20-173	210.09	3.88	3.053	250.4	2.322	46.69
6-20-173A	209.01	3.88	2.778	299.0	1.700	3.50
7-20-175A	250.30	2.70	2.402	291.3	1.715	5.05
8-20-176A	67.26	0.86	0.177	335.3	1.510	5.12
9-22-179B	110.46	2.91	0.877	309.5	1.483	1.78
10-22-180B	187.18	2.91	1.478	328.2	1.936	10 .05
11-22-182B	115.32	1.99	0.567	455.3	1.413	1.20
12-22-183	190.08	1.99	0.961	450.1	1.402	1.05
13-22-184	310.26	1.99	1.563	359.3	2.530	108.16
14-22-186	83.32	3.90	0.939	341.1	1.570	2.723
15-22-187	105.03	3.90	1.098	335.7	1.726	4.64
16-22-188	153.45	3.91	1.743	285.4	2.075	17.76
17-22-189	298.83	3.91	3.712	308.8	2.481	46.13
18-22-192	227.13	0.916	0.386	371.9	2.456	255.10
19-23-193	344.20	0.916	0.964	400.6	2.361	116.32
20-23-197	207.20	4.413	2.904	247.3	2.377	49.02
21-24-202	575.56	0.840	0.826	605.5	1.480	1.23
22-24-206	217.00	3.840	3.075	257.0	2.263	35.52

Table J-5. Parameters n and α obtained by matching peak discharge and its time for different events on butyl plus gravel surface of CSU Rainfall-Runoff Experimental Facility, Fort Collins, Colorado.

Code	Rainfall duration (Sec)	Rainfall intensity (In/hr)	Peak discharge (In/hr)	Time to peak discharge (Sec)	n	α
1-8-38B	136.02	1.089	0.583	216.5	2.149	165.54
2-8-38B	78.98	2.387	1.012	181.4	1.663	11.92
3-8-40B	51.76	4.287	1.463	149.2	1.602	9.39
4-9-41B	86.21	0.461	0.129	261.8	1.811	55.07
5-9-42B	111.07	1.148	0.486	232.0	1.871	36.96
6-9-43B	81.51	2.383	1.027	194.7	1.562	6.72
7-9-44B	53.98	4.394	1.452	180.3	1.441	3.60
8-10-45D	79.17	2.374	0.919	200.9	1.631	3.06
9-10-46B	69.12	4.094	1.660	152.1	1.823	22.22
10-10-47B	124.63	1.130	0.552	246.0	1.697	13.16
11-10-48B	161.36	0.487	0.217	324.9	1.855	37.09
12-11-50B	134.17	0.510	0.175	358.4	1.713	15.16
13-11-51B	122.18	1.074	0.560	241.0	1.564	7.06
14-11-52B	74.74	4.442	2.144	174.6	1.425	3.17
15-12-54B	128.63	1.094	0.612	211.3	1.908	49.22
16-12-55B	93.91	2.207	1.089	175.1	1.844	28.95
17-12-56B	63.91	4.28	1.667	148.3	1.791	20.04
18-13-57B	130.74	0.489	0.153	317.1	2.108	191.29
19-13-58B	145.03	1.069	0.589	265.9	1.649	9.17
20-18-134	100.50	2.100	1.400	123.6	2.268	305.47
21-18-135	90.86	3.83	2.53	110.9	2.317	271.60
22-18-136	223.69	0.96	0.853	248.7	2.120	105.22
23-18-137	144.62	2.10	1.637	186.0	2.368	312.61
24-18-138	131.25	3.83	3.166	143.3	2.553	417.47
25-25-215	87.04	3.61	1.52	206.0	1.623	6.28

Table J-6. Parametets n and α obtained by matching peak discharge and its time for different events on bricks, random plots of gravel and butyl surface of CSU Rainfall-Runoff Experimental Facility, Fort Collins, Colorado.

Code	Rainfall duration (Sec)	Rainfall intensity (In/hr)	Peak discharge (In/hr)	Time to peak discharge (Sec)	n	α
1-35-389	103.62	1.886	1.293	173.6	1.369	3.477
2-35-390	177.32	1.886	1.822	216.2	0.989	0.508
3-35-391	48.30	0.790	0.181	197.5	1.638	25.76
4-35-392	105.80	0.790	0.447	191.8	1.625	17.48
5-35-394	38.52	4.003	1.183	142.0	1.418	5.264
6-35-396	139.55	4.003	3.659	166.0	1.415	3.24
7-36-400	63.90	0.867	0.243	172.3	1.915	124.35
8-36-401	90.02	0.867	0.381	163.6	2.091	309.79
9-36-402	128.71	0.867	0.537	195.1	1.898	67.92
10-36-403	22.33	3.699	0.639	120.6	1.598	20.02
11-36-404	65.38	3.699	1.955	120.4	1.718	22.04
12-37-410	53.64	3.555	1.118	162.8	1.646	12.10
13-37-411	52.99	3.555	1.033	165.9	1.703	15.58
14-37-412	121.55	3.555	2.835	176.4	1.331	2.266
15-37-414	51.24	1.686	0.404	185.4	1.775	34.88
16-37-415	121.45	1.686	1.110	199.6	1.512	5.91
17-37-418	123.87	0.770	0.428	229.8	1.594	11.29
18-37-419	177.62	0.771	0.625	238.2	1.493	5.84
19-37-421	134.35	0.396	0.165	272.1	1.990	143.49
20-37-422	206.53	0.396	0.295	329.5	1.297	1.72
21-38-428	35.56	4.073	0.855	145.5	1.743	25.33
22-38-429	38.51	4.073	0.967	148.7	1.665	15.95
23-28-430	80.12	4.073	2.205	130.9	2.016	63.30
24-38-431	123.79	4.073	3.253	137.8	2.496	334.65
25-38-432	151.89	1.807	1.457	222.0	1.270	1.60
26-38-434	99.57	1.807	0.940	175.1	1.882	42.75
27-38-435	117.57	0.824	0.447	245.6	1.417	3.93
28-39-441	58.47	3.717	2.121	119.9	1.358	4.42
29-39-443	57.95	0.892	0.221	190.3	1.893	105.51
30-39-444	82.80	0.892	0.399	179.1	1.675	25.66

Table J-6. (continued)

Code	Rainfall duration (Sec)	Rainfall intensity (In/hr)	Peak discharge (In/hr)	Time to peak discharge (Sec)	n	α
31-39-444A	92.36	3.720	2.929	144.6	1.209	1.79
32-40-427	44.14	4.242	0.912	169.1	1.844	29.09
33-40-460	176.08	0.480	0.263	297.1	1.883	50.14
34-40-461	287.69	0.501	0.477	349.2	1.098	0.53
35-40-466	108.85	0.970	0.371	253.6	1.815	29.91
36-40-467	152.58	0.970	0.678	231.9	1.57I	8.19
37-40-473	111.25	1.930	0.918	265.0	1.416	2.54
38-40-473A	146.69	1.930	1.435	206.5	1.628	8.95
39-40-474	46.71	1.930	0.320	237.5	1.74	21.58
40-40-480	137.84	4.242	3.596	181.2	1.399	2.65
41-40-481	182.14	4.242	4.073	216.0	1.105	0.74
42-41-488	179.65	0.479	0.277	245.5	2.184	248.13
43-41-489	247.93	0.439	0.390	302.1	1.474	4.84
44-41-495	184.41	0.995	0.813	243.1	1.517	5.59
45-41-496	251.88	0.995	0.965	271.5	1.480	3.92
46-41-503	159.78	2.034	1.700	189.3	1.986	46.45
47-41-507	50.65	4.052	1.158	135.6	2.068	104.13
48-41-508	99.06	4.052	2.721	146.9	1.751	15.64
49-41-509	148.76	4.052	3.471	168.8	2.228	78.24
50-41-510	189.14	4.052	3.562	206.2	2.589	197.24
51-42-512	424.71	0.468	0.432	510.9	1.308	0.95
52-42-515	68.95	0.456	0.079	297.9	1.837	66.47
53-42-516	148.74	0.456	0.238	278.5	1.672	17.74
54-42-518	318.60	0.456	0.406	373.7	1.848	26.43
55-42-521	103.79	0.878	0.376	234.7	1.676	16.96
56-42-522	165.50	0.878	0.643	261.3	1.360	2.50
57-42-523	232.62	0.878	0.768	294.0	1.402	2.54
58-42-530	183.27	1.886	1.732	244.3	1.065	0.61
59-42-532	27.28	4.189	0.546	186.2	1.629	11.50
60-42-533	68.42	4.189	1.765	147.6	1.803	22.02
61-42-534	97.30	4.189	2.762	140.2	1.928	34.30
62-42-535	127.57	4.189	3.258	183.7	1.415	2.81
63-42-536	27.99	4.189	0.519	192.1	1.723	19.27

Table J-6.(continued)

Code	Rainfall duration (Sec)	Rainfall intensity (In/hr)	Peak discharge (In/hr)	Time to peak discharge (Sec)	n	α
64-43-540	287.35	0.450	0.271	389.5	2.166	126.03
65-43-541	234.01	0.450	0.316	268.1	2.485	1,597.78
66-43-547	343.20	1.084	0.997	360.9	2.559	311.15
67-43-551	217.09	2.024	1.720	244.7	2.266	88.96
68-43-555	132.89	4.206	2.803	198.1	1.713	7.70
69-43-556	194.84	4.206	3.709	211.3	2.583	168.33
70-43-557	262.40	4.206	4.104	292.9	1.167	0.647
71-44-564	135.81	0.468	0.144	358.2	1.955	70.65
72-44-565	209.16	0.468	0.261	332.4	2.038	98.88
73-44-566	283.01	0.468	0.371	317.6	2.444	788.02
74-44-570	103.71	4.219	2.386	153.0	2.331	160.77
75-44-571	148.84	4.219	3.252	172.3	2.375	120.62
76-44-572	196.58	4.219	3.816	234.8	1.460	2.269
77-44-575	151.22	2.107	1.364	227.1	1.815	15.86
78-45-578	184.48	1.112	0.777	252.7	1.929	37.43
79-45-581	121.38	4.171	3.729	142.7	2.288	136.22
80-46-587	200.19	1.072	0.849	244.5	2.031	66.32
81-46-590	111.68	4.351	3.756	148.5	1.289	2.25
82-47-599	179.88	1.039	0.861	227.7	1.633	10.74
83-47-602	99.5	4.166	3.656	138.6	1.140	1.40

APPENDIX K

VARIABILITY OF PARAMETER α WITH PARAMETER n

Table K--1. Variability of parameter α with parameter n on butyl surface of CSU Rainfall-Runoff Experimental Facility, Fort Collins, Colorado.

Code	Rainfall Intensity (In/hr)	Rainfall Duration (sec)	Peak Runoff (In/hr)	Parameter α for select values of n							
				1.25	1.5	1.75	2.0	2.25	2.50	2.75	3.0
1-1-8A2	4.189	33.95	1.556	2.80	11.40	47.57	196.0	814.8	3,385.0	14,072.5	58,535.8
2-1-11B	1.075	85.09	0.590	1.94	8.84	40.77	187.6	880.6	4,002.2	18,579.6	86,097.8
3-2-18B	1.032	69.59	0.405	1.13	5.45	26.93	131.7	649.3	3,198.8	15,770.9	77,779.5
4-2-19B	2.130	51.68	0.803	1.30	5.67	25.10	110.6	490.4	2,172.0	9,626.2	42,686.1
5-2-20B	3.358	42.21	1.516	1.68	6.75	27.53	113.6	454.7	1,862.5	7,609.0	31,107.1
6-3-21B	0.898	65.59	0.354	0.63	3.21	16.62	87.8	442.7	2,292.1	11,874.8	61,555.8
7-3-22B	2.135	66.00	1.073	0.66	2.71	11.23	46.8	197.2	801.9	3,335.0	13,881.4
8-3-23B	4.389	52.98	2.066	0.65	2.36	8.64	32.0	115.5	424.7	1,559.5	5,730.6
9-4-24B	0.976	352.33	0.863	0.65	2.07	6.81	22.4	73.6	242.1	795.7	2,597.2
10-4-25B	2.243	122.48	0.912	0.73	2.52	8.88	31.9	109.4	385.4	1,358.5	4,791.1
11-5-27B	1.088	80.78	0.472	1.57	7.24	33.93	161.2	737.6	3,459.8	16,208.4	75,983.5
12-5-28B	2.321	77.64	1.614	2.42	9.49	35.80	138.1	540.1	2,137.2	8,286.6	31,853.1
13-6-30B	1.038	77.79	0.418	1.54	7.21	34.60	169.0	786.5	3,762.3	18,011.1	86,275.6
14-6-31B	2.391	70.75	1.307	2.00	7.78	30.80	121.5	489.3	1,910.8	7,589.4	30,159.2
15-6-32B	4.42	32.69	1.057	1.81	7.29	30.59	125.9	520.6	2,518.6	8,953.4	37,148.6
16-17-116	0.98	48.01	0.124	0.85	5.51	24.69	134.9	741.3	4,074.8	22,403.1	123,191.7
17-17-117	0.89	56.69	0.277	1.79	9.47	51.46	272.7	1,477.3	7,959.7	42,910.6	231,431.7
18-17-118	0.89	102.49	0.575	1.98	8.91	41.21	188.9	873.7	4,057.8	19,223.1	86,421.8
19-17-119A	1.860	48.07	0.641	2.04	9.36	40.00	203.1	948.8	4,428.7	20,684.3	96,652.9
20-17-119B	1.860	47.38	0.596	1.93	8.84	41.78	192.5	908.0	4,255.7	19,956.5	93,625.9
21-17-120	1.860	88.80	1.401	2.38	9.51	37.05	145.5	587.0	2,303.1	9,195.3	36,794.2
22-17-121	1.860	119.84	1.839	2.92	9.66	33.47	122.7	443.2	1,610.2	5,876.2	21,515.0
23-17-124	3.690	68.80	3.123	3.32	11.66	41.12	147.2	515.3	1,807.5	6,432.0	22,966.0
24-26-324	0.390	29.32	0.019	0.06	0.78	3.63	39.6	385.0	3,497.0	30,506.5	259,314.1

Table K-1. Continued

Code	Rainfall Intensity (In/hr)	Rainfall Duration (sec)	Peak Runoff (In/hr)	Parameter α for select values of n							
				1.25	1.5	1.75	2.0	2.25	2.50	2.75	3.0
49-27-319	2.035	45.54	0.619	1.97	8.94	41.77	205.3	934.5	4,094.5	18,962.4	87,856.0
50-28-340	0.415	47.79	0.062	1.32	9.75	68.00	407.1	2,775.7	18,929.3	129,123.0	88,595.7
51-28-341	0.415	144.25	0.287	1.80	9.27	46.02	234.0	1,205.3	6,283.2	32,115.0	162,471.8
52-28-342	0.415	252.45	0.411	1.78	7.10	30.34	131.3	572.4	2,511.1	11,064.7	48,921.0
53-28-343	0.814	65.58	0.245	1.55	8.07	43.31	227.6	1,208.3	6,420.2	34,131.2	181,525.1
54-28-345	0.814	120.21	0.665	2.40	10.76	48.37	211.7	978.2	4,350.0	19,724.2	89,528.6
55-28-346	2.035	38.71	0.450	1.72	8.18	39.00	188.9	911.1	4,379.3	21,230.3	102,530.8
56-28-347	2.035	81.47	1.522	2.71	10.81	42.08	165.4	665.8	2,609.9	10,415.1	41,661.8
57-28-348	2.035	128.06	1.919	2.32	8.01	26.96	93.1	332.9	1,172.9	4,068.0	14,370.0
58-28-349	4.135	30.57	1.282	2.77	11.63	50.25	211.8	911.4	3,903.2	16,725.5	71,701.2
59-28-350	4.135	53.19	2.845	3.50	13.05	46.81	171.9	645.0	2,409.1	8,897.1	32,498.8
60-29-353	0.814	134.53	0.729	2.45	10.38	45.20	195.5	860.8	3,760.5	16,634.3	71,949.8
61-29-355	0.814	94.87	0.502	2.21	10.47	50.24	240.3	1,163.5	5,657.4	26,954.8	130,171.4
62-29-358	4.135	27.63	1.080	2.60	11.25	50.08	217.4	954.9	4,197.3	18,457.3	81,193.4
63-29-360	4.135	63.29	3.560	3.89	13.25	47.19	167.1	591.1	2,026.4	7,148.9	25,401.2
64-30-364	0.814	77.61	0.340	1.79	8.97	45.67	236.5	1,173.7	5,968.7	30,375.5	154,681.5
65-30-365	0.814	141.36	0.790	2.72	11.29	47.33	199.4	874.5	3,726.8	16,078.6	69,573.7
66-31-368	0.814	69.45	0.307	1.85	9.49	49.84	258.6	1,354.0	7,083.6	37,085.0	194,258.8
67-33-377	3.642	26.69	0.796	2.33	10.56	47.52	219.4	1,004.3	4,599.0	21,067.9	96,540.2
68-33-378	3.642	65.20	2.698	3.14	11.14	39.65	142.5	524.7	1,885.7	6,862.0	25,062.1
69-33-379	3.642	103.29	3.568	2.86	8.78	27.27	87.81	277.8	882.5	2,828.5	9,093.9
70-33-380	0.772	41.37	0.123	1.46	9.75	46.2	310.0	1,875.6	11,353.4	68,741.2	416,295.6
71-33-381	0.772	93.99	0.444	2.08	10.02	48.94	238.3	1,179.3	5,704.8	28,052.4	137,688.7
72-33-382	0.772	146.98	0.609	1.79	7.78	34.13	145.7	625.5	2,725.2	11,938.3	52,326.5

Table K - 1. Continued

Code	Rainfall Intensity (In/hr)	Rainfall Duration (sec)	Peak Runoff (In/hr)	Parameter α for select values of n							
				1.25	1.5	1.75	2.0	2.25	2.50	2.75	3.0
25-26-325A	0.390	86.81	0.128	1.44	8.39	50.28	296.4	1,763.0	10,455.5	52,281.4	372,300.7
26-26-325B	0.415	81.58	0.128	1.43	8.34	50.00	293.5	1,756.2	10,455.5	62,281.4	371,153.3
27-26-326A	0.39	134.72	0.238	1.69	8.83	46.10	245.8	1,311.2	7,026.5	36,803.3	195,715.8
28-26-326B	0.415	126.60	0.238	1.67	8.71	46.66	243.3	1,306.0	6,847.1	36,500.8	194,221.9
29-26-327A	0.80	55.05	0.215	1.71	9.37	52.91	296.0	1,624.4	9,060.4	50,560.8	282,251.4
30-26-327B	0.814	54.10	0.215	1.72	9.36	52.86	291.1	1,623.2	9,054.5	50,531.2	282,104.1
31-26-328	0.80	113.28	0.543	2.01	9.09	42.01	192.6	835.4	4,209.3	19,427.8	88,454.4
32-26-330A	2.035	94.68	1.796	2.94	10.96	41.14	156.4	594.4	2,261.5	8,597.5	32,400.0
33-26-330B	1.800	107.05	1.796	3.57	12.75	46.58	172.4	644.0	2,421.4	9,148.7	34,694.2
34-26-331A	4.135	19.37	0.667	2.48	13.00	55.77	268.1	1,289.3	6,201.8	29,838.0	143,588.4
35-26-332	4.135	57.3	3.149	3.62	13.17	46.89	168.5	619.4	2,220.7	8,097.1	29,580.6
36-26-333A	4.135	78.65	3.615	3.05	10.00	32.97	110.2	368.2	1,231.4	4,030.5	13,505.1
37-26-333B	4.04	80.50	3.615	3.11	10.05	33.34	109.8	368.7	1,227.0	4,151.1	13,615.6
38-27-310	4.039	22.09	0.640	2.08	10.25	44.22	206.9	968.8	4,535.9	21,243.0	99,508.9
39-27-311	4.039	49.92	2.591	3.48	12.95	48.82	183.5	696.7	2,655.3	10,350.9	38,001.8
40-27-312	4.039	58.18	3.133	3.67	13.35	47.62	171.3	622.1	2,260.9	8,266.9	30,217.2
41-27-315	1.798	51.54	0.619	1.99	9.04	42.05	192.6	891.7	4,125.1	19,094.7	88,430.7
42-27-318	0.799	45.59	0.152	1.53	8.80	52.50	296.3	1,734.2	10,154.2	59,471.7	348,402.2
43-27-321	0.390	37.19	0.027	0.63	4.48	32.75	242.4	1,799.0	13,352.1	99,064.5	734,634.6
44-27-322	0.390	71.40	0.110	1.57	9.58	60.56	374.1	2,338.2	14,623.3	91,497.3	572,716.6
45-27-323A	0.390	117.60	0.202	1.64	8.88	48.77	267.1	1,501.1	8,070.5	44,426.9	244,767.2
46-27-323B	0.415	110.51	0.202	1.63	8.80	48.37	269.0	1,454.2	8,016.3	44,153.2	243,367.3
47-27-317	2.035	142.56	1.921	2.03	6.83	22.38	75.2	261.8	898.0	3,032.5	10,438.3
48-27-319	0.814	116.30	0.612	2.20	10.10	45.22	204.6	946.3	4,267.4	19,583.9	90,075.6

Table K-2. Variability of parameter α with parameter n on butyl plus dam surface of CSU Rainfall-Runoff Experimental Facility, Fort Collins, Colorado.

Code	Rainfall Intensity (In/hr)	Rainfall Duration (sec)	Peak runoff (In/hr)	Parameter α for Select Values of n							
				1.25	1.5	1.75	2.0	2.25	2.50	2.75	3.0
1-50-630	0.515	81.48	0.061	0.51	3.46	15.93	88.2	499.0	2,823.0	15,973.2	90,392.5
2-50-631	0.515	163.70	0.233	0.87	4.04	19.11	91.40	423.7	2,069.0	9,507.7	45,026.4
3-50-632	0.515	229.21	0.386	1.05	4.57	19.36	82.8	362.8	1,548.5	6,726.2	29,285.5
4-50-633	0.515	295.58	0.480	1.10	4.40	17.13	67.8	271.3	1,119.1	4,435.3	17,931.3
5-50-635	1.082	88.66	0.310	0.94	4.24	19.65	89.1	408.8	1,876.6	8,618.2	39,593.7
6-50-636	1.082	162.70	0.759	1.24	4.88	18.52	71.9	282.6	1,124.5	4,382.6	10,957.4
7-50-637	1.082	234.02	0.958	1.12	3.83	13.62	48.3	171.4	608.9	2,160.4	7,615.5
8-50-638	1.082	294.62	1.032	1.00	3.16	10.29	33.7	114.5	378.1	1,265.6	4,248.6
9-50-640	2.086	63.36	0.483	0.97	4.05	17.16	72.3	306.4	1,299.3	5,510.9	23,382.7
10-50-641	2.086	193.96	1.976	1.39	4.20	12.91	39.9	127.7	402.9	1,252.9	3,964.0
11-51-644	0.512	95.47	0.077	0.53	2.81	15.58	83.2	452.6	2,463.3	13,419.9	73,072.8
12-51-645	0.512	273.34	0.444	1.07	4.32	17.63	72.9	301.3	1,246.0	5,011.5	20,742.6
13-51-647	1.026	83.24	0.277	0.96	4.47	21.40	99.0	471.8	2,230.2	10,546.2	49,888.8
14-51-648	1.026	259.15	0.893	0.97	3.33	11.56	40.7	143.1	503.6	1,728.9	6,094.4

Table K-3. Variability of parameter α with parameter n on gravel (20 lbs/yd^2) surface of CSU Rainfall-Runoff Experimental Facility, Fort Collins, Colorado.

Code	Rainfall Intensity (In/hr)	Rainfall Duration (sec)	Peak Runoff (In/hr)	Parameter α for select values of n							
				1.25	1.5	1.75	2.0	2.25	2.50	2.75	3.0
1-14-149	0.807	272.39	0.798	1.29	4.39	14.87	54.7	198.2	726.1	2,647.2	9,727.1
2-14-149A	0.807	246.82	0.722	1.09	3.97	14.88	55.4	210.3	791.2	3,013.3	11,219.3
3-14-150	0.807	67.73	0.166	0.96	4.97	24.00	137.2	725.5	3,837.4	20,303.4	107,451.9
4-14-151A	1.871	215.49	1.562	0.92	2.69	9.11	29.1	90.6	283.1	899.6	2,860.2
5-14-151B	1.871	225.13	1.592	0.90	2.79	8.66	27.3	84.3	260.4	816.2	2,574.2
6-14-152A	1.871	57.53	0.481	1.18	5.19	23.45	105.0	460.8	2,056.1	9,177.9	40,981.6
7-14-152B	1.871	56.48	0.479	1.20	5.32	24.13	105.0	478.6	2,145.1	9,619.3	43,151.0
8-14-153A	2.886	207.48	2.330	0.82	2.35	6.80	18.7	54.1	155.6	448.4	1,296.4
9-14-153B	2.686	57.64	0.718	1.12	4.51	18.59	19.0	304.5	1,240.3	5,054.7	20,607.7
10-14-155	3.782	204.58	3.486	0.99	2.60	6.81	18.0	48.1	131.7	347.4	935.8
11-14-156	3.782	53.72	0.989	1.10	4.12	15.89	59.7	227.1	864.6	3,292.4	12,541.7
12-14-61B	0.458	138.67	0.153	0.75	3.72	19.06	95.4	487.8	2,480.5	12,621.0	64,227.6
13-14-62B	1.099	132.71	0.421	0.74	2.98	12.34	50.5	208.7	861.6	3,558.7	14,707.9
14-14-63B	2.311	100.97	0.887	0.86	3.10	11.43	41.6	152.8	560.9	2,059.7	7,569.0
15-14-64B	4.49	86.97	1.702	0.87	2.75	8.90	28.5	92.0	296.9	958.7	3,097.7
16-15-65B	0.468	130.16	0.139	0.71	3.55	18.45	93.5	481.8	2,477.1	12,742.0	65,571.3
17-15-66B	1.127	123.56	0.419	0.77	3.17	13.29	55.0	229.9	960.3	4,013.4	16,782.4
18-15-67B	2.385	84.02	0.730	0.84	3.14	12.11	45.5	174.4	665.6	2,542.0	9,712.1
19-15-68B	4.502	81.78	1.489	0.81	2.60	8.55	27.6	90.9	298.0	977.2	3,206.1

Table K-4. Variability of parameter α with parameter n on gravel (50 lbs/yd^2) surface of CSU Rainfall-Runoff Experiment Facility, Fort Collins, Colorado.

Code	Rainfall Intensity (In/hr)	Rainfall Duration (sec)	Peak Runoff (In/hr)	Parameter α for select values of n							
				1.25	1.5	1.75	2.0	2.25	2.50	2.75	3.0
1-20-169	0.86	258.51	0.635	0.75	2.74	0.91	36.2	135.6	495.6	1,853.6	6,741.5
2-20-170	1.85	67.83	0.440	0.90	3.75	16.30	69.4	297.7	1,278.7	5,494.1	23,614.2
3-20-171	1.85	254.54	1.446	0.68	2.06	6.35	18.7	57.1	174.4	535.6	1,645.8
4-20-172	3.85	51.41	0.766	0.88	3.32	13.65	42.1	184.4	707.0	2,712.0	10,406.4
5-20-173A	3.88	209.01	2.778	0.64	1.72	4.47	11.8	32.1	85.0	228.5	616.5
6-20-173B	3.88	210.09	3.05	0.72	1.92	5.15	13.4	35.2	93.6	250.4	670.8
7-20-174A	2.70	55.84	0.594	0.95	3.67	15.65	65.1	264.8	1,086.6	4,460.3	18,314.5
8-20-175A	2.70	250.30	2.402	0.78	2.10	5.82	16.0	44.8	124.3	352.3	953.9
9-20-176A	0.86	67.26	0.177	0.95	4.85	25.00	130.3	679.0	3,540.7	18,470.3	96,376.6
10-22-178B	2.90	41.51	0.310	0.62	2.70	11.80	50.8	220.9	960.4	4,176.3	18,163.8
11-22-179B	2.91	110.46	0.877	0.56	1.87	6.36	21.3	72.3	245.3	832.4	2,826.0
12-22-180B	2.91	187.18	1.478	0.52	1.51	4.45	13.1	39.9	115.2	341.7	1,014.3
13-22-181B	1.99	46.65	0.221	0.61	3.01	13.96	61.4	284.9	1,321.5	6,132.0	28,457.1
14-22-182B	1.99	115.32	0.567	0.55	1.98	7.39	26.9	99.4	366.8	1,354.4	5,003.6
15-22-183	1.99	190.08	0.961	0.53	1.68	5.44	17.8	57.0	185.4	602.7	1,960.3
16-22-184	1.99	310.26	1.563	0.52	1.49	4.28	12.0	33.6	95.9	275.12	790.7
17-22-185	3.91	47.17	0.481	0.57	2.78	8.73	34.1	133.2	520.3	2,033.0	7,945.0
18-22-186	3.90	83.20	0.940	0.58	1.92	6.59	22.1	74.7	253.0	856.8	2,903.0
19-22-187	3.90	105.03	1.098	0.52	1.61	5.20	16.4	52.3	167.0	533.5	1,705.2
20-22-188	3.91	153.45	1.743	0.53	1.51	4.35	12.8	36.7	105.3	305.0	884.4
21-22-189	3.91	298.83	3.712	0.66	1.53	3.60	8.5	21.0	50.7	121.0	293.4
22-23-191	0.916	64.98	0.093	0.45	2.31	12.16	61.6	319.1	1,655.0	8,584.2	44,530.0

Table K-4 (Continued)

Code	Rainfall Intensity (In/hr)	Rainfall Duration (sec)	Peak Runoff (In/hr)	Parameter α for select values of n							
				1.25	1.5	1.75	2.0	2.25	2.50	2.75	3.0
23-23-192	0.916	227.13	0.386	0.44	1.62	6.13	23.5	86.8	327.6	1,237.4	4,677.2
24-23-193	0.916	344.20	0.694	0.53	1.79	5.93	19.8	67.9	226.9	770.0	2,620.0
25-23-195	4.413	41.09	0.385	0.43	1.66	6.60	26.3	105.1	419.6	1,675.3	6,683.1
26-23-196	4.413	124.31	1.462	0.52	1.55	4.69	14.0	42.2	127.0	382.8	1,154.6
27-23-197	4.413	207.2	2.904	0.62	1.64	4.20	10.97	29.0	76.6	203.8	530.7
28-24-199	0.902	80.88	0.124	0.50	2.82	14.54	56.35	277.5	1,366.6	6,732.5	33,172.0
29-24-200	0.840	240.18	0.458	0.56	2.10	7.93	29.94	115.5	430.7	1,639.3	6,233.7
30-24-202	0.840	575.56	0.826	0.48	1.33	3.87	11.72	34.6	103.8	312.3	942.8
31-24-205	3.84	40.38	0.329	0.46	1.82	7.56	30.26	123.6	505.0	2,063.6	8,433.2
32-24-206	3.84	217.00	3.075	0.71	1.88	5.02	13.00	33.9	89.6	238.23	633.9
33-24-207	3.84	134.80	1.711	0.63	1.84	5.53	16.87	49.7	149.5	449.5	1,352.3

Table K-5. Variability of parameter α with parameter n for butyl plus gravel surface of CSU Rainfall-Runoff Experimental Facility, Fort Collins, Colorado.

Code	Rainfall Intensity (In/hr)	Rainfall Duration (sec)	Peak Runoff (In/hr)	Parameter α for select values of n							
				1.25	1.5	1.75	2.0	2.25	2.50	2.75	3.0
1-8-37B	0.494	138.97	0.171	0.76	3.71	18.63	92.0	459.0	2,288.7	11,418.9	56,999.3
2-8-38B	1.089	136.02	0.583	1.04	4.22	17.27	70.5	294.2	1,185.3	4,865.8	19,992.2
3-8-39B	2.387	78.98	1.012	1.30	4.93	19.10	75.2	284.3	1,099.7	4,257.7	16,494.5
4-8-40B	4.287	51.76	1.460	1.50	5.46	20.42	75.2	279.9	1,040.8	3,873.3	14,420.6
5-9-41B	0.461	86.20	0.129	1.11	6.22	36.01	203.5	1,163.8	6,658.9	38,121.0	218,316.2
6-9-42B	1.148	111.07	0.486	1.02	4.26	18.20	78.9	329.2	1,404.1	5,994.6	25,608.7
7-9-43B	2.383	81.51	1.027	1.27	4.79	18.43	71.9	270.1	1,037.1	3,985.0	15,322.1
8-9-44B	4.394	53.98	1.452	1.36	4.89	18.00	64.8	238.5	872.5	3,133.5	11,694.7
9-9-71B	0.440	45.80	0.054	1.03	8.65	47.35	321.6	2,184.5	14,844.0	100,887.1	685,782.7
10-9-77B	0.440	81.23	0.097	0.95	5.43	31.88	190.6	1,105.2	6,497.6	38,216.8	224,841.3
11-9-78B	0.440	120.40	0.159	0.98	5.11	27.32	144.0	766.6	4,077.3	21,700.5	115,555.0
12-9-79B	0.440	169.65	0.254	1.09	5.21	25.27	122.1	599.9	2,882.7	14,074.6	68,592.2
13-9-80B	0.440	203.95	0.292	1.03	4.68	21.69	99.7	465.3	2,150.5	10,149.9	46,316.6
14-9-82B	0.859	26.76	0.055	0.58	3.75	23.61	156.7	1,042.0	6,928.5	46,016.0	305,260.0
15-9-83	0.859	53.91	0.157	1.15	6.04	33.18	179.9	991.8	5,469.4	30,170.5	166,465.2
16-9-84	0.859	60.23	0.197	1.21	6.40	34.17	182.3	976.6	5,235.0	28,073.2	150,591.2
17-9-85	0.859	113.02	0.432	1.30	5.84	26.61	121.9	549.6	2,511.0	11,462.1	52,364.3
18-9-86	0.859	182.05	0.713	1.37	5.46	21.80	85.1	348.4	1,378.8	5,553.3	22,387.6
19-9-87	2.019	33.32	0.280	1.23	7.23	31.03	150.6	756.5	3,802.1	19,113.5	96,101.2
20-9-88B	2.019	65.27	0.726	1.43	5.95	25.31	106.2	450.2	1,906.7	8,080.6	34,263.1
21-0-89	2.019	104.14	1.120	1.31	4.83	18.10	67.6	257.3	950.2	3,584.5	13,488.7
22-9-90	2.019	132.34	1.463	1.36	4.77	16.48	57.5	206.0	719.5	2,543.2	8,923.3

Table K-5. (Continued)

Code	Rainfall Intensity (In/hr)	Rainfall Duration (sec)	Peak Runoff (In/hr)	Parameter α for select values of n							
				1.25	1.5	1.75	2.0	2.25	2.50	2.75	3.0
23-9-91	2.019	142.45	1.525	1.30	4.51	15.23	52.3	179.6	626.8	2,178.2	7,697.6
24-9-93	4.228	25.48	0.578	1.42	7.34	33.00	120.8	539.6	2,410.8	10,772.7	48,145.7
25-9-94	4.228	54.69	1.442	1.40	5.06	18.74	68.25	251.5	925.8	3,409.8	12,565.0
26-9-95	4.228	68.64	1.972	1.49	5.10	17.68	61.94	211.7	735.1	2,553.6	8,876.6
27-9-96	4.228	77.26	2.059	1.35	4.48	15.09	51.16	169.9	573.6	1,933.6	6,523.9
28-9-97	4.228	102.91	2.705	1.32	4.04	12.60	40.00	122.2	384.2	1,232.6	3,742.4
29-9-98	4.228	128.68	3.403	1.31	3.96	11.73	33.78	98.0	288.2	852.4	2,522.0
30-9-99	4.228	151.90	3.765	1.31	3.56	9.99	27.89	78.8	221.3	636.0	1,744.1
31-9-100	4.228	189.86	4.102	1.190	3.03	7.82	20.25	54.7	143.4	380.5	1,013.1
32-10-45D	2.374	79.17	0.919	1.17	4.45	17.30	66.50	257.8	998.7	3,871.5	15,016.7
33-10-46D	4.094	69.12	1.660	1.27	4.37	15.33	54.69	186.2	650.9	2,277.2	7,972.2
34-10-47B	1.130	124.63	0.552	1.04	4.24	17.64	73.81	302.5	1,260.4	5,243.6	21,832.6
35-10-48B	0.487	161.36	0.217	0.84	3.96	19.08	92.99	439.1	2,115.5	10,189.8	49,116.0
36-11-49B	2.350	102.91	1.15	1.10	3.93	14.25	52.10	186.5	678.1	2,464.0	8,960.2
37-11-50B	0.510	134.17	0.17	0.79	3.81	19.14	94.54	472.3	2,357.3	11,771.1	58,808.8
38-11-51B	1.074	122.18	0.56	1.16	4.84	20.44	86.02	371.3	1,536.8	6,504.5	27,552.4
39-11-52B	4.44	74.74	2.14	1.38	4.55	15.26	51.55	170.5	573.1	1,924.4	6,466.9
40-12-53B	0.459	106.64	0.139	0.93	4.97	27.22	145.12	793.2	4,306.9	23,397.9	127,165.1
41-12-54B	1.094	128.63	0.612	1.18	4.82	19.92	82.42	346.7	1,418.3	5,908.7	24,581.6
42-12-55B	2.207	93.91	1.089	1.27	4.70	17.72	67.27	250.6	947.4	3,578.2	13,525.5
43-12-56B	4.28	63.91	1.667	1.33	4.60	16.29	57.01	201.2	709.6	2,504.2	8,843.8
44-13-57B	0.489	130.74	0.153	0.74	3.67	18.75	93.65	478.3	2,428.8	12,340.8	62,732.9

Table K-5. (Continued)

Code	Rainfall Intensity (In/hr)	Rainfall Duration (sec)	Peak Runoff (In/hr)	Parameter α for select values of n							
				1.25	1.5	1.75	2.0	2.25	2.50	2.75	3.0
45-13-58B	1.069	145.03	0.589	1.00	4.00	16.18	65.21	268.2	1,069.3	4,348.5	17,660.2
46-13-59B	2.394	99.76	1.089	1.04	3.76	13.70	50.46	180.5	659.2	2,404.7	8,777.8
47-16-11B	0.85	100.32	0.460	1.65	7.64	35.86	167.97	803.8	3,722.4	17,541.4	82,735.2
48-18-133	0.96	94.81	0.427	1.37	6.24	28.99	165.1	620.1	2,878.4	13,365.0	62,099.0
49-18-134	2.10	100.50	1.400	1.70	6.22	23.30	86.4	325.9	1,215.7	4,631.6	17,080.5
50-18-135	3.83	90.86	2.525	1.64	5.28	17.47	67.3	189.2	627.6	2,103.0	6,859.5
51-18-136	0.96	233.69	0.853	1.16	4.16	15.37	57.1	209.7	775.4	2,926.6	10,552.8
52-18-137	2.10	144.62	1.637	1.32	4.50	15.48	51.0	173.3	590.7	2,024.0	6,944.3
53-18-138	3.83	131.25	3.166	1.41	4.20	12.51	36.4	111.5	329.6	991.8	2,987.4
54-25-210	0.87	17.97	0.081	2.04	14.91	105.66	765.0	5,641.9	40,161.1	291,079.0	2,109,826.6
55-25-214	3.61	25.16	0.364	1.03	4.75	22.74	103.6	483.1	2,254.4	10,521.1	49,105.7
56-25-215	3.61	87.04	1.516	1.02	3.43	11.70	40.5	134.77	458.9	1,563.7	5,331.9

Table K-6. Variability of parameter α with parameter n for brick, random plats of of gravel and butyl surface of CSU Rainfall-Runoff Experimental Facility, Fort Collins, Colorado.

Code	Rainfall Intensity (In/hr)	Rainfall Duration (sec)	Peak Runoff (In/hr)	Parameter α for select values of n							
				1.25	1.5	1.75	2.0	2.25	2.50	2.75	3.0
1-35-388	1.894	27.59	0.301	1.94	10.15	53.59	287.1	1,538.1	8,242.9	44,186.3	236,910.0
2-35-389	1.886	103.61	1.293	1.84	6.97	26.14	98.9	379.1	1,449.1	5,595.1	21,042.8
3-35-390	1.886	177.32	1.822	1.66	5.26	16.89	54.5	183.2	597.6	1,974.9	6,545.8
4-35-391	0.790	48.30	0.182	1.72	9.77	56.32	324.3	1,875.8	10,845.8	62,762.5	363,301.8
5-35-392	0.790	105.80	0.447	1.75	8.14	38.36	180.3	863.1	4,024.8	19,103.6	90,521.5
6-35-394	4.003	38.52	1.183	1.99	7.94	32.68	131.2	536.4	2,186.4	8,916.6	36,378.2
7-35-394	4.003	88.31	2.69	1.81	5.93	19.18	62.50	207.1	678.6	2,277.3	7,371.4
8-35-396	4.003	139.55	3.66	1.63	4.64	13.26	38.0	110.7	327.8	944.8	2,742.7
9-36-399	0.867	20.61	0.052	0.65	4.30	28.35	202.7	1,452.5	10,382.4	74,003.0	526,129.7
10-36-400	0.867	61.90	0.243	1.47	7.55	40.20	208.5	1,100.4	5,794.5	30,528.2	160,897.4
11-36-401	0.867	90.02	0.381	1.56	7.38	35.61	174.0	821.7	3,967.9	19,147.7	90,460.2
12-36-402	0.867	128.71	0.537	1.50	6.47	28.30	123.4	544.8	2,414.8	10,502.4	46,256.5
13-36-403	3.699	22.33	0.639	2.30	10.94	49.15	241.8	1,153.7	5,506.2	26,285.5	125,508.8
14-36-404	3.690	65.38	1.955	2.00	7.17	25.98	93.9	347.3	1,224.0	4,495.4	16,351.2
15-36-405	3.699	103.02	0.661	0.35	1.14	3.71	11.8	38.3	124.7	406.1	1,322.6
16-37-410	3.555	53.64	1.118	1.45	5.48	21.36	81.2	315.5	1,219.2	4,713.7	18,232.6
17-37-411	3.555	52.99	1.033	1.35	5.13	20.10	76.7	298.3	1,156.7	4,487.3	17,414.2
18-37-412	3.555	121.55	2.835	1.57	4.90	15.36	46.9	144.2	448.5	1,408.4	4,417.2
19-37-414	1.686	51.20	0.404	1.39	6.36	30.34	141.7	667.6	3,147.8	14,847.9	70,058.5
20-37-415	1.686	121.45	1.110	1.47	5.43	20.48	76.7	289.3	1,095.0	4,189.7	15,609.3
21-37-416	1.686	189.61	1.646	1.61	5.15	16.67	54.2	184.4	608.6	2,035.5	6,818.1
22-37-417	0.771	49.74	0.097	0.91	6.19	29.10	167.5	968.9	5,605.4	32,435.2	187,712.8
23-37-418	0.771	123.87	0.428	1.42	6.37	29.0	132.4	614.1	2,761.8	12,704.1	58,251.7
24-37-419	0.771	177.62	0.625	1.47	6.09	25.20	101.3	424.3	1,761.9	7,348.2	30,681.2

Table K-6. Continued

Code	Rainfall Intensity (In/hr)	Rainfall Duration (sec)	Peak Runoff (In/hr)	Parameter α for select values of n							
				1.25	1.5	1.75	2.0	2.25	2.50	2.75	3.0
25-37-420	0.396	51.23	0.039	0.76	5.16	34.65	235.0	1,535.0	1,087.0	73,504.2	499,065.2
26-27-421	0.396	134.35	0.165	1.08	5.64	30.00	162.1	840.1	4,459.4	23,690.7	125,935.0
27-27-422	0.396	206.53	0.295	1.27	6.04	28.06	131.6	632.4	2,958.1	14,088.4	67,253.1
28-38-435	0.824	52.39	0.142	1.15	6.45	34.1	197.1	1,106.0	6,207.9	34,854.3	195,732.8
29-38-436	0.824	117.57	0.447	1.44	6.47	26.5	133.6	619.1	2,768.3	12,678.0	57,917.2
30-38-428	4.073	35.56	0.855	1.53	6.24	26.43	106.1	439.4	1,821.6	7,553.8	31,331.9
31-38-429	4.073	38.51	0.967	1.57	6.21	25.52	102.8	417.2	1,694.7	6,886.8	27,994.3
32-38-430	4.073	80.12	2.205	1.56	5.16	17.32	58.0	198.5	657.2	2,214.1	7,466.3
33-38-431	4.073	123.79	3.253	1.49	4.46	13.46	39.6	117.0	350.9	1,057.6	3,191.1
33-38-432	1.807	151.89	1.457	1.44	5.00	17.54	58.6	206.6	721.0	2,528.6	8,876.8
34-38-433	1.807	38.26	0.291	1.13	6.35	32.50	156.9	782.9	3,906.7	19,500.7	97,359.1
35-38-434	1.807	99.57	1.940	1.39	5.34	20.82	81.0	333.0	1,235.7	4,833.2	18,920.1
36-38-437	0.824	222.03	0.763	1.37	5.25	19.63	74.3	284.7	1,115.1	4,235.0	16,356.9
37-39-440	3.717	25.87	0.652	1.93	8.87	40.76	182.2	836.8	3,844.3	17,667.0	81,209.8
38-39-441	3.717	58.47	2.121	2.52	9.23	34.25	126.8	477.3	1,754.1	6,556.9	24,465.3
39-39-443	0.892	57.95	0.221	1.45	7.55	40.96	218.0	1,162.7	6,232.3	33,421.5	179,286.5
40-39-444A	0.892	82.80	0.399	1.75	8.42	41.18	203.8	975.5	4,781.8	23,392.7	114,515.9
41-39-444B	3.717	92.36	2.930	2.15	7.11	23.64	76.5	249.1	822.3	2,733.2	3,085.6
42-40-459	0.480	87.65	0.073	0.60	3.34	18.65	105.3	594.9	3,316.6	19,013.3	107,485.3
43-40-460	0.480	176.08	0.263	1.01	4.68	22.00	103.2	494.5	2,286.7	10,852.0	51,292.5
44-40-461	0.501	287.69	0.477	1.24	4.79	19.04	76.1	315.3	1,269.3	5,182.5	21,218.1
45-40-465	0.970	25.79	0.063	0.67	4.11	25.62	166.2	1,080.7	7,026.3	45,640.0	296,164.0
46-40-466	0.970	108.85	0.371	1.02	4.50	20.20	89.7	401.6	1,797.3	8,040.4	36,061.3
47-40-467	0.970	152.58	0.678	1.38	5.65	22.41	90.8	372.9	1,549.7	6,309.4	25,486.7
48-40-468	0.970	264.42	0.937	1.18	4.02	13.80	47.6	178.9	595.9	2,104.6	7,454.4
49-40-471	1.930	198.80	1.863	1.42	4.37	13.56	42.3	137.3	432.9	1,382.5	4,427.8

Table K-6 Continued

Code	Rainfall Intensity (In/hr)	Rainfall Duration (sec)	Peak Runoff (In/hr)	Parameter α for select values of n							
				1.25	1.5	1.75	2.0	2.25	2.50	2.75	3.0
50-40-472	1.93	146.70	1.435	1.34	4.56	15.52	53.4	188.1	645.3	2,252.4	7,881.7
51-40-473	1.93	111.25	0.918	1.07	3.94	14.74	55.6	204.9	768.2	2,876.9	10,781.9
52-40-474	1.93	46.71	0.32	1.02	4.85	19.40	101.5	473.7	2,212.2	10,332.9	48,273.8
53-40-477	4.242	44.4	0.912	1.19	4.53	17.10	67.8	263.3	1,023.4	3,979.5	15,479.3
54-40-478	4.242	89.34	2.583	1.55	4.96	15.95	51.5	166.3	538.3	1,745.1	5,666.7
55-40-480	4.242	137.84	3.60	1.42	4.05	11.60	38.7	95.8	272.8	783.0	2,283.4
55-40-481	4.242	182.14	4.073	1.32	3.32	8.67	22.7	61.7	163.9	439.4	1,181.8
56-41-486	0.479	52.73	0.042	0.60	3.80	24.0	154.3	991.7	6,377.3	41,015.9	263,803.5
57-41-487	0.439	109.71	0.111	0.79	4.21	23.27	125.4	684.0	3,731.7	20,367.6	111,203.3
58-41-488	0.479	179.65	0.227	1.05	4.84	22.65	105.7	500.9	2,323.2	10,946.6	51,483.8
59-41-489	0.439	247.93	0.390	1.31	5.54	24.31	106.7	466.3	2,043.9	9,136.7	39,046.7
60-41-492	0.983	39.24	0.100	0.87	5.03	28.83	166.5	962.2	5,561.6	32,151.3	185,884.1
61-41-493	0.995	87.05	0.314	1.09	5.03	23.87	110.5	523.2	2,462.5	11,597.1	54,640.7
62-41-495	0.995	184.41	0.813	1.34	5.12	19.68	73.6	290.6	1,104.2	4,278.7	16,596.5
63-41-496	0.995	251.88	0.965	1.27	4.32	14.88	51.6	186.2	653.4	2,319.9	8,261.8
64-41-498	0.983	114.61	0.467	1.22	5.27	23.14	102.6	444.1	1,955.7	8,605.1	37,891.5
65-41-502	2.000	69.43	0.657	1.27	5.20	21.91	90.2	379.4	1,586.7	6,639.9	27,798.4
66-41-503	2.034	159.78	1.700	1.39	4.60	15.25	51.5	169.0	557.2	1,868.5	6,270.9
67-41-507	4.052	50.65	1.158	1.36	5.05	19.37	72.7	275.6	1,045.8	3,971.3	15,086.1
68-41-508	4.052	99.06	2.721	1.57	4.87	15.53	49.1	157.4	489.7	1,624.6	5,094.2
69-41-509	4.052	148.76	3.471	1.33	3.76	10.67	30.7	88.2	245.0	701.8	2,022.6
70-41-510	4.052	189.14	3.562	1.03	2.73	7.27	19.6	52.7	142.2	388.2	1,018.8
71-42-512	0.486	424.17	0.432	.70	2.62	9.62	35.7	133.9	513.8	1,908.9	7,222.4
72-42-515	0.456	68.95	0.079	0.96	5.78	35.17	207.3	1,258.9	7,648.9	46,486.4	282,585.5
73-42-516	0.456	148.74	0.238	1.19	5.84	29.09	144.4	735.0	3,588.2	17,910.3	89,474.3
74-42-518	0.456	318.6	0.456	0.95	3.75	15.30	61.6	253.6	1,033.1	4,360.7	17,100.6

Table K-6 Continued

Code	Rainfall Intensity (In/hr)	Rainfall Duration (sec)	Peak Runoff (In/hr)	Parameter α for select values of n							
				1.25	1.5	1.75	2.0	2.25	2.50	2.75	3.0
75-42-520	0.878	36.46	0.072	0.75	4.33	26.34	159.5	967.0	5,864.5	35,568.7	215,721.9
76-42-521	0.878	103.79	0.370	1.26	5.75	26.73	126.0	571.8	2,053.0	12,317.7	57,227.6
77-42-522	0.878	165.5	0.643	1.36	5.53	22.23	90.4	376.5	1,530.5	6,298.7	25,745.7
78-42-523	0.878	132.6	0.768	1.56	4.27	15.82	59.4	222.9	837.2	3,147.7	11,590.7
79-42-527	1.886	40.97	0.254	1.03	4.86	22.14	113.4	550.4	2,671.8	12,974.1	63,011.3
80-42-528	1.886	98.77	0.824	1.14	4.33	16.81	66.1	250.6	975.4	3,787.1	14,713.1
81-42-529	1.886	154.93	1.694	1.67	5.55	18.89	63.9	219.9	751.1	2,600.4	8,811.0
82-42-530	1.886	183.27	1.732	1.42	4.54	14.57	47.1	124.4	516.2	1,666.0	5,490.0
83-42-532	4.189	27.28	0.546	1.31	6.75	24.56	106.7	469.8	2,068.6	9,109.8	40,124.5
84-42-533	4.189	68.42	1.765	1.41	4.84	16.87	59.7	203.6	769.3	2,473.0	8,628.4
85-42-534	4.189	97.30	2.762	1.55	4.81	15.28	48.1	152.9	487.5	1,570.4	4,922.8
86-42-535	4.189	127.57	3.258	1.39	4.05	11.77	34.5	101.9	301.6	898.0	2,674.2
87-42-536	4.189	27.99	0.519	1.21	6.23	22.21	96.0	420.1	1,838.1	8,043.7	35,205.0
88-43-538	0.45	87.89	0.044	0.37	2.15	12.63	70.0	401.9	2,309.0	13,266.3	76,228.4
89-43-539	0.45	180.94	0.134	0.50	2.35	11.36	53.5	256.6	1,227.8	5,869.0	28,087.8
90-43-540	0.45	287.35	0.271	0.63	2.60	10.98	46.2	197.1	843.8	3,523.8	14,963.1
91-43-541	0.45	234.01	0.316	0.98	4.39	18.93	83.5	373.2	1,660.7	7,488.1	32,944.5
92-43-544	1.084	171.42	0.557	0.79	3.00	11.63	44.9	178.1	674.3	2,616.4	10,160.6
93-43-546	1.084	249.36	0.789	0.76	2.67	9.19	32.0	114.2	397.7	1,401.0	4,903.9
94-43-547	1.084	343.20	1.000	0.74	2.34	7.38	23.4	75.3	247.3	783.8	2,535.6
95-43-549	2.024	75.21	0.461	0.77	3.12	12.72	51.9	212.3	868.8	3,557.4	14,570.6
96-43-550	2.024	145.02	1.129	0.92	3.11	10.74	36.9	129.1	439.2	1,522.8	5,270.8
97-43-551	2.024	217.09	1.720	0.97	2.98	9.16	28.6	87.2	266.7	827.3	2,574.2
98-43-554	4.206	64.63	1.102	0.90	3.13	11.22	39.2	138.7	490.8	1,737.8	6,155.2
99-43-555	4.206	132.89	2.803	1.06	3.05	8.95	26.0	76.9	224.9	671.6	1,941.0
100-43-556	4.206	194.84	3.709	0.99	2.58	6.74	17.8	47.2	125.2	331.5	868.6

Table K-6. Continued

Code	Rainfall Intensity (In/hr)	Rainfall Duration (sec)	Peak Runoff (In/hr)	Parameter α for select values of n							
				1.25	1.5	1.75	2.0	2.25	2.50	2.75	3.0
101-43-557	4.206	262.40	4.104	0.85	2.00	4.75	11.4	28.3	68.6	168.0	412.8
102-44-563	0.468	60.65	0.050	0.64	4.23	25.0	154.1	961.3	5,998.5	37,435.4	233,654.6
103-44-564	0.468	135.81	0.144	0.74	3.66	18.8	94.4	480.8	2,445.5	12,444.9	63,357.7
104-44-565	0.468	209.16	0.261	0.84	3.74	16.9	76.6	353.0	1,579.8	7,209.7	32,843.8
105-44-566	0.468	282.01	0.371	0.90	3.77	15.9	65.3	269.5	1,129.4	4,758.4	20,063.4
106-44-569	4.219	46.79	0.760	0.93	3.51	13.4	50.5	193.6	743.0	2,962.4	10,953.1
107-44-570	4.219	103.71	2.386	1.18	3.63	11.30	35.1	111.1	342.6	1,075.2	3,368.1
108-44-571	4.219	148.84	3.252	1.112	3.16	8.8	24.9	70.6	200.7	574.3	1,643.4
109-44-572	4.219	196.58	3.816	1.03	2.64	6.9	17.9	47.4	124.5	332.4	870.2
110-44-574	2.107	71.45	0.473	0.80	3.26	13.3	54.6	223.5	917.2	3,766.2	15,469.4
111-44-575	2.107	151.22	1.364	1.06	3.42	11.6	38.7	131.1	445.3	1,498.4	5,074.5
112-45-577	1.112	71.42	0.175	0.65	3.11	14.5	71.3	343.8	1,657.3	7,990.8	38,536.9
113-45-578	1.112	184.48	0.778	1.05	3.97	14.5	54.2	205.0	785.1	2,945.2	10,968.0
114-45-580	4.171	40.70	0.756	1.11	4.37	17.5	67.9	270.5	1,078.2	4,298.4	17,140.3
115-45-581	4.171	121.38	3.279	1.48	4.44	13.4	39.3	116.2	348.6	1,050.9	3,170.4
116-46-586	1.072	70.47	0.176	0.71	3.48	16.3	79.6	388.3	1,895.2	9,252.6	45,180.5
117-46-587	1.072	200.19	0.849	1.13	4.18	15.6	56.8	208.1	773.0	2,886.7	10,788.9
118-46-589	4.351	36.13	0.699	1.13	4.45	18.0	72.9	296.4	1,204.3	4,895.4	19,903.6
119-46-590	4.351	111.68	3.756	1.90	5.65	16.9	51.2	155.0	455.6	1,376.8	4,109.3
120-47-598	1.039	57.83	0.193	1.03	5.28	27.2	138.1	713.1	3,684.5	19,043.0	98,445.1
121-47-599	1.039	179.88	0.861	1.40	5.32	20.30	75.7	296.8	1,123.1	4,326.7	16,687.9
122-47-601	4.166	30.24	0.516	1.10	5.56	19.62	82.9	355.0	1,529.7	6,574.7	28,263.6
123-47-602	4.166	99.58	3.656	2.28	7.03	21.82	68.6	215.4	677.3	2,128.4	8,589.7
124-48-607	0.494	32.43	0.029	0.41	2.63	18.96	139.6	1,029.1	7,567.5	5,548.0	405,638.5

Table K-6. Continued

Code	Rainfall Intensity (In/hr)	Rainfall Duration (sec)	Peak Runoff (In/hr)	Parameter α for select values of n							
				1.25	1.5	1.75	2.0	2.25	2.50	2.75	3.0
125-48-608	0.494	238.81	0.377	1.04	4.48	19.00	81.3	355.8	1,518.3	6,590.0	28,658.7
126-48-611	1.010	92.81	0.309	0.97	4.39	20.46	92.7	430.7	1,988.1	9,180.7	42,413.4
126-48-614	4.337	34.54	0.744	0.97	5.22	20.34	85.6	352.1	1,448.2	5,957.4	24,512.4
126-48-615	4.337	103.80	3.851	2.19	6.51	20.03	61.5	188.4	580.5	1,820.0	5,453.1
128-49-617	1.071	223.64	1.046	1.46	5.05	17.56	61.4	224.4	797.2	2,861.1	10,300.6
129-49-618	1.071	72.17	0.225	0.89	4.21	20.84	97.9	474.8	2,302.8	4,391.2	17,211.8
130-49-620	4.401	41.27	0.926	1.25	4.81	17.61	379.5	286.1	1,120.6	1,251.3	3,717.3
131-49-621	4.401	118.85	4.057	1.99	5.74	16.57	48.3	142.4	430.0	25,902.7	143,314.8
132-49-622	1.071	42.88	0.127	0.94	6.27	28.19	155.1	846.6	4,682.3	11,172.4	54,219.2

APPENDIX L

FORMULATION OF SINGLE-STEP LAX-WENDROFF FINITE DIFFERENCE SCHEME

L. 1 DERIVATION OF THE SCHEME

The dimensionless equation of continuity for the converging section follows:

$$\frac{\partial h}{\partial t} + u\frac{\partial h}{\partial x} + h\frac{\partial u}{\partial x} = q + \frac{h(1 - r)u}{[1 - (1 - r)x]} \tag{L-1}$$

Using $u = h^{n-1}$, Eq. (L-1) can be written as

$$\frac{\partial h}{\partial t} + \frac{\partial h^n}{\partial x} - \{q + \frac{(1 - r)h^n}{[1 - (1 - r)x]}\} = 0 \tag{L-2}$$

From the Taylor Series expansion we can write

$$h(x, t + \Delta t) = h(x,t) + \Delta t\frac{\partial h}{\partial t} + \frac{(\Delta t)^2}{2}\frac{\partial^2 h}{\partial t^2} + 0(\Delta t)^3 \tag{L-3}$$

Write Eq. (L-2) as

$$\frac{\partial h}{\partial t} = - \frac{\partial h^n}{\partial x} + \{q + \frac{(1 - r)h^n}{[1 - (1 - r)x]}\} \tag{L-4}$$

Differentiation of Eq. (L-4) with respect to t gives

$$\frac{\partial^2 h}{\partial t^2} = - \frac{\partial}{\partial t}[\frac{\partial h^n}{\partial x}] + \frac{\partial q}{\partial t} + \frac{\partial}{\partial t}\{\frac{(1 - r)h^n}{[1 - (1 - r)x]}\}$$

or

$$\frac{\partial^2 h}{\partial t^2} = - \frac{\partial}{\partial x}[\frac{\partial h^n}{\partial t}] + \frac{\partial q}{\partial t} + \frac{(1 - r)nh^{n-1}}{[1 - (1 - r)x]}\frac{\partial h}{\partial t} \tag{L-5}$$

Substitution of Eqs. (L-4) and (L-5) into Eq. (L-3) yields

$$h(x, t + \Delta t) = h(x, t) + \Delta t \left\{- \frac{\partial h^n}{\partial x} + q + \frac{(1-r)h^n}{[1 - (1 - r)x]}\right\} +$$

$$\frac{(\Delta t)}{2}\left[- \frac{\partial}{\partial x}(\frac{\partial h^n}{\partial t}) + \frac{\partial q}{\partial t} + \frac{(1 - r)nh^{n-1}}{[1 - (1 - r)x]} - \left(\frac{\partial h^n}{\partial x} + q\right.\right.$$

$$\left.\left. + \frac{(1 - r)h^n}{[1 - (1 - r)x]}\right)\right]$$

$$= h(x, t) + \Delta t\left\{ - \frac{\partial h^n}{\partial x} + q + \frac{(1 - r)h^n}{[1 - (1-r)x]} \right\} +$$

$$(\Delta t)^2 \left[- \frac{\partial}{\partial x} \left(nh^{n-1} \left\{ - \frac{\partial h^n}{\partial x} + q + \frac{(1 - r)h^n}{[1 - (1 - r)x]} \right\} \right) + \frac{\partial q}{\partial t} \right.$$

$$\left. + \frac{(1 - r)nh^{n-1}}{[1 - (1 - r)x]} \left(- \frac{\partial h^n}{\partial x} + q + \frac{(1 - r)h^n}{[1 - (1 - r)x]} \right) \right]$$

$$= h(x, t) - \left\{ \frac{\partial h^n}{\partial x} - q - \frac{(1 - r)h^n}{[1 - (1 - r)x]} \right\} \left\{ \Delta t + \right.$$

$$\left. \frac{(\Delta t)}{2} \frac{(1 - r)nh^{n-1}}{[1 - (1 - r)x]} \right\}$$

$$+ \frac{(\Delta t)^2}{2} \left[\frac{\partial}{\partial x} \left\{ nh^{n-1} \left[\frac{\partial h^n}{\partial x} - \left\{ q + \frac{(1 - r)h^n}{[1 - (1 - r)x]} \right\} \right] \right\} \right.$$

$$\left. + \frac{\partial q}{\partial t} \right] \qquad \text{(L-6)}$$

Equation (L-6) gives a second order approximation for $h(x, t + \Delta t)$, and is the basis of the finite difference formulation.

Using notations of Fig. 7-1, Eq. (L-6) can be written as

$$h_j^{i+1} = h_j^i - \left[\left\{ \frac{(h_{j+1}^i)^n - (h_{j-1}^i)^n}{2\Delta x} \right\} - q_j^i - \frac{(1 - r)(h_j^i)^n}{[1 - (1 - r)x_j^i]} \right] \left[\Delta t + \right.$$

$$\left. \frac{(\Delta t)^2}{2} \frac{(1 - r)n(h_j^i)^{n-1}}{[1 - (1 - r)x_j^i]} \right] + \frac{(\Delta t)^2}{2} \left[\frac{n}{\Delta x} \left\{ \frac{h^i_{j+1} + h^i_j}{2} \right\}^{n-1} \left\{ \frac{(h_{j+1}^i)^n - (h_j^i)^n}{\Delta x} \right. \right.$$

$$\left. \left. - \left\{ \frac{q_{j+1}^i + q_j^i}{2} \right\} - \frac{(1-r) \left\{ \frac{h_{j+1}^i + h_j^i}{2} \right\}^n}{1 - (1 - r)\left\{ \frac{x^i_{j+1} + x^i_j}{2} \right\}} \right\} - \frac{n}{\Delta x} \left\{ \frac{h_j^i + h_{j-1}^i}{2} \right\}^{n-1}$$

$$\left\{ \frac{(h_j^i)^n - (h_{j-1}^i)^n}{\Delta x} - \frac{q_j^i + q_{j-1}^i}{2} - \frac{(1-r)\left\{\frac{h_j^i + h_{j-1}^i}{2}\right\}^n}{1-(1-r)\left\{\frac{x_j^i + x_{j-1}^i}{2}\right\}} \right\}$$

$$+ \left[\frac{q_j^{i+1} - q_j^i}{\Delta t} \right] \Bigg] \qquad \text{(L-7)}$$

L. 2 DERIVATION OF STABILITY CRITERIA

Stability is essential for the convergence of a difference scheme. In an unstable scheme small numerical errors introduced in the computational method are amplified and dominate the solution. A linear stability analysis for the above difference scheme is given. Although the method is not rigorous for nonlinear equations it does serve to identify the unsuitability of the difference scheme, and determine appropriate step length for conditional stability.

In a linear stability analysis it is assumed that instabilities first appear in a very small region of space so that if the coefficients of the derivatives are smooth functions, they can be approximated as constants in this region. Write the Eq. (L-2) as

$$\frac{\partial h}{\partial t} + n h^{n-1} \frac{\partial h}{\partial x} - \frac{(1-r)h^{n-1}h}{[1-(1-r)x]} = q \qquad \text{(L-8)}$$

Linearize Eq. (L-8) and write as

$$\frac{\partial h}{\partial t} + n \bar{h}^{n-1} \frac{\partial h}{\partial x} - \frac{(1-r)\bar{h}^{n-1}h}{[1-(1-r)x]} = q \qquad \text{(L-9)}$$

Now at any point, (j,k), the numerical solution h_j^k equals the true solution $h(k\Delta t, j\Delta x)$ plus an error term ε_j^k.

Then
$$h_j^k = h(k\Delta t, j\Delta x) + \varepsilon_j^k \qquad \text{(L-10)}$$

here Δt = time increment, and

Δx = space increment.

Since the system of Eqs. (L-9) - (L-10) is linear, it may suffice to consider only one term of the Fourier Series expression for the error term. That is,

$$\varepsilon_{M}^{N} = \varepsilon_{o} \, \mathrm{Exp}[i(M\sigma\Delta x + N\gamma\Delta t)] \tag{L-11}$$

where ε_o = constant,

σ = wave number in space,

γ = wave number in time, and

$i = \sqrt{-1}$

It is assumed that the errors are perturbations added to the solution of the linear system. If the linearized finite difference equation is written in terms of the correct solution plus the error term (Eq. L-10) and then the exact solution is subtracted, a differential equation in the error terms can be obtained. That is

$$\frac{\partial \varepsilon}{\partial t} + a \frac{\partial \varepsilon}{\partial x} - \frac{b\varepsilon}{[1 - (1 - r)x]} = 0 \tag{L-12}$$

where

$$a = n\bar{h}^{n-1}$$

$$b = (1 - r)\bar{h}^{n-1}$$

The differential Eq. (L-12) is then written in finite-difference form. For the stability of a scheme the ratio of successive error terms must be smaller than unity, e.g.,

$$\left| \frac{\varepsilon_j^{k+1}}{\varepsilon_j^{k}} \right| < 1 \tag{L-13}$$

which establishes a stability criterion.

From Eq. (L-12),

$$\frac{\partial \varepsilon}{\partial t} = \frac{b\varepsilon}{[1 - (1 - r)x]} - a \frac{\partial \varepsilon}{\partial x} \tag{L-14}$$

$$\frac{\partial^2 \varepsilon}{\partial t^2} = \frac{\partial}{\partial t}\left[\frac{b\varepsilon}{1 - (1 - r)x}\right] - \frac{\partial}{\partial x}\left[\frac{\partial \varepsilon}{\partial t}\right]$$

$$= \frac{b}{[1-(1-r)x]}\left\{\frac{b\varepsilon}{1-(1-r)x} - a\frac{\partial \varepsilon}{\partial x}\right\} - a\frac{\partial}{\partial x}\left\{\frac{b\varepsilon}{1-(1-r)x} - a\frac{\partial \varepsilon}{\partial x}\right\}$$

$$= \frac{b^2\varepsilon}{[1-(1-r)x]^2} - \frac{ab}{[1-(1-r)x]}\frac{\partial \varepsilon}{\partial x} - ab\frac{\partial}{\partial x}\left\{\frac{\varepsilon}{1-(1-r)x}\right\} + a^2\frac{\partial^2 \varepsilon}{\partial x^2}$$

$$= \frac{b^2\varepsilon}{[1-(1-r)x]^2} - \frac{ab}{[1-(1-r)x]}\frac{\partial \varepsilon}{\partial x} - ab\left\{\frac{1}{[1-(1-r)x]}\frac{\partial \varepsilon}{\partial x} + \frac{(1-r)\varepsilon}{[1-(1-r)x]^2}\right\} + a^2\frac{\partial^2 \varepsilon}{\partial x^2} \qquad \text{(L-15)}$$

From the Taylor Series expansion,

$$\varepsilon(x,\ t + \Delta t) = \varepsilon(x,\ t) + \Delta t\frac{\partial \varepsilon}{\partial t} + \frac{(\Delta t)^2}{2}\frac{\partial^2 \varepsilon}{\partial t^2} + 0(\Delta t^3) \qquad \text{(L-16)}$$

Substituting Eqs. (L-14) and (L-15) into Eq. (L-16) leads to

$$\varepsilon(x,t + \Delta t) = \varepsilon(x,t) + \Delta t\left\{\frac{b\varepsilon}{[1-(1-r)x]} - \frac{a\partial \varepsilon}{\partial x}\right\} + \frac{(\Delta t)^2}{2}$$

$$\left\{\frac{b^2\varepsilon}{[1-(1-r)x]^2} - \frac{ab}{[1-(1-r)x]}\frac{\partial \varepsilon}{\partial x} - \frac{ab}{[1-(1-r)x]}\frac{\partial \varepsilon}{\partial x} - \frac{ab\varepsilon(1-r)}{[1-(1-r)x]^2}\right\} + \frac{(\Delta t)^2}{2}a^2\frac{\partial^2 \varepsilon}{\partial x^2} \qquad \text{(L-17)}$$

Write Eq. (L-17) in the finite difference form as:

$$\varepsilon_j^{k+1} = \varepsilon_j^k + \Delta t\left\{\frac{b\varepsilon_j^k}{[1-(1-r)x]} - a\frac{\varepsilon_{j+1}^k - \varepsilon_{j-1}^k}{2\Delta x}\right\} + \frac{(\Delta t)^2}{2}$$

$$\left\{\frac{b^2\varepsilon_j^k}{[1-(1-r)x]^2} - \frac{2ab(\varepsilon_{j+1}^k - \varepsilon_{j-1}^k)}{[1-(1-r)x]2\Delta x} - \frac{ab\varepsilon_j^k(1-r)}{[1-(1-r)x]^2}\right\}$$

$$+ a^2\frac{(\Delta t)^2}{2}\left\{\frac{\varepsilon_{j+1}^k - 2\varepsilon_j^k + \varepsilon_{j-1}^k}{(\Delta x)^2}\right\} \qquad \text{(L-18)}$$

Let $M = N = 0$ for the point j, k in Eq. (L-18), then

$$\varepsilon_j^k = \varepsilon_o; \quad \varepsilon_j^{k+1} = \varepsilon_o \exp(i\gamma\Delta t); \quad \varepsilon_{j+1}^k = \varepsilon_o \exp(i\sigma\Delta x); \quad \varepsilon_{j-1}^k$$

$$= \varepsilon_o \exp(-i\sigma\Delta x)$$

Substituting these expressions into Eq. (L-18) and dividing by ε_o leads to:

$$\frac{\varepsilon_j^{k+1}}{\varepsilon_j^k} = e^{i\gamma\Delta t} = 1 + \Delta t\left\{ \frac{b}{[1-(1-r)x]} - a\,\frac{e^{i\sigma\Delta x} - e^{-i\sigma\Delta x}}{2\Delta x} \right\}$$

$$+ \frac{(\Delta t)^2}{2}\left\{ \frac{b^2}{[1-(1-r)x]^2} - \frac{ab(e^{i\sigma\Delta x} - e^{-i\sigma\Delta x})}{[1-(1-r)x]2\Delta x} \right.$$

$$\left. - \frac{ab(1-r)}{[1-(1-r)x]^2}\right\} + a^2\,\frac{(\Delta t)^2}{2}\left\{\frac{e^{i\sigma\Delta x} - 2 + e^{-i\sigma\Delta x}}{(\Delta x)^2}\right\} \qquad \text{(L-19)}$$

Utilizing the appropriate trignometric identities, Eq. (L-19) can be written as:

$$e^{i\gamma\Delta t} = 1 + \Delta t\left\{\frac{b}{[1-(1-r)x]} - ai\,\frac{\sin\sigma\Delta x}{\Delta x}\right\} + \frac{(\Delta t)^2}{2}$$

$$\left\{\frac{b^2}{[1-(1-r)x]^2} - \frac{ab2i\,\sin\sigma\Delta x}{[1-(1-r)x]\Delta x} - \frac{ab(1-r)}{[1-(1-r)x]^2}\right\}$$

$$+ \frac{(\Delta t)^2}{2}\,a^2\left\{\frac{2\cos\sigma\Delta x - 2}{(\Delta x)}\right\} \qquad \text{(L-20)}$$

or

$$e^{i\gamma\Delta t} = 1 - ai\,\frac{\Delta t}{\Delta x}\sin\sigma\Delta x + (a\,\frac{\Delta t}{\Delta x})^2\,(\cos\sigma\Delta x - 1)$$

$$+ \frac{\Delta t b}{[1-(1-r)x]} + \frac{(\Delta t)^2}{2}\,\frac{b^2}{[1-(1-r)x]^2} - \frac{(\Delta t)^2}{2\Delta x}\,ab$$

$$\frac{2i\,\sin\sigma\Delta x}{[1-(1-r)x]} - \frac{(\Delta t)^2(1-r)}{2(1-(1-r)x]^2}\,ab \qquad \text{(L-21)}$$

For stability, the quantity $e^{i\gamma\Delta t}$ must be within the unit circle on the complex plane. The real part of Eq. (L-21) follows

$$1 + \left(\frac{a\Delta t}{\Delta x}\right)^2 (\cos\sigma\Delta x - 1) + \frac{b\Delta t}{[1-(1-r)x]} + \frac{1}{2}\left\{\frac{b\Delta t}{1-(1-r)x}\right\}^2 -$$

$$\left\{\frac{\Delta t}{[1-1(-r)x]}\right\}^2 \frac{ab}{2}(1-r)$$

or

$$1 + \left\{a\frac{\Delta t}{\Delta x}\right\}^2(\cos\sigma\Delta x - 1) + \frac{b\Delta t}{[1-(1-r)x]}\left\{1 + \frac{1}{2}\frac{b\Delta t}{[1-(1-r)x]}(1-a(1-r)\right\}$$

and the imaginary part,

$$-ai\frac{\Delta t}{\Delta x}\sin\sigma\Delta x - \frac{(\Delta t)^2}{2}ab\frac{i\sin\sigma\Delta x}{[1-(1-r)x]} = -ai\frac{\Delta t}{\Delta x}\sin\sigma\Delta x\left\{1 + \frac{\Delta tb}{[1-(1-r)x]}\right\}$$

Squaring the real and imaginary parts leads to:

$$\left|\left[1 + \left\{a\frac{\Delta t}{\Delta x}\right\}^2(\cos\sigma\Delta x - a) + \frac{b\Delta t}{[1-(1-r)x]}\left\{1 + \frac{b\Delta t}{2(1-(1-r)x)}(1-a(1-r))\right\}\right]^2 + \left[a\frac{\Delta t}{\Delta x}\sin\sigma\Delta x\left(1 + \frac{1+\Delta tb}{(1-(1-r)x)}\right)\right]^2\right| \leq 1 \qquad \text{(L-22)}$$

which gives the stability criterion.

Consider now the most critical conditions when the left hand side of Eq. (L-22) is evaluated at various values of $\sigma\Delta x$. See Table D-1. Terms of smaller magnitudes will be dropped; specifically terms involving $0(\Delta t)$ will be ignored.

Table D-1. Stability criterion.

$\sigma\Delta x$	$\sin\sigma\Delta x$	$\cos\sigma\Delta x$	Criterion
0	0	0	$\left\|1\right\| \leq 1$
$\pi/2$	1	0	$\left\|1 - (a\frac{\Delta t}{\Delta x})^2 + (a\frac{\Delta t}{\Delta x})^4\right| \leq 1$
π	0	-1	$\left\|1 - 4(a\frac{\Delta t}{\Delta x})^2 + 4(a\frac{\Delta t}{\Delta x})^4\right| \leq 1$
$3\pi/2$	-1	0	$\left\|1 - 3(a\frac{\Delta t}{\Delta x})^2 + (a\frac{\Delta t}{\Delta x})^4\right| \leq 1$

From the above analysis, it is clear that the criterion stated above is satisfied when

$$(a \frac{\Delta t}{\Delta x})^2 \leq 1$$

$$a \frac{\Delta t}{\Delta x} \leq 1$$

$$\frac{\Delta t}{\Delta x} \leq \frac{1}{n(\bar{h})^{n-1}} \qquad \text{(L-23)}$$

Equation (L-28) shows that the point (k+1, j) must lie within the zone of determinacy of the line from (k, j-1) to (k, j+1). The Lax-Wendroff scheme is linearly stable subject to the condition Eq. (L-23).

APPENDIX M

PARAMETER VARIABILITY ON AGRICULTURAL WATERSHEDS

Table M-1. Variability of parameter α on Watershed C, Riesel (Waco, Texas.

Serial number	Date of rainfall event	Observed hydrograph peak (in/hr)	Parameter α
1	6-10-1941	0.882	3.118
2	6-23-1959	0.625	1.834
3	7-9-1961	0.050	6.849
4	5-13-1957	0.566	2.788
5	7-16-1961	0.149	3.705
6	6-4-1962	0.314	3.159
7	5-9-1957	0.112	7.823
	Statistics of Parameter α		
Mean			4.182
Variance			5.039
Standard Deviation			2.245
Coefficient of Variation			0.537

Table M-2. Variability of parameter α on Watershed D, Riesel (Waco), Texas.

Serial number	Date of rainfall event	Observed hydrograph peak (in/hr)	Parameter α
1	5-6-1955	0.273	26.400
2	5-3-1957	0.670	8.800
3	6-23-1959	0.604	8.800
4	12-31-1959	0.070	9.600
5	7-16-1961	0.164	4.600
6	7-23-1961	0.046	10.345
7	6-4-1962	0.223	3.484
8	5-10-1965	0.894	3.914
	Statistics of Parameter α		
Mean			9.589
Variance			75.625
Standard Deviation			8.696
Coefficient of Variation			0.967

Table M-3. Variability of parameter α on Watershed G, Riesel (Waco), Texas.

Serial number	Date of rainfall event	Observed hydrograph peak (in/hr)	Parameter α
1	7-14-1941	0.091	3.739
2	2-14-1959	0.384	3.974
3	6-23-1959	0.049	3.445
4	11-4-1959	0.074	4.406
5	12-31-1959	0.052	5.344
6	7-16-1961	0.068	3.663
7	7-23-1961	0.021	6.119
8	3-29-1965	0.950	1.695
	Statistics of Parameter α		
Mean			4.048
Variance			1.750
Standard Deviation			1.323
Coefficient of Variation			0.327

Table M-4. Variability of parameter α on Watershed W-1, Riesel (Waco), Texas.

Serial number	Date of rainfall event	Observed hydrograph peak (in/hr)	Parameter α
1	3-12-1953	1.130	5.213
2	5-13-1957	1.640	3.373
3	6-4-1957	1.090	5.123
4	6-23-1959	1.890	16.117
5	6-15-1961	0.270	12.100
6	7-16-1961	0.132	4.900
7	6-9-1962	2.180	6.825
8	3-29-1965	2.313	2.063
	Statistics of Parameter α		
Mean			6.953
Variance			22.414
Standard Deviation			4.734
Coefficient of Variation			0.681

Table M-5. Variability of parameter α on Watershed W-2, Riesel (Waco), Texas.

Serial event	Date of rainfall event	Observed hydrograph peak (in/hr)	Parameter α
1	5-22-1951	0.046	3.587
2	3-12-1958	0.760	2.363
3	4-24-1957	2.040	1.612
4	5-13-1957	1.540	1.773
5	6-23-1957	1.420	2.192
6	6-25-1961	0.201	1.946
7	6-9-1962	0.943	2.337
8	3-29-1965	1.832	1.357
	Statistics of Parameter α		
Mean			2.199
Variance			0.515
Standard Deviation			0.718
Coefficient of Variation			0.325

Table M-6. Variability of parameter α on Watershed W-6, Riesel (Waco), Texas.

Serial number	Date of rainfall event	Observed hydrograph peak (in/hr)	Parameter α
1	4-27-1949	0.438	0.580
2	4-24-1957	2.200	1.246
3	5-13-1957	1.640	1.102
4	6-23-1957	1.600	1.690
5	6-18-1961	0.230	0.601
	Statistics of Parameter α		
Mean			1.044
Variance			0.218
Standard Deviation			0.467
Coefficient of Variation			0.448

Table M-7. Variability of parameter α on Watershed W-10, Riesel (Waco), Texas.

Serial number	Date of rainfall event	Observed hydrograph peak (in/hr)	Parameter α
1	3-12-1953	1.070	2.687
2	4-24-1957	2.790	1.467
3	4-24-1957	2.79	3.306
4	6-4-1957	0.853	3.182
5	6-23-1959	1.960	1.224
6	5-23-1961	0.422	2.939
7	6-25-1961	0.334	3.004
8	6-9-1962	0.824	1.282
9	3-29-1965	1.770	1.363
	Statistics of Parameter α		
Mean			2.298
Variance			0.873
Standard Deviation			0.934
Coefficient of Variation			0.407

Table M-8. Variability of parameter α on Watershed Y, Riesel (Waco), Texas.

Serial number	Date of rainfall event	Observed hydrograph peak (in/hr)	Parameter α
1	3-31-1957	0.150	4.071
2	4-24-1957	1.810	4.556
3	6-4-1957	1.430	4.446
4	6-23-1959	0.661	3.359
5	7-16-1961	0.060	0.615
6	6-25-1961	0.205	3.984
7	6-9-1962	0.711	4.201
8	3-29-1965	2.047	3.017
	Statistics of Parameter α		
Mean			3.53
Variance			1.662
Standard Deviation			1.289
Coefficient of Variation			0.365

Table M-9. Variability of parameter α on Watershed Y-2, Riesel, (Waco), Texas.

Serial number	Date of rainfall event	Observed hydrograph peak (in/hr)	Parameter α
1	3-26-1946	0.50	2.536
2	4-24-1957	1.68	2.644
3	5-13-1957	1.24	2.192
4	6-4-1957	1.79	3.031
5	6-23-1959	0.796	2.284
6	7-16-1961	0.072	2.772
7	6-25-1961	0.253	4.026
8	6-9-1962	0.899	3.360
9	3-29-1965	2.352	2.184
	Statistics of Parameter α		
Mean			2.781
Variance			0.373
Standard Deviation			0.610
Coefficient of Variation			0.219

Table M-10. Variability of parameter α on Watershed Y-4, Riesel (Waco), Texas.

Serial number	Date of rainfall event	Observed hydrograph peak (in/hr)	Parameter α
1	3-12-1953	0.558	1.673
2	4-24-1957	1.610	1.300
3	6-13-1957	1.140	1.319
4	6-4-1957	1.590	1.701
5	6-23-1959	0.789	5.282
6	6-25-1961	0.325	4.557
7	7-16-1961	0.062	2.400
8	6-9-1962	0.663	1.754
9	3-29-1965	2.500	3.471
	Statistics of Parameter α		
Mean			2.607
Variance			2.184
Standard Deviation			1.478
Coefficient of Variation			0.566

Table M-11. Variability of parameter α on Watershed Y-6, Riesel (Waco), Texas.

Serial number	Date of rainfall event	Observed hydrograph peak (in/hr)	Parameter α
1	5-6-1955	0.373	5.595
2	6-4-1957	0.931	0.694
3	6-23-1959	1.030	7.390
4	5-25-1961	0.211	5.157
5	6-15-1961	0.815	15.001
6	5-13-1957	0.803	0.520
7	6-9-1962	1.000	3.700
8	3-29-1965	2.692	1.784
9	4-24-1957	1.050	1.14
	Statistics of Parameter α		
Mean			5.164
Variance			22.125
Standard Deviation			4.704
Coefficient of Variation			0.911

Table M-12. Variability of parameter α on Watershed Y-7, Riesel (Waco), Texas.

Serial number	Date of rainfall event	Observed hydrograph peak (in/hr)	Parameter α
1	5-6-1955	0.590	18.74
2	5-24-1957	2.360	2.002
3	5-13-1957	2.030	2.581
4	6-4-1957	1.370	2.315
5	6-23-1959	1.760	29.459
6	5-22-1961	0.152	64.281
7	7-16-1961	0.069	1.689
8	6-9-1962	0.953	1.528
9	3-29-1965	2.275	1.146
	Statistics of Parameter α		
Mean			13.749
Variance			459.032
Standard Deviation			21.425
Coefficient of Variation			1.558

Table M-13. Variability of parameter α on Watershed Y-8, Riesel (Waco), Texas.

Serial number	Date of rainfall event	Observed hydrograph peak (in/hr)	Parameter α
1	3-12-1953	0.639	0.846
2	4-24-1957	2.710	1.355
3	5-13-1957	2.230	1.736
4	6-4-1957	2.150	2.300
5	6-23-1959	1.680	3.790
6	6-8-1961	0.078	1.000
7	6-9-1962	1.860	1.672
8	3-29-1965	2.249	2.123
	Statistics of Parameter α		
Mean			2.005
Variance			1.278
Standard Deviation			1.130
Coefficient of Variation			0.564

Table M-14. Variability of parameter α on Watershed Y-10, Riesel (Waco), Texas.

Serial number	Date of rainfall event	Observed hydrograph peak (in/hr)	Parameter α
1	5-6-1955	0.595	3.821
2	4-24-1957	2.700	1.371
3	5-13-1957	1.910	1.508
4	6-4-1957	2.400	1.333
5	6-23-1959	0.703	1.333
6	5-25-1961	0.366	4.382
7	6-15-1961	0.338	5.000
8	6-9-1962	0.394	1.152
9	3-29-1965	2.726	5.000
	Statistics of Parameter α		
Mean			2.487
Variance			2.619
Standard Deviation			1.618
Coefficient of Variation			0.651

Table M-15. Variability of parameter α on Watershed SW-12, Riesel (Waco), Texas.

Serial number	Date of rainfall event	Observed hydrograph peak (in/hr)	Parameter α
1	3-12-1953	2.170	2.750
2	6-4-1957	0.610	1.339
3	6-23-1959	0.714	1.232
4	6-9-1962	0.468	2.674
5	3-29-1965	4.005	1.891
	Statistics of Parameter α		
Mean			1.977
Variance			0.513
Standard Deviation			0.716
Coefficient of Variation			0.362

Table M-16. Variability of parameter α on Watershed SW-17, Riesel (Waco), Texas.

Serial number	Date of rainfall event	Observed hydrograph peak (in/hr)	Parameter α
1	3-12-1953	1.610	0.858
2	3-31-1957	0.441	0.962
3	4-24-1957	2.900	0.709
4	5-12-1957	1.740	0.529
5	6-24-1959	2.170	0.928
6	6-25-1961	0.604	1.727
7	7-16-1961	0.348	0.640
8	6-9-1962	3.790	1.381
9	3-29-1965	2.440	0.342
	Statistics of Parameter α		
Mean			0.897
Variance			0.184
Standard Deviation			.429
Coefficient of Variation			0.479